

Downstream change in channel hydraulics along  
the River Severn, UK

by

John S. Couperthwaite

A thesis submitted to the  
Faculty of Science  
of the  
University of Birmingham  
for the degree of  
DOCTOR OF PHILOSOPHY

School of Geography  
University of Birmingham  
Edgbaston  
Birmingham  
B15 2TT  
England

May 1997

UNIVERSITY OF  
BIRMINGHAM

**University of Birmingham Research Archive**

**e-theses repository**

This unpublished thesis/dissertation is copyright of the author and/or third parties. The intellectual property rights of the author or third parties in respect of this work are as defined by The Copyright Designs and Patents Act 1988 or as modified by any successor legislation.

Any use made of information contained in this thesis/dissertation must be in accordance with that legislation and must be properly acknowledged. Further distribution or reproduction in any format is prohibited without the permission of the copyright holder.

1927517X



UK 041 0133

## Abstract

An understanding of the longstream distribution of hydraulic processes is important for evaluating the processes which control the catchment-scale variation of channel stability, sediment transport and siltation, flood generation and aquatic habitats. However, little attention has been given to quantifying the detailed spatial and temporal variability of channel hydraulic parameters, despite considerable attention to reach-scale processes. The aim of this study was to understand the mechanisms controlling the spatial and temporal variation of channel hydraulics parameters at the basin scale, using a combined field and modelling approach. Field measurements were made at 25 logarithmically-spaced sites along the River Severn between the source and the near-tidal limit at Saxons Lode, under 3 flow conditions (low, medium and high) defined by exceedence frequencies. A flow event, occurring between 15-24 February 1989, was simulated by the 1-D hydraulic model, MIKE11. The simulated reach consisted of cross sections spaced at 1 km intervals between 4 km and 254 km downstream from the source of the Severn.

Channel hydraulic parameters showed considerable variability in both space and time, reflecting cross-section geometry variation downstream. Mean velocity increased with distance downstream from  $0.23 \text{ m s}^{-1}$  to  $1.72 \text{ m s}^{-1}$  under steady, bankfull flow conditions. However, unsteady flows simulated by MIKE11 demonstrated a longitudinal decline in the mean velocity of the wave peak associated with the rapid movement and minimal attenuation of the flood wave through the unconfined upper Severn. Flow resistance (Manning's  $n$  and Darcy-Weisbach  $f$ ) decreased downstream from the source ( $n = 0.32$  to  $0.06$ ), although under low flow conditions it increased from  $n = 0.3$  to  $1.1$  downstream to the non-alluvial - alluvial channel transition at Llanidloes; thereafter it exhibited a steady downstream decline. Reach mean shear stress and unit stream power peaked near the source (5-10 km downstream; drainage area  $< 50 \text{ km}^2$ ) at  $120 \text{ N m}^{-2}$  and  $290 \text{ W m}^{-2}$  and further downstream at the Ironbridge Gorge (170 km) ( $38 \text{ N m}^{-2}$ ;  $40 \text{ W m}^{-2}$ ).

The detailed model results revealed discontinuities in the downstream distribution of channel hydraulics, particularly at Llanidloes and the Ironbridge Gorge; these are believed to be controlled by changes in the geology of the basin which affects the channel slope and lateral confinement. The pattern of fluvial energy reflects this lithological control, but high rates of energy expenditure do not coincide with recorded estimates of lateral channel adjustment. Bank resistance is predicted to exert a significant control on the relationship between flow hydraulics and bank erosion rates. Variations in sediment storage through the basin recorded by previous studies are found to be tentatively related to downstream patterns of total and unit stream power. It is also predicted that large scale discontinuities in reach-scale channel hydraulics may affect the zonation of aquatic habitats through the basin. This study has implications for understanding and modelling fluvial processes at a basin scale, the prediction of floods and the management of aquatic habitats.

for mum and dad

## **Acknowledgements**

I would like to express my gratitude to my supervisors, Dr Damian Lawler and Dr John West, for their unfailing support and encouragement. Many thanks also goes to NERC for providing financial support, and the School of Geography and School of Civil Engineering, University of Birmingham, for the use of their facilities. I would like to thank Richard Johnson, Ray Hodson and John Willows who all dedicated many hours of their time to help build and install field equipment, and assisted in the field on numerous occasions. I am also indebted to Dan Cornford, Paul Wood and Louise Bull for all their assistance and advice with the modelling, field work and writing. Thanks go to all the other past and present postgraduates in Geography and Civil Engineering who have been a pleasure to work with. I would also like to thank Jamie Peart for always being helpful and cheerful, and letting me use the school's minibus, despite the rumours. I also greatly appreciate the keen, willing, and sometimes able, assistance offered in the field by the following: Maureen Agnew; Rosie Albutt; Carol Dukes; James Grove; David Hannah; Alan Hills; Chris Rose; Matt Stanway; Alan Stokes; and Julie Wong.

I am very grateful to the Institute of Hydrology at Plynlimon for allowing me access to the Experimental Catchment, and providing me with flow data. I am also indebted to David Pettifer at the EA for the cross section and flow data from the Severn for the MIKE11 model, and for his time and help during the early modelling stages. Severn Trent EA have also been very helpful and forthcoming with flow data, especially Rosie Powell, Brian Sheldon, Andy Roberts, Susannah Solway and Alison Williams. Thanks go to British Waterways Board for allowing access to the lower Severn. Thanks also to the many landowners along the Severn who have granted permission for me to ramble over their fields and scare their cattle. Hazel Eldridge also deserves a special mention for her hospitality amidst the wilderness of Plynlimon.

On less academic matters, I would like to thank Gretchell Coldicott, and the secretaries, for their constant cheerfulness and interest in postgraduate affairs. San has been a pleasure to drink with. Emma, Phil, Stu, Dan, Nadia, Rosie, Sarah, Vicky, Katherine, Briony and Rod have been fun to live with. Finally, a special thanks goes to Louise Jackson for putting up with my river stories.

# CONTENTS

Title page	
Abstract	
Dedication	
Acknowledgements	
Contents .....	i
List of figures .....	ix
List of tables .....	xx
List of plates .....	xxii
List of symbols .....	xxiv
List of abbreviations .....	xxvii

## CHAPTER 1 INTRODUCTION

<b>1.1 Introduction .....</b>	<b>1</b>
<b>1.2 Background to the study .....</b>	<b>1</b>
<b>1.3 Aims and objectives .....</b>	<b>2</b>
<b>1.4 Research issues.....</b>	<b>3</b>
<b>1.5 Thesis structure .....</b>	<b>4</b>

## CHAPTER 2 THEORETICAL AND EMPIRICAL BACKGROUND

<b>2.1 Introduction .....</b>	<b>6</b>
<b>2.2 The fluvial system and channel hydraulics .....</b>	<b>6</b>
<b>2.3 Channel hydraulics in gravel-bed rivers .....</b>	<b>8</b>
<i>2.3.1 Introduction.....</i>	<i>8</i>
<i>2.3.1 Principles of fluid flow.....</i>	<i>9</i>
<i>2.3.2 Boundary layer theory and velocity profiles.....</i>	<i>12</i>
<b>2.4 Spatial and temporal variation of channel hydraulic parameters.....</b>	<b>15</b>
<i>2.4.1 Introduction.....</i>	<i>15</i>

2.4.2	<i>Non-uniform flow structure</i> .....	15
2.4.3	<i>Flow resistance</i> .....	15
2.4.4	<i>Mean velocity</i> .....	17
2.4.5	<i>Discharge - a channel forming variable ?</i> .....	18
2.4.6	<i>The significance of slope in channel hydraulics</i> .....	19
2.4.7	<i>Reach mean shear stress and stream power</i> .....	20
2.4.8	<i>Estimation of boundary shear stress and its space-time variability</i> .....	23
<b>2.5</b>	<b>Control of channel hydraulics over sediment transport processes</b> .....	<b>26</b>
2.4.1	<i>Introduction</i> .....	26
2.4.2	<i>Initiation of sediment transport</i> .....	26
2.4.3	<i>Mechanics of sediment transport</i> .....	27
2.4.4	<i>Downstream variation in sediment transport</i> .....	28
<b>2.5</b>	<b>Interaction between channel hydraulics, sediment transport and river channel form ....</b>	<b>29</b>
2.5.1	<i>Introduction</i> .....	29
2.5.2	<i>Spatial and temporal variation in channel form</i> .....	30
2.5.3	<i>Channel stability</i> .....	32
2.5.4	<i>Channel adjustment</i> .....	33
<b>2.6</b>	<b>Summary</b> .....	<b>34</b>
 <b>CHAPTER 3 RESEARCH DESIGN</b>		
<b>3.1</b>	<b>Introduction</b> .....	<b>35</b>
<b>3.2</b>	<b>Sampling strategy and rationale</b> .....	<b>35</b>
3.2.1	<i>Introduction</i> .....	35
3.2.2	<i>River selection</i> .....	35
3.2.3	<i>Study site selection</i> .....	36
3.2.4	<i>Cross section selection</i> .....	36
3.2.5	<i>Flow measurement strategy</i> .....	36
<b>3.3</b>	<b>Study area and study sites</b> .....	<b>38</b>
3.3.1	<i>The River Severn</i> .....	38
3.3.2	<i>Climate</i> .....	38
3.3.3	<i>Hydrology</i> .....	38
3.3.4	<i>Geological evolution of the Severn basin</i> .....	40

3.3.5 Channel characteristics .....	40
3.3.6 Location of study sites .....	46
<b>3.4 Channel survey and bed sampling techniques.....</b>	<b>47</b>
3.4.1 Introduction.....	47
3.4.2 Bankfull channel geometry.....	47
3.4.3 Planform geometry.....	50
3.4.4 Stage and preliminary flow classification.....	52
3.4.5 Flow geometry.....	52
3.4.6 Bed material sampling .....	53
<b>3.5 Measurement of water surface slope.....</b>	<b>56</b>
3.5.1 Introduction.....	56
3.5.2 Water surface survey.....	56
3.5.3 Trash line survey.....	57
<b>3.6 Measurement of flow velocity .....</b>	<b>57</b>
3.6.1 Introduction.....	57
3.6.2 Flow meter calibration.....	59
3.6.3 Flow measurement by wading.....	61
3.6.4 Flow measurement from a boat.....	63
3.6.5 Indirect estimation of flow velocity.....	67
<b>3.7 Calculation of discharge .....</b>	<b>67</b>
3.7.1 Introduction.....	67
3.7.2 Discharge calculation from flow velocity measurements .....	67
3.7.3 Estimation from volumetric stream gauging.....	68
3.7.4 IH / EA gauging station data.....	68
<b>3.8 Estimation of discharge in the Upper Severn.....</b>	<b>68</b>
3.8.1 Trash line survey information .....	68
3.8.2 Evaluation of discharge .....	70
<b>3.9 Field measurement and calculation of boundary shear stress.....</b>	<b>75</b>
3.9.1 Introduction.....	75
3.9.2 Field measurement techniques.....	75
3.9.3 Calculation of boundary shear stress .....	76
<b>3.10 Flow classification.....</b>	<b>80</b>
3.10.1 Introduction.....	80
3.10.2 Flow classification by flow frequency.....	80
3.10.3 Timing, method and location of flow measurement .....	80

<b>3.11 Sources of error</b> .....	<b>85</b>
------------------------------------	-----------

<b>3.12 Summary</b> .....	<b>87</b>
---------------------------	-----------

## **CHAPTER 4 DOWNSTREAM CHANGE IN CHANNEL HYDRAULICS ALONG THE RIVER SEVERN: FIELDWORK RESULTS**

<b>4.1 Introduction</b> .....	<b>88</b>
-------------------------------	-----------

<b>4.2 Downstream change in channel form</b> .....	<b>88</b>
--	-----------

4.2.1 <i>Introduction</i> .....	88
---------------------------------	----

4.2.2 <i>Bankfull channel geometry</i> .....	88
--	----

4.2.3 <i>Channel planform</i> .....	90
-------------------------------------	----

4.2.4 <i>Bed material size</i> .....	90
--------------------------------------	----

<b>4.3 Downstream change in low-flow hydraulics</b> .....	<b>95</b>
---	-----------

4.3.1 <i>Introduction</i> .....	95
---------------------------------	----

4.3.2 <i>Mean velocity</i> .....	97
----------------------------------	----

4.3.3 <i>Discharge</i> .....	97
------------------------------	----

4.3.4 <i>Water surface slope</i> .....	97
--	----

4.3.5 <i>Flow resistance</i> .....	99
------------------------------------	----

4.3.6 <i>Total and unit stream power</i> .....	100
--	-----

4.3.7 <i>Reach mean and boundary shear stress</i> .....	100
---	-----

<b>4.4 Downstream change in medium-flow hydraulics</b> .....	<b>104</b>
--	------------

4.4.1 <i>Introduction</i> .....	104
---------------------------------	-----

4.4.2 <i>Mean velocity</i> .....	104
----------------------------------	-----

4.4.3 <i>Discharge</i> .....	104
------------------------------	-----

4.4.4 <i>Water surface slope</i> .....	104
--	-----

4.4.5 <i>Flow resistance</i> .....	106
------------------------------------	-----

4.4.6 <i>Total and unit stream power</i> .....	107
--	-----

4.4.7 <i>Reach mean and boundary shear stress</i> .....	107
---	-----

<b>4.5 Downstream change in high-flow hydraulics</b> .....	<b>109</b>
--	------------

4.5.1 <i>Introduction</i> .....	109
---------------------------------	-----

4.5.2 <i>Mean velocity</i> .....	109
----------------------------------	-----

4.5.3 <i>Discharge</i> .....	109
------------------------------	-----

4.5.4 <i>Water surface slope</i> .....	112
--	-----

4.5.5 <i>Flow resistance</i> .....	112
------------------------------------	-----

4.5.6 <i>Total and unit stream power</i> .....	112
--	-----

4.5.7 Reach mean shear stress .....	115
<b>4.6 Inter-relationships between stage, channel hydraulics and channel form.....</b>	<b>115</b>
4.6.1 Introduction.....	115
4.6.2 Effect of stage on the downstream distribution of channel geometry.....	115
4.6.3 Effect of stage on the downstream distribution of channel hydraulics.....	117
<b>4.7 Spatial variation of channel hydraulic parameters.....</b>	<b>121</b>
4.7.1 Introduction.....	121
4.7.2 Hydraulic geometry of the River Severn.....	121
4.7.3 Inter-relationships between channel hydraulic parameters, at-a-site and downstream.....	124
<b>4.8 Summary .....</b>	<b>124</b>

## CHAPTER 5      MODELLING CHANNEL HYDRAULICS USING MIKE11

<b>5.1 Introduction .....</b>	<b>126</b>
<b>5.2 Modelling hydrodynamics using MIKE11.....</b>	<b>126</b>
5.2.1 Introduction: Considerations behind modelling channel hydraulics .....	126
5.2.2 Rationale for choosing MIKE11 .....	128
5.2.3 Data input requirements.....	129
5.2.4 Model computation.....	131
5.2.5 Model output .....	134
5.2.6 Channel roughness sensitivity analysis.....	134
<b>5.3 Flow event simulation: the February 1989 flow event.....</b>	<b>136</b>
<b>5.4 Model design and parameterization .....</b>	<b>138</b>
5.4.1 Introduction.....	138
5.4.2 Channel network and cross section data .....	138
5.4.3 Flow boundary conditions.....	142
5.4.4 Model calibration.....	143
5.4.5 Sensitivity analysis: the problem of floodplain storage.....	146
5.4.6 Model validation against field observations.....	146
<b>5.5 Summary .....</b>	<b>151</b>

## CHAPTER 6 DOWNSTREAM VARIATION OF CHANNEL HYDRAULICS ALONG THE RIVER SEVERN: MODEL RESULTS

<b>6.1 Introduction</b> .....	<b>152</b>
<b>6.2 Downstream distribution of channel geometry during the flow event</b> .....	<b>153</b>
6.2.1 <i>Temporal variation of channel geometry parameters</i> .....	153
6.2.2 <i>Spatial variation of channel geometry parameters</i> .....	153
<b>6.3 Downstream distribution of mean velocity during the flow event</b> .....	<b>156</b>
6.3.1 <i>Temporal variation of mean velocity</i> .....	156
6.3.2 <i>Spatial variation of mean velocity</i> .....	156
<b>6.4 Downstream distribution of discharge during the flow event</b> .....	<b>157</b>
6.4.1 <i>Temporal variation of discharge</i> .....	157
6.4.2 <i>Spatial variation of discharge</i> .....	160
<b>6.5 Downstream distribution of water surface slope during the flow event</b> .....	<b>160</b>
6.5.1 <i>Temporal variation of water surface slope</i> .....	160
6.5.2 <i>Spatial variation of water surface slope</i> .....	162
<b>6.6 Downstream distribution of total and unit stream power during the flow event</b> .....	<b>162</b>
6.6.1 <i>Temporal variation of total and unit stream power</i> .....	162
6.6.2 <i>Spatial variation of total and unit stream power</i> .....	163
<b>6.7 Downstream distribution of reach mean shear stress during the flow event</b> .....	<b>163</b>
6.7.1 <i>Temporal variation of reach mean shear stress</i> .....	163
6.7.2 <i>Spatial variation of reach mean shear stress</i> .....	167
<b>6.8 Summary</b> .....	<b>167</b>

## CHAPTER 7 CONTROLS AND IMPLICATIONS OF DOWNSTREAM CHANGES IN CHANNEL HYDRAULICS

<b>7.1 Introduction</b> .....	<b>168</b>
<b>7.2 The representativeness of hydraulic measurements in the Severn catchment</b> .....	<b>168</b>
7.2.1 <i>Introduction</i> .....	168
7.2.2 <i>The River Severn</i> .....	168
7.2.3 <i>Fieldwork measurements: techniques and results</i> .....	169
7.2.4 <i>Model simulation: techniques and results</i> .....	171

<b>7.3 Issues of model validation</b> .....	<b>171</b>
7.3.1 <i>Introduction</i> .....	173
7.3.2 <i>Disparity between field and model reach lengths</i> .....	173
7.3.3 <i>The representation of roughness in the model</i> .....	174
7.3.4 <i>Accuracy of the model simulation</i> .....	179
<b>7.4 Dynamics of floodwave propagation</b> .....	<b>179</b>
7.4.1 <i>Introduction</i> .....	179
7.4.2 <i>Mechanics of floodwave propagation</i> .....	180
7.4.3 <i>Impact of channel form and roughness on floodwave properties</i> .....	181
7.4.4 <i>Impact of flow magnitude on floodwave properties</i> .....	187
<b>7.5 Spatial variation of channel transport parameters: shear stress and stream power</b> .....	<b>187</b>
7.5.1 <i>Introduction</i> .....	187
7.5.2 <i>Evidence for a stream power peak in river basin studies</i> .....	188
7.5.3 <i>Geomorphic control over stream power variability</i> .....	190
<b>7.6 Channel hydraulics and lateral channel adjustment</b> .....	<b>192</b>
7.6.1 <i>Introduction</i> .....	192
7.6.2 <i>Interaction between channel hydraulics and bank erosion processes along the Severn</i> .....	192
7.6.3 <i>Significance of boundary and planform form resistance on channel form and processes</i> .....	196
<b>7.8 Channel hydraulics and sediment transport</b> .....	<b>197</b>
7.7.1 <i>Introduction</i> .....	197
7.7.2 <i>The potential of stream power for evaluating sediment storage in fluvial systems</i> .....	198
<b>7.8 Channel hydraulics and the zonation of macro-habitats</b> .....	<b>200</b>
7.8.1 <i>Introduction</i> .....	200
7.8.2 <i>The river continuum concept</i> .....	201
7.8.3 <i>The serial discontinuity concept</i> .....	202
7.9.4 <i>The importance of hydraulic parameters in ecological habitat assessment</i> .....	203
<b>7.9 Summary</b> .....	<b>205</b>

## CHAPTER 8 CONCLUSIONS

<b>8.1 Introduction</b> .....	<b>206</b>
<b>8.2 Summary of study results</b> .....	<b>206</b>
8.2.1 <i>Downstream distribution of channel hydraulic parameters</i> .....	206

8.2.2 Downstream distribution of stream power and shear stress.....	209
8.2.3 The potential for 1-D modelling of channel hydraulics at a catchment-scale.....	29
8.2.4 Downstream propagation of floodwaves.....	210
8.2.5 Downstream interaction between channel hydraulics, bank erosion and sediment transport.....	210
<b>8.3 Potential for further research.....</b>	<b>211</b>
<b>8.4 Summary .....</b>	<b>213</b>
<b>REFERENCES .....</b>	<b>214</b>

## APPENDICES

- I A summary of study site locations, and the timing and measurement technique applied to the collection of flow data
  
- II FORTRAN programs:
  - i. The computation of hydraulic parameters from MIKE11 simulation output files.
  - ii. The conversion of EA cross section and flow data information into suitable import files for MIKE11
  
- III ‘Downstream change in channel hydraulics and river bank erosion rates in the Upper Severn, UK’, Couperthwaite, J. S., Lawler, D. M., Bull, L. J. and Harris, N. M. 1996. *Proceedings of the Interceltic Colloquium on Hydrology and Water Management*, Brittany, France, 93-101.

## LIST OF FIGURES

### CHAPTER 1

- Figure 1.1 A flow diagram representing the overall structure of this thesis, with particular reference to the field and model components..... 5

### CHAPTER 2

- Figure 2.1 A simple representation of the inter-relationships between channel hydraulics, sediment transport and channel form in natural river systems (after Ashworth & Ferguson, 1986)..... 7
- Figure 2.2 A schematic representation of TOPMODEL (from Beven *et al.*, 1984, p. 121)..... 7
- Figure 2.3 Types of open-channel flow (from Chadwick & Morfett, 1986, p. 119)..... 9
- Figure 2.4 The vertical velocity profile in laminar and turbulent flow (from Petts & Foster, 1990, p. 97). .... 13
- Figure 2.5 An S-shaped vertical velocity profile, characteristic of steep mountain rivers with coarse gravel / cobble beds (from Bathurst, 1993, p. 86)..... 13
- Figure 2.6 A series of velocity profiles downstream from a Smooth-Rough perturbation in the boundary roughness (from Livesey, 1995, p. 92)..... 14
- Figure 2.7 Primary and secondary flow velocities at a meander bend, Penstrowed, River Severn, Wales (from Thorne & Hey, 1984, p. 494)..... 16
- Figure 2.8 Channel stability of Danish streams defined by unit stream power (from Brookes, 1988, p. 98). .... 21
- Figure 2.9 The distribution of historical channel change rates in the Upper Severn and Wye catchments (from Lewin, 1987, p. 167)..... 21
- Figure 2.10 The spatial distribution of reach mean shear stress (tractive force) and unit stream power in the Henry Mountains, Utah (from Graf, 1982, p. 209)..... 22

Figure 2.11	The relationship between ten-year peak discharges and total stream power for, a) 1883 (pre-erosion period), and b) 1909 (post erosion period) (from Graf, 1983a, p. 382).....	23
Figure 2.12	The influence of sediment load on the shape of the vertical velocity profile (from Bathurst, 1993, p. 78).....	24
Figure 2.13	The boundary shear stress distribution across a simple trapezoidal channel ( $Fr = 3.24$ , Aspect Ratio = $B / H = 1.52$ ), showing primary flow isovels and secondary flow cells (from Knight <i>et al.</i> , 1994, p. 53). ....	25
Figure 2.14	The downstream variation of Caesium-134 along the River Severn (Walling & Quine, 1993). ....	29
Figure 2.15	A schematic diagram showing the downstream change of channel hydraulic parameters (from Knighton, 1987, p. 96). ....	30
Figure 2.16	The variation of mean velocity in the main channel, floodplain and composite cross section with stage at: a) Sangamon River; and b) Salt Creek (from Bhowmik & Demissie, 1982, p. 450).....	31
CHAPTER 3		
Figure 3.1	Map of the Severn catchment showing the course of the River Severn, the principle tributaries, the IH and EA gauging stations and the fieldwork study sites. ....	39
Figure 3.2a	Lake Lapworth and the course of the Severn channel prior to and during the glacial period. ....	44
Figure 3.2b	The development of the Ironbridge Gorge following the breaching of the Ironbridge col by the waters of Lake Lapworth.....	44
Figure 3.3	The geological structure of the Severn basin. ....	45
Figure 3.4	The longitudinal profile and bed slope of the River Severn, including several key site locations.....	46
Figure 3.5a	Surveying the channel cross section using the levelling technique (after Lawler, 1993). ....	48

Figure 3.5b	Cross section variables are calculated by dividing the section into subsections defined by the surveyed points. ....	48
Figure 3.6	A diagram showing the two flow classification schemes used in this study (after Richards, 1982). ....	53
Figure 3.7	The Wolman count method of surface sediment (Wolman, 1954). ....	54
Figure 3.8	Method of surveying the water surface slope, using a level or EDM. ....	57
Figure 3.9	Estimation of water surface slope, using the EDM surveying method, at Buildwas (22 March 1995). ....	58
Figure 3.10a	Mean velocity in the vertical may be calculated from either: a) a single point measurement at 60 % of the flow depth; b) two measurements at 20 % and 80 %; or c) multiple measurements through the flow depth (Herschy, 1985). ....	62
Figure 3.10b	The method of calculating the mean velocity in the vertical from multiple measurements (after Herschy, 1985). ....	62
Figure 3.11	A comparison between measured discharges at a MEDIUM flow level and 5 flow resistance equation estimates. ....	72
Figure 3.12	A comparison between measured and predicted discharge at a MEDIUM flow level. ....	73
Figure 3.13	A comparison between the Hey equation (1979) and the regression estimation technique against measured HIGH flow values. ....	73
Figure 3.14	Inter-granular flow, velocity profiles and the zero plane displacement (ZPD). ....	77
Figure 3.15	The calculation of boundary shear stress from velocity profiles: a worked example ....	78-9
Figure 3.16	Timing of flow measurement between 1 January 1994 and 7 March 1996 for: a) sites upstream, and including, Abermule; and b) sites downstream of Abermule. Codes refer to flow measurements listed in Table 3.14. ....	83

## CHAPTER 4

Figure 4.1	The spatial variation of bankfull water width downstream along the Severn.....	94
Figure 4.2	The spatial variation of bankfull mean depth downstream along the Severn.....	94
Figure 4.3	Downstream change in channel sinuosity along the Severn. ....	94
Figure 4.4	The spatial variation of grain size downstream along the Severn, expressed as the $D_{16}$ , $D_{84}$ and $D_{50}$ . ....	95
Figure 4.5	The spatial variation of mean velocity along the Severn, at a low-flow. ....	98
Figure 4.6	The spatial variation of discharge along the Severn, at a low-flow level.....	98
Figure 4.7	The spatial variation of water surface slope along the Severn, at a low-flow level.....	98
Figure 4.8	The spatial variation of Manning's $n$ roughness coefficient along the Severn at a low-flow level.....	99
Figure 4.9	The spatial variation of the Darcy-Weisbach friction factor, $f$ , along the Severn at a low-flow level.....	99
Figure 4.10	The spatial variation of total stream power along the Severn at a low-flow level.....	101
Figure 4.11	The spatial variation of unit stream power along the Severn at a low-flow level.....	102
Figure 4.12	The spatial variation of reach mean shear stress along the Severn at a low-flow level. ....	102
Figure 4.13	The spatial variation of boundary shear stress along the Severn at a low-flow level.....	102
Figure 4.14	The spatial variation of mean velocity along the Severn at a medium-flow level.....	105
Figure 4.15	The spatial variation of discharge along the Severn at a medium-flow level.....	105

Figure 4.16	The spatial variation of water surface slope along the Severn at a medium-flow level. ....	105
Figure 4.17	The spatial variation of Manning's $n$ roughness coefficient along the Severn at a medium-flow level. ....	106
Figure 4.18	The spatial variation of the Darcy-Weisbach friction factor, $f$ , along the Severn at a medium-flow level. ....	106
Figure 4.19	The spatial variation of total stream power along the Severn at a medium-flow level. ....	108
Figure 4.20	The spatial variation of unit stream power along the Severn at a medium-flow level. ....	108
Figure 4.21	The spatial variation of reach mean shear stress along the Severn at a medium-flow level. ....	108
Figure 4.22	The spatial variation of boundary shear stress along the Severn at a medium-flow level. ....	109
Figure 4.23	The spatial variation of mean velocity along the Severn at a high-flow level. ....	111
Figure 4.24	The spatial variation of discharge along the Severn at a high-flow level. ....	111
Figure 4.25	The spatial variation of water surface slope along the Severn at a high-flow level. ....	111
Figure 4.26	The spatial variation of Manning's $n$ roughness coefficient along the Severn at a high-flow level. ....	113
Figure 4.27	The spatial variation of the Darcy-Weisbach friction factor, $f$ , along the Severn at a high-flow level. ....	113
Figure 4.28	The spatial variation of total stream power along the Severn at a high-flow level. ....	114
Figure 4.29	The spatial variation of unit stream power along the Severn at a high-flow level. ....	114

Figure 4.30	The spatial variation of reach mean shear stress along the Severn at a high-flow level. ....	114
Figure 4.31	The spatial and temporal variation of water width along the Severn. ....	116
Figure 4.32	The spatial and temporal variation of mean depth along the Severn.....	116
Figure 4.33	The spatial and temporal variation of hydraulic radius along the Severn. ....	116
Figure 4.34	The spatial and temporal variation of mean velocity along the Severn.....	118
Figure 4.35	The spatial and temporal variation of discharge along the Severn.....	118
Figure 4.36	The spatial and temporal variation of water surface slope along the Severn.....	118
Figure 4.37	The spatial and temporal variation of Manning's $n$ roughness coefficient along the Severn.....	119
Figure 4.38	The spatial and temporal variation of the Darcy-Weisbach friction factor, $f$ , along the Severn.....	119
Figure 4.39	The spatial and temporal variation of total stream power along the Severn.....	120
Figure 4.40	The spatial and temporal variation of unit stream power along the Severn. ....	120
Figure 4.41	The spatial and temporal variation of reach mean shear stress along the Severn.....	120
Figure 4.42	A tri-axial graph of downstream hydraulic geometry exponents (after Park, 1977) including the results from this study of the River Severn.....	122
Figure 4.43	The spatial and temporal variation of the hydraulic geometry parameters: a) width; b) mean depth; c) mean velocity; d) water surface slope; and e) roughness, for the 25 study sites on the Severn, under low- ( $F \geq 70\%$ ) and high- flow conditions ( $F \leq 10\%$ ).....	125
 CHAPTER 5		
Figure 5.1	A simple representation of the modelling procedure adopted for this study. ....	127

Figure 5.2	The centred 6-point Abbott scheme (Danish Hydraulics Institute, 1990). .....	130
Figure 5.3	The schematization of the channel network topography and flow simulation requirements of MIKE11. ....	130
Figure 5.4	The significance of storage in MIKE11, demonstrated using in-channel (A) and over-bank (B) flow in two channels having the same discharge. ....	132
Figure 5.5	The cross section is divided into a series of rectangular channels by MIKE11 to cope with irregular channel morphologies (Danish Hydraulics Institute, 1990). ....	133
Figure 5.6	The effect of floodplain storage on the attenuation of the floodwave (represented by peak stage). ....	135
Figure 5.7	The effect of varying floodplain area on the volume of water stored on the floodplain. ....	135
Figure 5.8	The significance of channel roughness on stage in a simple rectangular channel, for three constant flows ( $Q = 50, 150$ and $350 \text{ m}^3 \text{ s}^{-1}$ ). ....	135
Figure 5.9	Daily weather maps (1200 GMT) from 13 - 20 February 1989, showing the synoptic weather conditions prior to and during the simulated flow event. ....	136
Figure 5.10	A isohyet distribution of the total precipitation (mm) recorded at 37 monitoring stations throughout the Severn basin during the rainstorm event (17 - 20 February 1989). ....	137
Figure 5.11	Precipitation recorded at hourly intervals at the Tanllwyth remote weather station in the Plynlimon catchment. ....	137
Figure 5.12	A schematic representation of the River Severn showing the simulated channel reach, major tributary inputs and weirs (not to scale). ....	139
Figure 5.13	A schematic representation of the reaches simulated in the model. ....	141
Figure 5.14	A comparison between flow hydrographs measured at EA gauging stations and simulated in the model, presented in upstream - downstream order, ie: A) Caersws; B) Montford; C) Buildwas; D) Bewdley. ....	144

Figure 5.15	The simulation of floodplain storage at Montford, using total floodplain widths varying from 0 - 1000 m.....	147
Figure 5.16	A comparison between measurements of reach mean shear stress (●) made at 15 field sites under a range of flows with estimate of shear stress (○) simulated by MIKE11 during a flow event in February 1989.....	148
Figure 5.17	A comparison between measurements of unit stream power (●) made at 15 field sites under a range of flows with estimate of unit stream power (○) simulated by MIKE11 during a flow event in February 1989.....	149
Figure 5.18	A comparison between modelled reach mean shear stress (maximum and minimum) and measured shear stress at low, medium and high flows. ....	150
Figure 5.19	A comparison between modelled unit stream power (maximum and minimum) and measured unit stream power at low, medium and high flows. ....	150
 CHAPTER 6		
Figure 6.1	The temporal variation of water width at: a) Dolwen; b) Crew Green; and c) Buildwas.....	154
Figure 6.2	The spatial variation of water width along the Severn, expressed as a maximum and minimum of the data series at each cross section. ....	154
Figure 6.3	The temporal variation of hydraulic radius at: a) Dolwen; b) Crew Green; and c) Buildwas.....	155
Figure 6.4	The spatial variation of hydraulic radius along the Severn, expressed as a maximum and minimum of the data series at each cross section. ....	155
Figure 6.5	The temporal variation of mean velocity at: a) Dolwen; b) Crew Green; and c) Buildwas.....	158
Figure 6.6	The spatial variation of mean velocity along the Severn, expressed as a maximum and minimum of the data series at each cross section. ....	158
Figure 6.7	The temporal variation of discharge at Dolwen, Crew Green and Buildwas.....	159

Figure 6.8	The spatial distribution of instantaneous discharge along the Severn, defined at three time periods: a) 1500 h, 18 February; b) 1500 h, 19 February; c) 2100 h, 20 February.....	159
Figure 6.9	The temporal variation of water surface slope at: a) Dolwen; b) Crew Green; and c) Buildwas.....	161
Figure 6.10	The spatial variation of water surface slope along the Severn, expressed as a maximum and minimum of the data series at each cross section.....	161
Figure 6.11	The temporal variation of total stream power at: a) Dolwen; b) Crew Green; and c) Buildwas.....	164
Figure 6.12	The spatial variation of total stream power along the Severn, expressed as a maximum and minimum of the data series at each cross section. ....	164
Figure 6.13	The temporal variation of unit stream power at: a) Dolwen; b) Crew Green; and c) Buildwas.....	165
Figure 6.14	The spatial variation of unit stream power along the Severn, expressed as a maximum and minimum of the data series at each cross section. ....	165
Figure 6.15	The temporal variation of reach mean shear stress at: a) Dolwen; b) Crew Green; and c) Buildwas.....	166
Figure 6.16	The spatial variation of reach mean shear stress along the Severn, expressed as a maximum and minimum of the data series at each cross section. ....	166
 CHAPTER 7		
Figure 7.1	The longitudinal profile of the River Severn (Wheeler, 1979, p. 252).....	169
Figure 7.2	The reach-scale variation of several hydraulic parameters along the study reach at Tanllwyth ( $Q = 0.009 \text{ m}^3 \text{ s}^{-1}$ ). ....	170
Figure 7.3	A comparison between the NRA cross section data (surveyed in 1976) and the field survey (1995) at a) Abermule and b) Bewdley.....	171
Figure 7.4	An evaluation of the influence of reach length on the determination of water surface slope, showing a) the difference between bed elevations	

	and elevation derived from slope calculations, and b) the residual slope elevation. ....	175
Figure 7.5	The downstream variation of Manning's $n$ values used in the model to simulate the bank top, bank and bed roughness. ....	176
Figure 7.6	A comparison between roughness coefficients measured in the field and simulated in the model at complementary sites which have a complete low-, medium- and high-flow record. ....	177
Figure 7.7	The relationship between roughness and discharge. (a) represents sites which exhibit an inverse relationship, and b) represents those sites where a positive or unclear relationship holds. ....	178
Figure 7.8	The spatial pattern of the momentum equation components at selected period during the simulated February 1989 event at: 0900, 16 February; 0900, 18 February; 1500, 18 February; 2100, 18 February; 0900, 19 February; 2100, 20 February. ....	182
Figure 7.9	The downstream transformation of flow event along the Severn channel, occurring in a) September 1994; b) December 1994; c) February 1995; and May 1995. ....	183-184
Figure 7.10	A comparison between a) the Rashid and Chaudry (1995) study of over-bank flow and b) the calibration curve for Bewdley (model simulation vs. EA measured flow). ....	185
Figure 7.11	Downstream variation in the wave peak velocity of the floodwave between EA gauging stations for 9 events between 1989 - 1995. ....	186
Figure 7.12	Downstream variation of peak discharge measured at EA gauging stations for 9 events between 1989 - 1995. ....	187
Figure 7.13	A comparison between measured a) total, and b) unit stream power values from this study and from the Lecce (1993) study of 4 channels in the Blue River basin, Wisconsin. ....	189
Figure 7.14	Trends for a) reach mean shear stress, b) total and unit stream power, and c) mean velocity, against drainage area for sites within the USA (Leopold & Wolman, 1957). ....	190

Figure 7.15	A comparison between the modelled hydraulic parameters (Lawler, 1992) and predicted downstream trends from the field study for high-flows (approximate bankfull flow). .....	191
Figure 7.16	The theoretical control of channel morphology on the temporal variability of flow energy (after Magilligan, 1992). .....	192
Figure 7.17a	The downstream pattern of water width and reach mean shear stress. ....	193
Figure 7.17b	The inverse relationship between water width and reach mean shear stress, calculated from the maximum simulated at-a-site values. ....	193
Figure 7.18	A conceptual model for the downstream change in the dominance of bank erosion processes (from Lawler, 1992; p. 137). .....	194
Figure 7.19	A comparison between unit stream power measured at a high-flow level with estimates of bank erosion rates (Lewin, 1987) along the upper Severn. ....	195
Figure 7.20	The downstream distribution between reach mean shear stress, discharge and bank erosion in the upper reaches of the Severn at a medium-flow level (Couperthwaite, <i>et al.</i> , 1996). .....	195
Figure 7.21	The downstream variation in the lower and upper bank silt-clay content (% weight) in the upper Severn (Couperthwaite, <i>et al.</i> , 1996; Harris, in prep). .....	197
Figure 7.22	The downstream variation of stream power and sediment storage along the Severn, using sediment data from Walling and Quine (1993). .....	199
Figure 7.23	A conceptual model for the faunistic zonation pattern in natural stream associated with the longitudinal gradient of hydraulic processes in river basins (from Statzner & Higgler, 1986; p. 136). .....	202
Figure 7.24	A comparison between the a conceptualization of the Serial Discontinuity Concept, the downstream distributions of channel slope and stream power from this study on the River Severn. ....	204

## LIST OF TABLES

### CHAPTER 2

Table 2.1	Variation of flow resistance coefficients for different channel types (from Bathurst, 1993, p. 75).....	17
-----------	---	----

### CHAPTER 3

Table 3.1	Selection criteria for study site location.....	37
Table 3.2	A summary of previous and current research in the Severn basin in the field of fluvial geomorphology. ....	41-2
Table 3.3	The location and type of EA (former NRA) gauging stations along the Severn (listed in downstream order, beginning near the source) (NRA Hydrometric Yearbook, 1992). ....	43
Table 3.4	Location and characteristics of fieldwork study sites.....	49
Table 3.5	Possible errors during channel geometry and slope surveys, using either the level or EDM.....	51
Table 3.6	Errors characterising surface bed material sampling.....	55
Table 3.7	Results from the calibration of Ott C2 and Braystoke flow meters.....	59
Table 3.8	Possible errors during current metering (after Herschy, 1978, 1985). ....	65
Table 3.9	Performance of the various flow resistance equations against the measured (medium) flow data.....	72
Table 3.10	The performance of the Hey (1979) equation against the measured (high) flow data.....	74
Table 3.11	The performance of the regression analysis against the measured (high) flow data.....	74
Table 3.12	A statistical comparison of the Hey equation and regression analysis.....	75
Table 3.13	A classification of flow magnitude based on discharge exceedance frequencies. ....	81

Table 3.14	The location and timing of field visits for: a) all sites upstream of, and including, Abermule; and b) all sites downstream from Abermule.....	82
Table 3.15	A schematic representation of the various techniques used to estimate hydraulic parameters along the Severn. ....	84
Table 3.16	Estimated errors associated with the various measurement techniques .....	86
 CHAPTER 4		
Table 4.1	A summary of curve-fit relationships for the variables measured during the fieldwork programme.....	89
Table 4.2	The channel hydraulic parameters measured under low-flow conditions at 25 sites along the Severn.....	96
Table 4.3	The channel hydraulic parameters measured under medium-flow conditions at 25 sites along the Severn. ....	103
Table 4.4	The channel hydraulic parameters measured under high-flow conditions at 25 sites along the Severn.....	110
Table 4.5	Downstream hydraulic geometry relations for gravel-bed rivers and canals.....	123
 CHAPTER 5		
Table 5.1	Location and dimensions of the broad-crested weirs included in the model simulation.....	140
Table 5.2	The location of the upstream and downstream flow boundaries in each simulated reach.....	140
Table 5.3	The performance of the MIKE11 simulation against measured flows at EA gauging stations. ....	145
 CHAPTER 6		
Table 6.1	The location and characteristics of the three sites chosen to represent the simulated temporal variation of channel hydraulics. ....	152

## LIST OF PLATES

### CHAPTER 3

Plate 3.1	Water surface slope surveying, using the EDM (at Pool Quay).....	60
Plate 3.2	Calibration of current meters in a flume.....	60
Plate 3.3	Flow measurement by wading (at Upper Hafren 3).....	64
Plate 3.4	Flow measurement from a boat (at Bewdley).....	64
Plate 3.5	The current meter array design for flow measurement from a boat. ....	66
Plate 3.6a	Good evidence for trash lines in the field (Severn Flume).....	69
Plate 3.6b	Poor evidence for trash lines in the field (Upper Hafren 3).....	69

### CHAPTER 4

Plate 4.1	The study reach at Bewdley under low-flow conditions in June 1994, looking upstream from the EA Ultra-sonic gauging station. ....	91
Plate 4.2	The study reach at Saxons Lode under low-flow conditions in January 1995, looking upstream from the EA Ultra-sonic gauging station. ....	91
Plate 4.3	The steep upland reach at Upper Hafren 3 in Plynlimon under low-flow conditions (July 1994), looking downstream towards the Hafren Forest plantation.....	92
Plate 4.4	The study site at Caersws under low-flow conditions in June 1994, looking upstream at the bank and flow monitoring equipment used by Bull (1996). ....	92
Plate 4.5	The meandering reach upstream of the study site at Pool Quay under high-flow conditions (January 1996). ....	93
Plate 4.6	The meander sequence between the Buildwas study site and the Ironbridge Gorge under low-flow conditions in June 1995. ....	93

**CHAPTER 7**

<b>Plate 7.1</b>	<b>A hydraulic jump situated upstream of the study section at Upper Hafren</b>	
	3.....	172
<b>Plate 7.2</b>	<b>The study section at Tanllwyth was located centrally across a pool. ....</b>	<b>172</b>
<b>Plate 7.3</b>	<b>The presence of vegetation on the upper bank acts as an additional</b>	
	<b>roughness element at high flows.....</b>	<b>178</b>

## LIST OF SYMBOLS

a.s.l	= above sea level
$a$	= ratio of hydraulic radius to the perpendicular distance from the channel perimeter to the point of maximum velocity
$A_{EDM}$	= horizontal angle measured from the Electro-magnetic Distance Meter ( $^{\circ}$ )
$A$	= water prism area ( $m^2$ )
$\alpha_c$	= coefficient (accounting for energy losses in discharge and the upstream velocity head)
$A_i$	= area of water prism subsection, $i$ ( $m^2$ )
$A_t$	= total area of cross section ( $m^2$ )
$b$	= gradient of a line, and regression coefficient
$c_w$	= wave celerity ( $m\ s^{-1}$ )
$C$	= Chezy roughness coefficient
$C_v$	= Courant velocity coefficient
$d$	= flow depth (m)
$\bar{d}$	= mean flow depth (m)
$d_0$	= flow depth at the channel bed level (m)
$d_i$	= depth of subsection, $i$ (m)
$d'_i$	= interval distance between depth measurements (m)
$D_{16}, D_{50}, D_{84}$	= grain size of the $n^{th}$ percentile (m)
$DA_{gauged}$	= drainage area of the gauged catchment ( $m^2$ )
$\Delta h$	= difference in elevation between adjacent cross sections (m)
$\Delta t$	= time difference between model computations (s)
$\Delta u$	= difference in mean velocity between adjacent cross sections ( $m\ s^{-1}$ )
$\Delta y$	= distance between adjacent cross sections (m)
$E_{EDM}$	= distance measured from the Electro-magnetic Distance Meter (m)
$f$	= Darcy-Weisbach friction factor
$F$	= flow frequency (%)
$Fr$	= Froude number
$g$	= acceleration due to gravity ( $m\ s^{-2}$ )
$\gamma_s$	= specific gravity of sediment ( $N\ m^{-3}$ )
$\gamma_w$	= specific gravity of water ( $N\ m^{-3}$ )
$h$	= stage (m)
$h_{EDM}$	= elevation measured from the Electro-magnetic Distance Meter (m)
$H$	= high-flow ( $F \leq 10\%$ )

$H_{BM}$	= elevation above a bench mark (m)
$H'_{BM}$	= regression estimate for elevation above a bench mark (m)
$H_s$	= available energy head above the weir crest (m)
$i$	= the sequence of velocity readings, taken from the bed upwards
$\kappa$	= von Karman constant
$k_s$	= equivalent roughness of sand (m)
$L$	= low-flow ( $F \geq 70\%$ )
$L_R$	= reach length (m)
$L_C$	= length of the channel, measured from an estimated centre line (m)
$M$	= medium-flow ( $10 \leq F \leq 70\%$ )
$n$	= Manning's roughness coefficient
$n$	= number of subsections
$n_r$	= number of revolutions
$n_v$	= number of point velocity readings in the vertical
$P_i$	= wetted perimeter of subsection, $i$ (m)
$P_t$	= total wetted perimeter of cross section (m)
$q$	= discharge of a subsection ( $m^3 s^{-1}$ )
$Q$	= discharge ( $m^3 s^{-1}$ )
$Q^t_{\text{gauged}}$	= the discharge gauged at time, $t$ ( $m^3 s^{-1}$ )
$R$	= hydraulic radius (m)
$\rho$	= water density ( $kg m^{-3}$ )
$Re$	= Reynolds number (dimensionless)
$s$	= water surface slope ( $m m^{-1}$ )
$s_c$	= channel slope ( $m m^{-1}$ )
$s_e$	= energy slope ( $m m^{-1}$ )
$s_f$	= friction slope ( $m m^{-1}$ )
$S$	= sinuosity
$S_0$	= bed slope ( $m m^{-1}$ )
$\tau$	= reach mean shear stress ( $N m^{-2}$ )
$\tau_b$	= boundary shear stress ( $N m^{-2}$ )
$t$	= time (seconds)
$t_p$	= time period
$\tau^*_{ci}$	= critical dimensionless shear stress of the $i^{\text{th}}$ percentile fraction of the surface bed material ( $N m^{-2}$ )
$\tau_i$	= shear stress acting on a particle ( $N m^{-2}$ )
$T_p$	= time difference between peak discharge (s)
$\nu$	= kinematic viscosity of water ( $m^2 s^{-1}$ )

$u$	= point flow velocity ( $\text{m s}^{-1}$ )
$\bar{u}$	= mean flow velocity ( $\text{m s}^{-1}$ )
$u^*$	= shear velocity ( $\text{m s}^{-1}$ )
$u_{0.2}$	= flow velocity at 20 % of the vertical depth ( $\text{m s}^{-1}$ )
$u_{0.6}$	= flow velocity at 60 % of the vertical depth ( $\text{m s}^{-1}$ )
$u_{0.8}$	= flow velocity at 80 % of the vertical depth ( $\text{m s}^{-1}$ )
$u_i$	= the $i^{\text{th}}$ measurement of streamwise velocity from the bed ( $\text{m s}^{-1}$ )
$u_v$	= mean vertical velocity of the $i^{\text{th}}$ vertical ( $\text{m s}^{-1}$ )
$U_s$	= freestream velocity ( $\text{m s}^{-1}$ )
$V$	= volume of water ( $\text{m}^3$ )
$\Omega$	= total stream power ( $\text{W m}^{-1}$ )
$w$	= water width (m)
$w_i$	= width of subsection, $i$ (m)
$w_s$	= structure width (m)
$W$	= wake function
$\omega$	= unit stream power ( $\text{W m}^{-2}$ )
$W_{\text{BF}}$	= bankfull water width (m)
$y$	= vertical distance from the channel boundary (m)
$y'$	= distance downstream (km)
$Y$	= cumulative distance downstream (km)
$z$	= boundary layer thickness (m)
$\Delta x$	= space step (m)
$\Delta t$	= time step (seconds)
$\emptyset$	= Ott C2 propeller diameter (m)

## LIST OF ABBREVIATIONS

$^{134}\text{Cs}$	= Caesium 134 radio-isotope
DD	= Distance downstream (km)
DTM	= Digital Terrain Model
DX-MAX	= Maximum grid spacing in MIKE11
EA	= Environment Agency
ECM	= Electromagnetic Current Meter
EDM	= Electromagnetic Distance Meter
h-Q	= Stage - discharge boundary
h-t	= Stage - time boundary
IDC	= Intermediate Disturbance Concept
IH	= Institute of Hydrology
LBT	= Left bank top
NRA	= National Rivers Authority
RBT	= Right bank top
RCC	= River Continuum Concept
SDC	= Serial Discontinuity Concept
SE	= Standard error
TBM	= Temporary bench mark
w/d	= Width / depth ratio
$W_{BF}$	= Bankfull width
WELB	= Waters edge left bank
WERB	= Waters edge right bank
ZPD	= Zero plane displacement

### Study sites

Aber	= Abermule
Bewd	= Bewdley
B'north	= Bridgnorth
Bws	= Buildwas
Caer	= Caersws
CG	= Crew Green
Dol	= Dolwen
Dyff	= Dyffryn
HFalls	= Hafren Falls

HFor	= Hafren Forest
Llan	= Llandinam
MS	= Mount Severn
Mont	= Montford
New	= Newtown
PB	= Picnic Bridge
PQ	= Pool Quay
Rhy	= Rhydyronnen
SG	= Severn Gorge
SL	= Saxons Lode
SF1	= Severn Flume
SFord	= Severn Ford
Tan	= Tanllwyth
UH1	= Upper Hafren 1
UH2	= Upper Hafren 2
UH3	= Upper Hafren 3

# CHAPTER 1

## INTRODUCTION

### 1.1 Introduction

The spatial variability of hydraulic processes in river basins is important for the understanding of channel stability, sediment transport and siltation, aquatic habitats and flood prediction. The continuity between stream flow, sediment load, channel form and basin controls along a river channel emphasise the need for an appraisal of the patterns and controls of the major channel hydraulic parameters at a basin scale. The interaction between these, the sedimentary boundary and aquatic vegetation determines the potential for erosion, the capacity of the flow to transport material, the stability and diversity of biotic communities and the impact of extreme flow events on the surrounding floodplain. The effective management of water resources therefore requires an appreciation of the hydraulics of flow and the link between these related processes.

This study examines the distribution of channel hydraulic parameters through the Severn basin, from the source to Saxons Lode, using a combined field and modelling approach; these parameters describe the dimensions, motion and characteristics of flow and include: water width; mean depth; mean velocity; water surface slope; flow resistance; reach mean and boundary shear stress; and gross and unit stream power. Previous contributions to this research area have tended to concentrate on the fluvial processes occurring at a smaller spatial scale (eg: Magilligan, 1992; Lecce, 1993) and are difficult to apply to basin-scale studies in the fields of, for example, bank erosion and sediment transport. This chapter presents the context of this study. It first discusses the background to the research problem, then focuses on the specific aims, objectives and hypotheses of this research. Finally, the structure for the thesis is presented, describing the contents of each chapter. In addition, Figure 1.1 illustrates the linkages between the field and modelling methodologies in this study, and the benefits of a combined approach.

### 1.2 Background to the study

The interaction between channel form, boundary roughness and 3-D flow structure has been well documented in the past, at scales varying from individual clasts (Brayshaw *et al.*, 1983), to bedforms (Leeder, 1983; Best, 1992) and bend and reach scales (eg: Dietrich, 1987; Ferguson, 1986). This has led to important advances. However, the spatial and temporal relationship between channel hydraulics and channel form at a catchment-scale has been largely overlooked (Lewin, 1987). Several studies have adopted either a composite basin approach (Leopold & Maddock, 1953; Leopold & Wolman, 1957; Graf, 1982), or examined small - medium sized basins in a range of fluvial environments (eg: River Severn (Lewin, 1983, 1987); Allt Dubhaig (Ferguson & Ashworth, 1991); River Coe (McEwen, 1994); Galena River (Magilligan, 1992); Blue River (Lecce, 1993)). Few have attempted to quantify detailed flow processes throughout an entire basin; the methodology for this approach is described in Chapters 3 and 5.

Although considerable information exists on the longstream distribution of mean velocity (Leopold, 1953; Mackin, 1963; Carlston, 1969), the magnitude, patterns and controls of other more important flow variables, including total and unit stream power, boundary and reach mean shear stress, and flow resistance, are not clearly understood (Knighton, 1987) (see Chapter 2). The hydraulic geometry theory (Leopold & Maddock, 1953) highlighted the downstream adjustment of channel and flow parameters in response to imposed climatological, hydrological and lithological controls, but failed to define the longstream variability and nature of adjustment between channel hydraulic parameters; this will be discussed further in Chapters 2 and 7. Furthermore, the belief that discharge is dominant in geomorphic activity in hydraulic geometry has been undermined by research highlighting the importance of more sensitive measures of energy in the fluvial system (Nanson & Croke, 1992) (section 2.4.7). Begin (1981), Graf (1982, 1983a), Lewin (1983, 1987) and Lawler (1992) suggest that lateral channel adjustment and channel form are closely related to the spatial variation of fluvial energy (shear stress and stream power), which has been shown to be predominantly controlled by lithologically-induced slopes (Ferguson & Ashworth, 1991; Magilligan, 1992; Lecce, 1993) and bank resistance (Harris, in prep); these points are described in Chapters 2 and 7. This supports the regime and extremal theories that a stable channel form is reached as energy expenditure is minimised (Yang, 1976; Yang & Stall, 1973). The redistribution of sediment from in-channel, tributary and bank sources is known to be selectively entrained (Ashworth & Ferguson, 1986; 1989), transported (Ashworth *et al.*, 1992) and deposited (Carling, 1983) by the flow, although the control of basin-scale hydraulic processes is unknown (Chapters 2 and 7).

The simulation of channel hydraulics in natural channels has concentrated on reach-scale analyses of palaeohydraulic flows (O'Connor & Webb, 1988; Wohl, 1992), 2-D and 3-D flow structure (Cunge *et al.*, 1980; Alabyan, 1996) and the impact of management schemes on hydrological processes (Beyer & Portner, 1994; Macilwaine *et al.*, 1994). Catchment-scale modelling has been restricted to general hydrological models (eg: TOP model and SHE) or dambreak reconstructions (Carling & Glaister, 1988; Wolff & Burges, 1994; Mishra & Seth, 1996) with only a limited concern for the spatial variability of hydraulic processes (Magilligan, 1992). However, the advantage of a high resolution, catchment-scale, approach to channel hydraulic simulation presents an opportunity to evaluate the detailed distribution of flow variables in space and time (see Chapter 5) and therefore complements traditional approaches.

### 1.3 Aims and Objectives

Against this background of research, a number of aims and objectives may be identified. The research addresses the overall problem of the influence of river flow on the stability of river channels and quality of the aquatic habitat. Specific attention is given to quantifying the magnitude of the spatial and temporal variations of hydraulic parameters and the causes for these variations. This was accomplished through a combined field monitoring programme and model simulation. The following objectives were developed to achieve this aim:

1. To quantify the downstream distribution of channel hydraulic parameters under steady and unsteady flow conditions. Both field measurements and model simulation results (Chapters 4 and 6,

respectively) will be used to evaluate trends and investigate the impact of tributaries, channel form and basin lithology.

2. To quantify the distribution of stream power and shear stress along a channel, with stage and during a flow event (Chapters 4 and 6). The channel hydraulic information will be used to determine the hydrological and lithological controls on this distribution (Chapter 7). The presence and location of the hypothesised energy peak in the basin will be identified.
3. To simulate the spatial and temporal variability of channel hydraulics along a channel using a 1-D hydraulic model. This will require topographic and hydrological information for a river channel at the basin scale, and the application of an existing model (Chapter 5).
4. To evaluate the hydraulic controls affecting the propagation of floodwaves along a channel. This will allow for an examination of the temporal variation of at-a-site hydraulics, and the interaction between downstream changes in channel size, shape and slope and wave characteristics (velocity and attenuation) (Chapter 7).
5. To consider the implications for lateral channel adjustment, sediment transport and the zonation of aquatic habitats in response to variations in hydraulic processes along a river channel (Chapter 7).

This research will therefore attempt to increase our understanding of flow processes at basin scales by defining: the spatial distribution of channel hydraulic parameters at pre-defined flow frequencies and at the event timescale; how these processes are inter-related in time and space; the controls on the fluvial energy distribution; and the interaction between channel form, fluvial energy, channel mobility and sediment transfer. This is achieved using a unique data-set of directly measured hydraulic characteristics at sites along the channel, and model information simulated at a high resolution. The combination of these methods and hydraulic parameters has not been measured before along a single channel through an entire river basin.

#### **1.4 Research issues**

The preceding sections have indicated the uncertainty in this research field and outlined the specific areas of interest for this study. The following issues are discussed in order of the preceding objectives.

It has been proposed that regional variations in basin geology (Brush, 1957; Magilligan, 1992; Lecce, 1993) and flow inputs (Richards, 1980; Reid *et al.*, 1989) will significantly alter the longstream pattern of channel hydraulics. However, no detailed measurements of hydraulics at this scale have been made to evaluate these claims. There is currently little understanding of the distribution and controls on mean velocity at this scale, and under varying flow frequencies, despite earlier studies by Leopold (1953), Mackin (1963) and Carlston (1969). It is likely that mean velocity will be highly variable between reaches, but increase with distance downstream and stage in response to greater depths and channel efficiencies and reduced flow resistance. In-channel roughness elements are expected to dominate the distribution of water

surface slope at low flows (Prestegard, 1983; Bathurst, 1993), but local and regional valley topography will be more significant at higher stages. Vegetation influences are likely to alter the variation of flow resistance and mean velocity with stage.

The spatial distribution of fluvial energy is likely to be dominated by changes in the geology throughout the basin, as found by Graf (1982, 1983a), Magilligan (1992) and Lecce (1993). Therefore, the energy is not expected to decrease gradually from the source (Knighton, 1987), or reach a peak in the upper reaches (Lewin, 1983, 1987; Lawler, 1992), but peak wherever the channel slope is steepened. This will occur in response to recent or long term channel adjustment (natural or anthropogenic), or by lateral valley confinement. Variations in channel size and shape through the basin will modify the temporal adjustment of fluvial energy to flow magnitude.

The MIKE11 model will be used to analyse catchment-scale hydraulic processes, and therefore extend the current reach-scale application of 1-D models (Magilligan, 1992; Wohl, 1992; Carling & Wood, 1994). It is likely that a balance must be achieved between the detailed simulation of hydraulic processes and the availability of topographical data. Also, the accuracy of the model simulation will depend upon the comparability of the field and modelling methodologies.

The hydraulic characteristics of floodwaves are likely to be substantially altered by downstream changes in the geometry, slope and storage capacity of the channel (Woltemade, 1993; Woltemade & Potter, 1994). Lateral channel confinement and the associated steepened channel slopes will prevent overbank flow and storage; this will limit attenuation and increase wave velocities (Mishra & Seth, 1996). During overbank flow, enhanced hydraulic roughness at low floodplain inundation are likely to reduce wave velocities, and further increases in stage will lower hydraulic roughness and increase wave velocity.

Downstream changes in the rate of channel adjustment are governed by the interaction between fluvial energy and bank resistance (Bull, 1979). Little information exists regarding the spatial variation of these three components, although it is likely that measures of fluvial energy, such as reach mean and boundary shear stress, are poor predictors of channel mobility without bank resistance information. Sediment transport and deposition are dependent upon the transport capacity, or energy, of the flow (Bagnold, 1966; Gomez, 1983; Reid & Frostick, 1986). Therefore, the spatial variation of fluvial energy is expected to be more closely related with selective transport processes. The longitudinal variation of hydraulics and channel stability may affect the distribution, stability and diversity of species within biotic communities. The 'zones of hydraulic transition' proposed by Statzner and Higler (1986) are, therefore, likely to correspond to these spatial patterns of hydraulic parameters in the basin.

## **1.5 Thesis Structure**

This thesis is divided into eight chapters. Chapter 1 has introduced the background to this research, the aims and objectives of this study and a summary of issues to be elucidated during this project (Figure 1.1). Chapter 2 reviews previous related research, focusing on the inter-relationship between hydraulic processes, sediment transport and channel form at the catchment scale (Figure 1.1).

Chapters 3 and 4 describe respectively the methodology and results from the fieldwork programme. The former describes the characteristics of the study basin and the rationale for site selection, together with the techniques used to survey the channel and compute the hydraulic characteristics of the flow; the latter reviews the downstream variation of each hydraulic parameter under varying flow frequencies.

Chapters 5 and 6 describe respectively the methodology and results from the model simulation of river hydraulics through the Severn basin. The former reviews the computational requirements of the model, and the results from the calibration and validation exercises; the latter presents the results from the model simulation of an unsteady flow event, describing the temporal variation of each hydraulic parameter during the event and with distance downstream.

Chapter 7 integrates the results from Chapters 4 and 6, to evaluate the spatial and temporal variation of channel hydraulics at the catchment-scale. This first considers whether the findings from this study are representative of the conditions along the Severn, and also whether the results from this basin are applicable in other basins. The controls on the propagation of floodwaves and the spatial variation of the hydraulic parameters through the basin are discussed. The implications of this study for channel stability, sediment transport and stream ecology are also explored.

Chapter 8 (Conclusions) summarises the main findings from this study. It also reviews some methodological problems, and provides suggestions for future initiatives to improve our understanding of basin-scale fluvial hydraulics.

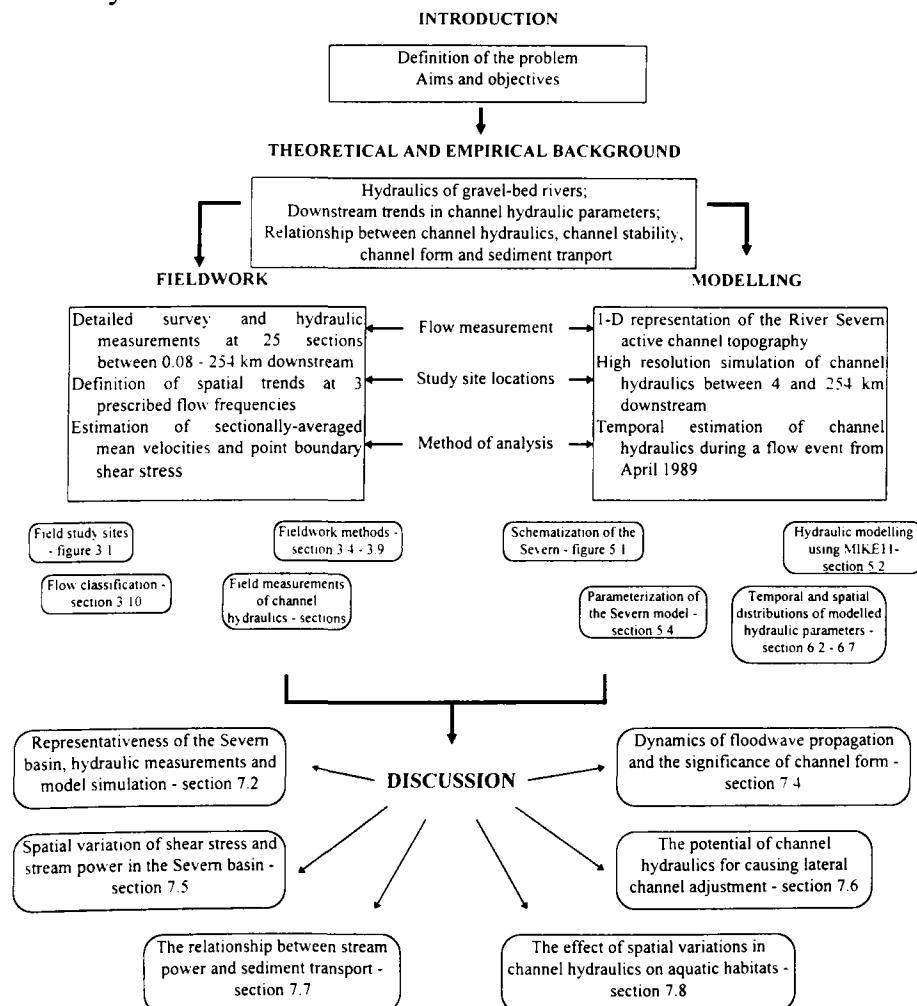


Figure 1.1

A flow diagram illustrating the structure of this thesis, and the combined field and modelling approach. Note that key sections and figures are included for easy reference.

## CHAPTER 2 THEORETICAL AND EMPIRICAL BACKGROUND

### 2.1 Introduction

This chapter presents the background to this study of channel hydraulics at a catchment-scale. It will include a review of the fluvial system, with particular emphasis on the role of channel hydraulics in explaining sediment transport and channel form. Channel hydraulics are commonly defined using a measure of discharge to explain channel form and the associated processes of sediment entrainment and transport, and channel adjustment. However, recent evidence suggests that shear stress and stream power are more useful measures for indicating the *effectiveness* of a flow (Magilligan, 1992; Nanson & Croke, 1992). Following a review of the place of channel hydraulics in the fluvial system, the various principles of channel hydraulics will be explained. This will lead on to a review of the hydraulic processes which occur at the boundary layer and their consequent effect on the spatial and temporal variation of channel hydraulics, particularly shear stress and stream power. The importance of these processes in defining sediment entrainment and transport will then be reviewed. Finally, the impact of hydraulics on river channel form through the impact of variations in sediment transport is discussed.

### 2.2 The fluvial system and channel hydraulics

The climate of the fluvial system ultimately determines the character of the drainage basin through a direct control on the hydrology, and indirect control on the basin physiography and lithology (Figure 2.1). The physiography defines the altitudinal range, size and shape of the basin. The lithology includes the bedrock geology (composition and structure), the tectonic status and the soil formation. These variables together determine the hydrological regime in the basin through their control over the water and sediment yield, which are free to vary in space and time. Drainage occurs through the channel network, developing a system of channels, whose size and geometry are intimately related to the channel hydraulics within them. The topographic form of the river channel at any position in the catchment thus reflects the spatially varied system controls.

The storage and release of flow through hydrological stores largely defines the magnitude and lag time of an event (Figure 2.2). However, the heterogeneity of basin topography, relief, micro-climate and hydraulic conductivity produces a differential response in the channel to precipitation inputs, both within a basin and between adjacent basins. A schematic representation of this hydrological system from TOPMODEL (Beven and Kirkby, 1979; Beven *et al.*, 1984) (Figure 2.2), shows how the product of flow inputs into a channel are an assemblage of flow components routed through interception, infiltration and saturated zone stores. In catchments where these controlling variables (climate, physiography and hydrology) remain constant over time, the flow characteristics in a reach define the flow *regime* of the reach. This regime varies throughout a catchment because of the spatially and temporally varied inputs into the channel network. Thus a river channel may be adjusted to a number of flow regimes along its length (Knighton, 1987).

Fluvial processes operate at a variety of scales within a catchment. At the micro-scale, flow - particle interaction causes shear between the two mediums which forms a turbulent boundary layer, whose magnitude is defined by the flow hydraulics (flow velocity and depth), boundary roughness and channel

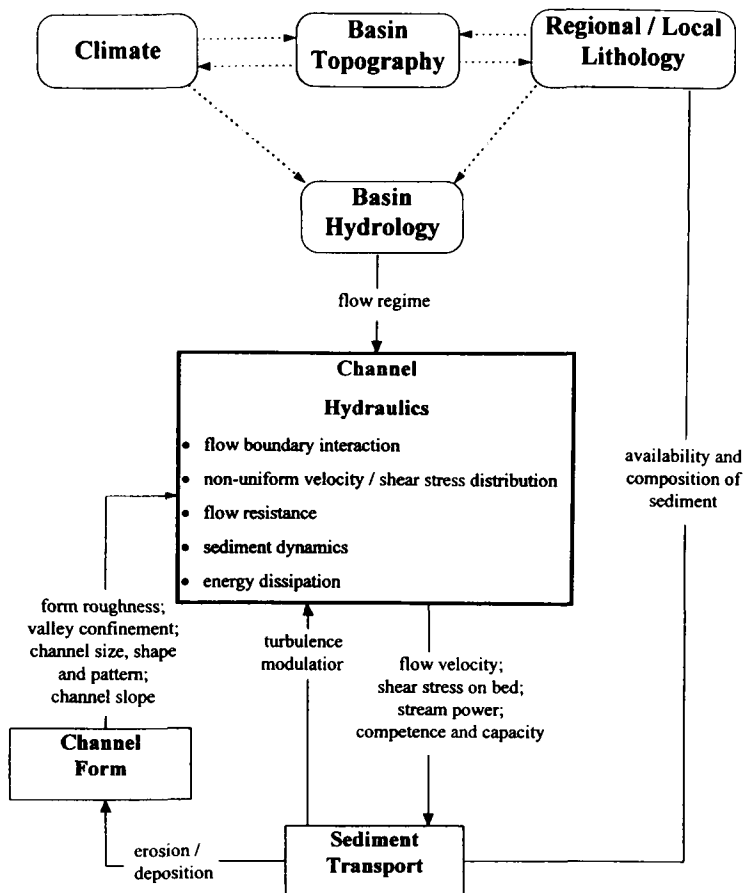


Figure 2.1 A simple representation of the inter-relationships between channel hydraulics, sediment transport and channel form in natural river systems (after Ashworth & Ferguson, 1986).

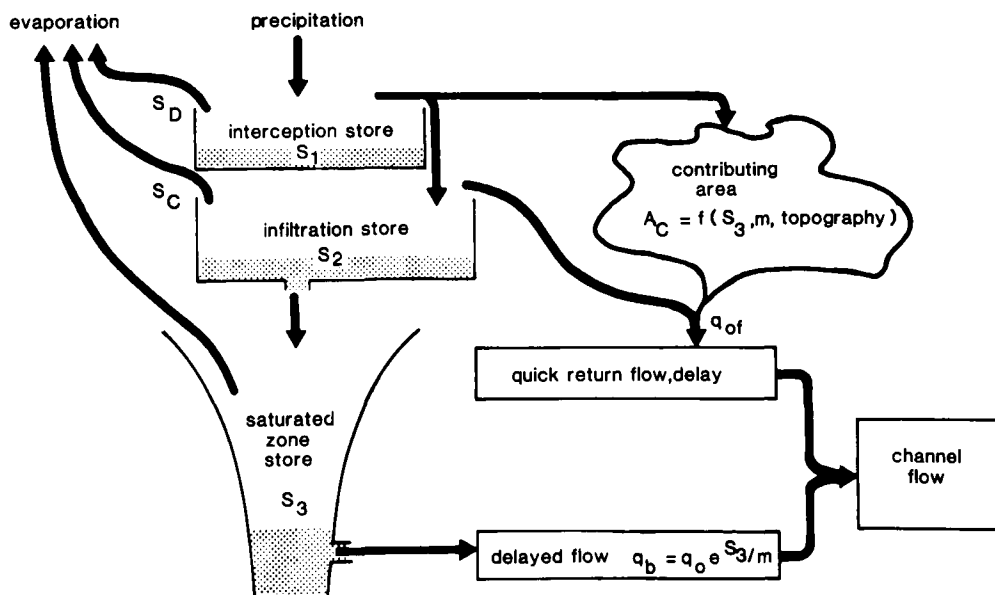


Figure 2.2 A schematic representation of TOPMODEL (from Beven *et al.*, 1984, p. 121)

form. Turbulence and shear generated in this region imposes a stress on the sediment boundary and encourages entrainment. At the meso-scale, river channel adjustment, at least in alluvial channels, is thought to create a form and pattern that will transport water and sediment efficiently through it (Leopold & Wolman, 1957). Non-uniform flow develops in channels in response to flow deflection around roughness elements, bars and meander bends, which creates secondary flow circulation and localised regions of high shear stress at the boundaries (Bathurst, 1977; 1979). At the macro scale, spatial adjustment in flow hydraulics due to variations in slope, discharge and boundary resistance alters the energy levels of flow at a reach scale and thus dictates river channel change at a meso and micro scale.

The mutual relationship between channel hydraulics, sediment transport (entrainment, movement and deposition), and channel form at all time and space scales in the fluvial system is thus evident. Figure 2.1 demonstrates how channel hydraulics have an integral role in defining the form of river channels and the processes operating within them. Flowing water in a channel will impart a shear stress on the boundary; if the stress is sufficient to entrain the particles present on the boundary then erosion will occur (Ashworth & Ferguson, 1989). The competence (the maximum grain size which can be entrained by the flow) and capacity of the flow (the volume of sediment a given flow can transport), defined by the stream power, will determine whether the sediment will be transported. This load in the water may dampen turbulent eddies in the flow and lead to a reduction in velocity and transport capacity. Erosion of the channel form will alter the size, and possibly shape and pattern of the channel; it may also change the roughness characteristics of the channel if, for example, fine particles are eroded to leave a coarse sublayer behind, or the channel pattern is altered. The resultant form of the channel will alter the distribution and magnitude of the velocity and boundary shear stress. It may also alter the hydraulic roughness, due to changes in the particle composition on the boundary or channel planform, or the stream power due to alterations in the slope or channel width. These feedback links are inherent within the system and determine the variability of the channel hydraulics over space and through time by altering the geometry of the channel, the slope, and the boundary roughness (Figure 2.1). At a local scale, channel geometry is substantially altered by meander bends, pool-riffles, bars and boulders, and along the channel by variations in bank cohesion and vegetation. At a catchment scale, the channel geometry is an assemblage of mutually inter-related reaches, dominated by the system controls indicated in Figure 2.1. Hence for this study it is necessary to interpret the form of a channel, and the processes operating within it, at a catchment-scale rather than at a reach-scale.

## **2.3 Channel hydraulics in gravel bed rivers**

### *2.3.1 Introduction*

The interface between flowing water and a deformable sediment boundary has been the focus of much research in recent years (eg: Hey *et al.*, 1982; Thorne *et al.*, 1987; Billi *et al.*, 1992). From studies of boundary layer theory, attention has concentrated on sediment mechanics, flow resistance and channel morphology, with considerable regard to the micro scale. Few studies have emphasised the transferability of such work to macro scale flow features at a reach and catchment scale. This section reviews channel hydraulics through the various scale domains by outlining the relationship these have with the river system.

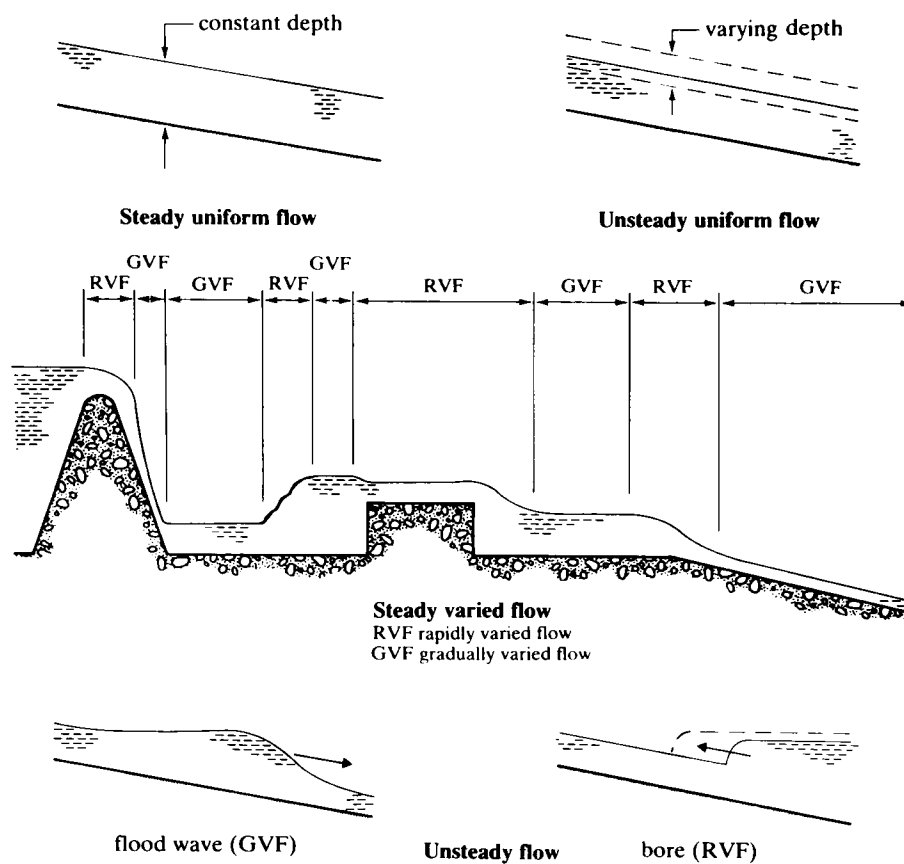


Figure 2.3 Types of open-channel flow (from Chadwick & Morfett, 1986, p. 119).

### 2.3.2 Principles of fluid flow

Natural open-channel flow is most commonly classified in terms of time and space (eg: Chow, 1959). If the flow, or discharge, is constant over time it is described as *uniform, or steady* (Figure 2.3); if, however, the flow varies over time, it is *non-uniform, or unsteady* (Figure 2.3). Flow is also classified according to whether the flow depth varies along the channel length: the flow is *uniform* if the depth remains constant (Figure 2.3); it is *rapidly varied* if the depth changes abruptly over a short channel length (eg: hydraulic jump) (Figure 2.3); and *gradually varied* if the change is less marked along the reach (eg: riffle) (Figure 2.3). For example, a flow is defined as steady-gradually varied if the depth varies with distance, but not with time. Most flow in natural channels is unsteady-gradually varied flow due to the time-varying discharge and irregular channel geometry (Chow, 1959). In some reaches, however, where the hydraulic depth is low or waterfalls and steps are present, the flow may be unsteady-rapidly varied.

The open-channel flow equations are principally based on the conservation of mass, momentum and energy within a reach. Chezy (1769, cited in Chow, 1959) used this simple scenario to equate the driving and resisting forces acting on a unit weight of water as it flows downstream [Equation 2.1]; this defines the average boundary shear stress acting along a channel reach, which is the tractive force of the flow acting on the boundary material.

$$\tau = \rho g R S_e \tag{2.1}$$

where,  $\tau$  = reach mean shear stress ( $\text{N m}^{-2}$ )  
 $\rho$  = water density ( $\text{kg m}^{-3}$ )  
 $g$  = acceleration due to gravity ( $\text{m s}^{-2}$ )  
 $R$  = hydraulic radius ( $\text{m}$ ) =  $A / p$   
 $s_e$  = energy slope (often substituted for the water surface slope,  $s$ , or channel slope,  $s_c$ ) ( $\text{m m}^{-1}$ )  
 $A$  = water prism area ( $\text{m}^2$ )  
 $p$  = wetted perimeter ( $\text{m}$ )

Water flowing downstream along a river channel conserves energy by converting potential energy into kinetic energy and heat. The available stream power is the time rate of energy expenditure, or the rate of doing work. It may be expressed as either:

- gross stream power,  $\Omega$  ( $\text{W m}^{-1}$ ), or the power per unit length of a defined channel (Rhoads, 1987) [Equation 2.2], or
- unit stream power,  $\omega$  ( $\text{W m}^{-2}$ ), or the power per unit wetted area of a defined reach (Rhoads, 1987) [Equation 2.3].

$$\Omega = \rho g Q s_e \quad [2.2]$$

$$\omega = \frac{\rho g Q s_e}{w} = \tau \bar{u} \quad [2.3]$$

where,  $\Omega$  = total stream power ( $\text{W m}^{-1}$ )  
 $\omega$  = unit stream power ( $\text{W m}^{-2}$ )  
 $w$  = water width ( $\text{m}$ )  
 $Q$  = discharge ( $\text{m}^3 \text{s}^{-1}$ )  
 $u$  = mean flow velocity ( $\text{m s}^{-1}$ )

A roughness coefficient was originally defined by Chezy (1768) to evaluate the mean velocity of a fluid with a given dimension and slope flowing through a pipe.

$$\bar{u} = \frac{C}{\sqrt{R s_e}} \quad [2.4]$$

where,  $C$  = Chezy coefficient of friction

This theory can be readily applied to natural channels (Chow, 1959). However, the coefficient is likely to change over time (Chow, 1959), within a reach (Ashworth *et al.*, 1992), or downstream (Leopold & Maddock, 1953; Bathurst, 1993). The factors causing this variability are associated with the relative smoothness of the bed, stage, vegetation, sediment transport, and variations in channel geometry and

alignment (Chow, 1959; Bray, 1982). An accurate evaluation of the coefficient is therefore difficult (Chow, 1959), although various empirical formulae (eg: Cowan, 1956; Limerinos, 1970; Hey, 1979; Jarrett, 1984) or example photographs (Barnes, 1967; Chow 1959) are available in the literature. In an assessment of the resistance equations, the Task Force on Friction Factors in Open Channels (1963) recommended the Darcy-Weisbach equation [2.5] because it is dimensionally correct and it is based on sound theoretical principles (Hey, 1979). However, the Manning's equation [2.6] has been widely adopted by engineers because it is simple, easy to use, and, most importantly, gives reasonably accurate results (Chow, 1959; Chadwick & Morfett, 1986). This study will consider both equations for determining mean velocity in an ungauged section.

Darcy-Weisbach Equation [2.5]

$$f = \frac{8gRs_e}{(\bar{u})^2}$$

Mannings Equation [2.6]

$$n = \frac{R^{0.67} s_e^{0.5}}{\bar{u}}$$

where,  $f$  = Darcy-Weisbach friction factor  
 $n$  = Manning's coefficient of roughness

These may also be used to calculate discharge, using a cross-section area - mean velocity product (continuity equation) (Equation 2.6).

$$Q = A\bar{u} = w\bar{d}\bar{u} \tag{2.7}$$

where,  $A$  = flow area (m<sup>2</sup>)  
 $\bar{d}$  = mean flow depth (m)

Although these 7 equations assume uniform conditions, they are commonly applied to reaches if local expansion or contraction of the channel is minimal, the channel geometry is regular and straight and the flow structure is neither converging or diverging (Ferguson & Ashworth, 1992). In such a reach, the water surface slope ( $s$ ) will closely approximate the energy gradient (Henderson, 1966; Prestegard, 1983), and the flow properties measured at a section ( $R$ ,  $w$ ,  $\bar{d}$ ,  $\bar{u}$  &  $Q$ ) are representative of the reach. The water may also be assumed to be clear, or sediment free, and therefore water density is constant. In natural channels, the rate of density change is small, although it is recognised that in highly sediment charged water it will alter significantly (Costa, 1988).

Flow in natural channels is predominantly *turbulent*; this implies that the water particles are moving in non-linear flow paths (ie: stochastic or coherent turbulent motion). The turbulent state is defined by the Reynolds number,  $Re$  [Equation 2.8], which is the ratio of viscous to inertial forces. Open channel flow is defined as turbulent if  $Re$  is large ( $\geq 2000$ ), ie: inertial forces greater than viscous forces. Flow

dominated by viscous forces (or *laminar* flow) is very uncommon in natural open-channels because it requires water particles to flow in smooth paths, or streamlines.

$$Re = \frac{\bar{u}R}{\nu} \quad [2.8]$$

where,     Re     = Reynolds number (dimensionless)  
           ν       = kinematic viscosity of water (m<sup>2</sup> s<sup>-1</sup>)

The Froude number, Fr [Equation 2.9], defines the effect of gravity on the inertial properties of flow. It is calculated from,

$$Fr = \frac{\bar{u}}{\sqrt{gd}} \quad [2.9]$$

where,     Fr     = Froude number (dimensionless)

If  $Fr < 1$ , the flow is subcritical and the wave celerity (velocity) is greater than the flow velocity, allowing water to travel upstream in the form of waves. If  $Fr > 1$ , the flow is supercritical, and the wave celerity is less than flow velocity, inhibiting waves from travelling upstream. The former is most likely to occur locally surrounding flow obstructions (boulders, weirs) or in extreme flow events in steep channels, whereas the latter predominates in most river channels.

### 2.3.3 Boundary layer theory and velocity profiles

The velocity of water flowing close to a channel boundary is reduced due to resistance at the interface between the two media (Petts & Foster, 1985). The degree of retardation is at a maximum adjacent to the boundary, where the flow velocity is reduced to zero. In reality the influence of the boundary extends to the surface (Bathurst, 1993), thus generating a *velocity profile* (Figure 2.4). However, the region where the shearing action is greatest (and the velocity gradient most pronounced) is commonly defined as the *boundary layer* (Chow, 1959). Since the boundary is not distinctive, its thickness,  $\delta$ , is ill-defined (see 3.5.8). Similarly, the elevation at which the flow velocity is zero (the Zero Plane Displacement (ZPD)) is difficult to ascertain in natural conditions, due to inter-granular flow through a composite gravel matrix (Jackson, 1981; Carling, 1992). Boundary shear stress, or the horizontal force exerted by the flow on the boundary, is thus defined by the velocity gradient in the boundary layer. This is derived from the 'von Karman - Prandtl law of the wall' (Schlichting, 1968):

$$\frac{u}{u_*} = \frac{1}{\kappa} \ln \left[ \frac{y}{k_s} \right] \quad [2.10]$$

and,

$$u^* = \sqrt{\frac{\tau}{\rho}}$$

[2.11]

- where,
- $u$  = velocity of flow in a vertical water column, height,  $y$  ( $\text{m s}^{-1}$ )
  - $u^*$  = shear velocity ( $\text{m s}^{-1}$ )
  - $\kappa$  = von Karman constant ( $\sim 0.4$  - see discussion in section 3.5.8)
  - $y$  = distance from the boundary (m)
  - $k_s$  = equivalent roughness of sand (m) (Nikuradse, 1933)

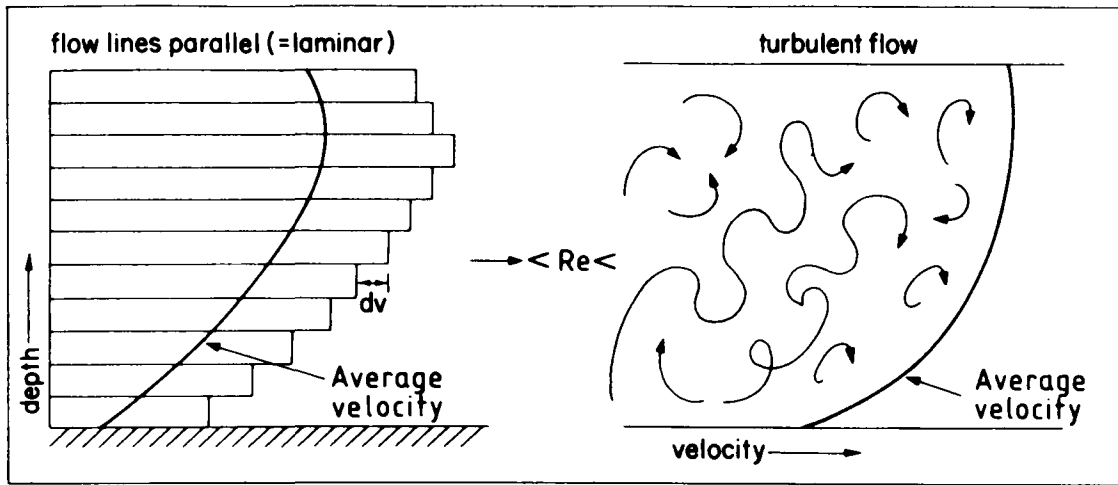


Figure 2.4 The vertical velocity profile in laminar and turbulent flow (from Petts & Foster, 1990, p. 97).

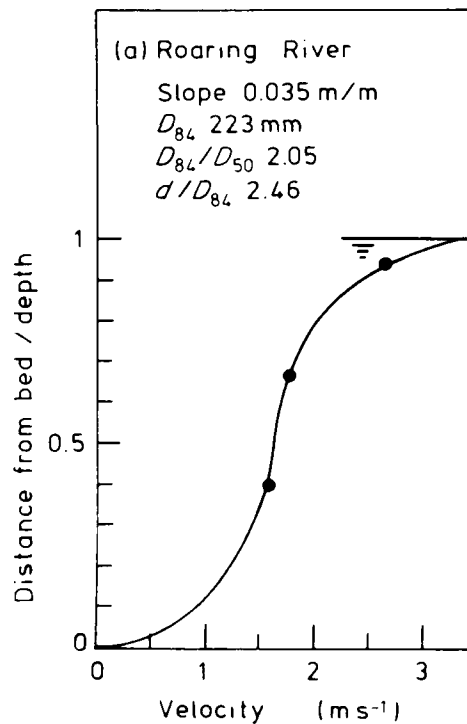


Figure 2.5 An S-shaped vertical velocity profile, characteristic of steep mountain rivers with coarse gravel / cobble beds (from Bathurst, 1993, p. 86).

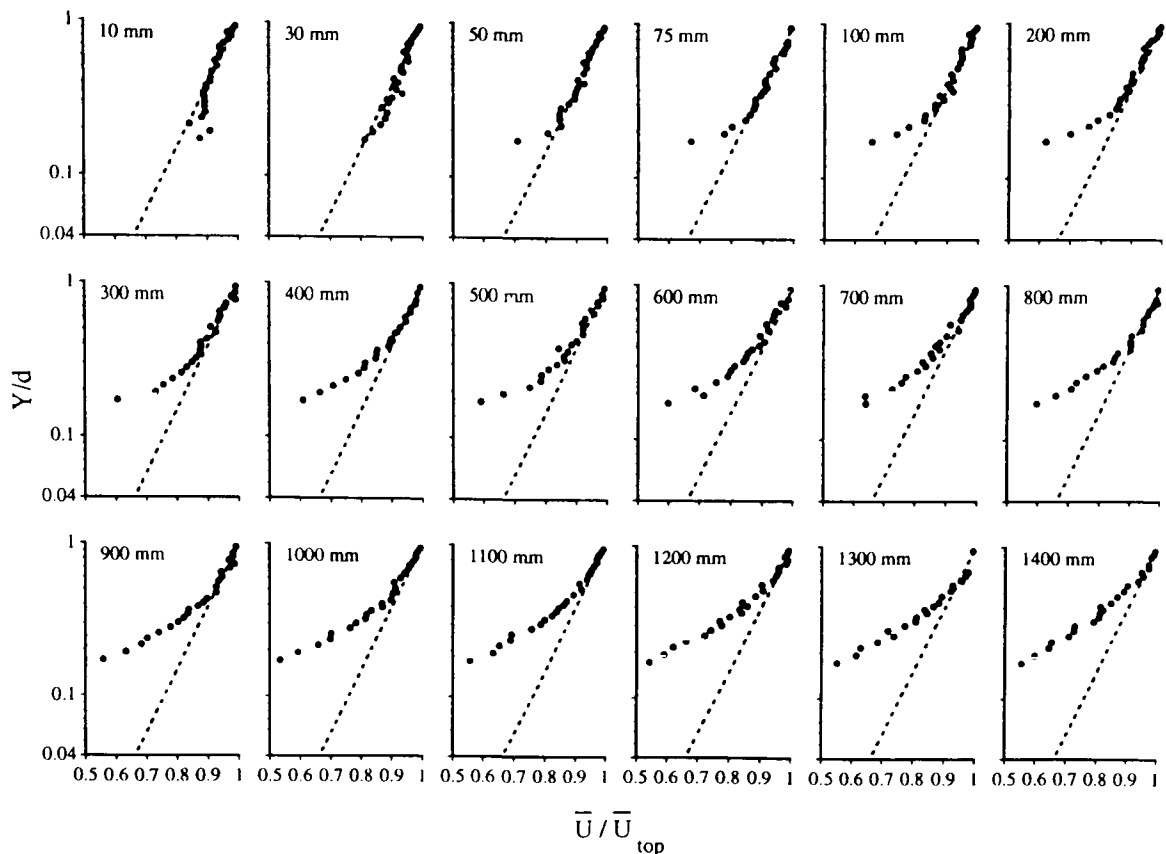


Figure 2.6 A series of velocity profiles downstream from a Smooth-Rough perturbation in the boundary roughness; a discontinuity occurs in the profile on account of flow deceleration close to the boundary. Each profile is measured from the left of the flume at varying distance steps. (from Livesey, 1996, p. 92).

The velocity profile is generated by a collection of roughness elements, from grains of various shapes and sizes, to obstacles, small-scale bed forms, and larger scale topographic forms (eg: riffles). Prandtl (1952) and von Karman (1934) demonstrated that within the boundary layer the majority of the flow (*inner* flow) can be described by logarithmic functions, whereas, in the *outer* flow this relationship does not hold due to secondary circulation and bedform defects, and boundary roughness effects (vortex shedding) (Bathurst, 1993).

Bathurst (1993) argued that the degree of divergence of the profile is dependent on the flow type (Nezu & Rodi, 1986), pressure gradient (Cebeci & Bradshaw, 1977), secondary circulation (Bathurst, 1982) and suspended sediment (Coleman, 1981; 1986), but independent of boundary conditions. However, in hydraulically rough channels, Jarrett (1990) and Bathurst (1993) observed that an S-shaped profile occurs on account of extreme drag by the coarse gravel bed material, with high velocity at the surface (Figure 2.5). Alternatively, where the free surface resistance is high, due to energy loss from wind friction or hydraulic jumps, the velocity at the surface may be reduced. Discontinuous / kinked velocity profiles are little understood, although an abrupt change in surface roughness upstream of the measurement position is the probable cause (Robert, 1990; Livesey, 1996) (Figure 2.6). Despite the obvious importance of velocity profiles for determining a) the control of the boundary over the flow structure, b) the shear stress exerted over the bed, and c) the related control over sediment entrainment, the scarcity of research into depth-limited flow velocity profiles (eg: Marchand *et al.*, 1984; Wiberg & Smith, 1987; Jarrett, 1990) in natural channels is surprising.

## 2.4 Spatial and temporal variation of channel hydraulic parameters

### 2.4.1 Introduction

The longitudinal and lateral variation of boundary roughness and channel geometry within a reach modifies the magnitude and distribution of point velocities, and thereby the resultant flow circulation pattern (Bathurst *et al.*, 1977; Bathurst, 1979; Bathurst *et al.*, 1979) (Figure 2.1). This results in localised scour and deposition of sediment due to the non-uniform distribution of boundary shear stress (Bathurst, 1979). Correspondingly, the water surface slope created by irregular flow circulation patterns modify the magnitude and temporal variation in stream power and reach mean shear stress. The force contained by the flow is therefore governed by factors other than volume alone (discharge). Recent research into channel change and sediment transport (Lewin, 1983, 1987; Graf, 1982; Reid & Frostick, 1986; Nanson & Croke, 1992; McEwen, 1994) suggests that stream power and shear stress are more representative than discharge and mean velocity in defining the effectiveness of a flow to modify the sediment boundary, and that the lithological form of a basin may have a significant effect on longstream fluvial processes (Magilligan, 1992). This section will therefore address these issues and review current theories regarding the distribution of these channel hydraulic parameters in fluvial systems.

### 2.4.2 Non-uniform flow structure

Flow in natural open channels is usually three-dimensional; this is typically characterised by the longstream, primary flow (dependent on discharge) and secondary flow (normal to the plane of the primary flow, and dependent on the cross section shape, pattern and boundary roughness). The resultant non-uniform flow distribution results in localised scour and deposition which is inter-related with the spatial variability in the topographical (Ippen & Drinker, 1962; Bathurst, 1979; Knight *et al.*, 1994) and sedimentological form (Knight, 1981; Ferguson *et al.*, 1989; Ashworth *et al.*, 1992) of the channel (Figure 2.1). Non-uniform flow is caused by the skewed vorticity of flow cells in a streamwise direction which form principally at the apex of meander bends (Thorne & Lewin, 1979; Hey & Thorne, 1975; 1984) (Figure 2.7). Secondary flow is not restricted to meandering channels where the skewed flow pattern induces circulation, but is also present in straight channels (Bhowmik, 1982). This is caused by natural perturbations of the flow over in-channel flow structures (eg: bedforms, pools-riffles or bars)). The feedback between the channel planform and flow structure exerts an important control in configuring the development of natural alluvial channels by the lateral and downstream variation in boundary shear stress and stream power distribution over time.

### 2.4.3 Flow resistance

‘The relative importance of the various sources of resistance varies through a river basin according to channel characteristics such as cross sectional shape, bed material size distribution and slope. Consequently the dominant resistance process also changes from one part of the channel network to another’ (Bathurst, 1993; p. 69) (Table 2.1). The representation of bed resistance (boundary resistance) thus requires both an adequate knowledge of the size distribution and an understanding of the relative impact of these features on the flow. Bed material sampling involves many difficulties (Hey & Thorne,

1984) caused by the variability in the size range and spatial distribution laterally and longitudinally in the channel. The size distribution of the bed is often characterised by a single grain size, from either  $D_{16}$ ,  $D_{50}$  or  $D_{84}$  (eg: Limerinos, 1970) (where  $D_n$  is the  $n^{\text{th}}$  percentile in a cumulative distribution of particle sizes). Although this cannot adequately explain the diversity in roughness, particle shape, orientation or protrusion, it can account for the resistance effects from the largest particles (Hey, 1979). The evaluation of flow resistance in boulder-bed channels considers only the effects of boulder spacing and relative submergence (Bathurst, 1993) because the disruption of the velocity profile by particle protrusion negates the use of conventional flow resistance equations (Wiberg & Smith, 1987). Thus, the factors influencing drag on individual boulders must be resolved and evaluated. This requires knowledge about the variation of the drag coefficient  $C_D$  due to energy losses from the free surface distortion and boulder shape, the accurate representation of the velocity profile, and an understanding of the resistance effects arising from boulder spacing and flow blockage in a cross section (Bathurst, 1993). The effect of bedform features, such as pebble clusters, transverse ribs and riffle-pool sequences, remains poorly understood. The hydraulic conditions responsible for the formation and boundary distribution of small-scale bedforms and riffle-pool sequences are well documented (Richards, 1976; Keller & Melhorn, 1978; Whittaker & Jaeggi, 1982). However, their effect on reach-scale channel roughness is still uncertain (Robert, 1990).

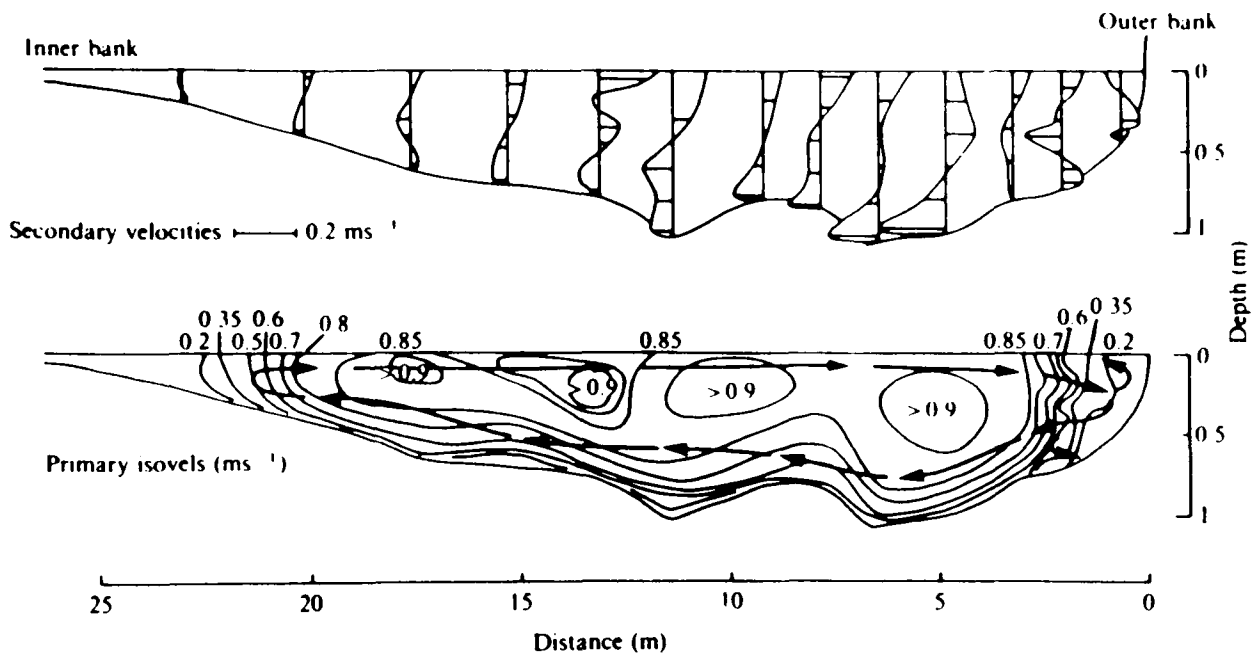


Figure 2.7 Primary and secondary flow velocities at a meander bend, Penstrowed, River Severn, Wales (from Hey & Thorne, 1984, p. 494).

Approximate range of

Type of channel	Channel slope (%)	Bed Material <sup>a</sup> D <sub>50</sub> (mm)	Darcy-Weisbach <i>f</i>	Manning <i>n</i>
Sand-bed	< 0.1	< 2	0.01 - 0.25	0.01 - 0.04
Gravel/cobble-bed	0.05 - 0.5	10 - 100	0.01 - 1.00	0.02 - 0.07
Boulder-bed	0.5 - 5	> 100	0.05 - 5	0.03 - 0.2
Step pool/fall	> 5	variable	0.1 - 100	0.1 - 5

<sup>a</sup>D<sub>50</sub> = bed material particle size for which 50 % of the material is finer

Table 2.1 Variation of flow resistance coefficients for different channel types (from Bathurst, 1993, p. 75).

Other factors affecting the roughness of the channel boundary include vegetation, channel size and shape, and discharge. The hydraulic effect of aquatic weed growth is to increase boundary roughness and channel capacity and retard the flow velocity; together these increase stage by enhancing the drag properties of the bank structure and dissipating the energy of the flow close to the channel boundary (Chow, 1959; Charlton *et al.*, 1978; Ferguson, 1981). Studies examining the relative stiffness (Kouwen & Li, 1980), density (Petryck & Bosmajian, 1975), and exposed area of aquatic vegetation (Petryck & Bosmajian, 1975) have as yet been concentrated in grass-lined and flume channels. However, the work by Powell (1978), Dawson (1978) and Watson (1987) has demonstrated the important inter-relationship between vegetation and roughness (Manning's *n*). These have demonstrated how the resistance imposed by the vegetation varies with stage, according to the density and flexural rigidity of the vegetation stand. This results in a marked variation in vegetation roughness at an event timescale, as the vegetation becomes prone under increasing discharge and mean velocities. Conversely, seasonal variations in growth impact upon the hydraulic conditions in a channel by decreasing discharge and mean velocity and increasing stage during summer months (Dawson, 1978). Temporal variations in discharge alter the relative (or hydraulic) roughness of the bed; this either 'drowns out' small scale roughness elements and decreases the significance of friction induced by the boundary, or intensifies secondary flow circulation and increases boundary roughness (Bridge & Jarvis, 1982). Similarly, variation in channel alignment induces form drag in response to the interaction between the primary and secondary flow circulation cells and the channel boundary (Bray, 1982).

#### 2.4.4 Mean velocity

Mean velocity is commonly perceived to decrease downstream, owing to the longstream reduction in slope and bed material size, and an increase in mean depth. This was shown to be false in the studies by Leopold and Maddock (1953) and Leopold and Wolman (1957). The former study examined

downstream and at-a-station trends in channel hydraulic parameters, using flow data from a range of US rivers basins; this revealed how mean velocity increased slightly downstream at a constant flow frequency. However, a re-examination of individual river reaches in the same dataset by Mackin (1963) indicated that the general downstream trend proposed by Leopold and Maddock (1953) actually included a series of downstream increases and decreases, suggesting that the composite nature of the analysis concealed the true longitudinal pattern. It was further argued that the downstream rate of change of mean velocity would vary under different flow frequencies, and that discharge was not an ideal parameter for studying downstream trends.

Carlston (1969) addressed these shortcomings using Rhodamine BA dye-injection methods to record the longstream variation of mean velocity along the Mississippi under two flow conditions and the Susquehanna and Potomac Rivers under a single flow condition. This showed that the magnitude of mean velocity varied greatly along a river and was equally likely to increase as decrease downstream. It was therefore concluded that over long reaches of river, mean velocity is nearly constant as the reduction in slope is compensated for by an increase in depth, and thus lower channel roughnesses.

The controls on the basin-scale distribution of mean velocity remain unclear despite these attempts to derive general downstream trends. Nevertheless, reach scale analyses of channel hydraulics (eg: Beven *et al.*, 1979; Beven & Carling, 1992) have highlighted the significance of instream roughness elements, such as riffles, boulders and vegetation, on longstream and temporal variations in mean velocities. Indeed, an analysis of mean velocity through two reaches along the River Severn (at Montford and Leighton, near Buildwas) by Beven and Carling (1992) showed how large coherent flow structures reduce flow velocities through a reach by enhanced flow resistance in comparison with velocities measured at a cross section. This raises several methodological issues concerning the measurement of mean velocity in a single cross section and the assumption of uniform flow conditions which will be discussed in Chapter 3.

#### 2.4.5 Discharge - a channel-forming variable?

The various theories developed to explain the diversity of channel geometries have principally used discharge as the controlling variable (Richards, 1977). One such theory is 'hydraulic geometry' (Leopold & Maddock, 1953) which defined functional relationships between discharge and channel width, depth, mean velocity and slope, both at-a-point and downstream. The trends take the form of power law functions:

$$\text{width, } w = aQ^b \quad [2.12]$$

$$\text{depth, } \bar{d} = cQ^f \quad [2.13]$$

$$\text{mean velocity, } \bar{u} = kQ^m \quad [2.14]$$

$$\text{slope, } s = gQ^z \quad [2.15]$$

From the continuity equation [Equation 2.7],  $b + f + m = 1$  and a.c.k = 1. The downstream values for the exponents, b, f & m demonstrated the 'uniformity of river cross-sections, planforms, and profiles, across a wide range of climatic, lithological, and (to a lesser extent) energy environments' (Thornes, 1977, p.

91), although these results were not for individual channel units but a collection of data from a variety of river channels of differing sizes (Park, 1977). Despite considerable success in providing a coherent framework for the applied fluvial scientist and insight into the controlling conditions in a given environment, the theory could not be relied upon for predictions beyond the range of conditions, nor for a cause-effect understanding of the system dynamics (Thornes, 1977; Ferguson, 1986). Various studies have adopted bankfull discharge (the discharge at a bankfull level in a cross section) as the control variable to define a critical measure of discharge. However, the confusion surrounding the definition of a 'dominant' discharge has led to a multiplicity of approaches. Richards (1977) summarises the particular difficulties in using a bankfull discharge with the following points: the definition of its return period is problematic (Wolman & Leopold, 1957); bankfull flow duration may increase downstream due to flood-peak attenuation, and channels may thus adjust to flows of a greater return period downstream (Harvey, 1969); and the definition of a bankfull channel geometry is uncertain in the field (Williams, 1978).

Discharge alone cannot explain the work done by the flow, or the 'geomorphic effectiveness' of the flow, in moving material and modifying the channel form. Large floods sometimes trigger extensive erosional activity in a channel, whereas at other times the erosional activity may be negligible. Indeed, Lawler (1992b) notes how a moderate flow (stage = 1.15 m) occurring on 20 October 1990 caused bank retreat of 11 mm, whilst 4 mm of bank deposition resulted from a larger event (stage = 2.30 m) on 8 February 1990. The magnitude of a channel-forming event must therefore be viewed relative to thresholds of the fluvial system (Schumm, 1973) and not in absolute terms (eg: Wolman & Miller 1960). The stream power (and shear stress) theory provides a suitable expression for the destabilizing force of a flow (Bull, 1979; Baker & Costa, 1987), which Graf (1982) has shown to be important in defining the uneven movement and storage of sediment in the system. In addition, large rates of channel migration have been attributed to high levels of stream power and shear stress in the Severn basin (Lewin, 1982; 1983; 1987), the River Coe in the Western Grampians (McEwen, 1994), and the Henry Mountains, Utah (Graf, 1982; 1983a).

#### *2.4.6 The significance of slope in channel hydraulics*

The slope of the water surface profile is controlled by physiography (Bray, 1982), bed material, the Froude number and discharge. At bankfull stages, the water surface slope closely approximates the energy gradient; at other stages, large variations in depth through a reach may account for differences of between 10 - 30 % (Prestegard, 1983). Prestegard (1983) has demonstrated that the theories of Sternberg (1875; cited in Hack, 1957) and Gilbert (1914), relating bed material to downstream decreases in gradient, are significant. She also emphasised that bed particle size influenced the local slope at a reach scale, as well as downstream along a channel. For most short, uniform reaches, however, the water surface slope provides a good estimate of the energy gradient (Prestegard, 1983). Nevertheless, because it is difficult to measure accurately, other variants of slope have been used (eg: channel slope (Carling, 1983), measured along the lowest bed elevation along a reach, or the valley slope (McEwen, 1994), measured along the bank top or estimated from detailed contoured maps). The water surface slope is therefore a significant variable for explaining spatial variation in stream power, reach mean shear stress and the roughness equations (eg: Manning's) because unsteady flow will significantly alter the water surface slope, reflecting for example, the temporal variation in fluid energy between the rising and

falling limb of a hydrograph. The principles behind reach- and catchment-scale variations in slope and the correct use of the water surface slope may therefore help in our understanding of downstream trends in stream power and shear stress.

#### *2.4.7 Reach mean shear stress and stream power*

The magnitude and space-time variability of stream power and shear stress in the fluvial system largely determine the potential of the channel to change, or migrate laterally (Graf, 1983a). This relationship was first identified by Gilbert (1880) who maintained that over time a channel would adjust its form to accommodate the energy of the flow. Subsequent studies have extended this idea to the graded stream (Mackin, 1948), extremal hypotheses (Langbein, 1964; Yang and Stall, 1973; Chang, 1979; Bettess and White, 1987), and regime theory, which all sought to link a stable channel morphology with the available energy in the flow, and sediment transport (Bagnold, 1960, 1966; Yang, 1972; Yang and Molinas, 1982). In an analysis of channel stability in Danish streams, Brookes (1988) identified a relationship between channel activity, planform and unit stream power. He discovered a marked difference between reaches which regained their sinuosity after straightening ( $> 100 \text{ W m}^{-2}$ ), reaches with bed or bank instability ( $> 35 \text{ W m}^{-2}$ ) and stable natural channels or straightened channels ( $< 35 \text{ W m}^{-2}$ ) (Figure 2.8). Similarly, Begin (1981) found that relative shear stress values ( $\tau/\tau_{\text{avg}}$ ) were greater in braided channels than meandering and straight channels.

Exactly how stream power and shear stress vary downstream and their link with channel activity remains unclear, although, it has been reported that stream power decreases downstream (Knighton, 1984; Richards, 1982). However, studies by Graf (1982, 1983a, 1983b), Lewin (1982, 1983, 1987), Lawler (1992a, 1995), Magilligan (1992), and Lecce (1993) indicated that this may not be the general case. The research by Lewin in the upper and middle Severn basin revealed high rates of floodplain reworking in the upper-middle reaches of the Severn, or the piedmont gap (Newson, 1981), between Llanidloes and Newtown (Figure 2.9) which was attributed to high rates of fluvial energy. Nevertheless, only a weak relationship was found between the historical rates of channel change and stream power. Brown (1987) used some of these data to compare floodplain sedimentation rates with stream power in the Severn basin. He concluded that decreasing stream power downstream was responsible for the increased channel stability in the lower Severn, which was attributable to the downstream reduction of slope. These findings are closely linked to the critical stream power theory proposed by Bull (1979). According to this 'a critical power threshold separates the modes of erosion and deposition and is dependent on the relative magnitudes of power needed to transport the average sediment load and on the stream power available to transport the load' (p.455). At the critical power threshold the channel is sensitive to change, and the process of lateral erosion dominates.

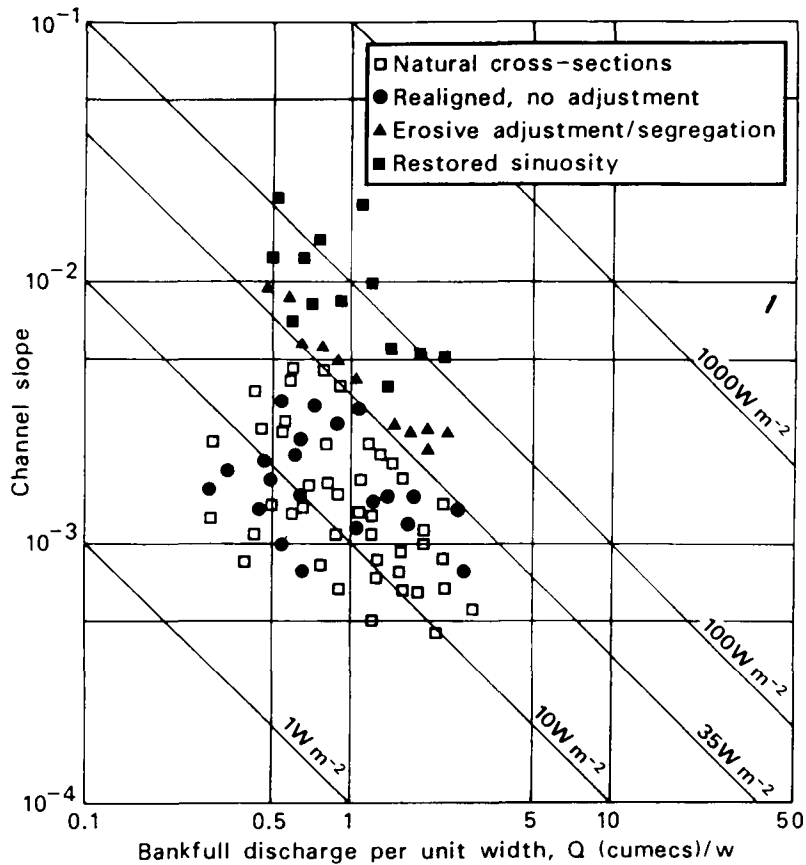


Figure 2.8 Channel stability of Danish streams defined by unit stream power (from Brookes, 1988, p. 98).

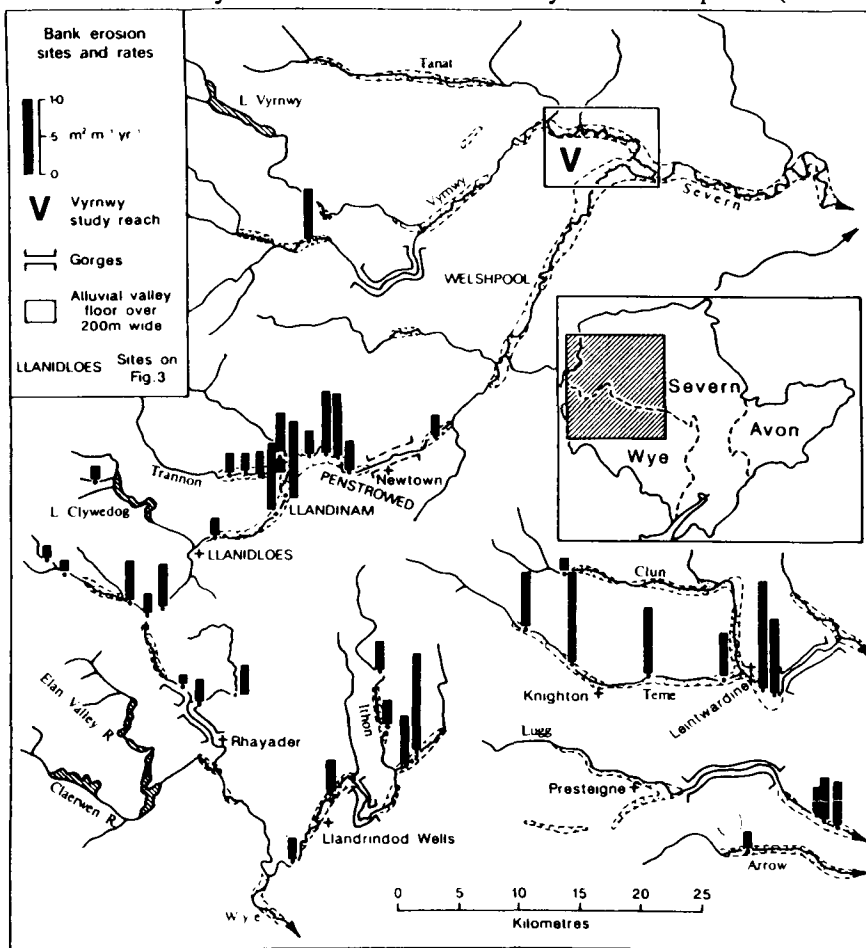


Figure 2.9 The distribution of historical channel change rates in the Upper Severn and Wye catchments (from Lewin, 1987, p. 167).

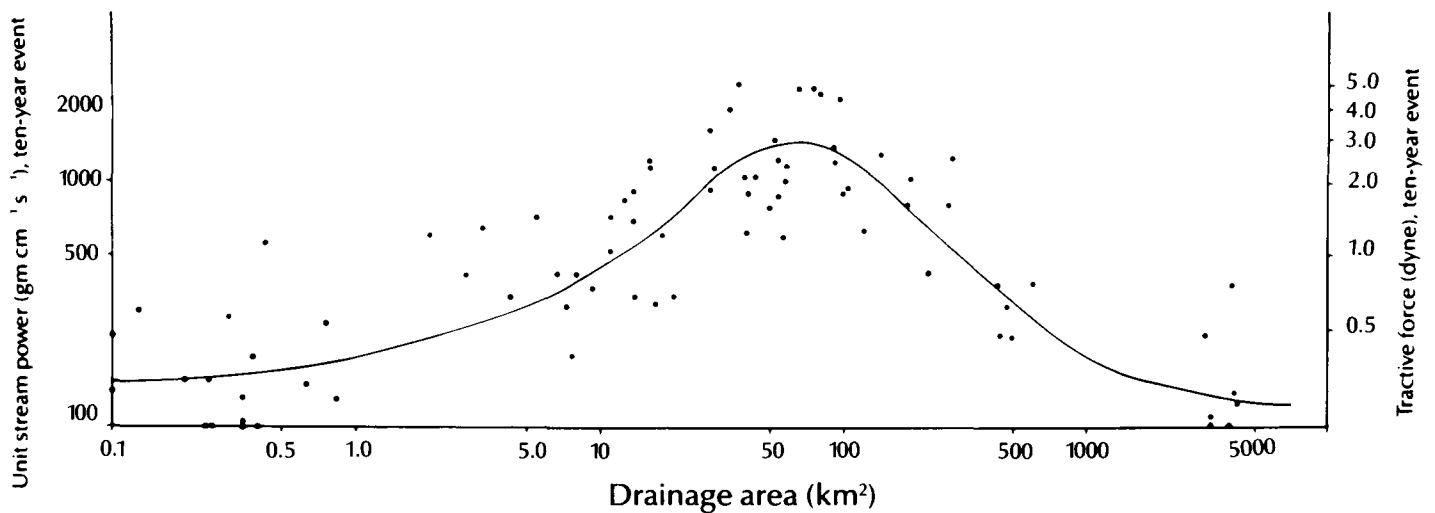


Figure 2.10 The spatial distribution of reach mean shear stress (tractive force) and unit stream power in the Henry Mountains, Utah (from Graf, 1982, p. 209). Note the different units ( $1 \text{ N m}^{-2} = 10 \text{ dyne cm}^{-1}$ ).

These results are consistent with the earlier findings of Graf (1982, 1983a) in which a zone of peak stream power and tractive force in the Walnut Gulch basin (Figure 2.10) corresponded to reaches having the largest channel width and highest rates of channel removal: indeed it is stated that, ‘...those reaches with sharply declining tractive force and total power are likely deposition sites, while those with sharp increases are likely erosion sites’ (Graf, 1983a; p.650). He also outlined the temporal control of channel form over hydraulic, and hence erosional processes, in an analysis of the long term evolution of arroyo systems in the Henry Mountains (Graf, 1983b). For this, he concluded that fluvial processes control the channel morphology only during catastrophic events, whereas the channel form controls the fluvial processes during the intervening period (Figure 2.11). The lithological control of the basin was also evident in the study by Magilligan (1992) of the Galena basin; his 1-D simulation of flow along the upper 500 km<sup>2</sup> of the basin demonstrated how resistant lithologies generated steep, confined reaches of high bed shear stresses, whilst the opposite occurred through less resistant lithologies. Lecce (1993) also discovered a stream power peak close to the source (basin area = 10 - 100 km<sup>2</sup>) in four tributaries of the Blue River, Wisconsin. The steep channel slopes in the mid-basin, generated by resistant lithologies, were believed to similarly control this distribution and be responsible for the spatial variation in channel shape and sediment storage. A similar study of the theoretical stream power peak by Lawler (1992a, 1995) applied simple numerical experiments using various functions of downstream change in discharge, slope and width. These illustrated both the possibility for a fluvial energy peak in river basins, as proposed by Graf (1982, 1983a, 1983b), Lewin (1983, 1987), and also the significance of channel and

valley morphology on the magnitude and spatial distribution of the stream power function (Magilligan, 1992).

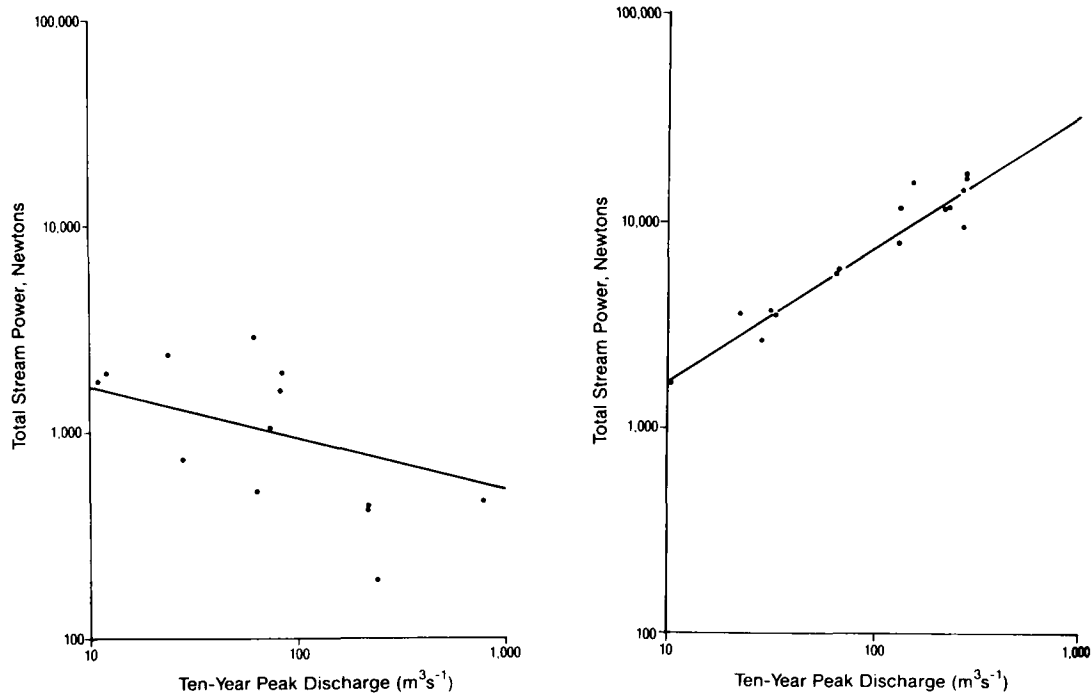


Figure 2.11 The relationship between ten-year peak discharges and total stream power for, a) 1883 (pre-erosion period), and b) 1909 (post erosion period) (from Graf, 1983a, p. 382).

#### 2.4.8 Estimation of boundary shear stress and its space-time variability

In natural river channels, uniform flow conditions can rarely be assumed. Thus, the estimation of a reach mean shear stress is difficult, and sufficient care must be taken to identify near-uniform flow conditions (section 3.2). Boundary shear stress, predicted from local velocity profiles, provides a more accurate, though laborious, measure. Accurate near-wall velocity measurement in turbulent flow over a coarse gravel bed are extremely difficult due to the problem of representing the 3-D velocity field instantaneously across the boundary layer. Rough approximations may be derived from rapid 2-D and 3-D devices (ECM) (Bathurst *et al.*, 1977; 1979) or slow 1-D impeller devices (Bridge & Jarvis, 1977; 1982; Beven & Carling, 1992; Ferguson & Ashworth, 1992), although the degree of uncertainty is high. This problem is often overcome by assuming a deeper boundary layer (50 %) and taking velocity measurements within this hypothetical region (Ferguson & Ashworth, 1992), or assuming that the entire profile is logarithmic. However, Kuhnle (1992) argues that if suspended sediment is present in the water

column, the velocity profile will not be logarithmic away from the boundary layer because the turbulence characteristics of the flow are altered. Coleman (1981) observed a reduction in near bed velocities and an increase in the outer flow velocities (Figure 2.12); this, he concluded, was caused by suspended sediment in the flow changing the wake function of the velocity-defect law:

$$\frac{u - U_s}{u^*} = \frac{2.303}{\kappa} \log \left[ \frac{y}{z} \right] + W \quad [2.16]$$

where,  $U_s$  = freestream velocity ( $m\ s^{-1}$ )  
 $z$  = boundary layer thickness (m)  
 $W$  = wake function

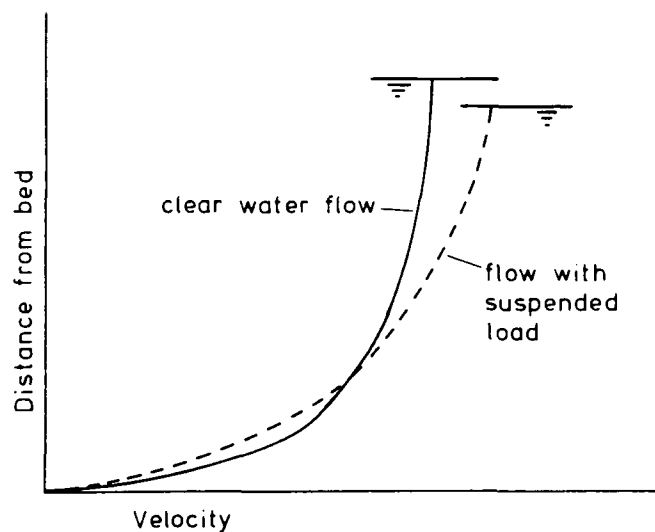


Figure 2.12 The influence of sediment load on the shape of the vertical velocity profile (from Bathurst, 1993, p. 78).

The prediction of boundary shear stress around the wetted perimeter of a channel is extremely problematical due to the irregularity of natural gravel beds and the difficulty of measuring flow in the boundary layer. Flume experiments by Knight *et al.* (1994) using both a simple and compound trapezoidal channel with varying aspect ratios demonstrated that the lateral distribution of shear stress is sensitive to the shape of the cross section (Figure 2.13). In this, no attempt was made to represent non-uniform channel geometries. However, field experiments by Bathurst (1977; 1979) on the River Severn at Caersws showed that secondary circulation, particularly in meander bends, significantly affects the distribution and magnitude of boundary shear stress by enhancing the skew-induced circulation relative

to the primary flow (Figure 2.7); this is maximised at a medium flow, whilst the primary flow component dominates at high discharges (Bathurst, 1979). The distribution of boundary shear stress has also been found to be affected by channel planform (Ippen & Drinker, 1962; Hooke, 1974; Bathurst, 1979; Begin, 1981); boundary roughness (Knight, 1981; Zippe & Graf, 1983; Kirkzog, 1989; Feuro & Baiamonte, 1994); sediment concentration (Vanoni, 1946; Vanoni & Nomicos, 1959; Wang, 1981); and discharge (Bathurst *et al.*, 1979).

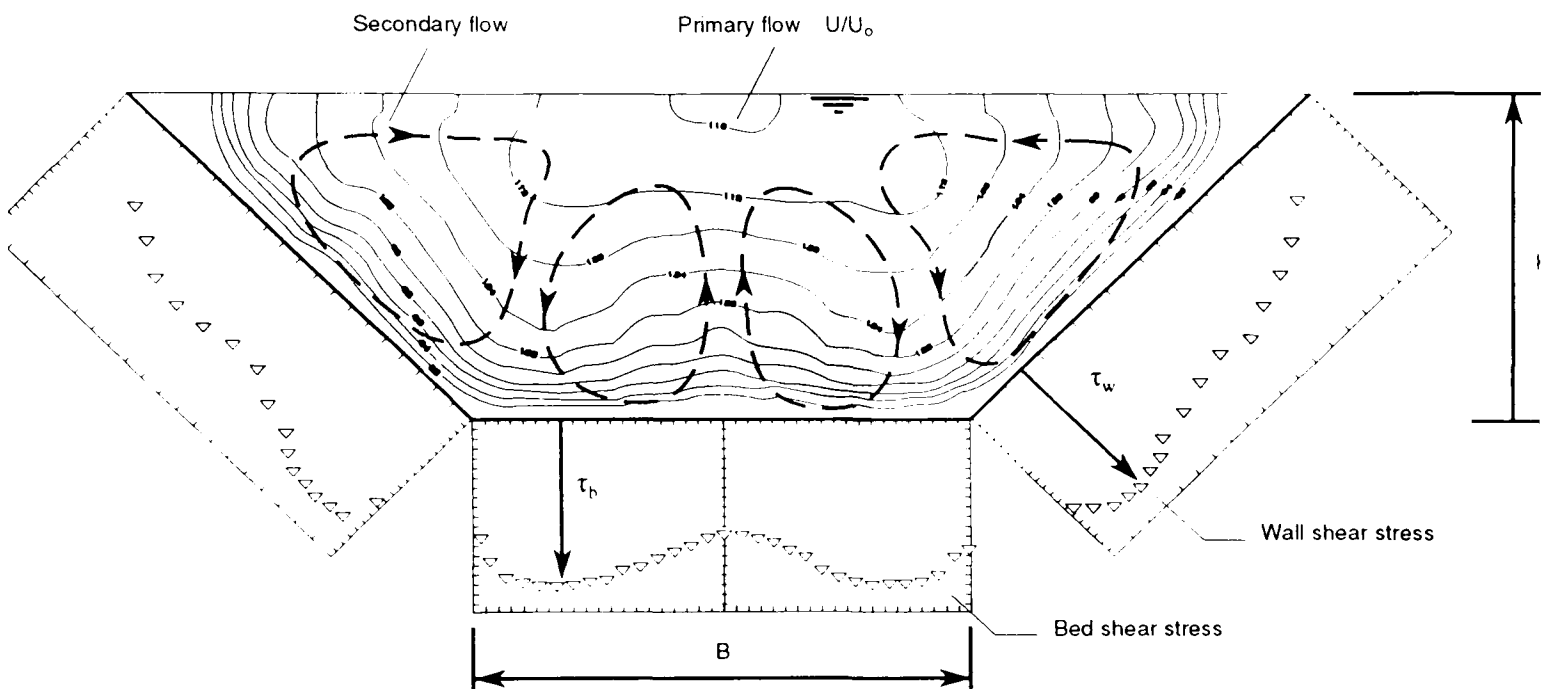


Figure 2.13 The boundary shear stress distribution across a simple trapezoidal channel ( $Fr = 3.24$ , Aspect Ratio =  $B / H = 1.52$ ), showing primary flow isovels and secondary flow cells (from Knight *et al.*, 1994, p. 53).

The magnitude of boundary shear stress varies widely across the channel in response to secondary flow circulation cells generated by irregular channel geometries, edge effects and interaction with dead-zones (Knight *et al.*, 1994). Figure 2.13 demonstrates that boundary shear stress peaks may occur at the base of the bank - bed intersection and in the channel centre, depending upon the aspect ratio of a trapezoidal channel. It also varies over time, as evidenced by bedload transport studies which show greater shear stresses on the rising limb of a flood wave (Reid *et al.*, 1985). The spatial variation of shear stress is also manifest in a longstream direction (Graf, 1982) (Figure 2.10), particularly as a result of downstream changes in channel and water surface slope, and the hydraulic roughness of the flow (dependent on the discharge, water depth and bed roughness) (Bathurst, 1993).

## 2.5 Control of channel hydraulics over sediment transport processes

### 2.5.1 Introduction

The hydraulic conditions responsible for the entrainment and removal of sediment vary through the fluvial system according to the spatial and temporal distribution of boundary shear stress and stream power. The measurement of sediment transport is beyond the scope of this study, but a review of the dominant processes will provide further insight into the relationship between channel hydraulics and channel morphology, particularly in the studies of channel form, channel stability, bed-material transport and palaeohydraulic reconstructions.

### 2.5.2 Initiation of sediment transport

The hydraulic conditions at the threshold of particle motion may be evaluated by equating the forces tending to entrain a particle with the forces tending to keep the particle at rest. The critical dimensionless shear stress parameter,  $\tau^*_{ci}$ , developed by Shields (1936) in a flume with uniform bed material, has been used to define a critical shear stress level for the onset of motion [Equation 2.17] (eg: Meyer-Peter & Muller, 1948).

$$\tau^*_{ci} = \frac{\tau_i}{(\gamma_s - \gamma_f)d_i} \quad (\text{after Andrews, 1983}) \quad [2.17]$$

where,  $\tau^*_{ci}$  = critical dimensionless shear stress of the  $i^{\text{th}}$  percentile fraction of the surface bed material

$\tau_i$  = shear stress acting on a particle ( $\text{N m}^{-2}$ )

$\gamma_s$  = specific gravity of sediment ( $\text{N m}^{-3}$ )

$\gamma_f$  = specific gravity of water ( $\text{N m}^{-3}$ )

In natural gravel bed rivers, however, the uncertainty in the hydraulic conditions, and non-uniform size and distribution of particles has led to considerable refinements to the theory of particle entrainment (eg: Parker *et al.*, 1982; Andrews, 1983; Komar, 1987; Ashworth & Ferguson, 1989). In particular, the variation in grain size and packing may cause the size-selective entrainment theory to fail (eg: equal mobility (Andrews, 1983)); this has clear implications for many other studies which rely on the related argument of flow competence.

The simple empirical relationships developed between grain size and flow (eg: Gilbert, 1914; Hjulstrom, 1935; Shields, 1936) assume that the maximum size removed from the bed, or flow *competence*, is a measure of the flow strength. Thus, by relating the largest grain size collected (eg: in a Helley-Smith sampler (Helley & Smith, 1971) or bedload trap) to the shear stress or stream power (or velocity) for a given flow, a functional relationship may be derived (Meigh, 1987). The shear stress at incipient motion can therefore be estimated for a range of grain sizes (Andrews, 1983; Carling, 1983), or the magnitude of flow may be estimated for a given grain size moved (eg: palaeohydraulic reconstructions (Costa, 1983)).

This ignores the effects of relative protrusion / hiding of a particle above / below the bed surface (Fenton & Abbott, 1977), or particle shape, orientation and packing (Li & Komar, 1986; Komar, 1987); in addition, turbulent flow over a hydraulically rough boundary causes non-linear chaotic irregularity in the near bed velocity field, creating instantaneous velocities sufficient to entrain a particle at below-threshold levels (Culling, 1988). The theory of 'size-selective' entrainment (Ashworth & Ferguson, 1989) may therefore be limited to local bed conditions (Richards, 1990), while 'equal mobility' (all the surface bed material is entrained within a narrow range of shear stress due to the combined effects of hiding and protrusion) (Parker *et al.*, 1982; Andrews, 1983) has relevance where the gravel bed layer is heavily armoured.

Flow intensity in sediment transport studies is often represented by boundary shear stress estimated from the Duboys equation (Baker & Ritter, 1975; Carling, 1983; Komar, 1987) due to the difficulty of measuring point values of boundary shear stress repeatably in the field during unsteady flow conditions (Dietrich & Whiting, 1989). Field observations have shown that the temporal variation in shear stress at the onset of motion is significant. Reid *et al.* (1985) demonstrated that bed shear stress at initial motion was around three times greater than when bedload ceased, which they attributed to particle interlocking and hiding. However, Robert (1990) used the same dataset from Turkey Brook to show that a reduction in form drag at the onset of motion caused shear stress to actually decrease and particles on the bed to be more easily entrained. Similarly, Carling (1983) showed that threshold bed shear stress values were greater in narrow channels ( $w/d < 11$ ) compared with wide channels ( $w/d > 11$ ). He concluded that this was caused by the changing efficiency of entrainment with increasing discharge as various bank roughness components become submerged. Clearly, the impact of flow resistance at various scales plays a critical role in defining the onset of motion, and reach mean shear stress has some validity in entrainment studies.

### 2.5.3 Mechanics of sediment transport

The load carried by a natural stream may be divided into three components: *dissolved load* (fine material transported in solution); *wash / suspended load* (particles  $< 0.064$  mm and transported readily by suspension); and *bed-material load* (particles  $> 0.064$  mm and transported close to the bed) (Knighton, 1984). This section will focus on bed-material and suspended load because it is appreciated that transport of these components are significant for the understanding of lateral channel adjustment, contaminant transport, effluent disposal, reservoir siltation and aquatic habitats.

Sediment transport requires the flow intensity (eg: shear stress or stream power) to exceed a given critical threshold. The threshold level is difficult to predict due to the complex nature of a) the characteristics of bed material and its structural arrangement, and b) the flow circulation pattern, for the reasons explained in sections 2.4.2 & 2.4.3. Thus, 'the spatially and temporally variable stresses exerted on the bed combine with the availability of sediment, whether in the bed or supplied from local bank erosion or upstream, to determine the rates of transport of different sizes of bedload at different places and times. Since this transport is non-uniform and unsteady, erosion and deposition alter the initial channel geometry, and selective entrainment or deposition may alter the texture of the bed' (Ferguson & Ashworth (1992, p. 478). Conversely, sediment load modulates the turbulence intensity of the flow and thereby encourages further dissipation of energy (Figure 2.1). This dynamic relationship between the flow, transported sediment and channel form in gravel bed rivers has made the predictive equations developed theoretically and in flumes

(Meyer-Peter & Muller, 1948; Bagnold, 1960; 1966) difficult to apply in the natural gravel-bed environment. Given this limitation, field measurement techniques must be employed to gather information about the dominant processes controlling sediment transport.

The transport capacity of a given flow may be explained in terms of the stream power concept (Bagnold, 1966). The subsequent analysis of sediment transport in flume experiments (Yang, 1972) and in natural rivers (Reid *et al.*, 1985; Meigh, 1987) have demonstrated that stream power, calculated from gross channel characteristics, is a strong predictive variable. Indeed, Meigh (1987) showed that the cross-sectional mean bedload transport rate at Caers on the River Severn was strongly related to point boundary shear stress and stream power, but not reach mean shear stress. However, as with studies using boundary shear stress, the magnitude of the most recent preceding event and longitudinal variations in sediment availability will also affect the inter-relationship between flow and sediment transport (Gomez, 1983; Reid *et al.*, 1985). In the former, bedload transport rates on the recessional limb of a flood were 10 times greater than during the rising limb, and this was ascribed to the armour layer delaying initial entrainment. In the latter study, transport rates were high during the rising limb in response to the occurrence of a sequence floods which loosened the bed material, and therefore decreased the resistance to entrainment.

#### 2.5.4 Downstream variability in sediment transport

The downstream variation in sediment transport is controlled largely by sediment availability and channel hydraulics. Walling and Quine (1993) developed a sediment budget of the channel, using Caesium-134 radionuclides, to define the downstream variation in sediment storage and loss along the River Severn. They used two parameters of Caesium-134: *activity* ( $\text{mBq g}^{-1}$ ) refers to the level of Caesium-134 found in fine sediment deposits; *inventory* ( $\text{Bqm}^{-2}$ ) refers to product of the activity and the volume of sediment storage. It was found that conveyance losses on the floodplain and channel accounted for up to 23 % and 2 % of the total suspended load, respectively. They also evaluated conveyance losses between reaches (Figure 2.14). This showed that in steep upland reaches the high entrainment thresholds of coarse gravel bed material prevent entrainment until a moderately high magnitude event occurred (Figure 2.14). Further downstream, sediment entrainment of finer material deposits was dependent on local hydraulic conditions (Ashworth & Ferguson, 1989). Despite lower shear stress and stream power magnitudes in the piedmont zone and the middle reaches, the combination of non-uniform flow circulation and irregular boundary composition resulted in spatially and temporally variable boundary shear stresses, often in excess of local sediment boundary thresholds. As sediment transport is limited by the ability of the flow to carry a given load, the transport capacity of a flow at a reach- and catchment-scale was controlled by the spatial and temporal distribution of stream power, or shear stress. This manifest itself as a series of sediment storage and transport zones along the river channel intimately related to the downstream distribution of channel hydraulics (Figure 2.14) (eg: Graf, 1982, Figure 2.10).

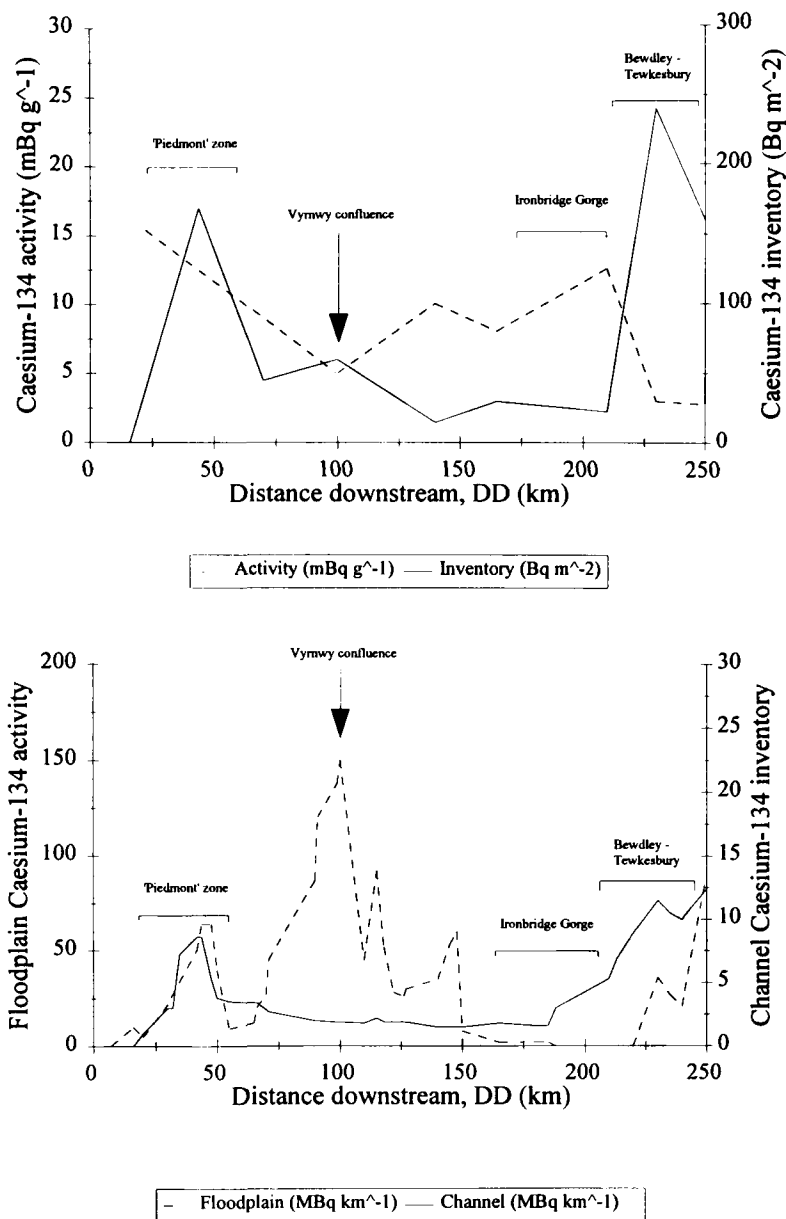


Figure 2.14 The downstream variation of Caesium-134 along the River Sever, defined as: activity (the level of Caesium-134 found in fine sediment deposits); and inventory (the product of the activity and the volume of sediment storage) (from Walling & Quine, 1993).

## 2.6 The interaction between channel hydraulics, sediment transport and river channel form

### 2.6.1 Introduction

The natural adjustment of alluvial channels to the flow and sediment regime creates a channel whose form will efficiently transport water and sediment through it. The mode of adjustment is controlled, in part, by the distribution of flow through the channel (and hence the magnitude and distribution of shear stress), and also the localised erosion and deposition of sediment at the boundary (see Figure 2.1). At a given point in time and space, the geometry (cross sectional form) has commonly been described in terms of the hydraulic controls (discharge, shear stress, stream power) (see section 2.5.1). The nature of the channel form (section 2.5.2) and the reasons for change (section 2.5.3) may be evaluated through the analysis of the variability of channel hydraulic parameters.

2.6.2 Spatial and temporal variability in channel form and flow processes

The river channel form is the cross-sectional shape and planform pattern between the active limits of the channel and floodplain. The form can be described in terms of its size (width, depth, area), shape (width: depth ratio, hydraulic radius); or the planform (eg: sinuosity). The three-dimensional channel form includes the longitudinal profile, defined by the channel and valley slope.

In his review of downstream channel adjustment, Knighton (1987) described the principle modes of downstream adjustment of channel and flow variables (Figure 2.15). Channel width and depth are shown to increase downstream largely due to the systematic increase in discharge and an increase in bank cohesion. However, width has been shown to be sensitive to abrupt changes in discharge at tributary confluences (Richards, 1980), channel slope (Ferguson, 1981), and both width and depth are found to be dependent on local lithologic conditions (Magilligan, 1992), bank material (Schumm, 1960; Ferguson, 1973) and bank vegetation (Charlton *et al.*, 1978; Murgatroyd & Ternan, 1983). The rate of change of slope decreases downstream, although the dominant controlling variable is disputed. The significance of bed material size (ie: bed resistance) has been emphasised in studies by Knighton (1975), Charlton *et al.* (1978), Leopold & Bull (1979), and Prestegard (1983), although the inherited valley fill gradient will impose an independent control over longer time-scales (Richards, 1977; Knighton, 1987). Pickup & Reiger (1979) note that the river channel is the result of all antecedent events, which Yu & Wolman (1987) describe as a ‘truncated memory’ because the existing channel geometry will exist until the discharge exceeds the entrainment threshold of the boundary material.

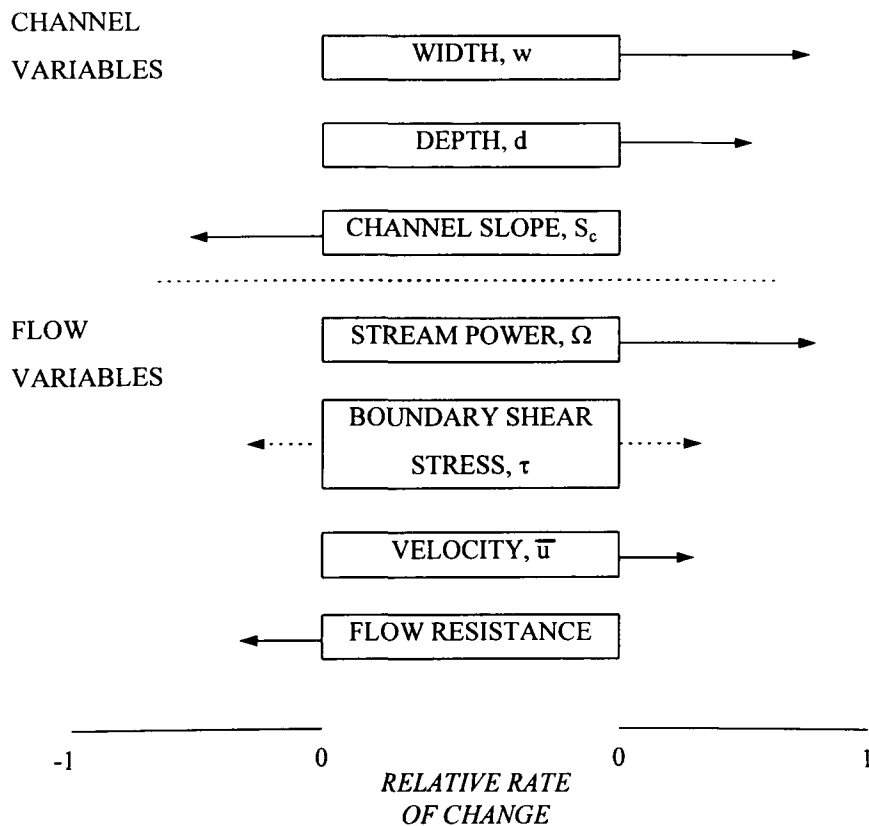


Figure 2.15 A schematic diagram showing the downstream change of channel hydraulic parameters (from Knighton, 1987, p. 96).

The propagation (or movement) of floodwaves through basins is also modified by downstream variations of the channel slope, topography and roughness. Up to a bankfull stage, mean velocity reaches a maximum as roughness elements are drowned out and the capacity of the channel is maximised (Bhowmik & Demissie, 1982) (Figure 2.16). After bankfull stage, inundation of the floodplain results in a reduction of the mean velocity caused by enhanced surface roughness and temporary flow storage. The interaction between unsteady flow and channel topography is described by Woltemade and Porter (1994). They show that attenuation of the flood peak, caused by floodplain storage, reduces the peak discharge and hence the mean velocities, depending upon the channel size and shape. Therefore, changes in the degree of confinement along the channel, modify the dynamics of the floodwave, although the degree of this control is unknown (Magilligan, 1992; Woltemade & Porter, 1994). This interaction between floodwaves and channel topography is discussed in greater detail in Chapter 7.

Knighton (1987) also suggested that total stream power will increase downstream (and unit stream power remain constant) due to the relationship with hydraulic geometry variables (see also Magiligan (1992)) (Figure 2.15). However, as noted in (section 2.4.7) it is still uncertain as to how these variables are spatially distributed. The downstream distribution of both boundary shear stress and velocity is uncertain due to the great variability which exists at a reach level and between river systems (Figure 2.15). Furthermore, flow resistance tends to decrease downstream in response to a reduction in bed material size (Brierley & Hickin, 1985; Bathurst, 1993), channel slope (Bathurst, 1993), and a general widening of channels (Carling, 1983). This general uncertainty in the downstream variability of flow variables indicates the lack of evidence existing in the literature.

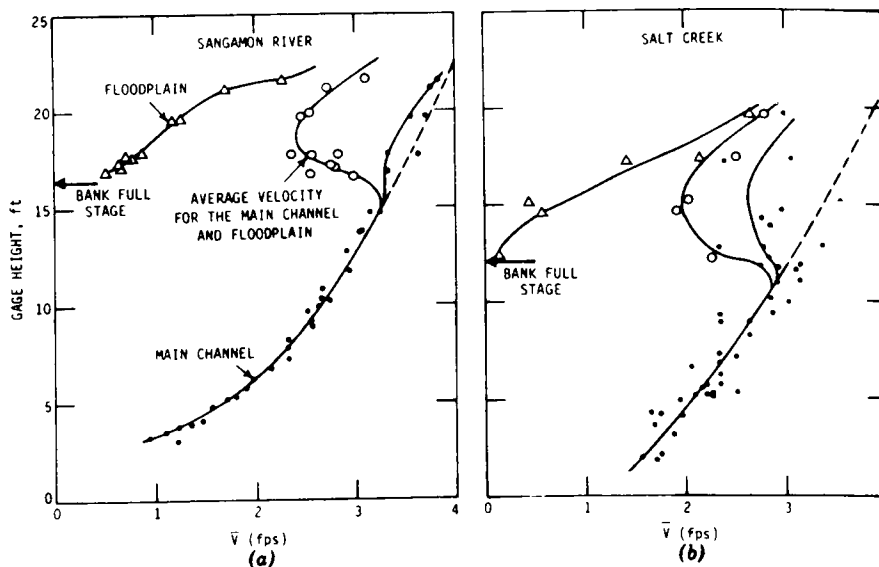


Figure 2.16 The variation of mean velocity in the main channel, floodplain and composite cross section with stage at: a) Sangamon River; and b) Salt Creek (from Bhowmik & Demissie, 1982, p. 450).

### 2.6.3 Channel stability

'Alluvial channels with erodible boundaries flow in self-formed channels which, when subject to relatively uniform governing conditions, are expected to show consistency of form, or average geometry adjusted to transmit the imposed water and sediment discharges. The problem is to determine the nature of the adjustment process and establish relationships which link control and response variables' (Knighton, 1987, p. 103). The unsteadiness and non-uniformity of natural rivers introduces a complex mode of behaviour which undermines the determinacy, or predictability, of the fluvial system (Allen, 1977; Ferguson, 1986). The variability of channel width and depth over time, determined by the pattern of discharge change, has led to the development of theories of regime, tractive force, minimum variance and other extremal hypotheses. These have sought to understand the spatial and temporal variability of channel form, which have themselves led to the development of theories defining the patterns carved by natural channels (Leopold & Wolman, 1957; Schumm, 1970, 1977; Schumm & Khan, 1972).

'Regime' theory was successfully devised to design a stable combination of width, depth and slope which allowed sediment transport (tractive force theory does not) but ensured that the transport capacity equalled the input sediment transport rate over a long time; this problem was solved using three equations: continuity, resistance and sediment transport (Lane, 1955). In recent years, it has been recognised that channels also adjust their planform in response to the natural flow regime (Yang, 1987). A suite of extremal hypotheses have subsequently been developed to provide a determinate solution to the problem. It is possible to distinguish between these hypotheses based upon their tendency to adopt either a statistical approach (eg: minimum variance, MV (Langbein, 1964; Williams, 1978)) or a physical approach (eg: minimum stream power, MSP (Chang, 1979), minimum unit stream power, MUSP (Yang, 1971a, b & c; 1972; 1973; Yang & Stall, 1973; 1976; Yang & Molinas, 1982), minimum energy dissipation rate, MEDR (Yang & Song, 1979; Brebner & Wilson, 1967), maximum sediment transport rate, MSTR (Kirkby, 1977), maximum friction factor, MFF (Davies & Sutherland, 1983), and maximum shear stress, MSS (Davies, 1987)).

The applicability of these hypotheses to natural channels is limited. Despite considerable promise, Davy & Davies (1979) noted that the entropy concept may only be used in laminar flow, and Hey (1978) points out that more variables are required to provide a determinate solution. Subsequently, Davies and Sutherland (1983; 1984) observed that all the physical approaches reduce to the latter two (MFF & MSS) in long term channel adjustment; during short term adjustment, discharge and slope are independent, therefore total stream power ( $=f(Qs)$ ) cannot be minimised because Q and s are fixed. They justifiably argued that 'because the shape achieved by a river's boundaries is formed by boundary material movement, which is in turn dictated by boundary shear stress, it is logical to seek an explanation for the shape of equilibrium channels in terms of boundary shear stress' (Davies & Sutherland, 1984, p. 742, comment). However, the future potential of this theory lies in the further exploration of dynamic fluvial systems, and in the consideration of 'energy transfer relations' in river channels (Davy & Davies, 1979, p. 105). Indeed, the distribution of species assemblages (or communities) along a river longitudinal profile has been linked to the energy and thermal gradients which exist in fluvial systems. This subject will be reviewed in Chapter 7, where the River Continuum Concept (Vannote *et al.*, 1980) and the Serial Discontinuity Concept (Ward & Stanford, 1983; 1995) will be discussed with reference to the results from this study.

#### 2.6.4 River channel adjustment

'The study of river channel changes...is no less than the study of equilibrium channel behaviour and the nature of excursions from those equilibrium conditions' (Hickin, 1983, p. 61). The reason for the excursion from equilibrium and the mode of channel adjustment are of interest to the fluvial geomorphologist and engineer. Explanations for these may be divided into natural and anthropogenic causes:

- Natural causes

An important factor controlling transient channel adjustment is the temporal variation of discharge. Extreme events (high magnitude - low frequency events) may cause significant departure from the equilibrium form such that the conditions may persist for long periods of time: this has been called a 'memory effect' (Stevens *et al.*, 1975; Wolman & Gerson, 1978; Hickin, 1983; Gupta, 1983). Subsequent smaller flows (ie: bankfull discharge) may reconstruct the floodplain (eg: Schumm & Lichty, 1963; Burkham, 1970) provided the alluvium material deposited by the high-magnitude event is not too coarse (Gupta, 1983). The geomorphic effect of such 'catastrophic' events is reviewed by Kochel (1988), drawing examples from US flood events. He concludes that the response is extremely difficult to predict because 'the interdependency of variables in fluvial systems causes flood response to vary among rivers in different climates' (Kochel, 1988, p. 183). In contrast, Wolman & Miller (1960) suggest that events of modest magnitude and relatively high frequency perform the most work by rivers on the landscape. The tendency to attach geomorphic significance to a 'dominant' (or bankfull) discharge, occurring every 1-2 years, is evident in the approaches taken by Leopold & Maddock (1953), Williams (1983) and Lewin (1982, 1983, 1987), for example. The overall *effectiveness* of a given flow must therefore be defined in terms of its ability to reshape the landscape and on the time period for the landscape to recover (Wolman & Gerson, 1978). Attention must thereby focus on the hydraulic controls, as (Baker & Costa, 1987, p. 1) declare, 'the geomorphic effectiveness of floods seems to be linked directly, not to their magnitude (discharge) or frequency (recurrence interval), but to the shear stress and stream power per unit boundary area relative to the resistance of the channel to erosion'

- Anthropogenic causes

The literature is full of examples of human-induced channel adjustment. The principle causes include flow regulation, channel stabilisation and urbanisation. The modification of the flow regime, through river impoundment or water abstraction, results in a reduction in peak discharge and an alteration of seasonal variability. The effect on the channel is to reduce its capacity by sedimentation (Park, 1975; Petts, 1984) or cause extensive scouring by altering the local hydraulic forces in the channel (ie: downstream from a reservoir). Channelisation measures to alleviate bank instability directly modify the natural channel cross section and planform and thereby have a direct influence on the hydraulics, sediment transport and ecological habitat in the reach. Urbanisation manifests itself through a modification of natural drainage. Flood events are greater and flashier due to rapid drainage from impermeable surfaces, and sediment supply is enhanced due to active construction. The effect on river

channel processes was monitored by Leopold (1973) over a 20 year period on Watts Branch, Maryland. He concluded that the most significant effect of urbanisation was on the enhanced frequency of overbank events.

## 2.7 Summary

This review of channel hydraulics has attempted to demonstrate both the complexity of the fluvial system and also the benefits of an improved understanding of channel hydraulics. It has been necessarily broad due to the need to provide an adequate background for this study and to highlight how channel hydraulics are important in a variety of fluvial processes.

The chapter has highlighted the limited understanding of hydraulic processes along an entire channel. Previous attempts to address this research gap have either measured or simulated hydraulic variables at a low spatial resolution (Magilligan, 1992; Lecce, 1993), or compared spatial trends using data from several river basins (Leopold & Maddock, 1953). Furthermore, spatial analyses of channel form (Graf, 1982, 1983a), bank erosion (Lewin, 1983, 1987; Lawler, 1992a, 1995) or sediment transport (Walling & Quine, 1993) have used these hydraulic results to evaluate mechanisms without a thorough knowledge of the detailed variation of channel hydraulic parameters at a catchment-scale, or the controls acting upon this distribution. This study therefore has the potential to combine the results from a downstream study with knowledge of micro- and reach- scale processes, to determine the variation of channel hydraulics at a catchment scale, and possibly evaluate the interaction with lateral channel adjustment and sediment transport processes.

## **CHAPTER 3 RESEARCH DESIGN**

### **3.1 Introduction**

The last chapter presented the overall background to this study of flow hydraulics, and described the reasons why hydraulics should be examined at a catchment scale. This chapter will describe in detail how such a strategy may be accomplished. The aims of this chapter are to describe the principles behind selecting the River Severn and the study sites, and to explain the field measurement of channel hydraulics; the methodology for simulating channel hydraulics is presented in Chapter 5. Firstly, it will discuss the criteria for selecting an appropriate river to study, the number and position of study sites along it and also the rationale for identifying a suitable cross section. The river and study sites selected will then be described. This is followed by a description of the flow measurement procedures, including how the surveying and current metering techniques were performed, how the various hydraulic variables were calculated and how errors may be incurred during the fieldwork measurement.

### **3.2 Sampling strategy and rationale**

#### *3.2.1 Introduction*

This study demands a strategy which ensures accurate measurement of all appropriate variables. It must be sufficiently robust to represent the large spatial variation along the Severn channel, and the temporal range of flows up to bankfull. This must be achieved with due consideration to fieldwork safety, equipment availability, logistical and financial support. The variety of techniques adopted for the fieldwork reflect these needs and demonstrate the flexibility of the designed approach.

#### *3.2.2 River selection*

The selection of a suitable study river demanded a consideration of the following factors:

- it should possess a flow regime and channel dimensions which enable the hydraulics to be measured safely and with minimal support;
- gauging stations must be available along the river to provide discharge information for fieldwork data, flow frequency, model calibration and verification;
- it should be close to Birmingham to ensure rapid, inexpensive river reconnaissance;
- artificial influences (eg: channelization) should be limited; in addition, pollution should be minimal for safety considerations;
- availability of previous published research on the river could be advantageous for the comparison of results and validation of model simulations.

### 3.2.3 Study site selection

The size, number and spacing of the study sites must achieve a balance between an adequate spatial coverage of the basin and a feasible, two year project. The size, or length, of each reach may be estimated by a variety of methods, including: a) geomorphologic units (eg: pools and riffles) (Keller & Melhorn, 1978; Richards, 1982; Clifford & Richards, 1992); b) geometrical distances (eg: a logarithmic scale) (Bathurst *et al.*, 1979; Graf, 1982); c) equal change in elevation or distance; or d) specific geomorphic interest (eg: cut-offs (Lewis & Lewin, 1980)). Methods (a), (b), and (d) are more commonly used because they are relatively easy to estimate in the field, and are based on sound geomorphic principles. However, with a prior knowledge of the valley slope, each reach length may be determined by allowing for a fall in elevation, for example of at least 0.01 m along the reach (c). Hence a combination of methods (a) and (c) were adopted to provide a consistent sampling framework across a wide spatial dimension.

The **number** of study sites must be sufficient to embrace the range of fluvial environments present on the river, but not place unrealistic demands on time and resources (human and financial). The **spacing** between each reach must be sufficient to define significant changes in the flow and morphological structure of the river. In natural river conditions the supposed mode of change in a downstream direction is commonly observed as a gradual modification of the channel planform, although tributaries and lithological controls may delineate clearly defined thresholds (Yatsu, 1955; Richards, 1980). However, as the hydraulic geometry theory demonstrated (Leopold & Maddock, 1953), channel width and depth increase logarithmically downstream in response to increasing discharge. Clearly, any systematic sampling of the river channel should therefore adopt a sample spacing of logarithmic (or allometric (Graf, 1982)) proportions, thus improving the spatial coverage and representation of the study site location.

### 3.2.4 Cross section selection

The choice of cross section location within the reach must first identify whether a section is representative of the reach, and second, whether the section will produce accurate flow measurements. This selection must consider the criteria described in Table 3.1, based on studies by Gregory and Walling (1973), Herschy (1978), Richards (1990a), Shaw (1988), Ferguson and Ashworth (1991), and McEwen (1994).

### 3.2.5 Flow measurement strategy

The flow measurement techniques must be appropriate for a diverse range of environments, and if several techniques are adopted, they must provide a compatible data-set. The 'range' of flows must also be considered. As flow measurement is difficult beyond bankfull, a suitable upper flow limit may be defined by the bankfull level; the summer residual flow in a channel also provides a convenient lower limit. However, stage is not a good indicator of the relative magnitude of a given flow because of irregularities in channel size and shape along a channel; rather, the return period or flow frequency

Table 3.1 Selection criteria for study site location.

Site selection criteria	Explanation
the reach should be straight, with an unbroken water surface	energy slope estimations and shear stress calculations require steady, uniform conditions with no expansion or contraction of the channel cross section along the reach
the cross section should be approximately uniform (trapezoidal or rectangular) with a level bed and clear bank surfaces	any irregularities in the cross section will decrease the accuracy of the channel geometry estimation, and therefore the discharge. A clearly defined bank surface is also helpful when estimating stage, and for slope-area approximations.
in-channel and bank vegetation should be minimal	vegetation will seasonally alter the roughness characteristics of the reach through flow drag (Watson, 1987). It will also interfere with flow velocity measurements by impeding the rotation of impeller current meters.
there should be a clearly definable bankfull limit at the study section	this improves the accuracy of predicting the bankfull level (for slope-area approximations (Lewin, 1983)) and prevents flow expansion at high flow levels.
the cross section should be representative of the reach and located centrally	measurements taken from the one section location can then be used to estimate reach averages. By locating it centrally in the reach, the water surface slope may be averaged by levelling upstream and downstream of the cross section.
the limits of the study reach should be clearly visible from the study section	this prevents relocation of the surveying equipment during surveying (Lawler, 1993).
the reach should be 5 - 10 channel widths long	this has been characterised as one geomorphic unit (Richards, 1982) and is commonly the distance separating a riffle-pool unit (Keller & Melhorn, 1978).
the reach should be a sensible distance from any control structure and there should be no influx of water from tributaries and / or outflow pipes	These may create acceleration or backwater effects, for example from the legs or supports of bridges. They may also potentially disrupt the flow structure of the reach and certainly alter the discharge distribution along it.

### 3.3 Study area

#### 3.3.1 The River Severn

The river chosen for this study is the River Severn (Figure 3.1). The Severn flows from the Plynlimon massif in central Wales, through the Shropshire plain and the Ironbridge gorge, and south through the cities of Worcester and Gloucester (Figure 3.1). The furthest part of the catchment lies within 100 km of Birmingham, and therefore provides an excellent location for frequent and rapid flow monitoring. In addition, it has been extensively studied in the past (Table 3.2). The flows of the Severn are also currently monitored: in the headwaters (Plynlimon), the Institute of Hydrology have an experimental catchment which monitors the effect of afforestation on the basin hydrology (Figure 3.1); further downstream, the EA have gauging stations on all major tributaries and on the main trunk of the river (Figure 3.1): these vary in their monitoring complexity from simple stage-discharge relationships to continuous ultra-sonic measurement (NRA Hydrological Yearbook 1992) (Table 3.3). This study will concentrate on the upper 250 km of the river, from the source in Plynlimon to the approximate tidal limit at Saxon's Lode, Tewkesbury (Figure 3.1).

#### 3.3.2 Climate

The Severn originates in the upland region of Central Wales at an altitude of 740 m. The climate is temperate humid, dominated by frontal rain from the SE in the form of intense depressional storms and sequences of storms (Howe *et al.*, 1967). The mean annual precipitation close to the source is high (2300 mm measured between 1968 - 1975 (A.J. Newson, 1976), although this decreases rapidly with decreasing altitude to approximately 400 mm in the estuarine region of the Bristol channel (Lawler, 1987). The majority of rainfall in Plynlimon is accounted for by westerly and cyclonic days which provided up to 85 % of the rainfall in the Plynlimon catchment between September 1973 - September 1975 (A. J. Newson, 1976). This is predominantly frontal rain from the west, accentuated by orographic influences; these rainfall events often provide significant volumes of rainfall in very short periods (M. D. Newson, 1976). To the east, the orographic effect diminishes, producing a decrease in the seasonality of precipitation and a threefold reduction in the magnitude of rainfall events (Lawler, 1987). The mean annual temperature of the catchment is 9.3 °C, although the temperature tends to decrease with increasing altitude at a lapse rate of 7.0 K km<sup>-1</sup>, 6.0 K km<sup>-1</sup> and 5.0 K km<sup>-1</sup> for maximum, mean and minimum temperature respectively (Meteorological Office, 1975, cited in Lawler, 1987).

#### 3.3.3 Hydrology

The Severn is a dynamic river whose instability in the upper reaches and frequent flood events have made it the subject of widespread research (Table 3.2). The areas commonly flooded are close to the Newtown region, the Vyrnwy confluence, the Shropshire plain, and downstream from Worcester (Figure 3.1). At Saxons Lode, the daily mean discharge ranges from 7.2 m<sup>3</sup> s<sup>-1</sup> to 496.3 m<sup>3</sup> s<sup>-1</sup>, with a typical 2-year flood having a discharge of 392.5 m<sup>3</sup> s<sup>-1</sup>. The flow regime of the Severn is, in part, managed by a series of artificial measures (eg: regulation, floodplain management and abstraction) which influence the natural variability of the river. Wood (1987) notes that without augmentation by reservoir releases,

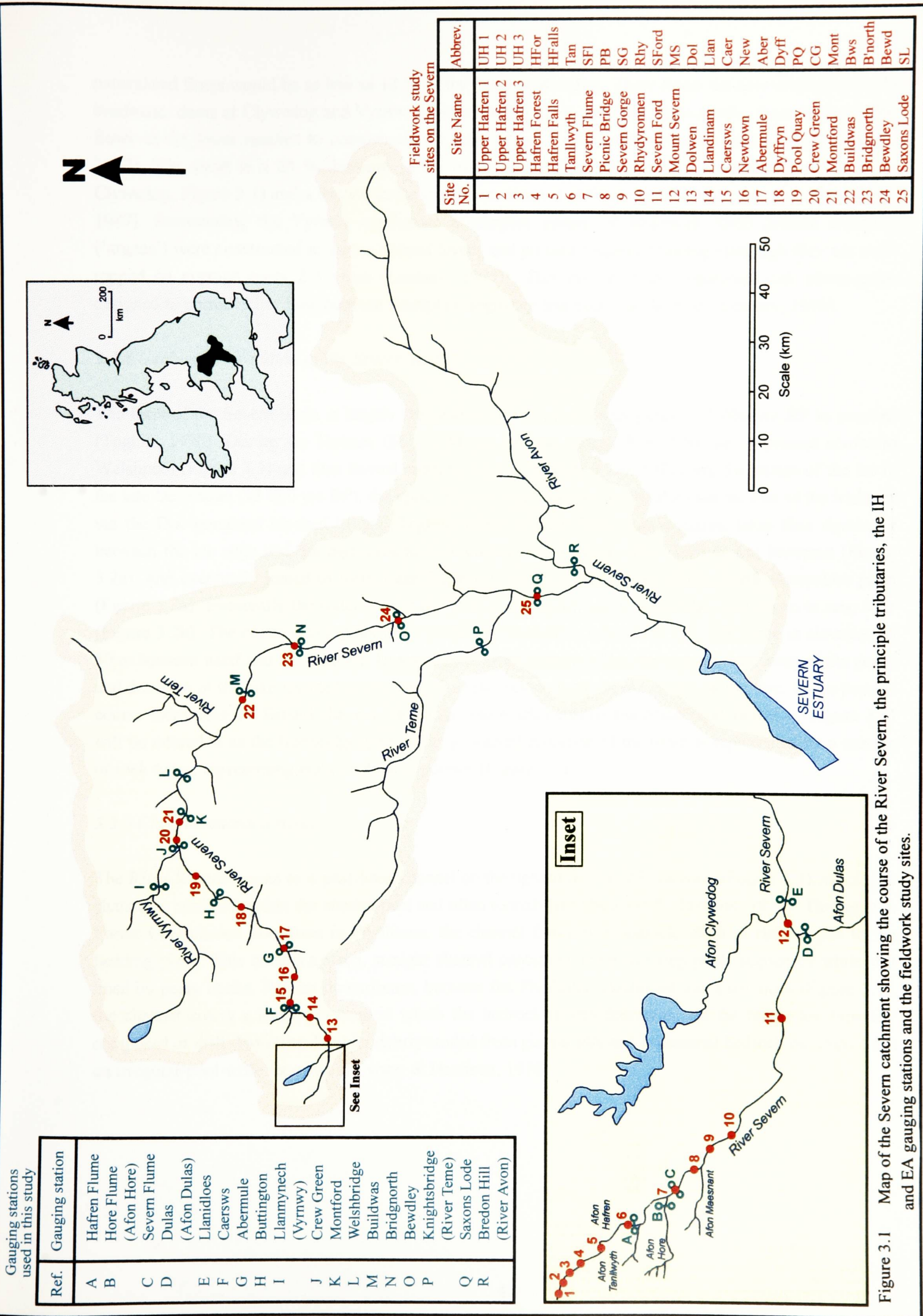


Figure 3.1 Map of the Severn catchment showing the course of the River Severn, the principle tributaries, the IH and EA gauging stations and the fieldwork study sites.

naturalised flows would be as low as 12 % of the mean at Bewdley. These flows are now controlled by the headwater dams at Clywedog and Vyrnwy, constructed in 1968 and 1881 respectively; these ‘top-up’ low-flows in the lower reaches to compensate for abstractions in the middle reaches of the channel (Higgs, 1987). The result is a 25 % decrease in the mean annual flood discharge at Caersws (downstream of Clywedog, Figure 3.1) and a decline in the recurrence interval at Caersws, Montford and Bewdley (Higgs, 1987). Surrounding the Vyrnwy confluence a complex system of earthwork flood defence measures (‘argaes’) were constructed to mimic natural levees and prevent frequent flooding (although they are overtopped on average every 2-3 years (Lindsay, 1995)). This system is also equipped with sluice-gates, designed to permit water flow between floodplain segments and back into the river (Lindsay, 1995).

#### *3.3.4 Geological evolution of the Severn basin*

The form of the Severn basin is largely the product of the post-glacial period (15 000 yrs BP to present) (Toghill, 1990). During the Tertiary (66 - 2 M yrs BP) the Severn flowed NE on its present course to Welshpool (Figure 3.1) and then flowed north to the Dee (Figure 3.2a). Following the retreat of the ice in the late Devensian (15 000 yrs BP), the upper Severn began to flow again, although the exit to the Irish sea via the Dee remained blocked by ice (Toghill, 1990) (Figure 3.2a). Large glacial lakes thus developed between the ice edge and the high ground surrounding the Wenlock edge, Telford and Newport (Figure 3.2a), and eventually joined to form Lake Lapworth which covered most of the North Shropshire plain (Figure 3.2a). Eventually the water rose to the level of the lowest col at Ironbridge, and began to seep over (Figure 3.2b). The col eroded rapidly and formed the Ironbridge gorge, due to a difference in elevation of 50 m between itself and the Coalport Brook, 1 mile away (Figure 3.2b). Subsequent deepening of the gorge and drainage of the lake resulted in the capture of the Severn from its old course to the Dee, to the present course today into the Bristol channel. Hereafter, the reach between Ironbridge and Bewdley (Figure 3.1) will be referred to as the Ironbridge gorge. The geological evolution of the basin is represented by a mosaic of rock types, representing eight geological periods (Figure 3.3).

#### *3.3.5 Channel characteristics*

The River Severn begins as a peat-lined channel on the upland moors of Plynlimon (Figure 3.1), where the channel is confined within the blanket peat and often roofed-over (Newson & Harrison, 1978). Through the Forest Commission plantation in Plynlimon, the channel flows over bedrock, often at right-angles to the bedding plane. This creates a steep, straight channel containing extensive step-pools sequences while still lined by peaty banks. Further downstream, between the Plynlimon catchment and Llanidloes (Figure 3.1), the channel enters a transition zone in which the bedrock is less dominant and the banks are typically composed of drift. However, boulder debris eroded from glacial tills and occasional bedrock outcrops form an irregular pool-riffle sequence (Newson & Harrison, 1978).

Table 3.2 A selection of previous and current research in the Severn basin in the field of fluvial geomorphology.

River reach	Author(s)	Subject
Plynlimon (Headwaters)	Painter <i>et al.</i> (1974)	Hydrology and forestry
	Newson, A.J. (1976)	Rainfall distribution and history
	Newson, M.D. (1976)	Physiography, deposits and vegetation
	Newson & Harrison (1978)	Channel studies
	Newson, M.D. (1980)	Geomorphic effectiveness of floods
	Newson, M.D. (1981)	Fluvial geomorphology
	Newson & Leeks (1987)	Sediment transport and yield
	Bonnett <i>et al.</i> (1989)	Monitoring sediment removal using radionuclides
	Kirby <i>et al.</i> , (1991)	Plynlimon research
	Hudson & Gilman (1993)	Hydrology of the Plynlimon catchment
	Bull <i>et al.</i> (1995)	Suspended sediment fluxes
	Bull (1996)	Bank erosion processes
	Couperthwaite <i>et al.</i> (1996)	Flow hydraulics and bank erosion processes
	Harris (in prep)	Bank erosion processes (unpublished thesis)
Plynlimon - Newtown	Bathurst <i>et al.</i> (1977)	Secondary flow measurement
	Bathurst (1979)	Shear stress in meander bends
	Bathurst <i>et al.</i> (1979)	Secondary flow and shear stress measurement
	Hey (1979)	Flow resistance estimation
	Hey & Thorne (1979)	Secondary flow measurement
	Thorne & Lewin (1979)	Bank erosion and bed material transport
	Lewin (1982)	Channel change
	Lewin (1983)	Channel change
	Lewis & Lewin (1983)	Alluvial cutoffs
	Hey & Thorne (1983)	Surface sediment sampling
	Higgs (1987)	Flooding and a change of hydrologic regime
	Lewin (1987)	Channel change
	Meigh (1987)	Bedload transport
	Newson & Leeks (1987)	Sediment transport and yield
	Bull <i>et al.</i> (1995)	Suspended sediment fluxes
	Carling (1995)	Instream habitat modelling
	Bull (1996)	Bank erosion processes
	Harris (in prep)	Bank erosion process (unpublished thesis)
	Couperthwaite <i>et al.</i> (1996)	Flow hydraulics and bank erosion
	Newtown - Shrawardine	Hey (1975) (cited in Lewin (1983))
Lewin (1983)		Channel change

	Lewin (1987) Lindsey (1995)	Channel change Vyrnwy confluence
Shrawardine - Buildwas	Wills (1924, 1938) Dury <i>et al.</i> (1972) Richards (1972) Kirkby (1972) Dury (1983)  Dury (1984) Carling (1991) Reynolds <i>et al.</i> (1991) Beven & Carling (1992) Carling & Wood (1993)  Shropshire County Council (1994) McCartney & Naden (1995)	Formation of the Ironbridge Gorge Underfit stream channels Underfit stream channels Underfit stream channels Underfit stream channels  Underfit stream channels Velocity reversal in pool-riffle sequences Retention areas and velocity distribution Flow velocities and roughness Velocity reversal in pool-riffle sequences - HEC- 2 simulation Site description for an SSSI Floodplain storage
Buildwas - Saxons Lode (Lower Severn)	Wills (1938) Beckinsale & Richardson (1964) Burrin (1980) Brown (1987) Dawson & Gardiner (1987) Marriott (1992)	Formation of the Ironbridge Gorge  Palaeo-reconstruction of river terraces  Valley fill sediments and floor morphology Holocene floodplain sedimentation Palaeo-reconstruction of river terraces Modelling of flood deposit
Severn basin	Ferguson (1981)  Brown (1987) Gregory & Lewin (1987) Higgs (1987) Lawler (1987) Lewin (1987) Mitchell & Gerrard (1987) Wood (1987) Rowan <i>et al.</i> (1992) Jolley & Wheeler (1993) Walling & Quine (1993)	Stream power comparison between rivers in the UK Sediment storage and supply Palaeohydrological research review Hydrological review Climatological review Geology and geomorphology of the basin Sediment storage and redistribution Hydrological review Sediment tracing of radionuclides Rainfall-runoff model Suspended sediment budget

Table 3.3 The location and type of EA (former NRA) gauging stations along the Severn (listed in downstream order, beginning near the source) (NRA Hydrometric Yearbook, 1992).

Station Name	Grid Reference	Instrumentation	Start of Record
Tanllwyth	SN843877	TF CH WT	01 / 1952
Severn Flume	SN 850872	TF CH	01 / 1952
Llanidloes	SN 955848	OC TG CH	06 / 1967
Dolwen	SN 996851	OC CH	06 / 1975
Caersws	SO 033917	OC TG CH	11 / 1962
Abermule	SO 164958	OC TG CH	06 / 1960
Crew Green	SJ 330158	OC TG CH	11 / 1983
Montford	SJ 412144	OC TG CH WT	06 / 1952
Welshbridge	SJ 489128	OC TG CH	12 / 1950
Buildwas	SJ 644044	US TG CH	09 / 1977
Bewdley	SO 782762	US TG CH WT	02 / 1968
Saxons Lode	SO 863390	US TG CH WT	06 / 1970

Key:

TF = Trapezoidal Flume  
 CH = Chart Recorder  
 OC = Open Channel Site

TG = Telegen 1150 Telemetry  
 WT = Water Temperature Sensor  
 US = Ultra-sonic Gauge

A channel transition occurs at Llanidloes, from non-alluvial to alluvial (Figure 3.1). This marks the break of slope of an unusually steep longitudinal profile by UK standards (Figure 3.4) (Wheeler, 1979) and the development of a floodplain (Brown, 1987). The Llanidloes - Welshpool reach is highly sinuous with high rates of lateral activity, making it the focus of much research (Table 3.2). Downstream from Welshpool the channel becomes more incised; the loss of conveyance capacity in the channel results in an increased frequency of over-banking (Hey, 1975, cited in Lewin, 1987). Between the Vyrnwy confluence and Buildwas, the channel is fairly straight, and floodplain is wide and frequently inundated (Lindsay, 1995). From Buildwas to Bewdley, the Severn steepens through the Ironbridge gorge and lateral migration is inhibited (Wills, 1924, 1938). At Worcester a series of four weirs serve to regulate the level of the lower Severn. Saxons Lode, near Tewkesbury represents the approximate tidal limit of the river and, therefore, the downstream limit to this study area.

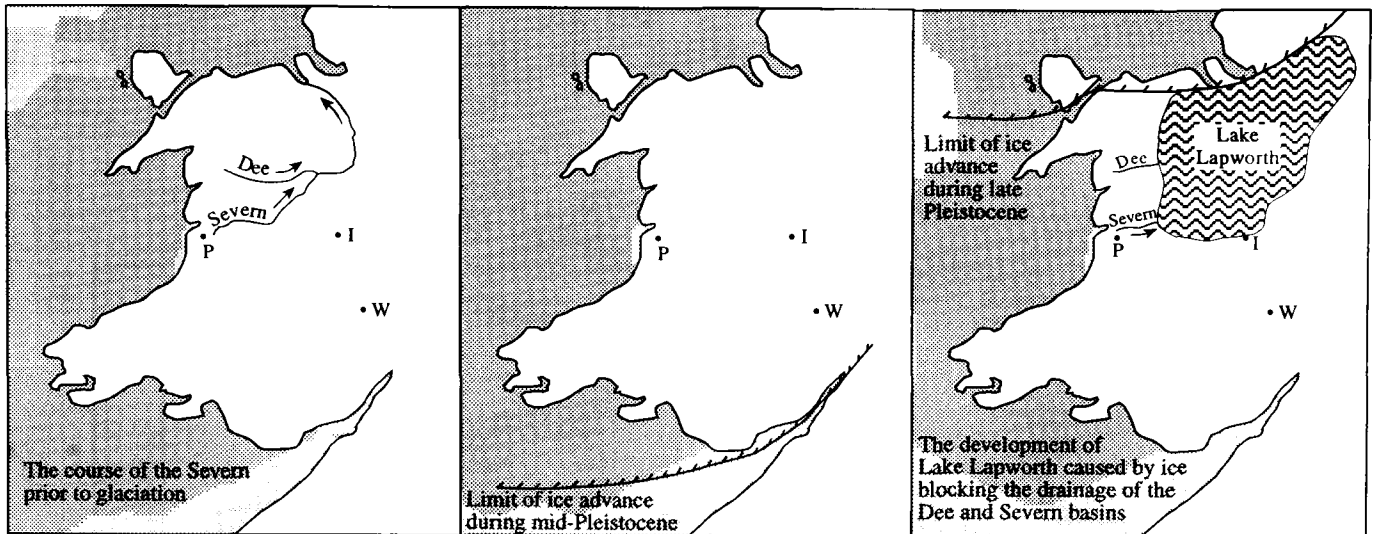


Figure 3.2a Lake Lapworth and the course of the Severn channel prior to and during the glacial period (P = Plynlimon; I = Ironbridge; W = Worcester).

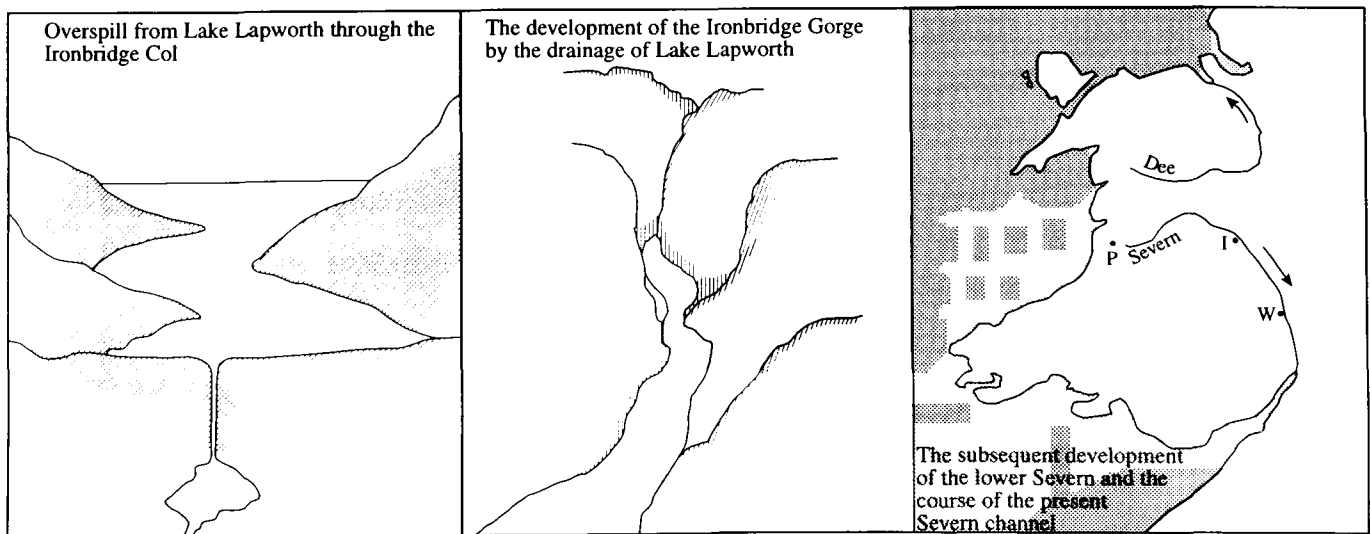


Figure 3.2b The development of the Ironbridge Gorge following the breaching of the Ironbridge col by the waters of Lake Lapworth (P = Plynlimon; I = Ironbridge; W = Worcester).

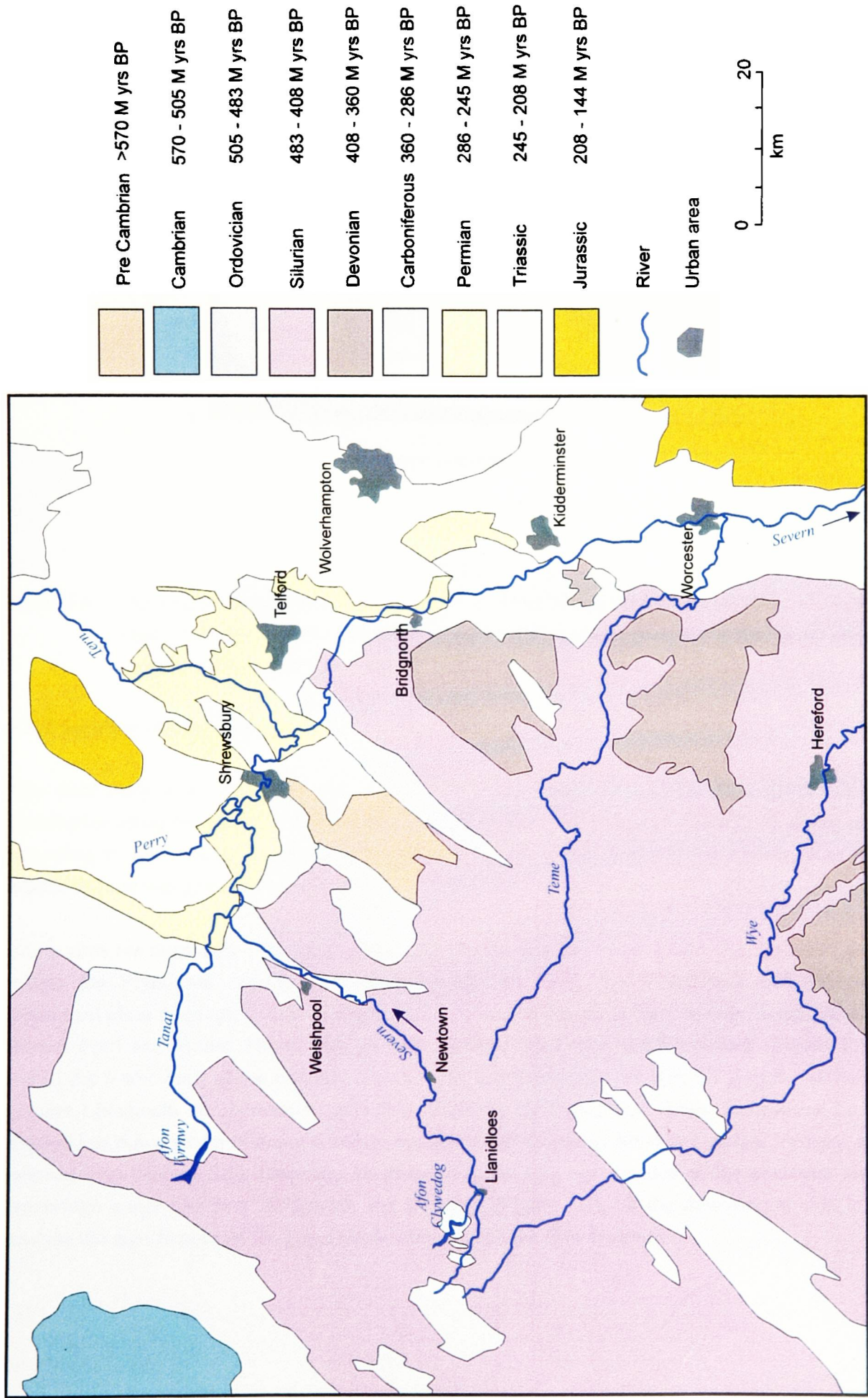


Figure 3.3 The geological structure of the Severn basin.

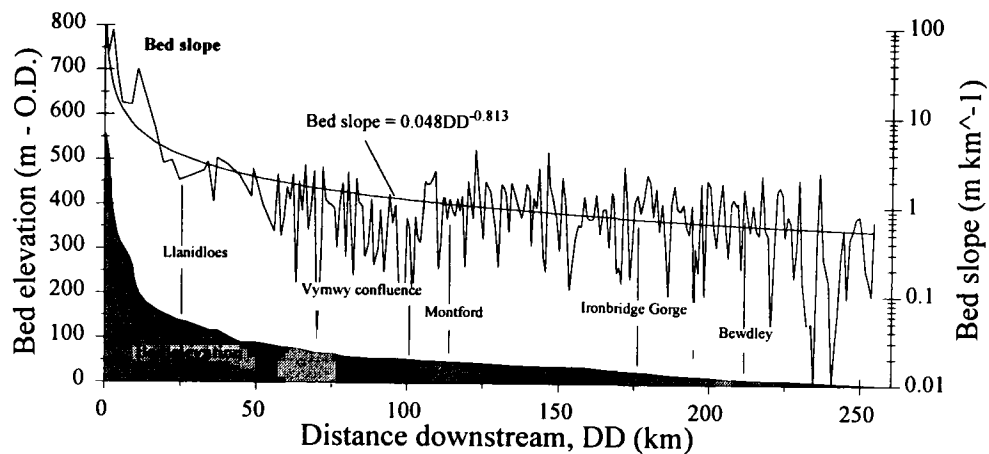


Figure 3.4 The longitudinal profile and bed slope of the River Severn, including several key site locations (see Figure 3.1). Bed slope is calculated from topographical cross section data at 1 km intervals used in the model simulation (Chapters 5 and 6).

### 3.3.6 Location of study sites

This field study is based on 25 study sites (Table 3.4 & Figure 3.1), located in a roughly logarithmic distribution along the Severn to reflect the supposed geometric increase in channel size downstream, and according to the criteria specified in 3.2.3 Each site was easily accessible and permission to use the adjoining land was granted in advance.

Study sites are numbered 1-25, beginning at the source (Figure 3.1 & Table 3.4). Sites 1-7 are located within the Plynllynon experimental catchment (Figure 3.1), two (Tanllwyth and Severn Flume) positioned close to gauging stations (Figure 3.1). Five sites (Picnic Bridge, Severn Gorge, Rhydyronnen, Severn Ford and Mount Severn) are situated between Plynllynon and Llanidloes (Figure 3.1), which marks the lower limit of the bedrock channel. The remaining sites all had EA gauging stations nearby (except Llandinam and Newtown) with five (Dolwen, Dyffryn, Crew Green and Saxons Lode) being located just downstream of major tributary confluences (Clywedog, Rhiw & Camlad, Vyrnwy, and Teme respectively) (Figure 3.1). One site, Buildwas (Figure 3.1), was located at the upstream side of the Ironbridge gorge and two, Bridgnorth and Bewdley (Figure 3.1), on the downstream side in order to analyse the significance of the gorge on the channel and the flow hydraulics.

### 3.4 Channel survey and bed sampling techniques

#### 3.4.1 Introduction

The section geometry and bed material characteristics were surveyed at the beginning of the study, and assumed to remain constant throughout the field programme (January 1994 - March 1996). Subsequent measurements of channel geometry in the section were used to check channel stability and determine the flow geometry. The channel geometry was measured to calculate the flow area, wetted perimeter and hydraulic radius for varying flow levels up to a bankfull level. The timing of flow measurements was initially defined with reference to stage at each study reach, but following the field study, the calculated discharge was used to reclassify the flow based on exceedance frequencies (section 3.10).

#### 3.4.2 Bankfull channel geometry

Each section was monumented on both left and right bank with plastic stakes located orthogonal to the channel, and at least one channel width from the bank edge (Figure 3.5a). This procedure ensured that results remained accurate for repeated site visits and allowed for the possibility of channel migration during the study (Lawler, 1993). These and other temporary bench marks (TBM's) were surveyed to the nearest Ordnance Survey benchmark using standard EDM or levelling techniques (eg: Pugh, 1975; Lawler, 1993; Elfick *et al.*, 1994). The cross section geometry was surveyed using either levelling (a Sokkisha level) or an Electromagnetic Distance Meter (EDM) (Zeiss Elta 4).

For narrow channels ( $W_{BF} < 20$  m) the levelling method was used. This required that normal precautions be taken, as described in Lawler (1993). During surveying, the staff may be placed at either: a) regular spaced intervals; b) changes or breaks of slope; or c) a combination of both. This study has adopted the latter because, although it is subjective, it gives greater scope for an accurate representation of the profile (Young, 1972). Measurements were recorded to the nearest millimetre, taking care to minimise the instrument and operator errors listed in Table 3.5. The results were tabulated in the manner described by Elfick *et al.* (1994, p.115).

For wide channels ( $W_{BF} > 20$  m) and if the elevation between the water level and the floodplain at low flow was too great to survey with the level, the EDM was used. The basic principles adopted for levelling were also used, except that the water depth was estimated at successive intervals across the channel, using the plumb-bob method (a weight suspended on a graduated line); this inevitably resulted in a slight loss of precision in measurements especially in strong flow (Table 3.5 & section 3.11), hence, water depth could only be read to the nearest 0.05 m using this method.

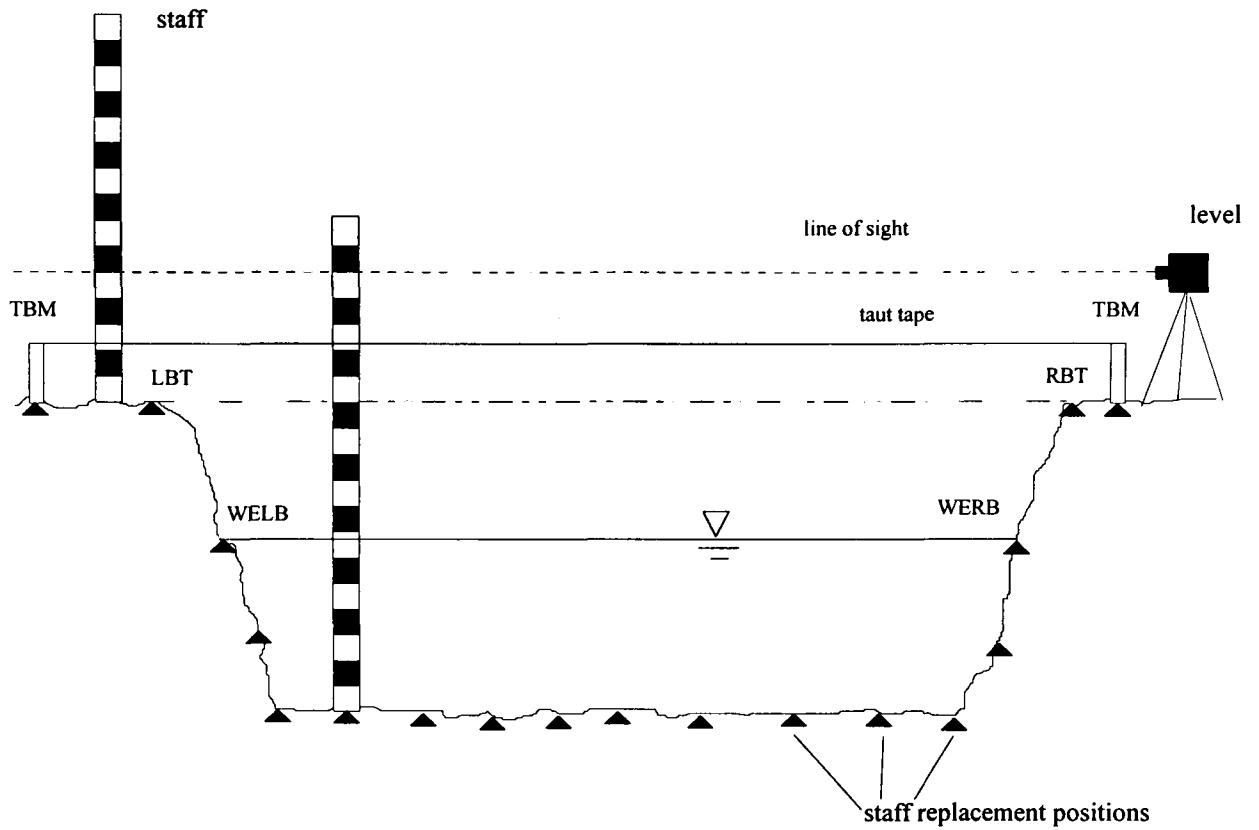


Figure 3.5a Surveying the channel cross section using the levelling technique (after Lawler, 1993).

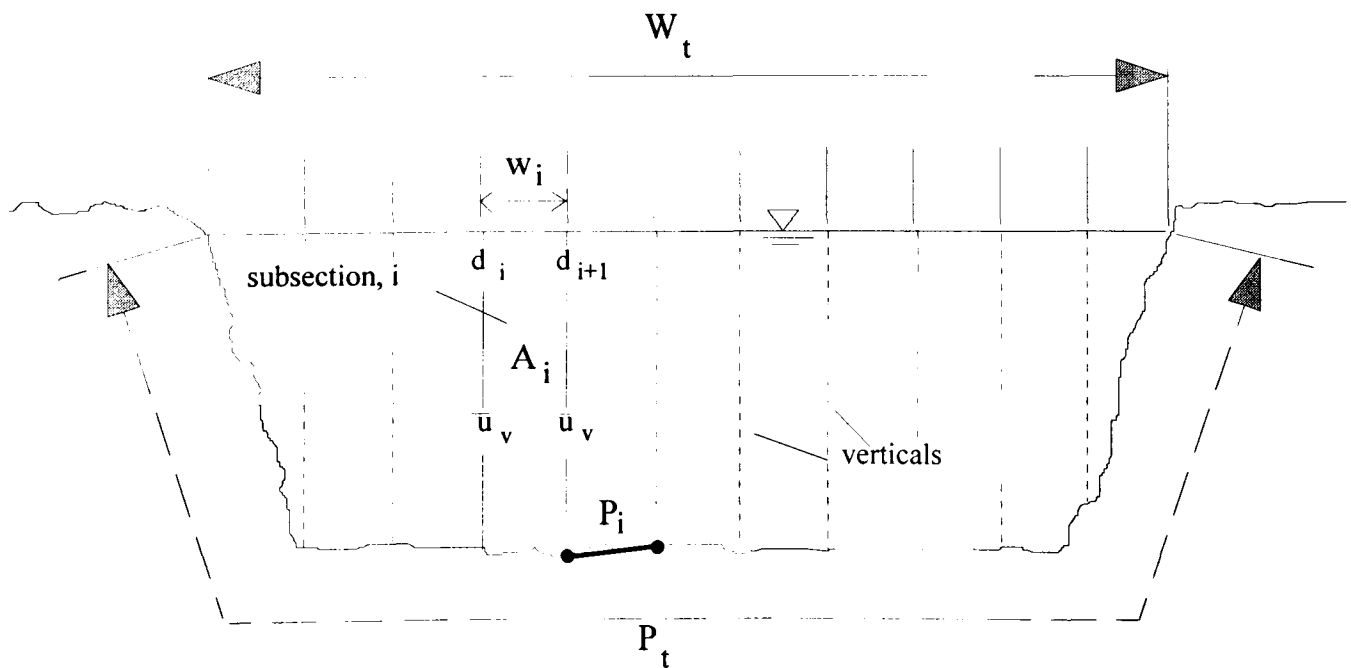


Figure 3.5b Cross section variables are calculated by dividing the section into subsections defined by the surveyed points, and using equations 3.1 - 3.6.

Table 3.4 Location and characteristics of fieldwork study sites

No.	Site name	Grid Reference	Distance downstream, km	Drainage basin area (km <sup>2</sup> )	Elevation (above datum), m	Stage datum	Check gauge	Site characteristics
1	Source 1	SN 823898	0.08	0.31	606.2	2	Interpolation	Deep, incised channel flowing through blanket peat, partly roofed, open moorland
2	Source 2	SN 825896	0.31	0.56	580.2	2	Interpolation	Deep, incised channel flowing through blanket peat, partly roofed, open moorland
3	Source 3	SN 828893	0.76	0.86	547.8	2	Interpolation	Deep, incised channel flowing through blanket peat, cobble bed, open moorland
4	Haflen Forest	SN 828890	1.23	1.15	524.4	2	Interpolation	Step-pool channel flowing through dense forest plantation, peaty banks
5	Haflen Falls	SN 837883	2.73	2.31	390.7	2	Interpolation	Riffle-pool channel, containing glacial boulder and drift deposits in bed and banks
6	Tanllwyth	SN 843877	3.71	3.76	347.8	2	Tanllwyth (IH)	Straight, riffle-pool reach, with composite banks
7	Severn Flume	SN 847873	4.26	8.62	334.3	1	Severn flume (IH)	Bedrock controlled, straight step-pool sequence, deep composite banks & rip-rap
8	Picnic Bridge	SN 856869	5.81	9.79	313.7	4	Interpolation	Bedrock controlled, sinuous step-pool sequence, composite banks
9	Severn Gorge	SN 871865	9.00	14.23	271.6	3	Interpolation	Bedrock controlled, straight, boulder channel, gravel bed, low composite banks
10	Rhydyronnen	SN 867869	9.23	14.73	266.4	3	Interpolation	Bedrock controlled, straight fall-pool sequence, gravel bed, composite banks
11	Severn Ford	SN 904846	11.11	24.75	204.3	3	Interpolation	Wide, shallow, riffle-pool sequence, low stable composite banks
12	Mount	SN 947841	16.88	98.5	165.7	3	Llanidloes (EA)	Bedrock controlled, wide, sinuous channel; large, active, composite banks
13	Severn							
13	Dolwen	SN 996852	22.22	187.0	147.6	1	Dolwen (EA)	Straight, riffle-pool channel, stable, composite banks
14	Llandinam	SO 885025	28.00	225.8	137	3	Interpolation	Sinuuous, riffle-pool sequences, wide shallow; low, active, composite banks
15	Caersws	SO 036920	34.10	375.0	119	1	Caersws (EA)	Sinuuous, wide; highly active composite banks
16	Newtown	SO 093910	44.93	457.0	109	3	Interpolation	Bedrock controlled, wide, shallow, straight; inactive, low composite bank
17	Abermule	SO 165958	55.92	580.0	83	1	Abermule (EA)	Straight, riffle-pools; high, stable, cohesive banks
18	Dyffryn	SJ 211012	70.30	855.0	75	3	Dyffryn (EA)	Straight, riffle-pools; high, stable, cohesive banks
19	Pool Quay	SJ 260118	83.20	943.0	67	1	Interpolation	Sinuuous, narrow, deeply incised channel, riffle-pools; large, cohesive, stable banks
20	Crew Green	SJ 345155	99.11	1915.0	54	1	Crew Green (EA)	Sinuuous, wide channel, prone to over-banking; unstable, friable bank material
21	Montford	SJ 396147	115.46	2025.0	53	1	Montford (EA)	Straight, wide channel; stable composite bank material
22	Buildwas	SJ 612048	166.45	3717.0	48	1	Buildwas (EA)	Sinuuous, wide channel; unstable glacial drift bank material
23	Bridgnorth	SO 722736	192.36	4059.0	30	1	Interpolation	Straight, wide, riffle-pool sequence; stable cohesive bank material
24	Bewdley	SO 782762	207.94	4325.0	17.4	1	Bewdley (EA)	Straight, high w:d, riffle-pools, tree-lined; stable, cohesive bank material
25	Saxons Lode	SO 863389	256.32	6850.0	7.5	1	Saxons Lode (EA)	Sinuuous, high w:d, tree-lined; unstable, friable bank material

Key (for stage references):

1 = EA stage board      2 = Stage board mounted on a scaffold or dexion support

3 = Nail datum      4 = other (eg. bridge support)

These measurements were used to calculate various parameters of the channel geometry, using the equations below (Figure 3.5b):

$$A_i = 0.5(d_i + d_{i+1})w_i \quad [3.1]$$

$$A_t = \sum_{i=1}^{i=n} A_i \quad [3.2]$$

$$P_i = \left( (d_{i+1} - d_i)^2 + w_i^2 \right)^{0.5} \quad [3.3]$$

$$P_t = \sum_{i=1}^{i=n} P_i \quad [3.4]$$

$$R = \frac{A_t}{P_t} \quad [3.5]$$

$$\bar{d} = \frac{\sum_{i=1}^{i=n} d_i}{n} \quad [3.6]$$

- where,
- $d_i$  = depth of subsection ,i (m)
  - $\bar{d}$  = mean flow depth (m)
  - $w_i$  = width of subsection, i (m)
  - $A_i$  = area of subsection, i ( $m^2$ )
  - $A_t$  = total area of cross section ( $m^2$ )
  - $P_i$  = wetted perimeter of subsection, i (m)
  - $P_t$  = total wetted perimeter of cross section (m)
  - $R$  = hydraulic radius of cross section (m)
  - $n$  = number of subsections

### 3.4.3 Planform geometry

The channel planform was photographed and the sinuosity (S) of the channel at each study site was estimated from 1: 10 000 Ordnance Survey maps to give an indication of the form resistance (Bray, 1982; Hey, 1979) imparted by the channel on the flow hydraulics. The reach length was defined as 20 bankfull channel widths, reflecting an approximate meander wave length (if 1 geomorphic unit is 5-7 channel widths, and a mean meander wavelength is 4 geomorphic units (Howard, 1992)).

Table 3.5 Possible errors during channel geometry and slope surveys, using either the level or EDM.

	Type	Description
Instrument errors	Instrument not in horizontal adjustment	The line of collimation is not parallel to the axis of the level vial
	Instrument not centred	Will cause the instrument head to deviate from the horizontal plane during rotation
	Tripod legs loose	Legs which are too loose or too tight prevent the free movement of the instrument head in the horizontal plane
Natural errors	Temperature variations	Heat may cause a metal staff to expand, the level bubble to shorten and create heat waves close to the ground
	Wind	Strong wind may cause the instrument to rock or vibrate, and makes the staff unsteady
	Settlement of the instrument	Adjustment of the instrument after the back sight reading may occur due to spongy surfaces, ice or smooth surfaces
	Flow level variation	Variation of the water surface during measurement must be checked, either by a repeat reading of the WELB or by re-reading a stage board
Operator errors	Bubble not centred	The level-bubble on the instrument may wander between backsights and foresights, or may be incorrectly centred before the backsight
	Faulty staff readings	This may be caused by poor weather, long sights, parallax or staff movement
	Recording notes	Transposition errors may result either by incorrect reading of the staff level, a written error or a calculation error
	Using different backsight and foresight positions	A well-defined location must be used, eg: stake, fencepost, mark on a building
	Location of the water edge	This can be caused by a time-varying water boundary, or the incorrect location of the staff
	Tape measure reading	Cross section and water slope measurements require accurate readings of distance from a <u>taut</u> tape measure
	Location of bank top	The location of the bank top may be defined in terms of the vegetation limit (Leopold & Skibitzke, 1967), the maximum break of slope or the minimum width-depth ratio (Wolman, 1955)
	Sagging tape	Extension of a tape over a wide channel may cause sagging which will create errors in the channel widths
	Tape measurement	The tape must be pulled taut, and read to the nearest centimetre



This was calculated from:

$$S = \frac{L_C}{L_R} \quad [3.7]$$

where,  $L_C$  = length of the channel, measured from an estimated centre line (m)  
 $L_R$  = reach length (m)

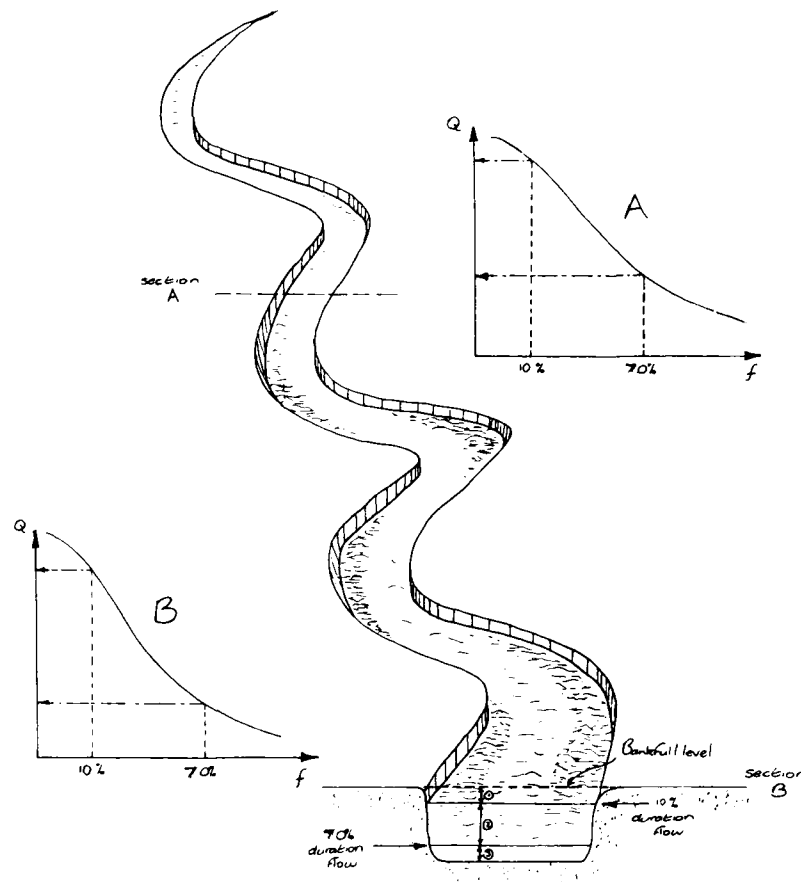
#### 3.5.4 Stage and preliminary flow classification

The stage at each site was determined with reference to a stage datum. For sites not positioned close to gauging station boards, stage boards had to be installed (Table 3.4). Flows were originally classified according to stage relative to a bankfull level (Figure 3.6). As flow data were not immediately available for the sites, this technique enabled flows to be measured (flow velocity, discharge, and water surface slopes) using a simple framework (low, medium and high flow measurement at each study site) which ensured non-duplication of results. Measured flows at each study site were later reclassified using flow duration curves to predict flow frequencies (Figure 3.6 and section 3.10).

#### 3.4.5 Flow geometry

The size and geometry of the water prism were calculated separately at low, medium and high flows. The two methods of determination were based on: a) direct; and b) indirect measurement procedures.

- a) Direct measurement of the water prism. In flow conditions suitable for wading or using a small inflatable boat, a tape was stretch orthogonally across the section. The water depth was measured at a minimum of twelve verticals across the channel, and estimated to the nearest 0.5 cm: the verticals typically coincided with velocity verticals (see sections 3.6.3 & 3.6.4). A 1 m ruler was used to measure depths of less than 1 m. At greater depths, a weight was suspended from a cable lowered from the boat, and water depths were read from a graduated scale on the winch. The channel geometry variables of water width, mean depth, area, wetted perimeter and hydraulic radius were calculated from equations [3.1 - 3.6].
- b) Indirect measurement of the water prism. For conditions unsafe for wading or using the boat, the left and right bank waters edge at the section were surveyed to a nearby temporary bench mark. This enabled the water surface elevation to be integrated with the previously surveyed bankfull channel geometry. Hence, by assuming that no change had occurred to the channel geometry, the geometry of the water prism was calculated using equations [3.1 - 3.6]. A trash line survey of the Upper Severn applied the same methodology by assuming the trash line indicated the maximum elevation of the water level during the flood (see section 3.5.3 for details of the water surface slope approximation & section 3.8 for details of the trash line survey)



No	Flow classification	Stage, h (Bankfull = 100 %)	Duration, F (frequency of occurrence, %)
1	High	$h \geq 80 \%$	$F \leq 10 \%$
2	Medium	$20 \leq h \leq 80 \%$	$70 \geq F \geq 10 \%$
3	Low	$h \leq 20 \%$	$F \geq 70 \%$

Figure 3.6 A diagram showing the two flow classification schemes used in this study. During data collection in the field, flows were classified according to ‘high’, ‘medium’ and ‘low’ stage (defined relative to bankfull). Following the fieldwork programme, flows were reclassified according to flow duration, ie: ‘high’ flow represents a flow occurring less than 10 % of the time (after Richards, 1982).

### 3.4.6 Bed material sampling

The non-tidal Severn is predominantly a gravel-bed river. Therefore, the grid method (Wolman, 1954) provides a convenient way for collecting and measuring fine-coarse gravel material over a broad spatial area, at most study sites. In the few reaches where this technique was ineffective (due to fine bed material sizes) the volumetric method was used (Kellerhals & Bray, 1971).

The grid method involves establishing a grid on the bed and sampling particles from each grid node (Figure 3.7). The grid was positioned upstream of the study section, because the upstream bed roughness influences the hydraulics in the study section. 100 individual particles were picked from the bed and the pebble b-axis was measured to the nearest 1 mm, using the method described by Wolman (1954). (Although, Hey & Thorne (1983) note that there is no significant difference between sample sizes of 40,

60 and 100.) The number of particle samplers was kept to a minimum, and all particles were measured by the same person to avoid sampling and measurement errors induced by bias (Marcus *et al.*, 1995) (section 3.11). The relative size of each size fraction was then determined by constructing a cumulative frequency curve. This technique truncates the lower limit of the sample size distribution because the sampler is physically incapable of collecting samples < 2 mm in diameter (Table 3.6); hence, the volumetric technique was chosen for finer bed material sizes.

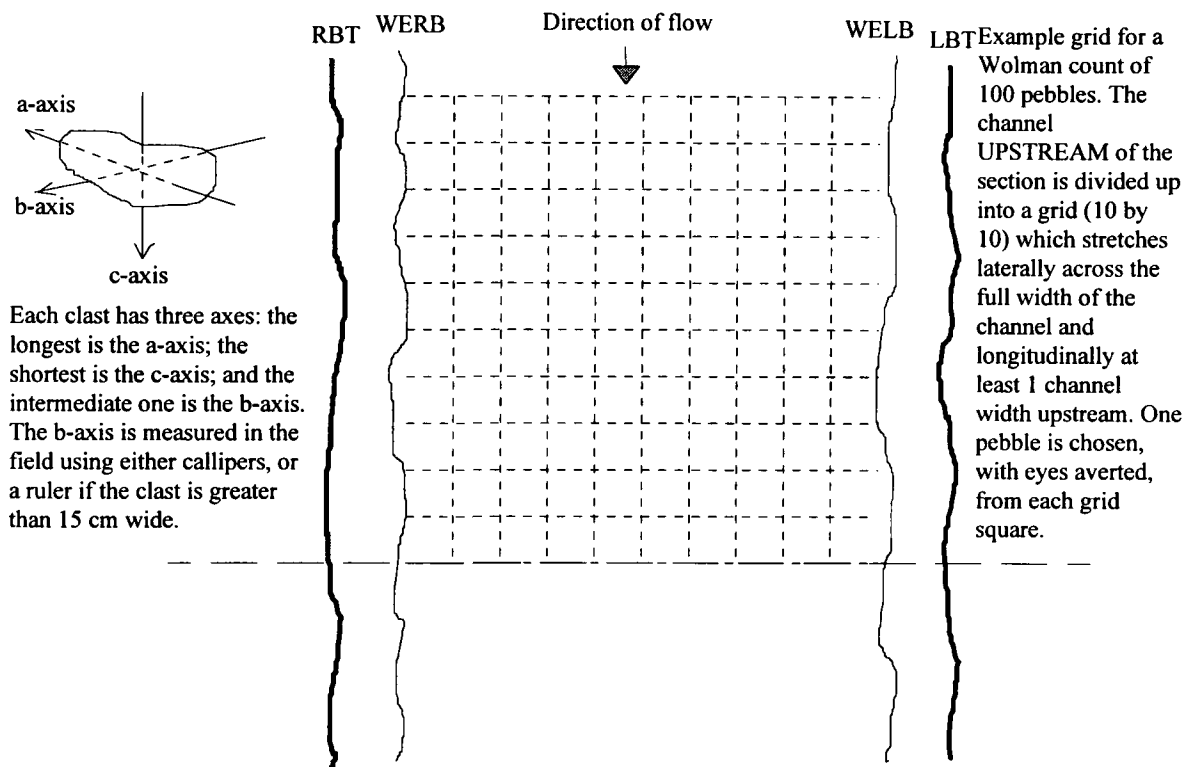


Figure 3.7 The Wolman count method of surface sediment sampling requires that pebbles are selected at random from the bed. Defining a grid ensures equal coverage of the reach upstream of the section (Wolman, 1954).

The volumetric method requires a predetermined volume of bed material to be removed, in this case by shovelling the sediment into a bag (Kellerhals & Bray, 1971). However, the surface and subsurface components were difficult to disaggregate so the sample may underestimate the surface bed material size (Table 3.6). In the laboratory, the sample was split into smaller sub-samples for analysis and dried. These sub-samples were crushed (if hardened) and sieved. The sediment within each sieve was weighed and tabulated, thus enabling a cumulative frequency curve of particle size by weight to be constructed. This technique has the potential to sample the full range of sediment sizes, but errors may occur, a) in the field, due to an inability to sample only the surface layer, or b) in the laboratory, caused by fine sediment clogging the sieve mesh and thus skewing the size-frequency distribution (Table 3.6).

Table 3.6 Errors characterising surface bed material sampling.

	Type	Description	Authors
Natural error	Spatial variability in gravel size	Short gravel bed reaches contain a diverse range of particle sizes, particularly over bars	Kellerhals & Bray (1971), Wolcott & Church (1991), Lisle (1995), Marcus <i>et al.</i> (1995), Paola & Seal (1995)
	Variation over time	Restructuring of the bed layer may occur during a high flow due to particle entrainment	Kellerhals & Bray (1971), Pickup (1976), Carling (1983)
	Surface layer sample	Surficial bed material may not entirely represent frictional bed resistance	Livesey (1996)
Human error	Measurement of the b-axis	Both identification and accurate measurement of the correct axis must be ensured	Marcus <i>et al.</i> (1995)
	Individual bias	Selection of particles and measurement of size may be consistently smaller or larger than other observers	Marcus <i>et al.</i> (1995)
	Single vs. multiple observers	Different collectors and measurers between sites will increase variability of results	Hey & Thorne (1983), Marcus <i>et al.</i> (1995)
	Choice of individual particle (Wolman Count)	It is difficult to identify and pick up the smaller particles in the size distribution (< 10 mm)	Wolman (1954), Leopold (1970), Kellerhals & Bray (1971), Fripp & Diplas (1993)
	Sample size	Sampling error decreases with an increase in sample size	Hey & Thorne (1983), Wolcott & Church (1991), Ferguson & Paola (in press)
	Use of a template	Templates are limited by the sample size distribution and the size of the holes.	Marcus <i>et al.</i> (1995)
	Unrepresentative sampling grid	The grid may not span the entire river or cover a sufficient proportion of the reach	Kellerhals & Bray (1971)
	Measurement and transcription errors	Errors may occur in taking a measurement from a ruler / callipers, or in the documentation of the result	
	Weight of sediment volume	Fine sediment may be lost between sieving and weighing	
	Sieve clogging	Sieve pores may become blocked by fine sediment, resulting in an underestimation of the fine particle fraction	
Analysis errors	Non-equivalent sampling procedures	Different sampling procedures may produce non-equivalent results	Leopold (1970), Kellerhals & Bray (1971), Hey & Thorne (1983), Church <i>et al.</i> (1987), Wolcott & Church (1991), Fripp & Diplas (1993)

## 3.5 Measurement of water surface slope

### 3.5.1 Introduction

An underlying principle behind selecting a straight reach with a reasonably uniform section is that the water surface slope can be used in calculations of flow resistance, stream power and shear stress because it closely approximates the energy, or friction, slope in the absence of nearby flow controls (Henderson, 1966). It is preferred to the channel bed and valley slope because the water surface slope varies as flood waves pass through the reach and thereby offers a more realistic representation of the energy of the flow at any moment in time. The slope may also be used to calculate the mean velocity and discharge of the section indirectly (using the Manning's and Darcy-Weisbach equations), reach mean shear stress, and total and unit stream power (Chapter 2).

### 3.5.2 Water surface survey

The water surface elevation was measured along the length of the study reach, defined here as 5 - 10 bankfull channel widths centred on the study section (Figure 3.8) (section 3.2.3). Slope was calculated from the linear regression of water surface elevation and distance downstream; the regression exponent represents the gradient of the best fit line, and hence, an approximate water surface slope.

There were two methods available for measuring the water surface slope: the levelling or the EDM surveying techniques:

- a) The level and staff technique. A minimum of ten water surface elevations were surveyed at equal, or representative, distances along the channel. The water slope was approximated using regression analysis, which allowed for errors associated with natural surface variability and human errors (Table 3.5 and section 3.11). The base of the staff was held on the water surface; ideally this was where it could be supported by a sloping bank-face and where the vertical fluctuations in the water surface were minimal (Table 3.5). This technique was used when, i) the channel width (and therefore reach length) was small ( $< 10$  m), so that one could comfortably view the whole reach, and ii) when the banks were low, thereby ensuring that the staff top remains horizontal viewing plane of the level.
- b) The EDM surveying technique. The EDM is free to move in the vertical plane and has an accuracy of  $\pm 0.005$  m up to a distance of 500 m (using the Zeiss Elta 4) (Plate 3.1). This gives the technique greater flexibility in difficult or large channel reaches. The operator records the distance,  $E_{EDM}$ , the horizontal angle,  $A_{EDM}$  and the vertical elevation,  $h_{EDM}$ , and from these the water surface slope was calculated using the method described in Figure 3.9. The EDM was used when, i) the water width was greater than 10 m, and ii) when the level of the floodplain was too high above the water surface to view the staff.

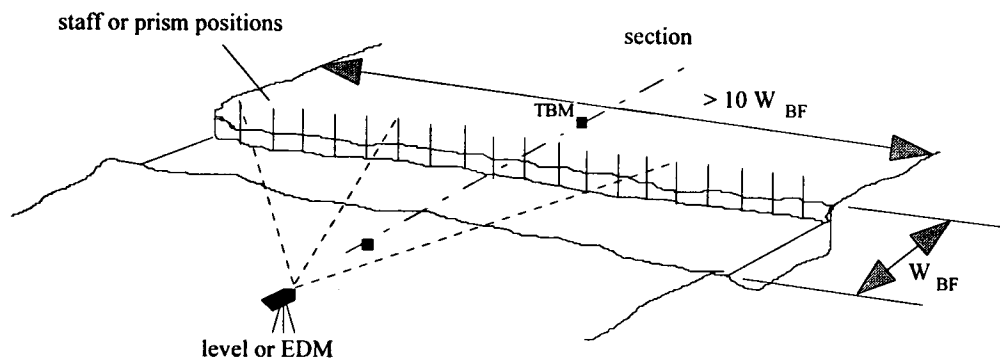


Figure 3.8 The water surface slope was surveyed, using a level or EDM, over a distance of 5 - 10 bankfull channel widths downstream along the channel, centred on the study section.

### 3.5.3 Trash line survey

Debris deposited by the December 1995 flow event provided sufficient information to reconstruct the maximum water surface elevation of the event in the upper reaches. Remnant trash lines were identified and surveyed along 11 out of the 12 upper study reaches, using the level and staff technique. It was assumed that the deposits represented the highest elevation of the flow during the flow event, and therefore, the water surface slope at peak discharge. This slope information and the reconstructed width and hydraulic radius (section 3.4.5) was used to evaluate the peak discharge along the channel; this case study is discussed in detail in section 3.8.

## 3.6 Measurement of flow velocity

### 3.6.1 Introduction

The aim of flow metering was to evaluate the at-a-site and downstream variability of flow hydraulics (mean velocity, boundary shear stress and isovel distributions). On account of equipment availability and time constraints, impeller devices were chosen in preference to Electromagnetic Current Meters (ECM's), thereby limiting flow velocity measurements to the longstream direction. The longitudinal flow velocity was measured directly, or estimated, at all sites, depending upon whether safety could be ensured during the measurement period.

No.	EDM measurements			Calculated values		Regression analysis	
	Distance (m)	Hor. angle (degrees)	Elevation (m)	Distance between sample points, (m)	Distance downstream (m)	Elevation above a bench mark (m)	Line of best fit for water elevation against distance downstream (m)
i	$E_{EDM}$	$A_{EDM}$	$h_{EDM}$	$y_i(a)$	$Y(b)$	$H_{BM}^c$	$H_{BM}^d$
1	255.794	343.994	-2.912		0	-2.787	-2.781
2	211.759	344.475	-2.897	14.154	14.155	-2.772	-2.785
3	189.545	346.408	-2.916	23.219	37.374	-2.791	-2.792
4	172.516	347.933	-2.930	17.696	55.070	-2.805	-2.797
5	151.565	350.111	-2.913	21.834	76.904	-2.788	-2.804
6	117.522	356.589	-2.957	37.234	114.138	-2.832	-2.815
7	101.704	1.978	-2.946	18.864	133.003	-2.821	-2.820
8	91.858	6.847	-2.956	12.821	145.823	-2.831	-2.824
9	72.967	19.152	-2.967	25.784	171.608	-2.842	-2.832
10	63.525	33.874	-2.979	19.837	191.444	-2.854	-2.838
11	59.613	55.215	-2.972	21.122	214.566	-2.847	-2.844
12	65.621	75.253	-2.964	22.577	237.143	-2.839	-2.851
13	83.868	92.210	-2.975	28.487	265.630	-2.850	-2.860
14	107.4	99.900	-2.969	26.754	292.384	-2.844	-2.867
15	121.57	103.111	-2.990	15.549	307.933	-2.865	-2.872
16	149.752	108.443	-2.996	30.851	338.784	-2.871	-2.881
17	217.096	115.603	-3.045	71.009	409.793	-2.920	-2.902
18	245.549	120.067	-3.035	33.660	443.453	-2.910	-2.912
19	272.519	124.139	-3.051	32.638	476.091	-2.926	-2.922
20	293.088	126.547	-3.058	23.752	499.842	-2.933	-2.929

where,

a) Distance between sampling points:

$$y_i = E_{i-1}^2 + E_i^2 - (2E_{i-1}E_i \cos(A_i - A_{i-1})) \quad [3.8]$$

b) Distance downstream:

$$Y_i = 0 \quad [3.9]$$

and

$$Y_{i+1} = Y_i + y_{i-1} \quad [3.10]$$

c) Elevation above a bench mark:

$$H_i = h_i - (-0.125) \quad [3.11]$$

d) Water surface slope is estimated from the regression of distance downstream,  $Y_i$ , against water elevation,  $H_i$ , ie:

$$H' = a + bY \quad [3.12]$$

where,

a = y-intercept

b = water surface slope, or the gradient of the line

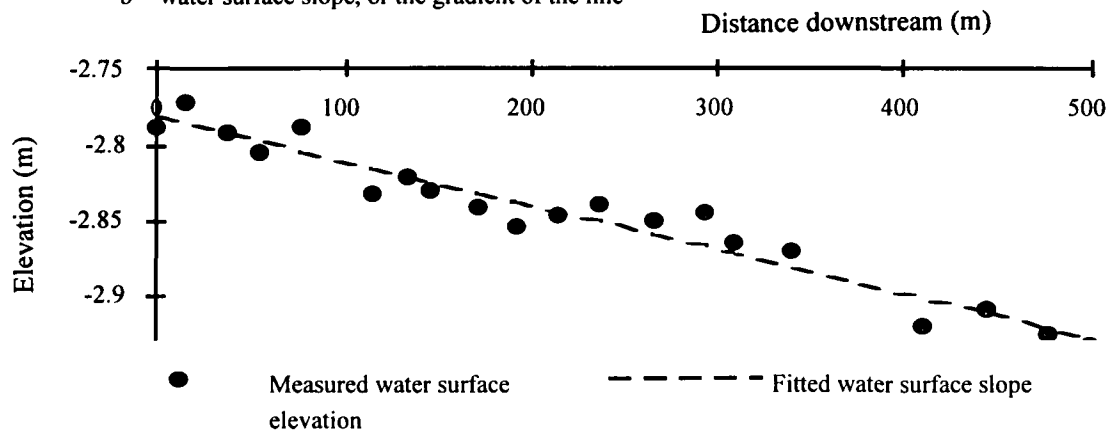


Figure 3.9 Estimation of water surface slope, using the EDM surveying method, at Buildwas (22 March 1995).  
Temporary bench mark = -0.125 m.

### 3.6.2 Flow meter calibration

Given the implications of accurate and precise velocity data, each meter was pre-calibrated separately using a straight 12 x 0.2 x 0.3 m flume (y, z, x) (Plate 3.2) to check and update the manufacturers calibrations. A trolley was used to pull the meter through the centre of the flume at a known and constant velocity; this was designed to minimise edge effects, caused by shear between the water and the flume bed and walls. The trolley was timed between two trip switches, spaced 8 m apart, giving the true velocity of the meter through the water. A counter attached to the current meter recorded the revolutions of the propeller. By comparing the trolley velocity with recorded revolutions, calibration equations for all six current meters and five Ott C2 propellers were established; for a list of results see Table 3.7. These results demonstrated that each of the current meters would measure flow velocity to an accuracy of within 1 % in flumes.

Table 3.7 Results from the calibration of Ott C2 and Braystoke flow meters (all regression equations were significant at  $p < 0.0001$ ).

Current meter	Impeller code	Calibration equation	$r^2$	F ratio
Ott C2 63501	38175	$\bar{u} = 0.255 n_r + 0.008$	0.999	15.4 <sup>a</sup>
	65412	$\bar{u} = 0.250 n_r + 0.012$	0.999	16.0 <sup>a</sup>
	94656	$\bar{u} = 0.256 n_r + 0.005$	0.999	15.2 <sup>a</sup>
	63945	$\bar{u} = 0.059 n_r + 0.038$	0.920	211.5 <sup>a</sup>
	65612	$\bar{u} = 0.105 n_r + 0.024$	0.999	90.4 <sup>a</sup>
Ott C2 37219	38175	$\bar{u} = 0.253 n_r + 0.013$	0.999	15.6 <sup>a</sup>
	64512	$\bar{u} = 0.255 n_r + 0.010$	0.999	15.4 <sup>a</sup>
	94656	$\bar{u} = 0.249 n_r + 0.017$	0.996	16.1 <sup>a</sup>
	63945	$\bar{u} = 0.058 n_r + 0.034$	0.996	300.6 <sup>a</sup>
	65612	$\bar{u} = 0.087 n_r + 0.072$	0.976	130.2 <sup>a</sup>
Ott C2 92500	38175	$\bar{u} = 0.254 n_r + 0.007$	0.999	15.5 <sup>a</sup>
	64512	$\bar{u} = 0.254 n_r + 0.008$	0.999	15.5 <sup>a</sup>
	94656	$\bar{u} = 0.247 n_r + 0.013$	0.999	16.4 <sup>a</sup>
	63945	$\bar{u} = 0.055 n_r + 0.042$	0.999	329.2 <sup>a</sup>
	65612	$\bar{u} = 0.106 n_r + 0.026$	0.999	89.5 <sup>a</sup>
Braystoke 1	1	$\bar{u} = 0.260 n_r + 0.015$	0.999	14.8 <sup>b</sup>
Braystoke 2	2	$\bar{u} = 0.271 n_r + 0.016$	0.999	13.6 <sup>b</sup>
Braystoke 3	3	$\bar{u} = 0.270 n_r + 0.009$	0.999	13.7 <sup>b</sup>

$\bar{u}$  = velocity (m s<sup>-1</sup>)

$n_r$  = number of revolutions per second

<sup>a</sup> F-Crit = 4.20 (at the 95 % confidence limit)

<sup>b</sup> F-Crit = 5.32 (at the 95 % confidence limit)



Plate 3.1 Water surface slope surveying, using the EDM (at Pool Quay).

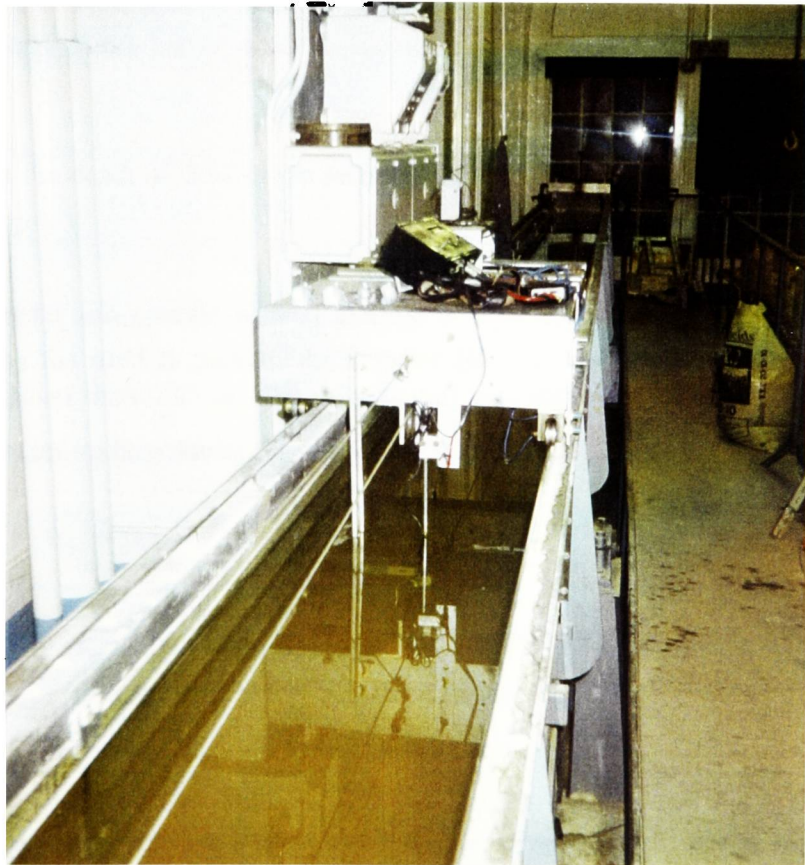


Plate 3.2 Calibration of current meters in a flume.

### 3.6.3 Flow measurement by wading

In suitable conditions (maximum flow depth < 0.7 m; maximum flow velocity < 2 m s<sup>-1</sup>), flow velocity was measured by wading in the channel, using either one or two Ott C-2 impeller current meters mounted on a single wading rod (Herschy, 1985; Jarrett, 1991) (Plate 3.3). This involved first stretching a tape taut across the plane of cross section. Depth measurements were made at a series of verticals across the channel, at roughly equal intervals. In areas of high discharge (Herschy, 1985) and close to the bank edge (Bathurst, 1979), the vertical number was increased to account for steep velocity gradients (Bathurst, 1979). An optimum number of verticals was chosen to balance accuracy with the time to complete the flow measurement; this ensured no significant increase in stage during the sampling period.

Flow velocity was measured at 10 - 15 verticals per cross section, as recommended by Herschy (1985). Flow-boundary interaction dictates the need to increase the number of measurements close to the boundary: the methodologies for velocity measurements in the vertical plane adopted by Bathurst (1979), Bathurst *et al.* (1979) and Bridge and Jarvis (1982) underlie this point. They specify height intervals of between 0.01 - 0.05 m near the bed and 0.1 - 0.2 m near the surface, or every 0.5 m in the intermediate depths. The impeller meter(s) was immersed in the water at each vertical and the number of revolutions of the impeller(s) was timed over 60 seconds (British Standards 1088; Bridge & Jarvis, 1977; Bathurst, 1979); this period was chosen as a compromise between the need to accurately represent the turbulent fluctuations of velocity and to measure flow conditions rapidly (Herschy, 1985) (Table 3.8). Impeller measurements were repeated at a representative number of heights in the vertical (Wilkinson, 1984), with at least 3 measurements close to the bed in order to calculate boundary shear stress (Bridge & Jarvis, 1977) (see section 3.5.8).

Depending upon the depth of flow in the section, the mean velocity in each vertical,  $u_i$ , was calculated in one of three ways:

- a) The Ott meter can operate without stalling in flow depths greater than 3 cm (this restriction was imposed by the need to prevent the impeller ( $\varnothing = 0.02$  m) from hitting the bed). Hence, in flow depths ( $d_i$ ) less than 0.05 m, the velocity ( $u_i$ ) was measured at 0.6  $d_i$ , where depth was measured from the water surface down) (Herschy, 1985) (Figure 3.10), ie:

$$\overline{u_v} = u_{0.6} \quad [3.13]$$

where,  $\overline{u_v}$  = mean vertical velocity of the  $i^{\text{th}}$  vertical (m s<sup>-1</sup>)  
 $u_{0.6}$  = flow velocity at 60 % of the vertical depth (m s<sup>-1</sup>)  
 $d_i$  = depth of water in the  $i^{\text{th}}$  vertical (m)

- b) For vertical depths between 0.05 m and 0.1 m, a mean vertical velocity ( $u_v$ ) was calculated from an average of the velocity at 0.2 $d_i$  and 0.8 $d_i$  (Herschy, 1985), (Figure 3.7) ie:

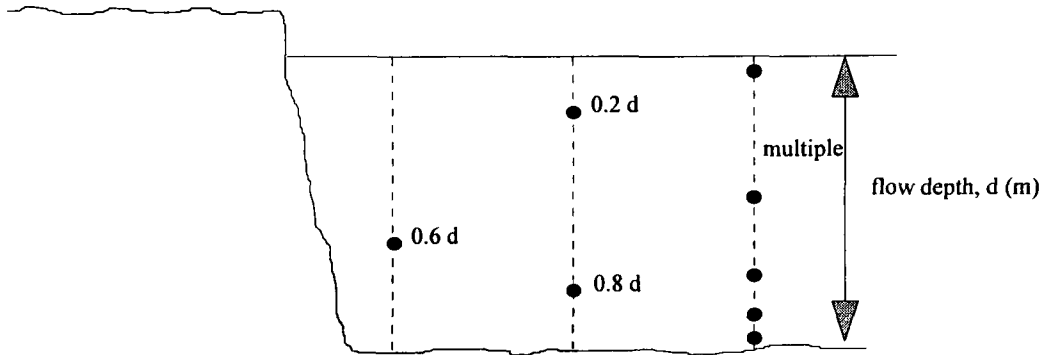


Figure 3.10a Mean velocity in the vertical may be calculated from either: a) a single point measurement at 60 % of the flow depth; b) two measurements at 20 % and 80 %; or c) multiple measurements through the flow depth (Herschy, 1985).

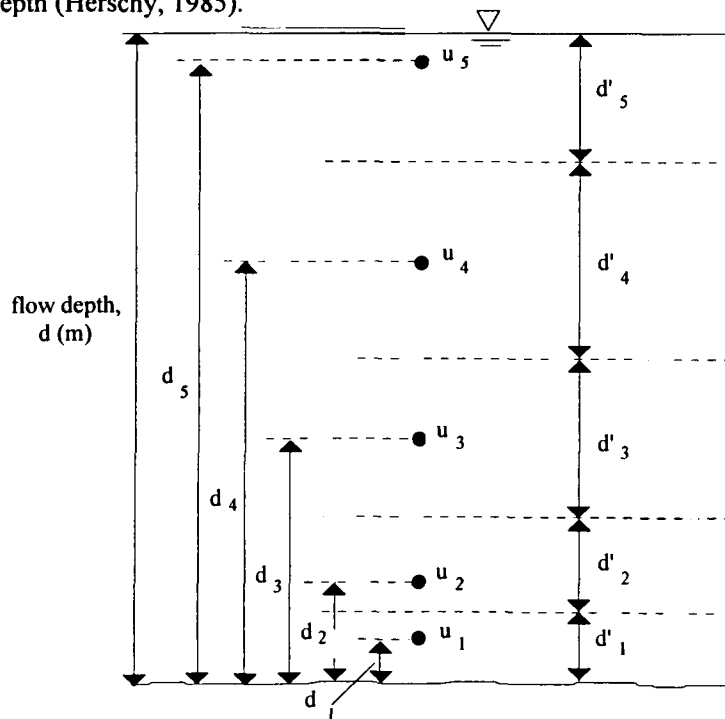


Figure 3.10b The method of calculating the mean velocity in the vertical from multiple measurements requires each point velocity measurement to be weighted according to the interval between successive measurements (after Herschy, 1985).

$$\bar{u}_v = \frac{(u_{0.2} + u_{0.8})}{2} \quad [3.14]$$

where,  $u_{0.2}$  = flow velocity at 20 % of the vertical depth ( $\text{m s}^{-1}$ )  
 $u_{0.8}$  = flow velocity at 80 % of the vertical depth ( $\text{m s}^{-1}$ )

- c) If the vertical depth was greater than 0.1 m, a minimum of three measurements of the vertical were taken (Figure 3.10). Whilst wading, at least one Ott C2 meter was mounted on a 1 m wading rod to decrease the measurement time period, and to maintain the correct vertical location (Ferguson & Ashworth, 1992) (Table 3.8). Between readings, the meters were adjusted manually to different heights in the vertical using a graduated pole, or a meter ruler.

#### 3.6.4 Flow measurement from a boat

If the flow depth was too great for wading ( $d \geq 0.7$  m), the measurements were made from an Avon inflatable boat. The same principles of flow measurement described above apply, although the techniques required to deploy the equipment and gather accurate measurements efficiently and safely are different. Care was first taken to secure a rope taut and low across the line of section, using either metal stakes or trees as supports. This helped the boat maintain a stable position and reduced errors in measured velocities associated with boat movement (Savini & Bodhaine, 1969) (Table 3.8). A winch was fastened tightly to the boat and from this an array of Ott and Braystoke impeller meters were suspended, using a metal cable (section 3.4.5 and Plate 3.4). Three Ott meters were arranged at heights of 0.07 m, 0.21 m and 0.38 m from the base of the 1 m wading rod, and three Braystoke meters at 0.5 m, 0.75 m and 1.0 m (Plate 3.5). This arrangement enabled flow velocities to be measured within 0.12 m from the bed, with minimal interference between impellers. A directional vane was fitted on the back of the wading rod to orientate the meters into the flow, and a streamlined weight was used on the base to hold the array vertical in high flow velocities. All six impeller meters were connected to dataloggers to provide synchronous measurements in each vertical.

Once the correct vertical was located, the array was lowered to the bed. The first set of measurements were taken. The array of meters were then raised a further 0.02 m and the velocities were recorded again, and this sequence was repeated once more. Therefore a minimum of three velocity measurements were recorded close to the bed to estimate the boundary shear stress from the velocity gradient (section 3.7.5). In deep water, the array would be pulled up to record six point velocities at 1 m intervals in each vertical. At least one measurement would be taken of the flow velocity just below the water surface.



Plate 3.3 Flow measurement by wading (at Upper Hafren 3).



Plate 3.4 Flow measurement from a boat (at Bewdley) (photograph by D. M. Lawler).

Table 3.8 Possible errors during current metering (after Herschy, 1978, 1985).

	Type	Description
Instrument error	Flow meter calibration equation	The estimated velocity in any of the impeller meters may be incorrect due to inaccurate calibration procedure
	Damage to the propeller	Damage after calibration will result in inaccurate velocities
	Faulty flow meter / lack of oil	Lack of lubrication or a faulty spindle will slow the impeller(s)
	Faulty timer	Electronic pulses from the meter may not be mis-recorded by the counter
	Inertial effects in low / turbulent flow	High, intermittent velocity bursts will lead to an overestimate of point flow velocity due to inertial effects in the impeller
Natural error	Low flow depth	Metering in depths (< 0.1 m) may cause snagging / stalling of impeller(s)
	Turbulent pulses	Turbulent bursts over short and long time-scales will create highly variable mean point velocities
	Unsteady surface	A broken surface will create highly variable velocities close to the surface
	Lateral / secondary flow	A significant proportion of the flow velocity may be unrecorded as it is secondary flow
	Vegetation	May cause stalling / snagging / damage to impeller
	Coarse gravel bed	May cause stalling / damage to impeller
Operator error	Incorrect time measurement	Velocities may not be timed over exactly 60 seconds
	Meters not pointing directly into the primary flow	Meters may be pointing upstream, and not into the primary flow
	Incorrect replacement of meters on bed after adjustment	Will record incorrect velocities, boundary shear stresses and zero plane displacements
	Wading rod not vertical	Rod may not be held / suspended vertically above the base
	Incorrect estimation of measurement height	This may be caused by the readjustment of meter elevation on wading rod, or winch
	Incorrect location of the vertical	An error in reading the tape, or locating the vertical
	Non-uniform flow through the reach	Roughness formulae are strictly only applicable to uniform flow
	Incorrect estimation of slope (see Table 3.5)	
	Incorrect estimation of hydraulic radius (see Table 3.5)	
	Incorrect estimation of channel area (see Table 3.5)	
Incorrect estimation of grain size (see Table 3.6)		

The point values of streamwise velocity were used to calculate the mean velocity in the vertical, using the method described in Figure 3.10 (Herschy, 1985), and evaluate the boundary shear stress (section 3.9) and the isovel distribution. The weighted mean velocity was calculated from,

$$\bar{u}_v = \sum_{i=1}^{i=n_v} u_i d'_i \quad [3.15]$$

$$d'_i = \frac{d_{i+1} + d_i}{2} - \frac{d_i + d_{i+1}}{2} \quad [3.16]$$

- where,
- $u_i$  = the  $i^{\text{th}}$  measurement of streamwise velocity from the bed ( $\text{m s}^{-1}$ ), eg: the first velocity measurement from the bed has  $i = 1$ , the second,  $i = 2$ , etc.
  - $d'_i$  = interval distance between depth measurements (m) (Figure 3.10b)
  - $d_i$  = the  $i^{\text{th}}$  measurement of distance from the bed (m)
  - $i$  = the sequence of velocity readings, taken from the bed upwards
  - $n_v$  = the number of point velocity readings in the vertical

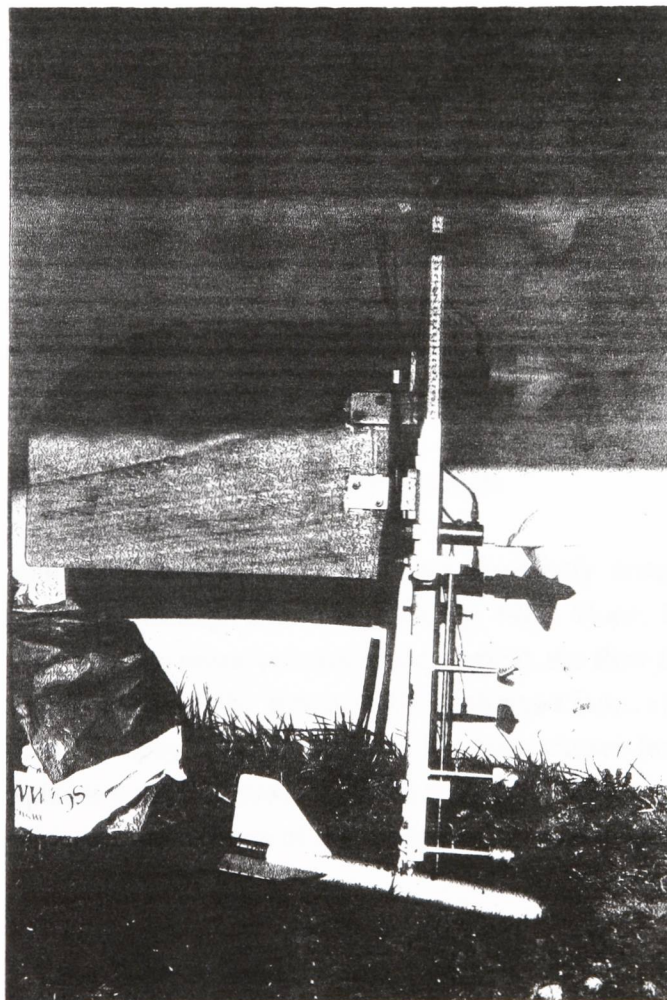


Plate 3.5 The current meter array design for flow measurement from a boat at the Bewdley study site (photograph by D. M. Lawler).

### 3.6.5 Indirect measurement of flow velocity

In conditions where it was unsafe to use the boat (flow velocity exceeded the maximum velocity of the boat ( $2 \text{ m s}^{-1}$ ) and/or water width exceeded the tape length ( $> 50 \text{ m}$ )), the flow velocity was estimated using either discharge data from EA gauging stations (3.7.3), or resistance equations in the absence of any velocity or discharge data. For sites close to a gauging station the stage at the section was surveyed and the cross sectional area of the water calculated. From the continuity equation,  $Q = A_t \bar{u}$ , the mean sectional velocity was calculated using discharge data for the time of measurement, kindly supplied by the Institute of Hydrology at Plynlimon or the EA. Similarly, for the trash line survey, mean velocity was calculated from the estimated peak discharge and channel area; for details of how discharge was derived during this survey, see section 3.8. The errors that may result from these direct and indirect methods of calculating mean flow velocity are described in Table 3.5 and section 3.11.

## 3.7 Calculation of discharge

### 3.7.1 Introduction

Discharge was calculated by several methods during this study because of difficulties in measuring flows at low stage in the headwaters, or at high stage in the lowlands. The majority of the measurements were derived from direct flow measurement. However, it was sometimes appropriate to employ alternative techniques when at the limits of the current metering capabilities; hence, in the upper ungauged reaches, discharges were measured volumetrically, whilst at high flows further downstream, EA-gauged flow information was used to eliminate the need to personally measure flows in dangerous conditions. The technique adopted for calculating discharge following the trash line survey will be reviewed in section 3.8 as this required a detailed analysis of available flow resistance methods; also, a review of when the different techniques were used is reviewed in section 3.10.3.

### 3.7.2 Discharge calculation from flow velocity measurements

The velocity-area technique (3.6.3) is a common and rigorously tested method for estimating the discharge of open channel flow through a section (Herschy, 1985; Shaw, 1988). Discharge is calculated from the sum of the product of the mean velocity in the vertical, the flow depth and water width between verticals (Equation 3.10 and Figure 3.5b). It may either be derived from, a) the mid-section method, or b) the mean-section method (Herschy, 1985). The latter has been chosen because the mid-section method places too great an emphasis on the accuracy of mean velocities in each vertical and the vertical depths. It may also omit a small area at the margin of the channel if velocity measurements are not made close to the banks.

$$Q = \sum \bar{u} A_t = \sum_{i=1}^{i=N} \left( \frac{u_i + u_{i+1}}{2} \right) \left( \frac{d_i + d_{i+1}}{2} \right) (w_{i+1} - w_i) \quad [3.17]$$

### 3.7.4 Discharge estimation from volumetric gauging

In small, upland reaches volumetric gauging provides the most accurate means of calculating discharge. This method involves capturing a volume of water in a container over a measured period of time; the stream discharge is therefore the volume per unit time, or:

$$Q = \frac{V}{t} \quad [3.18]$$

where,  $V$  = volume of water ( $m^3$ )  
 $t$  = time (seconds)

It is important that all the water flowing along a channel is captured. Hence, a natural (or engineered) control structure may be used to confine the flow through a small area, and thereby avoid any water loss from inter-granular or braided channel flow. This study relied upon small waterfalls in the headwaters to calculate discharge when the flow was too shallow to gauge with current meters. A graduated bucket was held beneath the waterfall until nearly full. The time period ( $t$ ) from the beginning of the experiment to the withdrawal of the bucket was timed. This was repeated five times to ensure a reasonably precise result.

### 3.7.3 IH / EA gauging station data

The Institute of Hydrology (IH) gauge flows at two stations in the Plynlimon catchment: Hafren Flume and Severn Flume (Figure 3.1 and Table 3.3). These data were used to evaluate the downstream variation of discharge at the ungauged upper study sites following the trash line survey of January 1996 (see section 3.8), and reclassify flows in this region by using the historical data record to calculate the flow frequency at each site. Discharge data from the network of Environment Agency (EA) gauging stations (Figure 3.1 and Table 3.3) were used when conditions were unsuitable for direct flow measurement (see sections 3.6 and 3.9). The discharge at the time of the water surface survey was then used in the channel hydraulic calculations. However, in ungauged reaches discharge was estimated, based on the gauged flow at the nearest upstream and downstream gauging stations.

## 3.8 Estimation of discharge in the Upper Severn

### 3.8.1 Trash line survey

Between December 1995 and January 1996, three large flow events occurred in the upper reaches of the Severn caused by a combination of heavy frontal rainfall and rapid snow melt. These events could not be measured directly in real time, on account of logistical problems, but reconnaissance surveys of remnant trash lines high on the bank-faces or floodplain enabled the water surface slope of the peak level to be reconstructed. The trash line consisted of broken reeds, pine needles, surface discoloration, fine sediment and small branches (Plate 6a). These deposits provided significant evidence for a recognisable upper



Plate 3.6a Good evidence for trash lines in the field (Severn Flume).



Plate 3.6b Poor evidence for trash lines in the field (Upper Hafren 3).

flow level, although the trace was not always convincing (Plate 6b); a level of confidence was, therefore, assigned to each measurement (0 = no confidence, 3 = very confident).

The trash-line surveys in the upper catchment yielded information about the stage (section 3.4.4), width (section 3.4.5), and water surface slope (section 3.5.3) of the flow at each site during the event. From these it was possible to ascertain various channel geometry parameters, such as the area, hydraulic radius and mean depth. Although this method was inevitably inaccurate due to the reliance on limited data and uncertainties relating to the mechanics of debris deposition (eg: Baker & Kochel, 1988), it provided an excellent opportunity to evaluate the channel hydraulics at high flows. Indeed, this technique has been widely used for the determination of bankfull hydraulic and geometric properties (Lewin, 1983; McEwen, 1994), flood flow levels (Jarrett, 1990) and the magnitude of catastrophic flood events (Baker & Costa, 1987).

### 3.8.2 Evaluation of discharge

Five flow resistance equations were chosen from the literature to test against the measured medium flow data in the upper reaches (equations 3.13 - 3.17); based upon their performance, the most successful would be chosen to estimate discharge at high flow in the ungauged reaches. These were chosen because they were all derived for gravel bed rivers, they are popular and have had proven success on a variety of data sets (Marcus *et al.*, 1992).

Limerinos (1970)

$$f = \left( \frac{1}{1.16 + 2 \log(R/D_{84})} \right)^2 \quad [3.19]$$

Lacey (1946-1947)

$$\bar{u} = 10.8d^{0.67}s^{0.33} \quad [3.20]$$

Hey (1979)

$$\frac{1}{\sqrt{f}} = 2.03 \log \frac{11.75R}{3.5D_{84}} \quad [3.21]$$

Jarrett (1984)

$$n = 0.39s^{0.38}R^{-0.16} \quad [3.22]$$

Bathurst (1985)

$$n = \frac{0.3194R^{1/6}}{4.0 + 5.62 \log(R/D_{84})} \quad [3.23]$$

where,  $D_{84}$  = grain size (84<sup>th</sup> percentile) (m)

The five equations consist of two separate forms:

- a) flow resistance dominated by particle size. The equations by Limerinos (1970), Hey (1979) and Bathurst (1985) apply a relative bed roughness coefficient ( $R/D_{84}$ ) to simulate the heterogeneous nature of the coarse boundary material. Burkham and Dawdy (1976) suggested that the roughness height of the gravel layer is 3.5 times the  $D_{84}$  grain size, hence Hey (1979) uses this coefficient,  $b$ , in his equation. Hey also attempted to approximate the roughness effect of the channel planform through a shape factor,  $a$  (where  $a$  is the ratio of the hydraulic radius to the perpendicular distance from the perimeter to the point of maximum velocity), based on the  $a$  coefficient in the Colebrook-White equation (in which  $a = \text{antilog}(E \kappa / 2.30)$ , where  $E$  is a coefficient). Here, the  $a$  coefficient was assumed to equal a value of 11.75, ie: near rectangular channel cross section with a width / depth ratio of 15.0.
- b) flow resistance related to hydraulic variables. Bray (1982) and Jarrett (1984) both used multiple regression between the Manning's  $n$  and slope. Slope has a strong control over flow resistance because as it increases, so too does bed particle size, wake turbulence and the energy lost from hydraulic jumps (Jarrett, 1990). This technique was favourable where no prior knowledge existed of the boundary roughness and has been proved as accurate as other techniques for high in-bank flows (Bray, 1982).

Table 3.9 and Figure 3.11 demonstrates the relative performance of these equations against the measured (medium flow) discharge data. The roughness coefficients ( $n$  and  $f$ ) were used in the Manning's or Darcy-Weisbach equations, according to the original use by the authors, to estimate mean velocity and discharge; this therefore assumes uniform flow conditions (unchanging cross section and velocity along a reach) and a water slope equal to the energy slope. In the upper reaches of the Severn, this was a total assumption, however reaches were chosen which closely approximated this ideal condition.

From Table 3.9 it is clear that all the equations perform well against the medium flow data set and are significant at the 95 % confidence limit. However, Figures 3.11 and 3.12 demonstrate that four of the equations consistently over-estimate the measured values and are highly variable; this is illustrated by the magnitude of the standard errors which are greater than 1.0. The Hey equation appears to fit the measured data set across the discharge range and has a standard error of only 0.27, although it too has a tendency to over-estimate discharge. The variability in these estimates may be explained, in part, by secondary flow effects in non-uniform reaches, obstructions, vegetation and sediment load, and by backwater effects through pools. However, the Hey equation was chosen to evaluate the discharges in the ungauged reaches at high flow, based upon the evidence presented above.

Table 3.9 Performance of the various flow resistance equations against the measured (medium) flow data

Author	Equation	r <sup>2</sup>	Significant F	Standard Error
Limerinos (1970)	$f = \left[ \frac{1}{1.16 + 2 \log \left( \frac{R}{D_{84}} \right)} \right]^2$	0.991	< 0.001	1.099
Jarrett (1984)	$n = 0.39s^{0.38}R^{-0.16}$	0.985	< 0.001	1.694
Hey (1979)	$\frac{1}{\sqrt{f}} = 2.03 \log \left( \frac{aR}{bD_{84}} \right)$	0.988	< 0.001	0.268
Lacey (1946-1947)	$\bar{u} = 9.6d^{0.67}s^{0.32}$	0.989	< 0.001	1.014
Bathurst (1985)	$\left( \frac{8}{\sqrt{f}} \right)^{0.5} = 5.62 \log \left( \frac{R}{D_{84}} \right) + 4$	0.991	< 0.001	1.161

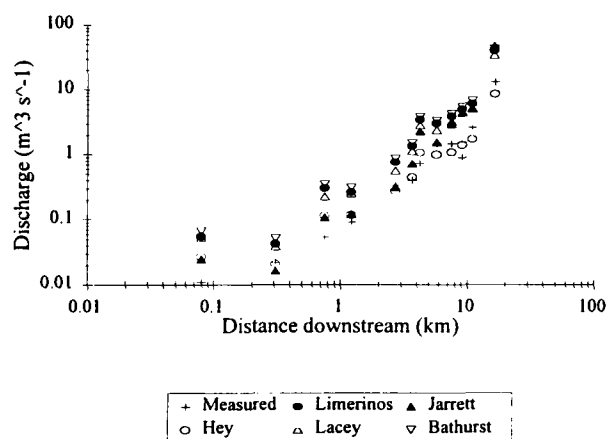


Figure 3.11 A comparison between measured discharges at a MEDIUM flow level and 5 flow resistance equation estimates.

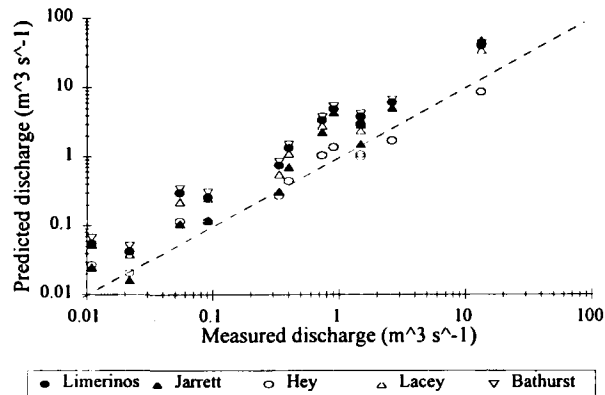


Figure 3.12 A comparison between measured and predicted discharge at a MEDIUM flow level.

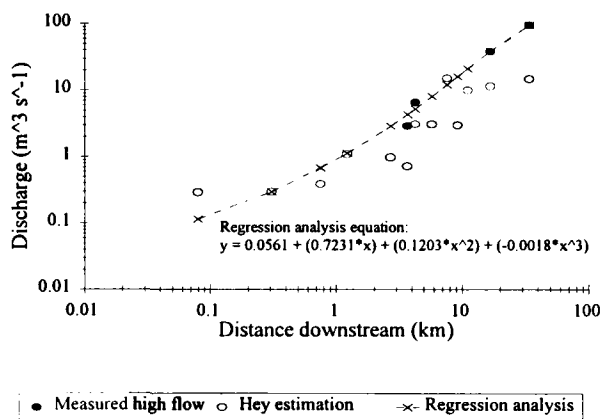


Figure 3.13 A comparison between the Hey equation (1979) and the regression estimation technique against measured HIGH flow values.

Figure 3.13 illustrates the performance of the Hey equation against four measured values of high discharge at gauging stations along the reach. It is clear that the difference in site geometry and bed material characteristics produces a highly variable downstream distribution of discharge. More importantly, the estimates fall below the measured values, particularly further downstream. This difference relates to an under-estimation of discharge at Llanidloes of  $26.51 \text{ m}^3 \text{ s}^{-1}$  and Caersws of  $78.59 \text{ m}^3 \text{ s}^{-1}$  and a failure to estimate the discharge to within 50 % at all four sites (Table 3.10). This level of inaccuracy was unacceptable, and therefore a regression analysis was tested.

Table 3.10 The performance of the Hey (1979) equation against the measured (high) flow data.

Distance downstream (km)	High Discharge			
	Measured Discharge ( $\text{m}^3 \text{s}^{-1}$ )	Predicted Discharge ( $\text{m}^3 \text{s}^{-1}$ )	Absolute difference (Obs - Pred) ( $\text{m}^3 \text{s}^{-1}$ )	Percentage difference (%)
3.71	2.89	0.72	2.18	75.09
4.26	6.48	3.10	3.38	52.16
16.88	37.84	11.33	26.51	70.06
34.10	93.05	14.46	78.59	84.46

A non-linear regression relationship was evaluated from the four measured discharge values and an additional data point at the source (0.08 km) (Figure 3.13). This additional point was included to increase the number of data points in the analysis and produce a reasonable estimate of discharge close to the source; a value of  $0.01 \text{ m}^3 \text{ s}^{-1}$  was assigned to this point, based on field evidence and resistance equation estimates. The regression method estimates measured discharge to within 50 % at all four gauged sites, and within 20 % at three sites (Table 3.11), although as Figure 3.13 illustrates, it fails to predict the step in discharge between the gauges at 3.71 and 4.26 km downstream. This step relates to the Hore confluence with the Severn between these two sites. Comparison between the Hey equation and the regression method demonstrate the improved level of accuracy in the latter (Tables 3.10 and 3.11) and a greater level of significance in the result (Table 3.12). This regression method was therefore used to evaluate discharge at the eight ungauged reaches where trash-line surveys were performed. Section 3.10 will describe how these and other measured discharges were classified in this study.

Table 3.11 The performance of the regression analysis against the measured (high) flow data

Distance downstream (km)	High Discharge			
	Measured Discharge ( $\text{m}^3 \text{s}^{-1}$ )	Predicted Discharge ( $\text{m}^3 \text{s}^{-1}$ )	Absolute difference (Obs - Pred) ( $\text{m}^3 \text{s}^{-1}$ )	Percentage difference (%)
3.71	2.89	4.303	1.41	48.9
4.26	6.48	5.181	-1.30	20.05
16.88	37.84	37.88	0.05	0.11
34.10	93.05	93.23	0.18	0.19

Table 3.12 A statistical comparison of the Hey equation and regression analysis

Test statistic	Hey estimate	Regression estimate
F ratio	11.99	2844.45
Significant p	0.074	0.000
r <sup>2</sup>	0.857	0.999
Standard Error	3.03	1.360

F-crit = 18.51 at a significance level of 0.05

### 3.9 Field measurement and calculation of boundary shear stress

#### 3.9.1 Introduction

Boundary shear stress was calculated in this study using the velocity gradient method. This was measured in the field by concentrating velocity measurements close to the channel bed, within the boundary layer. The use of this method in ‘natural’ channels is limited (Bridge & Jarvis, 1976, 1982; Ferguson & Ashworth, 1992), possibly as a result of the difficulties encountered when measuring flow velocity in the near-bed region (section 3.9.2) and validity of the assumptions employed to calculate boundary shear stress (section 3.9.3).

#### 3.9.2 Field measurement technique

Detailed flow velocity measurements in the near-bed region were made possible by concentrating flow velocity analysis close to the bed (3.6.2 and 3.6.3). A minimum of three measurements were made at each vertical, either by repeatedly altering the height of a current meter on a wading rod (3.6.2), or raising the array of meters suspended from the boat by small vertical increments (3.6.3). However, both methods were prone to difficulties. The repeated replacement of a wading rod in the same vertical on a rough bed is extremely difficult; similarly, the continuous movement of the boat would result in the deviation of the meters from the vertical. These would lead to velocity-depth measurements in a variety of verticals, and an unrelated velocity gradient. An alternative problem associated with this ‘replacement’ technique regards the quasi-periodic turbulent bursting in the boundary layer: the longitudinal velocity at a given depth is not constant over time, causing consecutive velocity measurements to record pulses of flow, and thereby distorting the vertical velocity gradient. The first problem was approached by minimising the number of meter replacements on the bed, by using several velocity meters mounted on a wading rod (Table 3.8). The latter problem was largely overcome by timing flows over 60 seconds and thereby avoiding short, high velocity bursts (Table 3.8).

### 3.9.3 Calculation of boundary shear stress

The estimation of boundary shear stress using the velocity gradient method is strictly only applicable to the lower 10 % of the flow (eg: Bathurst, 1979). From plots of velocity profiles in this region, boundary shear stress was calculated by, a) regressing point velocity against flow depth, or b) using the 'Prandtl-von Karman universal velocity distribution law' (Schlichting, 1979) for each point velocity measurement (Figure 3.14). The former has been preferred in this study due to the ease by which it may be used to calculate the boundary shear stress (Ferguson & Ashworth, 1992), and the consistency of the results in comparison with the latter (Figure 3.14). This technique assumes the following factors which must be considered:

- a) the von Karman value,  $\kappa$ , is constant;
  - b) boundary roughness and the zero plane displacement,  $d_0$ ;
  - c) the velocity profile is logarithmic;
  - d) the height of the boundary layer is approximately 10 % of the flow depth.
- a) the von Karman value,  $\kappa$ , is constant. The value of  $\kappa$  is usually obtained by plotting ( $u / u^*$ ) against  $\log (y / d_0)$ . This technique is valid in the lower regions of the flow where the profile is semi-logarithmic and  $\kappa$  may be assumed to be constant (Bathurst, 1982). However, when sediment is suspended in the flow, the  $\kappa$ -value has been found to vary between 0.2 (Vanoni & Nomicos, 1959) and 0.42 (Vanoni, 1946).  $\kappa$  is commonly assumed to be constant at the value of 0.4 (Nikuradse, 1932; Bridge & Jarvis, 1977; Bathurst, 1982), 0.41 (Coles, 1968) or 0.418 (Patel, 1968) which makes the estimation of boundary shear stress possibly inaccurate in sediment-laden flows.
- b) boundary roughness and the zero plane displacement,  $d_0$ . To calculate the shear stress at the true boundary between the fluid and the point of zero flow velocity, it is necessary to either position the measuring device at this point or extrapolate the flow velocity data from the upper layers down to this height,  $d_0$ . As Hinze (1975) notes, uncertainty is found if at the plane,  $y = 0$ , the wall is rough (Figure 3.14). When using wading rods or weights, the zero level of the bed is represented by the top of the clast below the measuring rod when it hits the channel bed (Wiberg & Smith, 1987; 1991). Therefore, to define the level of zero velocity (the zero plane displacement,  $d_0$ ) an assumption must be made about, i) the roughness distribution, or ii) the velocity distribution. The former (i), typically uses a displacement factor,  $k_s$ , calculated from the factorised grain size (ie:  $0.5D_{50}$  (Marchand *et al.*, 1984),  $0.1D_{84}$  (Whiting & Dietrich, 1989; Ferguson & Ashworth, 1992),  $3.5D_{84}$  (Leopold *et al.*, 1964; Burkham & Dawdy, 1976; Hey, 1979)), whereas for the latter (ii) it may be assumed that either the bed surface represents the point of zero velocity (Vanoni & Nomicos, 1959; Ghosh & Roy, 1970; Bathurst, 1979) or that the logarithmic velocity distribution may be extrapolated to the depth at which the velocity is zero (Zippe & Graf, 1983; Ferguson & Ashworth, 1992).

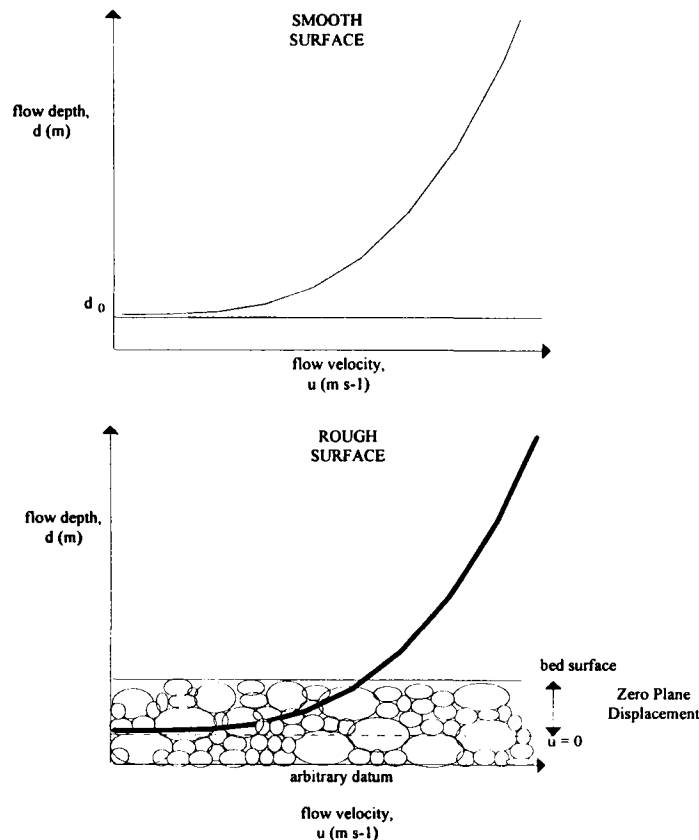


Figure 3.14 Inter-granular flow, velocity profiles and the zero plane displacement (ZPD).

- c) the velocity profile is logarithmic. The ‘law of the wall’ equation for a velocity profile is strictly only applicable in the near wall region where it is assumed that the shear in the fluid equals the shear at the bed (Richards, 1982). Boundary shear stress can therefore only be estimated from measurements made in this region. In the outer region of the flow, where turbulence is less influenced by shear at the boundary (Hinze, 1975), it is possible to define a permutation of the ‘law of the wall’ equation to describe the velocity distribution (ie: velocity defect law (Zippe & Graf, 1983; Kirkzog, 1989); parabolic law (Vedula & Achanta, 1985)).
- d) the height of the boundary layer is approximately 10 % of the flow depth. The direct (Pitot tubes) or indirect (velocity gradient) measurement of boundary shear stress is confined to the turbulent flow in the near-wall region. This region is commonly assumed to represent 10 % of the flow depth (Bathurst, 1979; Karim & Kennedy; 1987), however, 15 % (Bridge & Jarvis, 1977; Vedula & Achanta) and 20 % (Ferguson & Ashworth, 1992) have also been used due to the difficulty of measuring velocity with current meters close to the boundary.

This study will assume that the velocity profile is logarithmic only in the boundary layer, which extends to 10 % of the flow depth, as measured from the channel bed surface. The ZPD may be calculated by extrapolation of the velocity gradient in the boundary layer, and the von Karman value is assumed to be constant at 0.4.

Figure 3.14 The calculation of boundary shear stress from velocity profiles: a worked example

No.	Depth (m)	Standardised depth	ln (depth)	Velocity (m s <sup>-1</sup> )	Boundary shear stress (N m <sup>-2</sup> ): Regression method <sup>1</sup>	Boundary shear stress (N m <sup>-2</sup> ): Gradient method <sup>2</sup>
	d	d'(a)	ln(d)(b)	u	(c)	(d)
1	0.085	0.032	-2.465	0.405	3.73	3.10
2	0.105	0.040	-2.254	0.434		0.21
3	0.125	0.047	-2.079	0.440		5.65
4	0.210	0.079	-1.561	0.538		4.35
5	0.230	0.087	-1.470	0.553		2.30
6	0.250	0.094	-1.386	0.563		Average= 3.12
7	0.375	0.142	-0.981	0.646		
8	0.590	0.223	-0.528	0.744		
9	0.840	0.317	-0.174	0.790		
10	1.090	0.411	0.086	0.820		
11	1.640	0.621	0.498	0.817		
12	1.770	0.668	0.571	0.819		
13	1.935	0.730	0.660	0.839		
14	2.150	0.811	0.765	0.858		
15	2.400	0.906	0.875	0.883		
16	2.630	0.992	0.975	0.820		

a) Standardised depth is calculated from: 
$$d' = \frac{d}{2.65} \quad [3.25]$$

where, flow depth = 2.65. This is used to ascertain which velocity measurements lie within the boundary layer ( $d' \leq 0.1$ )

b) Flow depths are converted into natural logarithms for the 'regression method'

c) The regression method (Ferguson & Ashworth, 1992)<sup>1</sup> uses the 'law of the wall' equation,

$$\frac{u}{u^*} = \frac{1}{\kappa} \ln\left(\frac{y}{d_0}\right) \quad [3.26]$$

in which

$$u^* = \left(\frac{\tau}{\rho}\right)^{0.5} \quad [3.27]$$

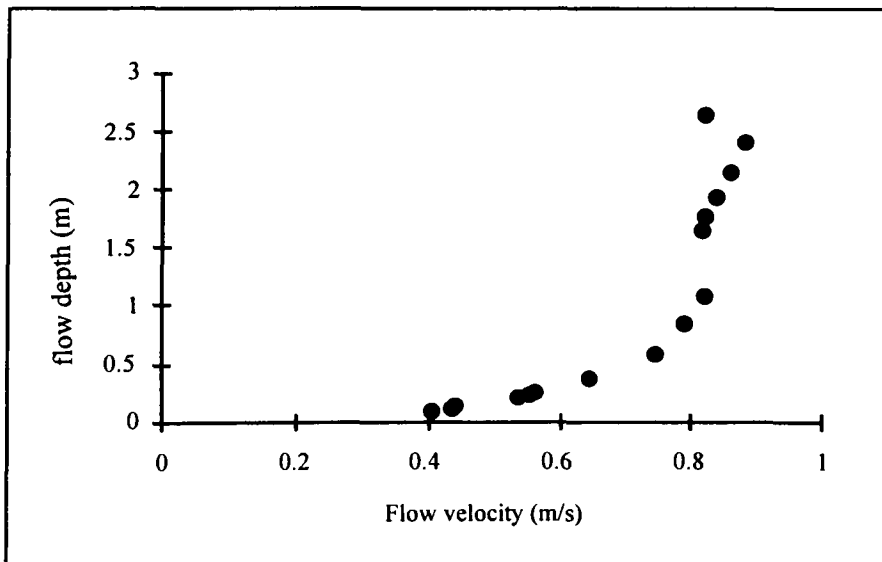
An average for the entire boundary layer is estimated by regressing the flow depth,  $d$ , against flow velocity,  $u$ . The x-coefficient, or gradient of the line,  $b$ , produced by the regression analysis is used in the following equation to calculate  $\tau_b$ .

$$\tau_b = 1000(\kappa b)^2 \quad [3.28]$$

d) The gradient method (Bridge & Jarvis, 1977; Bathurst, 1979)<sup>2</sup> is similar to the former in that it uses a formulae derived from (ii), however, shear stress is calculated from the average of each pair of velocity - depth measurements in the boundary layer. The equation is:

$$\tau_b = \rho \left[ \frac{(u_2 - u_1)}{\left( \frac{1}{K} \right) \ln \left( \frac{y_1}{y_2} \right)} \right]^2 \quad [3.29]$$

The results for each method are presented in the table. There is little difference between the estimates of boundary shear stress. The regression method is accurate to within 25 % using the method of error approximation described by Wilkinson (1984).



### 3.10 Flow classification

#### 3.10.1 Introduction

The preliminary flow classification offered a simple framework for identifying a range of flow magnitudes in the field. However, flow frequency is a more appropriate and established method of evaluating the flow magnitude. This section discusses the implications of this reclassification on the measured flow hydraulics (section 3.10.2) and reflects upon the methods used to measure flows at the 25 study sites (section 3.10.3).

#### 3.10.2 Flow classification by flow frequency

Channel hydraulics were measured at almost all 25 study sites for 3 separate flow levels (Table 3.13). These flow levels were defined in the field by the water stage / bankfull stage ratio (section 3.4.4). However, this form of classification is inappropriate when measuring a range of flows along a river; for example, a value of 0.8 from this ratio (defined as a high flow) may relate to a flow which is equalled or exceeded 90 % of the time at one section along the river, and 10 % at another. This is caused by the variation in channel dimension and shape, and hydrological regime through the catchment. It was therefore considered appropriate to redefine the flows in terms of the exceedance frequency,  $F$  (defined as the frequency a discharge is greater than a given magnitude). The revised classification is shown in Table 3.12. The flow levels originally defined as 'low' fall comfortably within the frequency bracket  $70 \leq F \leq 100$  %. Similarly, most of the 'high' flows have a frequency of between  $0 \leq F \leq 10$  %. The 'medium' flows typically fall somewhere between these limits ( $10 \leq F \leq 70$  %).

There are three general exceptions to this rule:

- a) The medium flow exceedance frequencies for the upper 3 sites are greater than 70 %.
- b) The high flow exceedance frequencies for the upper 2 sites are greater than 10 %.
- c) Flows measured at Llandinam do not fit this revised classification.

The first two anomalies can be explained by the reference gauge used. All sites upstream of Tanllwyth are classified using the flow duration curve from Hafren Flume. In the headwaters, the drainage network is dense and discharge increases rapidly downstream. Therefore, a discharge of  $0.1 \text{ m}^3 \text{ s}^{-1}$  has an exceedance frequency at the Hafren Flume of 50 %, but probably  $< 10$  % in the headwaters. As no data exists for the upper study sites, it will be assumed that the measured flows lie within equivalent exceedance frequency limits. The third anomaly is attributable to sampling at incorrect flow levels, and thus the hydraulics measured at Llandinam were considered only at the medium flow level.

#### 3.10.3 Timing, method and location of flow measurement

A variety of flow gauging techniques were adopted due to the diverse range of flow conditions at the spatial scale (headwaters to the lowlands) and also with increasing stage (low flow to bankfull). Table

3.14a and 3.14b illustrate where the different methods were used; note that abbreviations for study site names have been adopted and shall be used as figure labels throughout this chapter, see also Figure 3.1 for study site locations. The criteria for dividing the flow into three levels was defined in 3.4.4.

Table 3.13 A classification of flow magnitude based on discharge exceedance frequencies.

	Study site	IH* / EA Gauging station used	Frequency equalled or exceeded (%)		
			Low flow (F ≥ 70 %)	Medium flow (10 ≤ F ≤ 70 %)	High Flow (F ≤ 10 %)
1	Upper Hafren 1	Hafren Flume*	> 99	97	19
2	Upper Hafren 2	Hafren Flume*	> 99	94	19
3	Upper Hafren 3	Hafren Flume*	98	85	14
4	Hafren Forest	Hafren Flume*	98	67	2
5	Hafren Falls	Hafren Flume*	92	12	3
6	Tanllwyth	Hafren Flume*	89	12	< 1
7	Severn Flume	Severn Flume*	90	19	< 1
8	Picnic Bridge	Severn Flume*	70	9	3
9	Severn Gorge	Llanidloes	70	50	2
10	Rhydyronnen	Llanidloes	99	69	40
11	Severn Ford	Llanidloes	99	35	6
12	Mount Severn	Llanidloes	98.5	56	5
13	Dolwen	Caersws	70 & 46	18	5
14	Llandinam	Caersws	50	n.d	12
15	Caersws	Caersws	74 & 68	12	5 & 7
16	Newtown	Abermule	75	n.d	3
17	Abermule	Abermule	70	12	2.5
18	Dyffryn	Buttington	77	20	3
19	Pool Quay	Buttington	77	11	3
20	Crew Green	Montford	96	35	< 1
21	Montford	Montford	96	35	8
22	Buildwas	Buildwas	> 99	40	4
23	Bridgnorth	Bewdley	75	50	4
24	Bewdley	Bewdley	75 & > 99	50	5
25	Saxons Lode	Saxons Lode	> 99	40	5

Table 3.14 The location and timing of field visits for: a) all sites upstream of, and including, Abermule; and b) all sites downstream from Abermule. Figure 3.16a depicts field visits in terms of a reference flow at Abermule, and the latter (Figure 3.16b) as a reference flow from Bewdley.

a) Study sites upstream of Abermule

	Code	Study Site	Date
LOW	L1	Dol, Caer	18 Jul 1994
	L2	Rhy, SF, MS	21 Jul 1994
	L3	HFor, HFalls, Tan, SF, PB, SG	28 Jul 1994
	L4	Dol, Llan, Caer	20 Apr 1995
	L5	New	26 Apr 1995
	L6	UH1, UH2, UH3, HFor, HFalls, Tan, SF	9 Jun 1995
	L7	Aber	28 Jul 1995
MEDIUM	M1	HFalls, Tan	31 Jan 1995
	M2	PB, SF	1 Feb 1995
	M3	UH1, UH2, UH3, HFor	9 Feb 1995
	M4	SF, Rhy	16 Feb 1995
	M5	MS	23 Feb 1995
	M6	Dol, Llan	24 Feb 1995
	M6	Aber	10 Mar 1995
HIGH	H1	Dol, Caer	31 Jan 1995
	H2	Dol, Llan, Caer, New, Aber	17 Feb 1995
	H3	UH1, UH2, UH3, HFor, HFalls, Tan, SF, PB, Rhy, SF	23 Dec 1995

b) Study sites downstream from Abermule

	Code	Study Site downstream of Abermule	Date
LOW	L1	Bws	22 Mar 1995
	L2	Bewd	27 Apr 1995
	L3	B'north	3 Mar 1995
	L4	Dyff, PQ	19 May 1995
	L5	CG, Mont	16 Jun 1995
	L6	SL	18 Oct 1995
MEDIUM	M1	Dyff	9 Mar 1995
	M2	Mont	21 Mar 1995
	M3	PQ, CG	9 Jan 1996
	M4	Bws, B'north, Bewd, SL	7 Mar 1996
HIGH	H1	Bws, B'north, Bewd	3 Feb 1995
	H2	Dyff, PQ, CG	17 Feb 1995
	H3	Mont, SL	23 Dec 1995

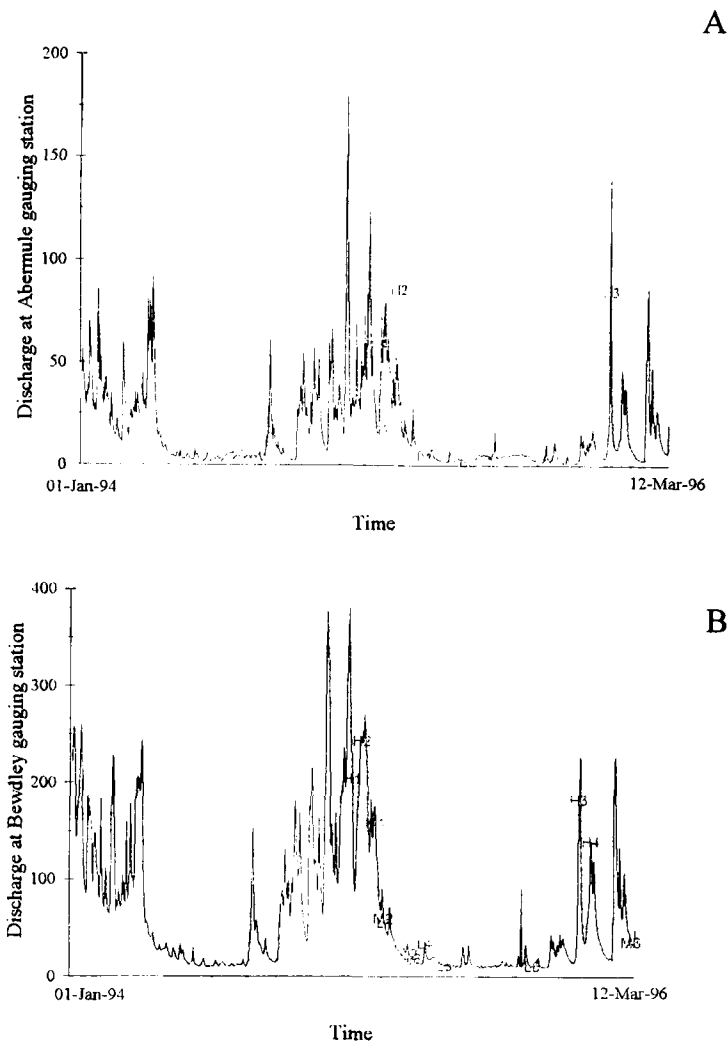


Figure 3.16 Timing of flow measurement between 1 January 1994 and 7 March 1996 for: a) sites upstream, and including, Abermule; and b) sites downstream of Abermule. Codes refer to flow measurements listed in Table 3.14.

The timing of the flow measurement during the 2 year fieldwork programme may be visualised by comparison of the date of the field visit with a reference flow (mean daily discharge ( $\text{m}^3 \text{s}^{-1}$ )) at two sites, Abermule (Figure 3.16a & Table 3.14a) and Bewdley (Figure 3.16b & Table 3.14b). These show which sites were visited on a particular date (between 1 January 1994 and 20 March 1995) and the corresponding flow magnitude. It is clear that the coarse tripartite division between the measured flows is replicated in the two graphs. However, these also indicate the degree of variability in the flow magnitudes for each division (eg: Figure 3.16b), particularly at a medium level and may contribute to a scatter in the spatial distribution of measured channel hydraulics. The infrequent nature of high flows is evident (ie: a mean daily flow of  $100 \text{ m}^3 \text{ s}^{-1}$  was exceeded on only three occasions between 1 January 1994 and 12 March 1995) as was the long, dry summer of 1995, which lasted from February to November (Figures 3.16a & 3.16b).

Table 3.17 A schematic representation of the various techniques used to estimate hydraulic parameters along the Severn.

Study site	Study site abbreviation	LOW flow	MEDIUM flow	HIGH flow
Upper Hafren 1	UH1	Current metering	Current metering	Current metering
Upper Hafren 2	UH2	Current metering	Current metering	Current metering
Upper Hafren 3	UH3	Current metering	Current metering	Current metering
Hafren Forest	HFor	Current metering	Current metering	Current metering
Hafren Falls	HFalls	Current metering	Current metering	Current metering
Tanllwyth	Tan	Current metering	Current metering	Current metering
Severn Flume	SF1	Current metering	Current metering	Current metering
Picnic Bridge	PB	Current metering	Current metering	Current metering
Severn Gorge	SG	Current metering	Current metering	Current metering
Rhydyronnen	Rhy	Current metering	Current metering	Current metering
Severn Ford	SFord	Current metering	Current metering	Current metering
Mount Severn	MS	Current metering	Current metering	Current metering
Dolwen	Dol	Current metering	Current metering	Slope-area
Llandinam	Llan	Current metering	Current metering	Slope-area
Caersws	Caer	Current metering	Current metering	Slope-area
Newtown	New	Current metering	Current metering	Slope-area
Abermule	Aber	Current metering	Current metering	Slope-area
Dyffryn	Dyff	Current metering	Current metering	Slope-area
Pool Quay	PQ	Current metering	Current metering	Slope-area
Crew Green	CG	Current metering	Current metering	Slope-area
Montford	Mont	Current metering	Current metering	Slope-area
Buildwas	Bws	Current metering	Current metering	Slope-area
Bridgnorth	B'north	Current metering	Current metering	Slope-area
Bewdley	Bewd	Current metering	Current metering	Slope-area
Saxons Lode	SL	Current metering	Current metering	Slope-area

Key: flow measurement techniques

Current metering
Slope-area
Volumetric estimation
Trash-line survey
No data

At low flow conditions in the headwaters of the Severn catchment, the mean flow was insufficient to use current meters; discharge was therefore estimated using the volumetric technique (Table 3.15). Where possible, the flow was gauged using the current meter technique, either by wading or from a boat (sections 3.6.3 & 3.6.4) (Table 3.15). All the 22 sites downstream from the Hafren Forest were gauged using this method at low flow, and 16 of the 25 sites at medium flows. Llandinam and Newtown could not be measured at this flow level because of the difficulty in reaching the sites at the correct flow magnitude. In conditions unsuitable for current meter gauging, slope and stage were surveyed and discharge data were gathered from neighbouring NRA gauging stations (section 3.4) (Table 3.15).

Each of these techniques have been applied to real-time flow conditions, but it proved extremely difficult to gauge flow at a high stage in the headwaters due to the rapid rise and fall of stage during an event in a region over 3 hrs drive-time from Birmingham. The trash-line survey was applied to evaluate the maximum stage of a flow event and thereby record the hydraulic variables at this high flow condition (Table 3.15). Discharge was estimated using the regression analysis technique, as described in section 3.8.

### **3.10 Sources of error**

The main components of error include: instrument error; sampling error; and observer error. Instrument errors may occur from incorrect calibration or assembly and were quantified for the individual techniques (eg: Table 3.7). Sampling errors are the result of unrepresentative / inappropriate sampling techniques. These errors were minimised by the careful choice of measurement techniques (sections 3.4, 3.5, 3.6), and a detailed sampling strategy (section 3.2). Observer error was reduced by limiting the number of observers during surveying (Table 3.5) (section 3.4 and 3.5), bed material sampling (Table 3.6) (section 3.4.6) and flow measurement (Table 3.8) (section 3.6). Another form of error concerns the 'nature of the observed phenomena' (Davidson, 1978). This involves the disturbance of the physical medium by the measurement apparatus. For example, the impeller meters are unavoidably intrusive within the water column and obstruct the natural movement of water, but precautions were made to limit the drag induced by extraneous components from the wading rod. Systematic errors were checked personally by calibrating the instruments (eg: flow meters, section 3.6.2) and duplicating measurements with more than one apparatus. Random errors were identified from anomalous measurements (outliers) and eliminated from further analysis.

The range of possible errors associated with surveying the channel geometry and water surface slope are presented in Table 3.16. These were quantified by calculating the variance of readings from a series of repeated measurements. The level and staff, had greater errors than the EDM on account of additional errors from manual tape measurements, particularly over long distances (Table 3.4 & Table 3.16). Additionally, the errors associated with variables derived from measured widths and depths (area, wetted perimeter and hydraulic radius) are greater due to the accumulation of errors during the calculation procedure (Table 3.16).

Surface bed material sampling is prone to a wide variety of errors created by the heterogeneity of the channel bed (natural errors) and ability to accurately sample the particle size range (human error) (Table 3.6); further errors may occur in post-processing if a variety of methods are used (analysis errors) (Table 3.6). Human errors were evaluated using the repeated measurement techniques, detailed in Hey & Thorne (1983) and Marcus *et al.* (1995) (Table 3.16).

Table 3.16 Estimated errors associated with the various measurement techniques.

Measurement	Technique	Variable	Variable error (%)
Channel geometry	Levelling	Width	5
		Depth	1
		Area	7
		Wetted perimeter	4
		Hydraulic radius	8
	EDM	Width	< 1
		Depth	1
		Area	4
		Wetted perimeter	3
		Hydraulic radius	5
Slope	Levelling	Water surface slope	5
	EDM	Water surface slope	1
Bed material	Wolman count	Grain size	
	Sieve analysis	Grain size	
Mean velocity	Current meter(s)	Point velocity	1
	Current meter(s)	Mean velocity	11
	Indirect (NRA flow data)	Mean velocity	5
	Indirect (Resistance equation)	Mean velocity	7
Discharge	Current meter(s)	Discharge	9
	Indirect (NRA flow data)	Discharge	≤ 20
	Indirect (Resistance equation)	Discharge	17
Flow resistance		Manning's $n$	12
		Darcy-Weisbach $f$	22
Shear stress		Reach mean	13
	Velocity gradient	Boundary	23
Stream power		Total	10
		Unit	11

Instrument errors associated with flow measurement (and channel surveying) were checked by calibrating the impeller meters prior to the field experiments (section 3.6.2 and Table 3.7); the calibration equations for each propeller agreed well with manufacturer calibrations, but sufficient variability resulted from different meter shafts - propeller combinations to warrant using the new calibration equations. Mean velocities and errors generated from EA data and the regression equations were calculated from other channel geometry and hydraulic variables, and hence, variable error is greater due to error propagation (Table 3.7).

### **3.11 Summary**

This chapter has described the methodology behind the fieldwork programme. The aim of the fieldwork programme was to measure the spatial variation of channel hydraulics along the Severn under a range of flow conditions. This has been achieved by adopting several measuring techniques to facilitate a safe, but accurate fieldwork programme.

## CHAPTER 4

### DOWNSTREAM CHANGE IN CHANNEL HYDRAULICS ALONG THE RIVER SEVERN: FIELDWORK RESULTS

#### 4.1 Introduction

This chapter discusses the results from the fieldwork programme along the Severn. The aim of this chapter is to develop an understanding of the longitudinal distribution of channel hydraulics, and the inter-relationships between individual channel hydraulics parameters and the spatial variation of channel form.

This chapter begins by describing the downstream variation of channel form variables. These were measured at the beginning of the study and are assumed to remain constant throughout the fieldwork programme (January 1994 - March 1996). This is followed by a review of the spatial variation of hydraulic parameters over three separate flow conditions, which ensures that variables discussed were measured under similar hydraulic conditions. Finally, the significance of stage on the downstream variability of channel geometry and channel hydraulics is considered. This final section discusses the impact of increasing flow level on the spatial variation of, firstly, channel geometry parameters, and secondly, the channel hydraulic parameters.

Trend lines fitted to the hydraulic parameters during this chapter represent the best-fit least-squares relationship; these are presented in Table 4.1. Furthermore, the ordinate axis of some figures have a logarithmic scale to reflect the spacing of the study sections; occasionally the abscissa axis is logged if the range of measured values covers several orders of magnitude. Throughout this chapter, reference will be made to study sites of the Severn basin: therefore, to avoid repetition, Figure 3.1 may be referenced whenever a site name is mentioned.

#### 4.2 Downstream change in channel form

##### 4.2.1 Introduction

This section shall begin by discussing how the channel geometry (4.2.2) and planform (4.2.3) vary from the headwaters to the near-tidal limit at Saxons Lode. In this study, it is assumed that there was negligible change in the bankfull channel geometry and planform during the 18 month fieldwork programme. It is also assumed that the bed material size and composition (4.2.4) in each study reach did not change significantly during this period. The effect of stage on the downstream distribution of the channel geometry is discussed in section 4.6.2.

##### 4.2.2 Bankfull channel geometry

The bankfull water width generally increased with distance downstream (Figure 4.1). From the headwaters, width increased gradually from approximately 1.0 m close to the source (Upper Hafren 1) to 70 m at Saxons Lode, as described by the function,  $\log(w) = 0.46 + 0.56\log(DD) + 0.22\log(DD)^2 - 0.10\log(DD)^3$  ( $n = 25$ ;  $p < 0.001$ ;  $r^2 = 0.95$ ). Downstream from Llandinam (22 km), the width became

Table 4.1 A summary of the curve fit relationships for the variables measured during the fieldwork programme

Flow Level	Variable	Curve Fit	b <sub>0</sub>	b <sub>1</sub>	b <sub>2</sub>	b <sub>3</sub>	r <sup>2</sup>	Significance, p	Figure number
LOW FLOW n = 30	Width	log-cubic	0.139	0.587	0.273	-0.109	0.951	< 0.0001	4.31
	Mean depth	power	0.090	0.536			0.93	< 0.0001	4.32
	Hydraulic radius	power	0.083	0.525			0.86	< 0.0001	4.33
	Mean velocity	power	0.112	0.138			0.623	< 0.0001	4.5 & 4.34
	Discharge	log-cubic	-1.925	-1.139	0.494	-0.178	0.94	< 0.0001	4.6 & 4.35
	Water surface slope	log-cubic	-1.400	-0.686	-0.594	0.175	0.71	< 0.0001	4.7 & 4.36
	Manning's <i>n</i>								4.8
	Darcy Weisbach <i>f</i>								4.9
	Total stream power	log-quadratic	0.674	0.453	-0.105		0.13	0.157	4.10 & 4.37
	Unit stream power	log-quadratic	0.394	-0.087	-0.141		0.21	0.043	4.11 & 4.38
Reach mean shear stress	log-quadratic	1.287	-0.209	-0.143		0.35	0.003	4.12 & 4.39	
MEDIUM FLOW n = 23	Width	log-cubic	0.204	0.622	0.292	-0.130	0.96	< 0.0001	4.31
	Mean depth	log-cubic	-0.788	0.503	0.174	-0.069	0.91	< 0.0001	4.32
	Hydraulic radius	log-cubic	-0.882	0.524	0.196	-0.0825	0.93	< 0.0001	4.33
	Mean velocity	power	0.283	0.226			0.78	< 0.0001	4.14 & 4.34
	Discharge	log-cubic	-1.239	1.499	0.554	-0.285	0.97	< 0.0001	4.15 & 4.35
	Water surface slope	log-cubic	-1.344	-0.609	-0.550	0.164	0.91	< 0.0001	4.16 & 4.36
	Manning's <i>n</i>								4.17
	Darcy Weisbach <i>f</i>								4.18
	Total stream power	log-quadratic	1.561	0.810	-0.243		0.59	< 0.0001	4.19 & 4.37
	Unit stream power	log-quadratic	1.192	0.275	-0.268		0.38	0.011	4.20 & 4.38
Reach mean shear stress	log-quadratic	1.689	-0.003	-0.227		0.68	< 0.0001	4.21 & 4.39	
HIGH FLOW n = 23	Width	log-cubic	0.325	0.584	0.267	-0.110	0.96	< 0.0001	4.31
	Mean depth	log-cubic	-0.438	0.274	0.240	-0.074	0.72	< 0.0001	4.32
	Hydraulic radius	log-quadratic	-0.486	0.249	0.086		0.88	< 0.0001	4.33
	Mean velocity	power	0.861	0.081			0.12	0.098	4.23 & 4.34
	Discharge	power	1.17	1.021			0.99	< 0.0001	4.24 & 4.35
	Water surface slope	log-cubic	-1.435	-0.453	-0.354	0.091	0.84	< 0.0001	4.25 & 4.36
	Manning's <i>n</i>								4.26
	Darcy Weisbach <i>f</i>								4.27
	Total stream power	log-quadratic	2.502	0.631	-0.166		0.58	< 0.0001	4.28 & 4.37
	Unit stream power	log-cubic	2.760	0.200	-0.676	0.187	0.52	0.002	4.29 & 4.38
Reach mean shear stress	log-cubic	1.950	-0.192	-0.215	-0.067	0.49	0.001	4.30 & 4.39	

more variable; this was accentuated by the positive outliers from the general trend at Caersws and Buildwas, and the negative outliers at Pool Quay, Crew Green and Montford. The former relate to highly sinuous channel reaches (see section 4.2.3), where study sections were located within the sequence of meander bends. By contrast, the latter coincide with the incised reach downstream of Welshpool, observed by Hey (1975, cited in Lewin, 1987), Lewin (1987), Brown (1987), and the underfit channel at Montford. This latter subject has been the focus of much debate by Dury *et al.* (1972), Richards (1972), Kirkby (1972) and Ferguson (1973).

The bankfull mean depth increased gradually downstream to Newtown (Figure 4.2); thereafter it continued to increase, but with a greater inter-reach scale variability (Figure 4.2) ( $\log(\bar{d}) = -0.31 + 0.23\log(DD) + 0.21\log(DD)^2 - 0.06\log(DD)^3$ ;  $n = 25$ ;  $p < 0.001$ ;  $r^2 = 0.85$ ). This is consistent with the bankfull width distribution (Figure 4.1), as both show a general increase from the source and a discontinuity in the distribution between Llandinam and Bridgnorth. Indeed, the incised reach, noted above, is reflected by the anomalously high depths in the Pool Quay - Montford reach (5 - 6 m) (Figure 4.2). This variation of channel geometry components downstream from the source reflect the morphological control exerted by channel form, bank resistance and erosion processes, and the hydrological impact of increasing discharge downstream. Clearly, site selection will also be responsible for the variance about the downstream trend exhibited in Figures 4.1 and 4.2.

#### 4.2.3 Channel planform

Figure 4.3 shows that channel sinuosity exhibited no clear downstream trend along the Severn. Between the source (Upper Hafren 1) and Saxons Lode, sinuosity predominantly decreased beneath the  $S = 1.5$  'meandering - straight' threshold value (Leopold & Wolman, 1957), where  $S$  is a function of the thalweg distance between two known points along a river divided by the straight line distance between those points; this was expected since straight reaches were chosen to approximate uniform flow conditions (section 3.2; Plate 4.1 & 4.2). However, the four main meandering reaches along the Severn were included because they were considered representative of the local channel form; these are: a) the moorland reach close to the source (Figure 4.3 & Plate 4.3); b) the 'piedmont' zone downstream from Llanidloes (Figure 4.3 & Plate 4.4); c) the incised channel downstream from Welshpool (Figure 4.3 & Plate 4.5); and d) upstream of the Ironbridge gorge (Figure 4.3 & Plate 4.6). Interestingly, reaches (b), (c) and (d) were prominent in the anomalous distributions of width and depth downstream from Llandinam (Figures 4.1 & 4.2), suggesting that channel planform may have a critical influence on the downstream distribution of channel hydraulic parameters.

#### 4.2.4 Bed material size

There was no significant spatial variation of bed material size along the entire non-tidal Severn. Figure 4.4 shows how the  $D_{16}$ ,  $D_{50}$  and  $D_{84}$  grain size percentiles are largely confined to a range of 20 - 100 mm, equivalent to the Wentworth grain size classification of coarse gravel to small cobbles (Church *et al.*, 1987). At Newtown, the bedrock crops-out within the reach and appears to enhance the particle size distribution, giving a value of  $D_{50} > 80$  mm (Figure 4.4). The three sites sampled volumetrically (Pool Quay, Crew Green and Saxons Lode), all greatly underestimated the general trend (Figure 4.4). These



Plate 4.1 The study reach at Bewdley under low-flow conditions in June 1994, looking upstream from the EA Ultra-Sonic gauging station.



Plate 4.2 The study reach at Saxons Lode under low-flow conditions in January 1995, looking upstream from the EA Ultra-sonic gauging station.

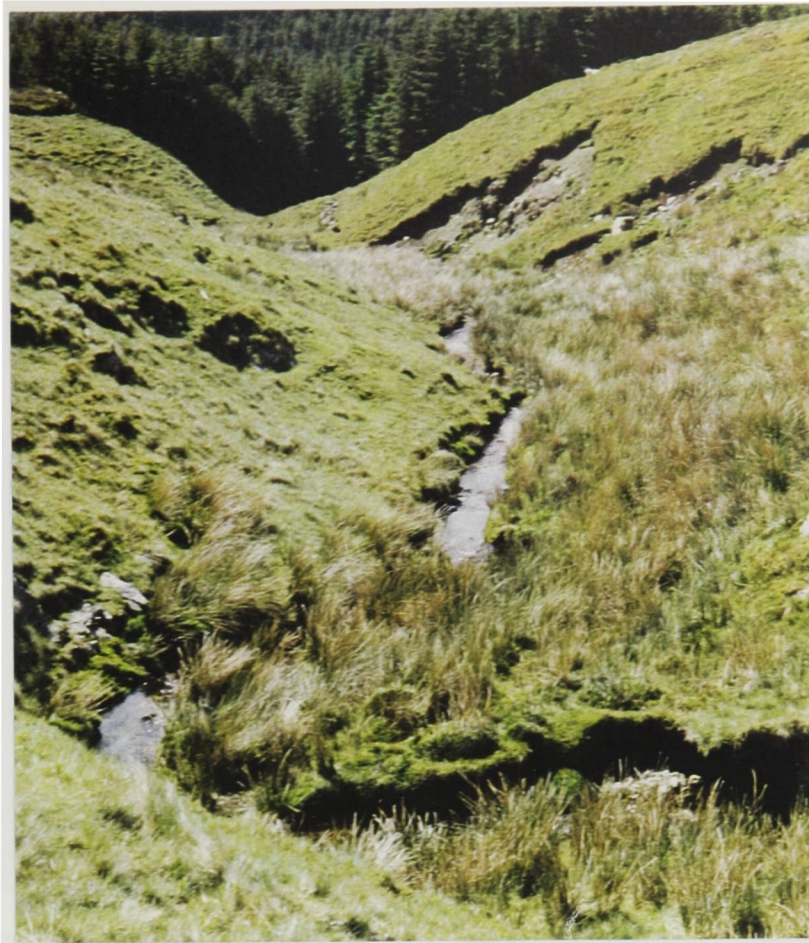


Plate 4.3 The steep upland reach at Upper Hafren 3 in Plynlimon under low-flow conditions (July 1994),, looking downstream towards the Hafren Forest plantation.

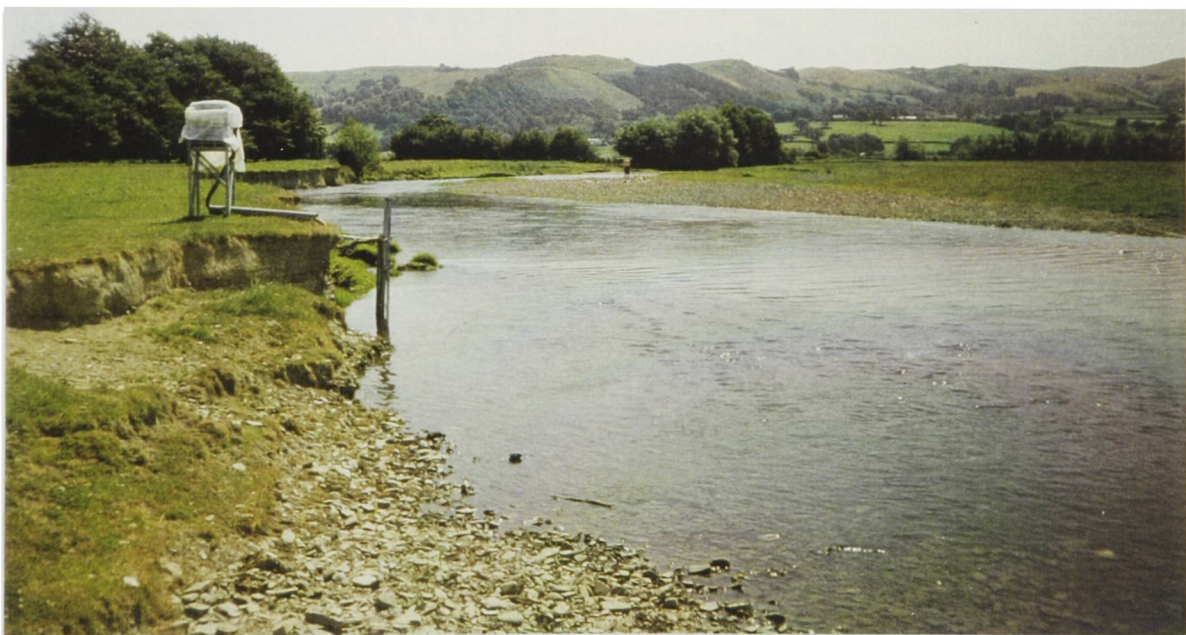


Plate 4.4 The study site at Caersws under low-flow conditions in June 1994, looking upstream at the bank and flow monitoring equipment used by Bull (1996). High rates of channel activity have been observed by Lewin (1983, 1987) through the ‘piedmont’ zone (Newson, 1981) in response to a sharp break in the channel and valley slope close to Llanidloes and a change in the structure and resistance of the bank material (see section 7.7).



Plate 4.5 The meandering reach upstream of the study site at Pool Quay under high-flow conditions (January 1996). This shows the high sinuosity of the channel between Abermule and the Vyrnwy confluence, and the influence of bank vegetation at higher, bankfull flows.



Plate 4.6 The meander sequence between the Buildwas study site and the Ironbridge gorge under high flow conditions in November 1996.

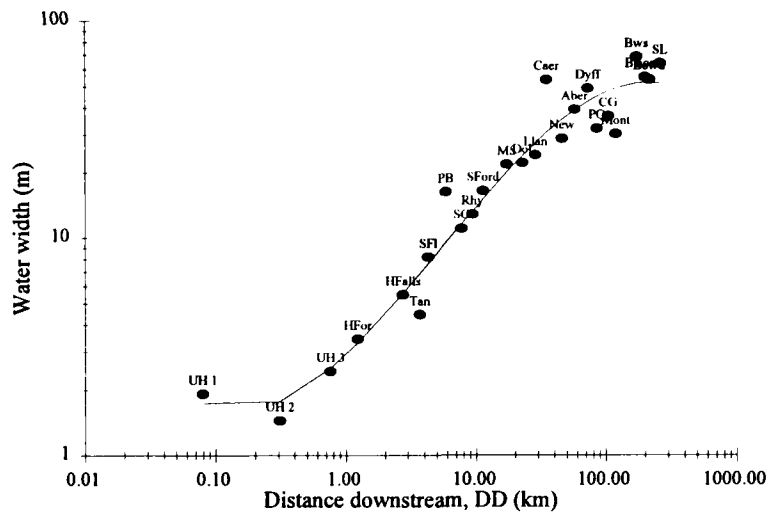


Figure 4.1 The spatial variation of bankfull water width downstream along the Severn.

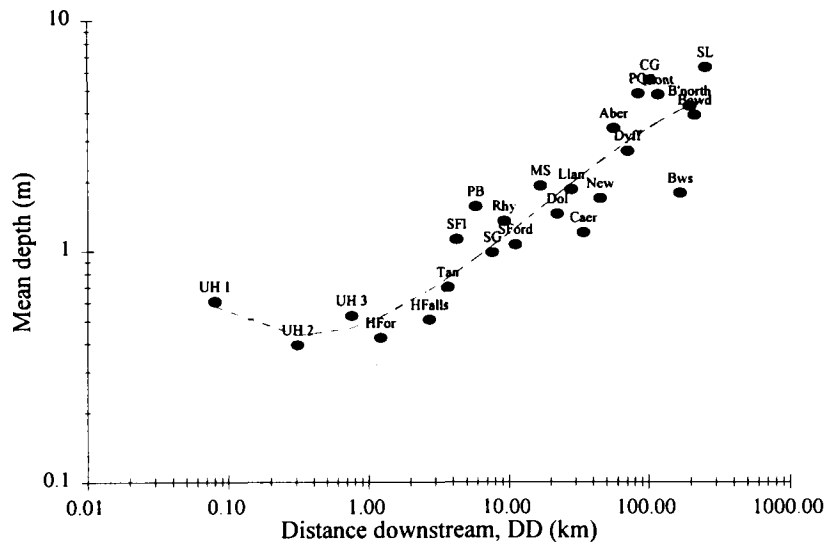


Figure 4.2 The spatial variation of bankfull mean depth downstream along the Severn.

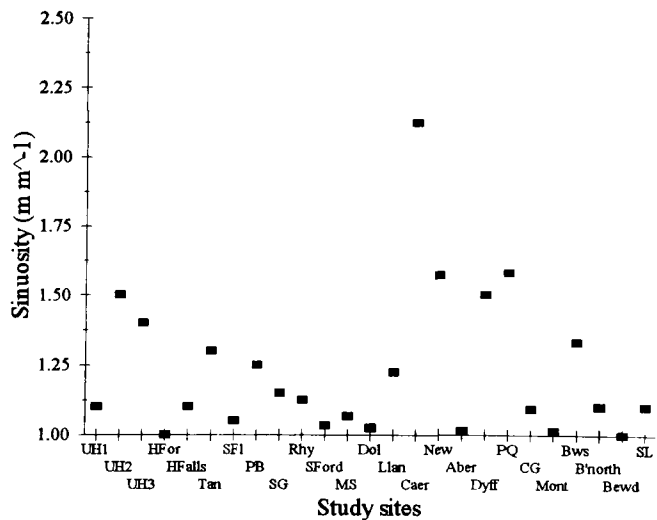


Figure 4.3 Downstream change in channel sinuosity along the Severn.

sites were sampled during the mid summer (1995) at one central channel location; hence, these samples may be unrepresentative for two reasons: a) silt may have been deposited on a gravel bed layer during the low summer flow; or b) the sample may reflect a localised area of silt on the channel bed. Alternatively, low boundary shear stresses and flow competence along these reaches may result in the deposition of fine sand and silt, and the accumulation of a fine particulate bed layer. The impact of channel management schemes, for example by channelisation or dredging, are difficult to evaluate although these would certainly alter the particle size distribution (Brookes, 1988), laterally and vertically in the section, and longitudinally along the reach; however, this will a subject for discussion in Chapter 7

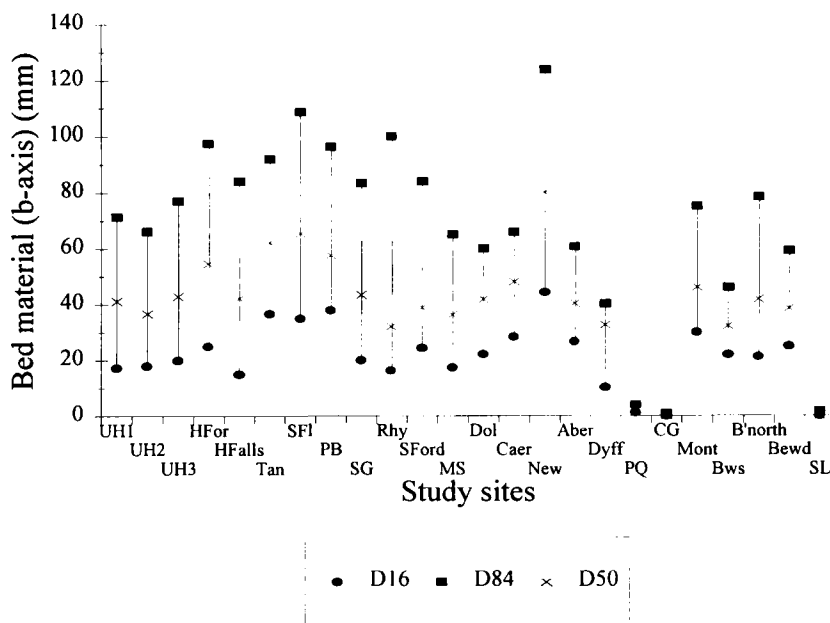


Figure 4.4 The spatial variation of grain size downstream along the Severn, expressed as the  $D_{16}$ ,  $D_{84}$  and  $D_{50}$ .

### 4.3 Downstream change in low-flow hydraulics

#### 4.3.1 Introduction

Low flows are classified in this study as having an exceedance frequency,  $F$ , of greater than or equal to 70 %; this corresponds to a flow of less than  $20 \text{ m}^3 \text{ s}^{-1}$  at Bewdley. Flows were measured at 22 sites using detailed velocity profiles across the section, either by wading or from a boat (section 3.6). At the three uppermost sites (Upper Hafren 1, 2 & 3), the mean flow level was too low to gauge using the velocity-area technique, hence discharge was estimated volumetrically (section 3.7.4 and 3.10.3). This section will review the downstream variability of each hydraulic variable considered in this study (Chapters 2 & 3, Table 4.2 and Appendix I). Later, in section 4.6.3, the effect of stage on the downstream variation of these hydraulic variables will be appraised.

Table 4.2 The channel hydraulic parameters measured at low flow at 25 sites along the River Severn

Site number	Site name	Distance downstream (km)	Elevation (m) (a.s.l)	Water width (m)	Mean depth (m)	Section area (m <sup>2</sup> )	Wetted perimeter (m)	Hydraulic radius (m)	w/d (m m <sup>-1</sup> )	Mean velocity (m s <sup>-1</sup> )	Section discharge (m <sup>3</sup> s <sup>-1</sup> )	Water surface slope (m m <sup>-1</sup> )	Bed material size			Manning's n	Darcy f	Reach mean shear stress (N m <sup>-2</sup> )	Boundary shear stress			Total stream power (W m <sup>-1</sup> )	Unit stream power (W m <sup>-2</sup> )
													D16 (mm)	D50 (mm)	D84 (mm)				min (N m <sup>-2</sup> )	max (N m <sup>-2</sup> )	mean (N m <sup>-2</sup> )		
1	Upper Hafren 1	0.08	606.21	0.97	0.04	0.04	1.03	0.04	23.10	0.08	0.003	3.67E-02	17.35	41.11	71.25	0.30	20.26	15.12				1.22	1.26
2	Upper Hafren 2	0.31	580.22	0.80	0.03	0.03	0.91	0.03	27.59	0.18	0.005	4.28E-02	18.00	36.67	66.25	0.11	3.03	11.76				1.92	2.40
3	Upper Hafren 3	0.76	547.76	1.15	0.11	0.13	1.33	0.10	10.65	0.21	0.029	2.98E-02	20.00	42.78	77.00	0.17	5.11	29.53				8.42	7.32
4	Hafren Forest	1.23	524.38	1.65	0.11	0.23	2.37	0.10	14.86	0.10	0.022	3.70E-02	25.00	54.55	97.50	0.43	30.79	35.21	0.00	1.17	0.20	7.99	4.84
5	Hafren Falls	2.73	390.72	2.25	0.12	0.22	2.45	0.09	19.40	0.14	0.031	1.35E-02	15.00	42.14	84.00	0.17	4.99	12.05	0.00	5.41	1.09	4.11	1.82
				2.40	0.12	0.31	2.61	0.12	19.35	0.13	0.041	2.82E-02				0.31	14.96	32.92				11.34	4.73
6	Tanllwyth	3.71	347.79	3.21	0.20	0.51	3.27	0.16	16.46	0.08	0.038	1.30E-02	36.67	62.22	92.00	0.44	28.04	19.77	0.01	0.10	0.06	4.85	1.51
				3.33	0.19	0.69	3.65	0.19	17.16	0.06	0.045	1.20E-02				0.56	42.56	22.37				5.30	1.59
7	Severn Flume	4.26	334.33	4.69	0.31	1.34	5.02	0.27	14.98	0.06	0.087	8.00E-03	35.00	65.50	108.75	0.57	39.77	20.95	0.00	3.28	0.51	6.83	1.46
				3.21	0.18	1.33	4.21	0.32	17.93	0.07	0.094	1.08E-02				0.68	53.05	33.37				9.96	3.10
8	Picnic Bridge	5.81	313.71	3.63	0.16	0.65	4.73	0.14	22.55	0.31	0.201	1.13E-02	37.86	57.50	96.25	0.09	1.26	15.19	0.05	2.76	1.11	22.28	6.14
9	Severn Gorge	7.62	271.57	6.60	0.30	1.87	6.74	0.28	22.30	0.13	0.238	6.00E-03	20.00	43.33	83.33	0.26	8.01	16.30	0.01	4.42	0.94	14.01	2.12
10	Rhydyronnen	9.23	266.39	7.40	0.25	2.19	8.65	0.25	29.13	0.05	0.106	7.57E-03	16.33	32.00	100.00	0.72	64.59	18.86	0.03	1.25	0.64	7.87	1.06
11	Severn Ford	11.11	204.27	15.57	0.15	1.67	11.05	0.15	101.76	0.07	0.112	1.44E-03	24.44	38.75	83.89	0.16	3.80	2.13	0.01	0.36	0.10	1.58	0.10
12	Mount Severn	16.88	165.71	11.50	0.48	7.99	15.77	0.51	23.91	0.03	0.238	2.70E-03	17.50	36.15	65.00	1.11	121.14	13.43				6.30	0.55
13	Dolwen	22.20	147.61	19.50	0.56	10.51	19.69	0.53	34.76	0.42	4.404	2.50E-03	22.14	41.67	60.00	0.08	0.60	13.07	2.08	10.31	5.12	108.01	5.54
				16.16	0.42	3.02	22.70	0.13	38.20	1.08	3.251	2.72E-03				0.01	0.02	3.55				86.75	5.37
14	Llandinam	28.00	135.20	16.80	0.45	4.12	22.15	0.19	37.09	0.69	2.825	1.51E-03				0.02	0.05	2.76				41.85	2.49
15	Caersws	34.10	118.70	17.30	0.44	7.80	17.78	0.43	39.05	0.47	3.701	9.00E-04	28.33	48.08	65.83	0.04	0.13	3.77	0.40	10.59	4.10	32.68	1.89
				29.52	0.52	16.33	30.43	0.54	57.10	0.27	4.439	1.73E-03				0.10	0.99	9.11				75.34	2.55
16	Newtown	44.93	109.00	22.90	0.81	18.73	23.22	0.81	28.17	0.18	3.415	2.00E-03	44.17	80.00	123.75	0.21	3.81	15.81	0.02	13.68	2.58	67.00	2.93
17	Abermule	55.92	83.00	26.79	0.77	19.36	27.38	0.71	34.79	0.26	5.010	6.50E-05	26.67	40.36	60.83	0.02	0.05	0.45	0.01	3.93	0.69	3.19	0.12
18	Dyffryn	70.30	75.02	34.40	0.85	29.46	36.79	0.80	40.66	0.18	5.180	3.96E-04	10.27	32.57	40.26	0.10	0.80	3.11				20.12	0.58
19	Pool Quay	83.20	63.03	13.05	1.00	17.35	20.17	0.85	13.12	0.33	5.680	5.33E-05	1.06	2.25	3.96	0.02	0.03	0.45	0.01	24.22	4.85	2.97	0.23
20	Crew Green	100.90	52.94	23.70	1.53	33.15	24.30	1.36	15.53	0.15	5.040	7.19E-05	0.04	0.12	0.62	0.07	0.33	0.96	0.02	2.14	0.63	3.55	0.15
21	Montford	115.46	52.00	23.10	1.25	25.67	23.60	1.09	18.49	0.20	5.173	3.50E-05	30.00	46.00	75.00	0.03	0.07	0.37	0.01	1.19	0.38	1.78	0.08
22	Buildwas	166.45	39.25	45.00	1.94	83.93	46.34	1.92	23.23	0.15	12.385	2.96E-05	22.00	32.31	46.00	0.06	0.20	0.56	0.17	13.86	4.00	3.60	0.08
23	Bridgnorth	192.36	30.52	45.70	1.13	52.68	46.11	1.14	40.59	0.34	17.717	9.40E-05	21.25	41.67	78.33	0.03	0.07	1.05	0.01	15.36	2.14	16.34	0.36
24	Bewdley	209.00	20.89	40.88	1.52	62.16	42.93	1.45	26.89	0.34	20.859	7.60E-04	25.00	38.46	59.17	0.11	0.77	10.80	0.01	6.62	1.46	155.52	3.80
25	Saxons Lodge	254.13	13.27	60.60	2.58	151.37	61.47	2.46	23.52	0.07	10.175	7.77E-04	0.05	0.16	1.63	0.76	33.23	18.77	0.01	0.41	0.10	77.56	1.28

### 4.3.2 Mean velocity

Figure 4.5 shows no clear spatial trend, but indicates an abrupt change in the downstream trend about Llanidloes (20 km downstream). The considerable scatter present in this spatial distribution is reflected in a low level of significance for the fitted line ( $\bar{u} = 0.11DD^{0.14}$ ;  $n = 30$ ;  $p < 0.001$ ;  $r^2 = 0.62$ ). A low mean velocity ( $\bar{u} < 0.2 \text{ m s}^{-1}$ ) persisted downstream to Mount Severn, punctuated by a slight peak at Picnic Bridge ( $\bar{u} = 0.31 \text{ m s}^{-1}$ ), 6 km from the source. Downstream from Llanidloes, an abrupt rise in mean velocity occurred in the reach between Dolwen and Caersws, peaking at Dolwen ( $\bar{u} = 1.08 \text{ m s}^{-1}$ ). Thereafter, mean velocity decreased steadily downstream from Caersws (34 km downstream from the source) to Saxons Lode (250 km). This decline was interrupted through the Ironbridge gorge by elevated values of mean velocity at Bridgnorth and Bewdley ( $\bar{u} \sim 0.35 \text{ m s}^{-1}$ ); this rise approximates to a flow velocity three times greater than in the reaches upstream and downstream of the gorge at Buildwas and Saxons Lode.

### 4.3.3 Discharge

Discharge increased with distance from the source, from  $0.003 \text{ m}^3 \text{ s}^{-1}$  at 0.08 km to  $20 \text{ m}^3 \text{ s}^{-1}$  at 210 km, represented to a first approximation by a log function (Figure 4.6). This rate of increase was high in the headwaters (almost three orders of magnitude over 20 km) and much reduced downstream (approximately one order of magnitude over 230 km); this is approximated by the power function,  $\log(Q) = -1.92 + 1.14\log(DD) + 0.49\log(DD)^2 - 0.18\log(DD)^3$  ( $n = 30$ ;  $p < 0.001$ ;  $r^2 = 0.94$ ). The swift increase in discharge close to the source is the result of the dense network of tributaries and enhanced orographic precipitation over the massif, which encourages rapid and efficient drainage. The log-log downstream distribution of discharge is non-linear due to the presence of positive (increased discharge) and negative (reduced discharge) 'steps': positive steps relate to tributary junctions (Richards, 1980), most notably the Afon Clywedog between Mount Severn and Dolwen; negative steps are possibly the result of groundwater losses through the Shropshire Plain or flow abstractions (Higgs, 1987). The resultant downstream distribution is characterised by a series of discontinuities and 'plateaux', about a general linear downstream trend. The plateaux, for example, occur in the reach between Dolwen and Montford because of the absence of major inflows: in reality, the Vyrnwy joins the channel through this reach, and smaller tributaries through other reaches, though they are not well represented due to the non-synchronous timing of the flow measurement programme (Chapter 3).

### 4.3.4 Water surface slope

Water surface slope decreased through four orders of magnitude as the Severn flows downstream from the source (Figure 4.7). The headwater region was characterised by slopes in excess of  $0.1 \text{ m m}^{-1}$ , whereas downstream at Buildwas the water surface slope was  $0.00002 \text{ m m}^{-1}$ . However, this trend is not linear ( $\log(s) = -1.40 - 0.69\log(DD) - 0.59\log(DD)^2 + 0.18\log(DD)^3$ ;  $n = 30$ ;  $p > 0.001$ ;  $r^2 = 0.71$ ), but dominated by a pronounced transition in the headwater region, from unusually steep and constant slopes greater than  $0.3 \text{ m m}^{-1}$  (3 % slope), to rapidly falling slopes downstream from the Plynlimon catchment. A second major change occurred close to a sharp break of slope in the strongly concave longitudinal profile at Llanidloes, as observed by Wheeler (1979). This cluster of sites is noticeably steeper than the

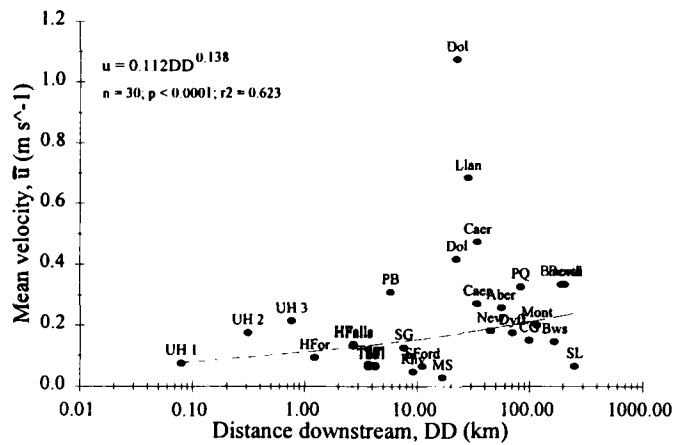


Figure 4.5 The spatial variation of mean velocity along the Severn, at a low-flow level, including the best-fit trend line and equation.

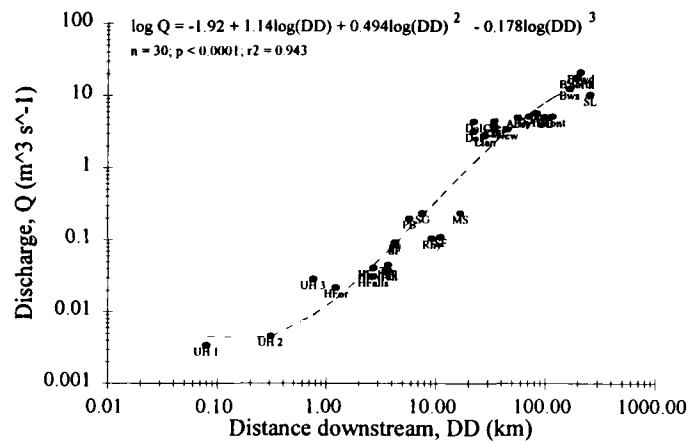


Figure 4.6 The spatial variation of discharge along the Severn, at a low-flow level, including the best-fit trend line and equation.

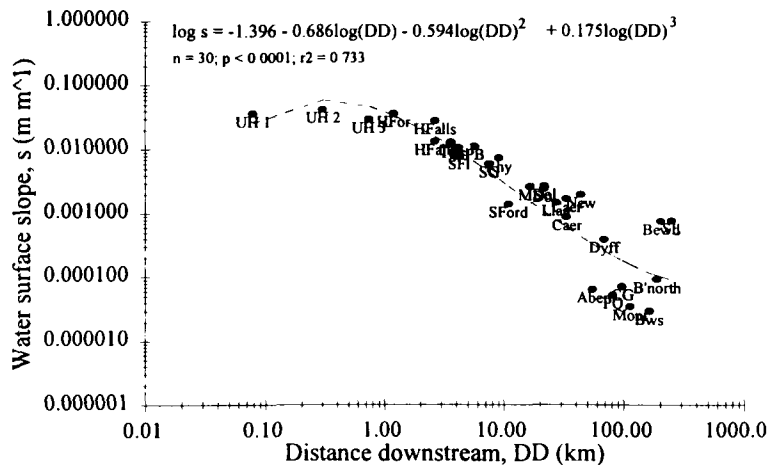


Figure 4.7 The spatial variation of water surface slope along the Severn, at a low-flow level, including the best-fit trend line and equation.

channel further downstream. Interestingly, these coincide with the ‘piedmont zone’ (Newson, 1981) which Lewin (1982, 1983, 1987) found to have the highest rates of channel mobility for the upper and middle reaches of the Severn. The Ironbridge gorge (170 - 210 km) region exerts a strong control on the longitudinal profile of the channel, and here the slopes rose sharply through Ironbridge and further to Bridgnorth and Bewdley. The pronounced scatter in slope values at this flow level may be attributed to the hydraulic effects of in-channel flow obstructions (eg: riffles, bars and vegetation) which at low flow levels disrupt the water surface profile by enhancing the boundary and channel roughness.

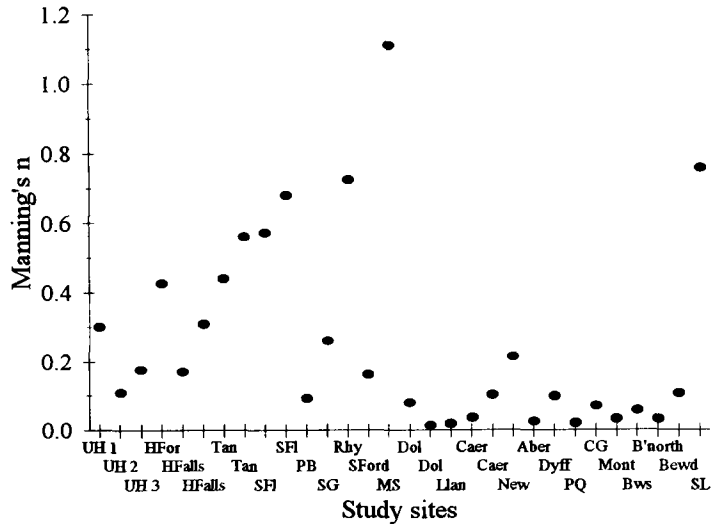


Figure 4.8 The spatial variation of Manning's  $n$  roughness coefficient along the Severn at a low-flow level.

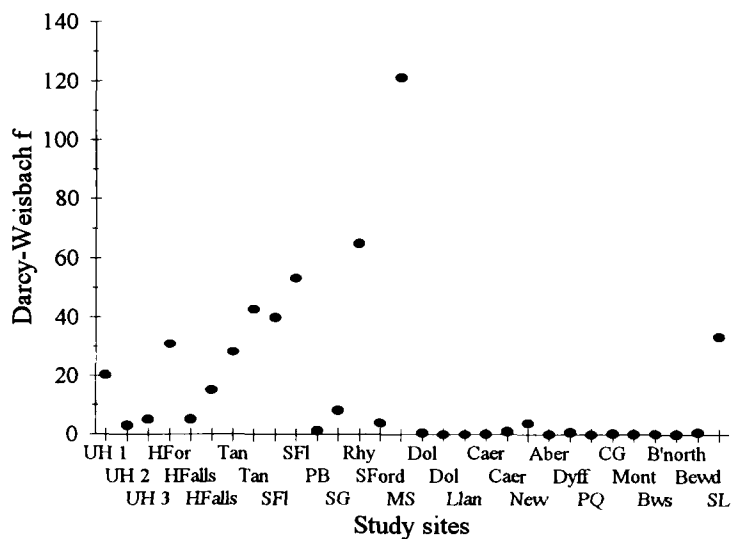


Figure 4.9 The spatial variation of the Darcy-Weisbach friction factor,  $f$ , along the Severn at a low-flow level.

#### 4.3.5 Flow resistance

The flow resistance parameters, Manning's  $n$  and Darcy-Weisbach  $f$ , did not decrease downstream from the headwaters (Knighton, 1987), but increased gradually between Upper Hafren 1 and Mount Severn ( $n = 1.11$ ), and then abruptly declined downstream ( $n < 0.1$ ) (Figures 4.8 and 4.9). Each study site in the upper

reach has  $n$ -values greater than 0.1, and thus fall within the 'step pool/fall' category, as classified by Bathurst (1993). The twelve lower sites downstream from Llanidloes had much reduced flow resistances and consequently may be classified in Bathurst's (1993) 'gravel/cobble-bed' channel category, with the exception of Newtown and Saxons Lode (Figure 3.1) which produced anomalous peaks of  $n = 0.21$  and  $0.76$ , respectively. It is interesting to observe that the sharp transition between these two reaches is located at the approximate non-alluvial - alluvial channel boundary (Brown, 1987) and may therefore provide an example of the local morphological control of channel type over the continuum of hydraulic processes.

#### 4.3.6 Total and unit stream power

Total stream power increased downstream from the source (Figure 4.10). Significantly, the non-alluvial headwater region between Upper Hafren 1 and Mount Severn produce a general increase in the downstream direction and little variability about this trend. In contrast, the alluvial channel (Dolwen - Saxons Lode) exhibits greater magnitudes of stream power, and greater variability. This distribution may be described by the log-log quadratic function (ie: a quadratic function fitted to a log-log relationship):  $\log(\Omega) = 0.67 + 0.45\log(DD) - 0.11\log(DD)^2$  ( $n = 30$ ;  $p = 0.157$ ;  $r^2 = 0.13$ ). Clearly, the enhanced variability is the result of the spatially varied components of the discharge - slope product. Figure 4.6 demonstrated that an abrupt rise in the level of discharge between Mount Severn and Dolwen was the result of the confluent tributary, Afon Clywedog, and only a moderate reduction in water surface slope (Figure 4.7); conversely, discharge altered little at Bridgnorth, Bewdley and Saxons Lode, but slope increased by an order of magnitude. Hence, the first total stream power peak was possibly the result of a rapid increase in discharge, and the latter, an increase in the water surface slope through the Ironbridge gorge and beyond. It may prove to be significant that the first peak in total stream power occurs in the reach shown to possess the highest rates of lateral channel activity on the Severn (Lewin, 1982; 1983; 1987), whilst the second peak occurs through the laterally confined gorge, underlining the physiographic control observed by Graf (1982, 1983a), Magilligan (1992) and Lecce (1993) (sections 2.4.7 & 7.6).

Unit stream power peaked in the upper reaches of the Severn ( $\omega = 7.32 \text{ W m}^{-2}$ ) and then decreased with distance downstream ( $\log(\omega) = 0.39 - 0.09\log(DD) - 0.14\log(DD)^2$ ;  $n = 30$ ;  $p = 0.043$ ;  $r^2 = 0.21$ ) (Figure 4.11). Despite considerable scatter, it is apparent that the lower limit decreases in a downstream direction, and the upper limit remains fairly constant ( $\omega \sim 7 \text{ W m}^{-2}$ ). The sudden transition in the level of unit stream power between Newtown and Abermule corresponds to a decrease of the same order of magnitude in the water surface slope between these sites (Figure 4.7), which was also discernible in the total stream power trend (Figure 4.10). Similarly, the control of water surface slope is also manifest in the reaches downstream of the Ironbridge gorge, where an enhanced bed and water surface gradient increases the unit stream power at Bridgnorth, Bewdley and Saxons Lode (Figure 4.11).

#### 4.3.7 Reach mean and boundary shear stress

Reach mean shear stress exhibits a slight downstream decline from the headwaters to Saxons Lode at low flow (Figure 4.12). A minor peak occurs in the headwaters between Upper Hafren 3 and Severn Flume ( $\tau > 30 \text{ N m}^{-2}$ ), and a general downstream decrease from the headwaters to Bridgnorth ( $\log(\tau) = 1.29 -$



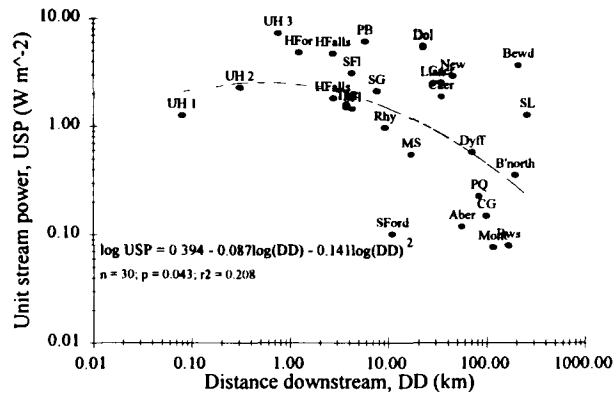


Figure 4.11 The spatial variation of unit stream power along the Severn at a low-flow level, including the best-fit trend line and equation.

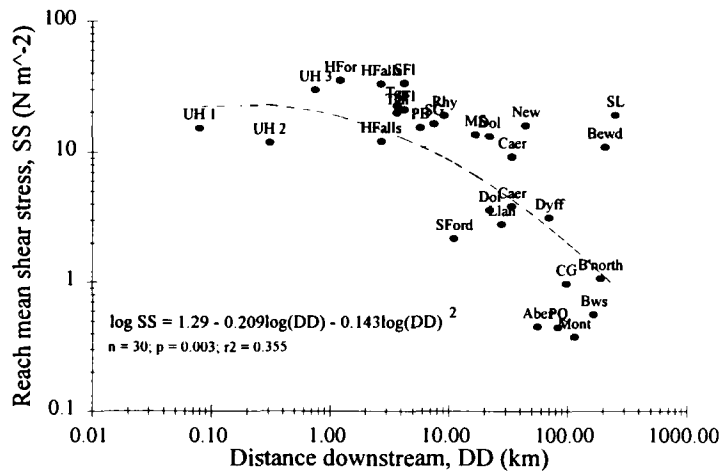


Figure 4.12 The spatial variation of reach mean shear stress along the Severn at a low-flow level, including the best-fit trend line and equation.

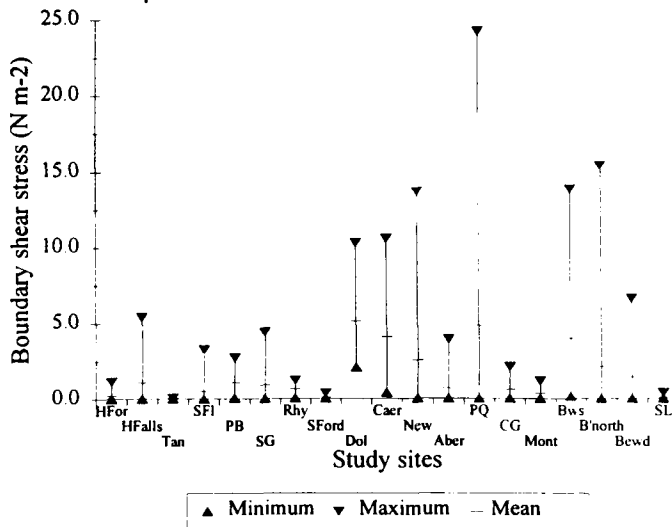


Figure 4.13 The spatial variation of boundary shear stress along the Severn at a low-flow level, including the best-fit trend line and equation.

Table 4.3 The channel hydraulic parameters measured at medium flow at 25 sites along the River Severn

Site number	Site name	Distance downstream (km)	Elevation (m)	Water width (m)	Mean depth (m)	Section area (m <sup>2</sup> )	Wetted perimeter (m)	w/d (m m <sup>-1</sup> )	Hydraulic radius (m)	Mean velocity (m s <sup>-1</sup> )	Section discharge (m <sup>3</sup> s <sup>-1</sup> )	Water surface slope (m m <sup>-1</sup> )	Manning's n	Darcy f	Reach mean shear stress (N m <sup>-2</sup> )	Boundary shear stress (N m <sup>-2</sup> )			Total stream power (W m <sup>-1</sup> )	Unit stream power (W m <sup>-2</sup> )
																min	max	mean		
1	Upper Hafren 1	0.08	606.21	1.20	0.09	0.10	1.27	13.13	0.08	0.14	0.01	3.34E-02	0.30	10.43	25.56				3.60	3.00
2	Upper Hafren 2	0.31	580.22	0.84	0.09	0.07	0.90	9.62	0.07	0.32	0.02	4.74E-02	0.11	2.65	33.95				10.23	12.18
3	Upper Hafren 3	0.76	547.76	1.35	0.18	0.24	1.55	7.34	0.15	0.22	0.05	4.47E-02	0.26	10.79	67.09				23.68	17.54
4	Hafren Forest	1.23	524.38	2.15	0.16	0.31	2.39	13.23	0.13	0.29	0.09	3.40E-02	0.16	4.24	43.69				30.35	14.12
5	Hafren Falls	2.73	390.72	3.60	0.23	0.58	2.93	15.82	0.20	0.57	0.33	2.98E-02	0.10	1.44	58.25	0.00	627.81	85.67	97.48	27.08
6	Tanllwyth	3.71	347.79	3.30	0.35	1.07	3.75	9.34	0.29	0.34	0.40	1.58E-02	0.15	3.15	44.29	0.00	7.08	0.93	61.85	18.74
7	Severn Flume	4.26	334.33	5.30	0.49	2.54	5.83	10.89	0.44	0.24	0.73	9.77E-03	0.20	5.62	41.81	0.00	1.55	0.37	69.90	13.19
8	Picnic Bridge	5.81	313.71	6.90	0.36	2.15	7.16	19.28	0.30	0.66	1.46	1.81E-02	0.09	0.99	53.36	0.60	91.83	19.97	259.16	37.56
9	Severn Gorge	7.62	271.57	7.70	0.52	3.36	7.23	14.92	0.46	0.40	1.47	5.21E-03	0.10	1.19	23.72	0.02	13.94	3.21	74.89	9.73
10	Rhydyronnen	9.23	266.39	8.10	0.64	4.43	7.88	12.76	0.56	0.18	0.90	4.07E-03	0.22	5.31	22.48	0.01	6.38	0.85	35.81	4.42
11	Severn Ford	11.11	204.27	11.50	0.52	5.75	11.92	22.00	0.48	0.47	2.60	4.24E-03	0.09	0.73	20.05	0.15	17.45	5.18	108.06	9.40
12	Mount Severn	16.88	165.71	17.30	1.52	24.97	18.25	11.39	1.37	0.44	13.13	1.64E-03	0.09	0.89	22.01	0.01	4.83	1.47	211.19	12.21
13	Dolwen	22.20	147.61	20.20	1.18	22.66	20.93	17.08	1.08	0.98	22.86	3.00E-03	0.06	0.26	31.87	0.06	20.03	3.29	672.83	33.31
14	Llandinam	28.00	135.20																	
15	Caersws	34.10	118.70	37.20	1.08	31.09	38.54	34.48	0.81	0.89	31.15	1.17E-03	0.03	0.09	9.26	0.01	29.29	5.17	357.51	9.61
16	Newtown	44.93	109.00																	
17	Abermule	55.92	83.00	30.40	1.52	43.65	31.27	20.03	1.40	0.76	32.53	4.80E-04	0.04	0.09	6.57	0.07	5.61	1.87	153.16	5.04
18	Dyffryn	70.30	75.02	35.00	1.82	56.37	34.77	19.24	1.62	0.54	34.06	3.00E-04	0.04	0.13	4.77	0.01	3.56	1.25	100.24	2.86
19	Pool Quay	83.20	63.03	17.65	2.37	39.59	19.82	7.45	2.00	1.57	62.35	5.16E-04	0.02	0.03	10.11				315.40	17.87
20	Crew Green	100.90	52.94	34.03	5.02	148.93	37.50	6.78	3.97	1.03	153.70	4.37E-04	0.05	0.13	17.01				658.15	19.34
21	Montford	115.46	52.00	24.70	2.34	54.99	27.25	10.56	2.02	0.65	36.17	3.40E-04	0.04	0.13	6.73	0.03	3.45	1.04	120.63	4.88
22	Buildwas	166.45	39.25	60.84	1.11	72.95	61.35	54.91	1.19	0.62	37.80	6.90E-05	0.02	0.02	0.80				25.59	0.42
23	Bridgnorth	192.36	30.52	46.34	1.24	65.76	47.01	37.40	1.40	0.82	38.00	8.56E-05	0.02	0.01	1.17				31.91	0.69
24	Bewdley	209.00	20.89	42.30	1.04	46.79	41.35	40.75	1.13	0.93	39.50	1.56E-03	0.05	0.16	17.34				605.23	14.31
25	Saxons Lode	254.13	13.27	62.35	3.22	212.85	64.14	19.37	3.32	0.97	60.50	1.79E-04	0.10	0.05	5.83				106.30	1.70

## 4.4 Downstream change in medium-flow hydraulics

### 4.4.1 Introduction

Medium flows were classified as having exceedance frequency limits of  $10 > F > 70$  %; this corresponds to a flow range of  $20 - 120 \text{ m}^3 \text{ s}^{-1}$  at Bewdley. The field results details are listed in Table 4.3 (and Appendix I). Flow variables were predominantly calculated from direct flow measurement (sections 3.6.2, 3.6.3 and 3.10.3).

### 4.4.2 Mean velocity

Mean velocity increased downstream from  $0.14 \text{ m s}^{-1}$  at Upper Hafren 1 to almost  $1.0 \text{ m s}^{-1}$  at Saxons Lode (Figure 4.14). This distribution is best described by a power function, of the form:  $\bar{u} = 0.28DD^{0.23}$  ( $n = 23$ ;  $p < 0.001$ ;  $r^2 = 0.78$ ). Despite this rising downstream trend, it is clear that there are two discrete clusters of sites, grouped upstream and downstream of Llanidloes (Figure 4.14). Upstream of Llanidloes, mean velocity increased to approximately  $0.5 \text{ m s}^{-1}$ . However, downstream of Llanidloes, mean velocity rose suddenly to  $0.98 \text{ m s}^{-1}$  at Dolwen (consistent with the low flow trend (Figure 4.5)) and thereafter became highly variable. For example, between Dyffryn (70 km) and Buildwas (166 km), mean velocity rose sharply at Pool Quay (83 km) from  $0.53 \text{ m s}^{-1}$  to  $1.57 \text{ m s}^{-1}$  and declined gradually at Buildwas ( $0.6 \text{ m s}^{-1}$ ). The enhanced variability of mean velocity through the lower reaches is perhaps a function of the more variable channel form, described in a bankfull state in 4.2.2 (Figures 4.1 & 4.2) and to be discussed in section 4.6.3. The implications of these trends will be discussed in Chapter 7.

### 4.4.3 Discharge

Figure 4.15 illustrates how discharge increased downstream at a medium-flow level. This distribution is best described by the log-log cubic function shown in Figure 4.15, ie:  $\log(Q) = -1.24 + 1.50\log(DD) + 0.55\log(DD)^2 - 0.28\log(DD)^3$ ;  $n = 23$ ;  $p < 0.001$ ;  $r^2 = 0.97$ ). Downstream from the source to Severn Ford (11km) (Figure 3.1), discharge increased in a uniform manner, although downstream reductions in discharge (eg: Rhydyronnen) reflect the difficulty of sampling all flows at the same steady state condition. From Dolwen to Bewdley, discharge remained remarkably constant at approximately  $20 - 30 \text{ m}^3 \text{ s}^{-1}$ . Again, the outliers at Pool Quay and Crew Green (Figure 4.15) may be the result of sampling inconsistencies, or alternatively, the suppressed downstream increase in flow may have been caused by water abstraction of over  $700 \text{ Ml d}^{-1}$  in the middle reaches for industries in Telford, Birmingham and the Midlands (Douglas, 1988).

### 4.4.4 Water surface slope

Water surface slope decreased with distance from the source (Figure 4.16), and is best described by the function:  $\log(s) = 1.34 - 0.61\log(DD) - 0.55\log(DD)^2 + 0.16\log(DD)^3$  ( $n = 23$ ;  $p < 0.001$ ;  $r^2 = 0.91$ ). Like the low-flow trend for water surface slope (Figure 4.7), this downstream trend is marked by a pronounced break of slope in the headwaters, between Upper Hafren 3 and Tanllwyth. From Tanllwyth, slope decreased from  $0.01 \text{ m m}^{-1}$  to  $0.00008 \text{ m m}^{-1}$  at Buildwas (Figure 4.16). Again, the significance of



the Ironbridge gorge was expressed by elevated water surface slopes at Bridgnorth and Bewdley, peaking at  $0.002 \text{ m m}^{-1}$  (Figure 4.16).

#### 4.4.5 Flow resistance

Flow resistance at a medium-flow declined gradually downstream from the source region of the Severn to Saxons Lode ( $n = 0.3$  to  $0.02$ ; and  $f = 10.5$  to  $< 0.5$ ) (Figures 4.17 & 4.18). In the upper study reaches (upstream of Mount Severn), the roughness coefficients ( $n$  and  $f$ ) were highly variable, with an upper limit of  $n = 0.9$  and a lower limit of  $n = 0.3$ . Further downstream,  $n$  and  $f$  remained fairly constant at approximately  $n = 0.04$  and  $f < 0.5$ . This distribution is significantly different to the low-flow trends, where the magnitude of the resistance coefficients was much greater and resistance actually increased downstream to Mount Severn (Figures 4.8 & 4.9), rather than decreasing. Clearly, the dominance of the various flow resistance components are governed by stage and channel topography, and it is the combination of these factors which has produced different downstream trends at low- and medium-flows.

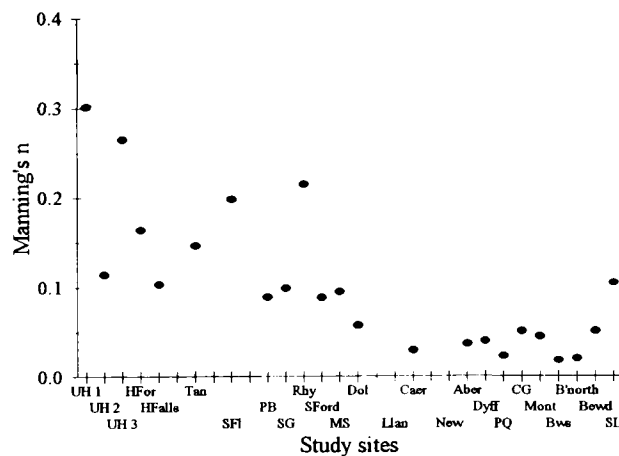


Figure 4.17 The spatial variation of Manning's  $n$  roughness coefficient along the Severn at a medium-flow level.

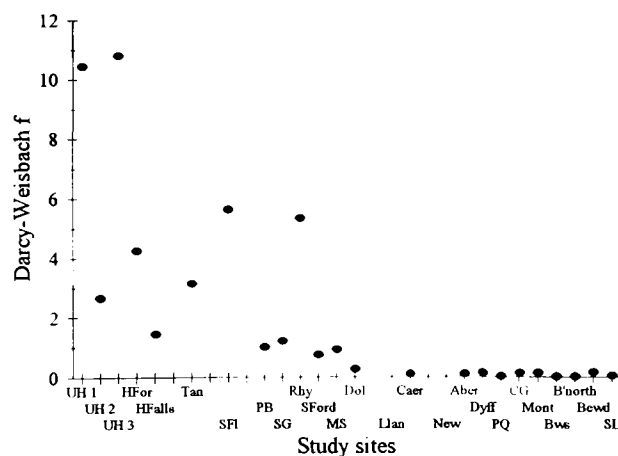


Figure 4.18 The spatial variation of the Darcy-Weisbach friction factor,  $f$ , along the Severn at a medium-flow level.

#### 4.4.6 Total and unit stream power

Total stream power remained low in the upper reaches ( $< 100 \text{ W m}^{-1}$ ), peaking in the mid-basin ( $672 \text{ W m}^{-1}$  at Dolwen) and declining to less than  $100 \text{ W m}^{-1}$  further downstream (Figure 4.19). This has been represented by upper and lower envelope curves which embrace the entire distribution (Figure 4.19). These indicate that upstream of Mount Severn (16 km), the maximum level of total stream power increases with distance downstream and the lower limit remains low, giving an increasing range of total stream power with distance from the source. Maximum levels of total stream power occur between 22 km (Dolwen) and 210 km (Bewdley) downstream (Figure 4.19). The degree of inter-reach scale variability is great. For example, downstream of Abermule most sites have total stream powers comparable with the upper reaches ( $< 200 \text{ W m}^{-1}$ ), except for Pool Quay, Crew Green and Bewdley whose total stream power exceed  $600 \text{ W m}^{-1}$  (Figure 4.19). These outliers can be explained by high discharges at the first two sites (Figure 4.15), and the water surface slope (Figure 4.16) at the latter.

The spatial variation of unit stream power also showed a mid-basin peak, but much closer to the source (Figure 4.20). This indicates that both minimum and maximum unit stream power increase rapidly away from the source for approximately 2 km. Thereafter, minimum unit stream power decreased gradually from  $13 \text{ W m}^{-2}$  to less than  $1 \text{ W m}^{-2}$  in the lower catchment. However, maximum unit stream power continued to rise to a peak of  $40 \text{ W m}^{-2}$  at almost 6 km downstream (Picnic Bridge), and then declined downstream. These envelope curves suggest that the inter-reach range of unit stream power varies considerably downstream, reaching a maximum between 5 and 30 km along the channel, close to the region of maximum channel activity found by Lewin (1987) (Figure 2.9).

#### 4.4.7 Reach mean and boundary shear stress

Reach mean shear stress increased to a peak of approximately  $60 \text{ W m}^{-2}$  between 1-6 km from the source (Figure 4.21). The best-fit line illustrates this general trend ( $\log(\tau) = 1.69 - 0.003\log(DD) - 0.23\log(DD)^2$ ;  $n = 23$ ;  $p > 0.001$ ;  $r^2 = 0.68$ ). The lower catchment has noticeably lower shear stresses, with peaks at Crew Green and Bewdley of  $> 20 \text{ N m}^{-2}$ . This is generally consistent with the low-flow trends (Figure 4.12), although the influence of stage has enhanced the magnitude of shear stress, particularly in the headwater region of the catchment.

Boundary shear stress shows no significant downstream trend at the thirteen sites measured at this flow level (Figure 4.22); this limited data set was the result of difficulties ensuring safety during flow measurement. The mean boundary shear stress was generally higher in the reaches upstream of Abermule. Hafren Falls and Picnic Bridge had noticeably greater shear stress values, largely as a result of a single unreasonably high value in one vertical (ie:  $627 \text{ N m}^{-2}$  at Hafren Falls). This was probably caused by experimental error. The minimum calculated shear stress was almost  $0 \text{ N m}^{-2}$  at all thirteen sites. These results illustrate the limitations behind field measurements of boundary shear stress using 1-D velocity profile techniques, where rough channel boundaries impede measuring devices and generate non-uniform turbulent flows.

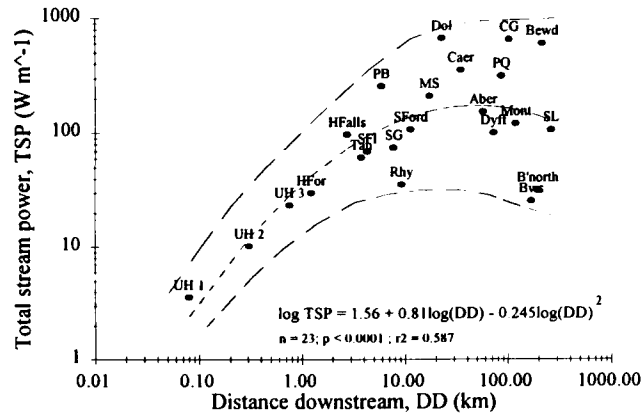


Figure 4.19 The spatial variation of total stream power along the Severn at a medium-flow level, including the best-fit trend line and equation.

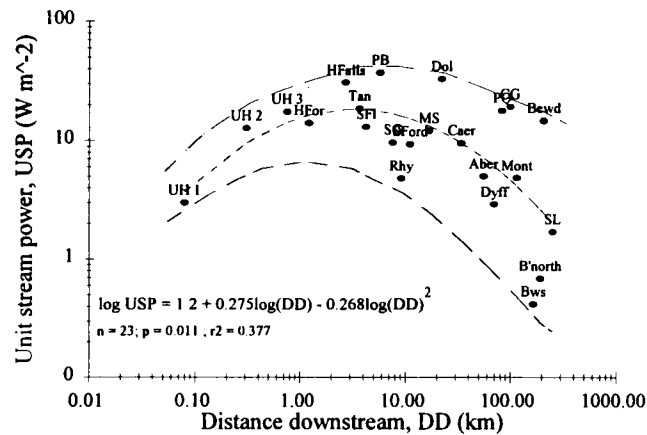


Figure 4.20 The spatial variation of unit stream power along the Severn at a medium-flow level, including the best-fit trend line and equation.

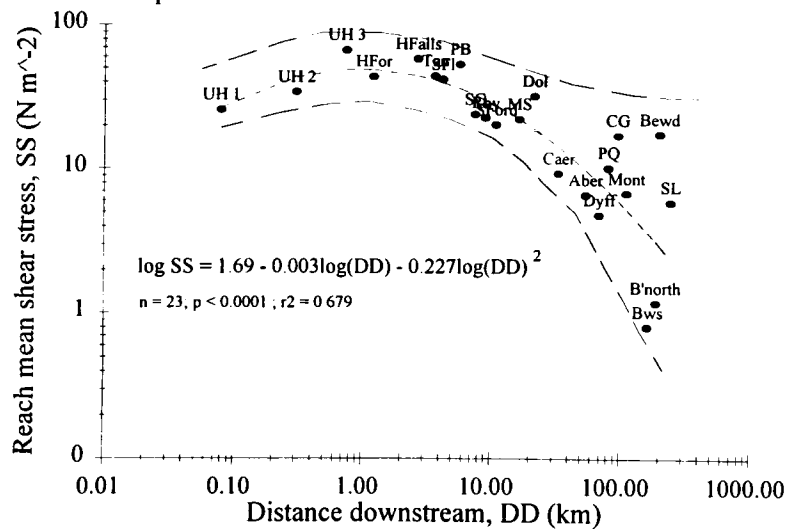


Figure 4.21 The spatial variation of reach mean shear stress along the Severn at a medium-flow level, including the best-fit trend line and equation.

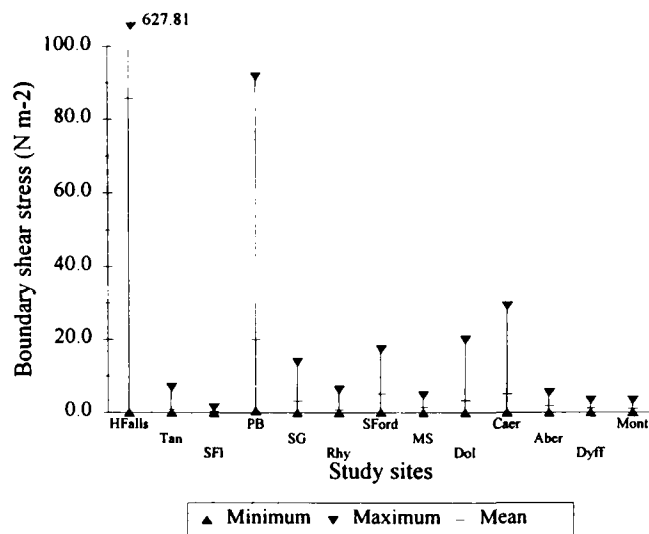


Figure 4.22 The spatial variation of boundary shear stress along the Severn at a medium-flow level.

## 4.5 Downstream change in high-flow hydraulics

### 4.5.1 Introduction

High flows were classified as having an exceedance frequency of  $F < 10\%$ ; this corresponds to flows of greater than  $120 \text{ m}^3 \text{ s}^{-1}$  at Bewdley. The field results for this section are tabulated in Table 4.4. These results include the trash line survey for the upper catchment and the indirect flow estimation methods; for details of the surveying technique and discharge estimation method, see sections 3.4.5, 3.7 and 3.8.

### 4.5.2 Mean velocity

Mean velocity generally increased downstream from the source to Saxons Lode (Figure 4.23). This trend is best described by the power function:  $\bar{u} = 0.86DD^{0.08}$ ;  $n = 23$ ;  $p = 0.098$ ;  $r^2 = 0.12$ ). The highest mean velocities were recorded in the upper reaches, between Hafren Falls and Severn Ford ( $\bar{u} > 1.5 \text{ m s}^{-1}$ ). These were calculated from the trash line survey, and thus may suggest a lack of accuracy. However, the discharge gauged at Tanllwyth was used to calculate the mean velocity at this site; hence, it is perhaps not unreasonable for such high velocities to occur in the headwater regions. Mean velocity was more variable in the lower catchment, but this only conceals a coherent inter-reach trend also largely present in the low- and medium-flow distributions (Figures 4.5 and 4.14).

### 4.5.3 Discharge

Discharge increased by almost four orders of magnitude between the headwaters to Saxons Lode (250 km downstream), from  $0.01 \text{ m}^3 \text{ s}^{-1}$  to almost  $300 \text{ m}^3 \text{ s}^{-1}$  (Figure 4.24). The log-log distribution (best described by the function:  $Q = 1.17DD^{1.02}$ ;  $n = 23$ ;  $p < 0.001$ ;  $r^2 = 0.98$ ) exhibits good agreement about the fitted trend line, indicating that tributary inputs along the Severn generally had a less significant influence on these results than for low- and medium-flows (Figures 4.6 & 4.15). An exception occurred

Table 4 4 The channel hydraulic parameters measured at high flow at sites along the River Severn.

Site number	Site name	Distance downstream (km)	Elevation (m) (a.s.l)	Water width (m)	Mean depth (m)	Section area (m <sup>2</sup> )	Wetted perimeter (m)	w/d (m m <sup>-1</sup> )	Hydraulic radius (m)	Mean velocity (m s <sup>-1</sup> )	Section discharge (m <sup>3</sup> s <sup>-1</sup> )	Water surface slope (m m <sup>-1</sup> )	Manning's n	Darcy f	Reach mean shear stress (N m <sup>-2</sup> )	Total stream power (W m <sup>-1</sup> )	Unit stream power (W m <sup>-2</sup> )
1	Upper Hafren 1	0.08	606.21	1.34	0.39	0.50	1.91	3.41	0.26	0.23	0.11	3.24E-02	0.32	12.47	83.03	36.50	27.26
2	Upper Hafren 2	0.31	580.22	1.45	0.39	0.46	2.07	3.68	0.22	0.64	0.29	4.66E-02	0.12	1.98	101.01	133.35	91.97
3	Upper Hafren 3	0.76	547.76	1.64	0.33	0.56	2.16	4.96	0.26	1.22	0.67	4.71E-02	0.07	0.64	118.80	311.72	190.07
4	Hafren Forest	1.23	524.38	3.60	0.45	1.58	4.44	8.02	0.36	0.71	1.12	3.31E-02	0.13	1.84	115.99	365.25	101.46
5	Hafren Falls	2.73	390.72	3.15	0.49	1.37	3.60	6.45	0.38	2.11	2.89	3.20E-02	0.04	0.21	119.05	907.83	288.20
6	Tanllwyth	3.71	347.79	3.44	0.39	1.43	4.36	8.77	0.33	2.02	2.90	1.89E-02	0.03	0.12	61.06	537.33	156.34
7	Severn Flume	4.26	334.33	9.12	1.09	9.07	11.34	8.39	0.80	0.71	6.48	3.21E-03	0.07	0.39	25.19	204.06	22.37
8	Picnic Bridge	5.81	313.71	7.08	0.63	4.34	7.80	11.15	0.56	1.84	7.97	2.06E-02	0.05	0.27	112.36	1609.65	227.51
9	Severn Gorge	7.62	271.57														
10	Rhydyronnen	9.23	266.39	11.08	1.23	12.89	13.68	8.99	0.94	1.21	15.56	2.91E-02	0.14	1.48	269.20	4442.96	401.13
11	Severn Ford	11.11	204.27	12.12	0.72	8.93	13.12	16.92	0.68	2.29	20.47	3.52E-03	0.02	0.04	23.52	706.86	58.32
12	Mount Severn	16.88	165.71	16.59	1.48	25.40	18.42	11.23	1.38	0.87	22.20	2.12E-03	0.07	0.30	28.68	461.70	27.82
13	Dolwen	22.20	147.61	21.76	0.39	27.03	22.73	56.38	1.19	1.52	41.09	2.86E-03	0.04	0.12	33.32	1152.90	52.93
				21.80	0.39	26.94	24.44	56.62	1.10	1.09	29.48	1.75E-03	0.04	0.13	18.95	506.08	23.24
14	Llandinam	28.00	135.20	21.37	0.91	20.22	23.76	23.41	0.85	1.54	31.09	2.58E-03	0.03	0.07	21.54	786.83	36.83
15	Caersws	34.10	118.70	53.28	0.54	48.69	55.38	99.59	0.88	0.83	40.21	2.02E-03	0.05	0.20	17.40	796.85	14.94
				51.56	0.49	44.91	53.65	104.37	0.84	1.11	49.79	1.84E-03	0.03	0.10	15.09	898.77	17.40
16	Newtown	44.93	109.00	35.00	0.65	40.00	52.25	53.52	0.64	1.38	55.00	6.33E-03	0.04	0.17	39.92	3415.35	97.58
17	Abermule	55.92	83.00	33.05	2.46	74.38	34.83	13.42	2.14	0.90	66.86	6.14E-04	0.05	0.13	12.87	402.71	12.18
18	Dyffryn	70.30	75.02	51.62	2.91	132.09	66.32	17.72	1.99	0.61	80.00	1.10E-03	0.09	0.47	21.49	863.28	16.72
19	Pool Quay	83.20	63.03	27.62	4.05	94.60	30.75	6.82	3.08	0.90	85.00	1.37E-03	0.09	0.41	41.35	1142.37	41.35
20	Crew Green	100.90	52.94	67.20	5.76	216.61	71.45	11.66	3.03	1.28	277.23	1.18E-03	0.06	0.17	35.07	3209.16	47.76
21	Montford	115.46	52.00	36.99	4.90	164.26	41.29	7.55	3.98	0.67	110.25	9.46E-04	0.11	0.66	36.90	1022.73	27.65
22	Buildwas	166.45	39.25	67.20	1.94	130.89	67.97	34.69	1.93	1.72	224.54	1.18E-03	0.03	0.06	22.22	2599.20	38.55
23	Bridgnorth	192.36	30.52	50.51	2.97	163.12	52.88	17.01	3.08	1.40	228.51	7.00E-04	0.04	0.09	21.18	1569.15	31.07
24	Bewdley	209.00	20.89	49.94	3.53	187.58	53.57	14.15	3.50	1.22	229.17	1.44E-04	0.02	0.03	4.95	323.73	6.48
25	Saxons Lode	254.13	13.27	63.49	3.80	253.68	65.86	16.70	3.85	1.09	275.46	7.34E-04	0.06	0.19	27.73	1983.48	31.24

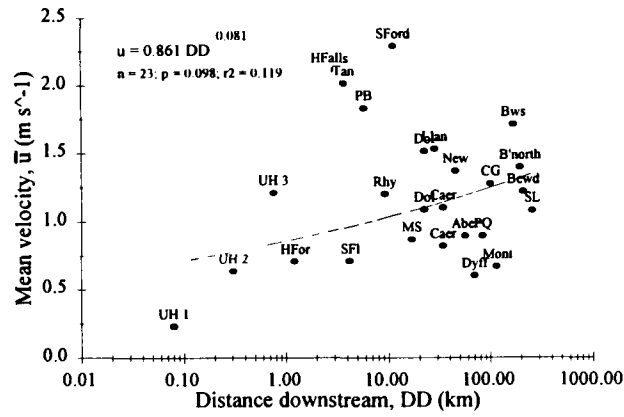


Figure 4.23 The spatial variation of mean velocity along the Severn at a high-flow level, including the best-fit trend line and equation.

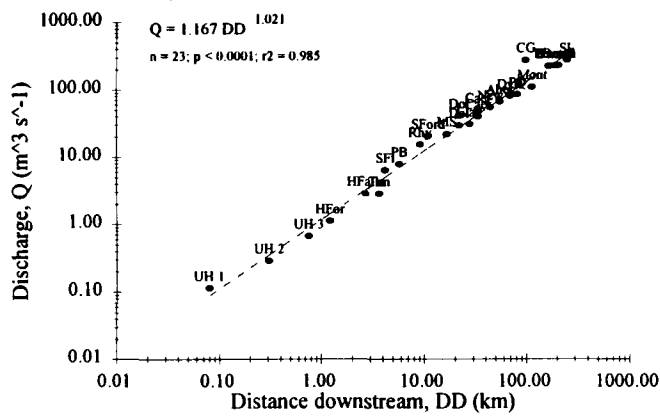


Figure 4.24 The spatial variation of discharge along the Severn at a high-flow level, including the best-fit trend line and equation.

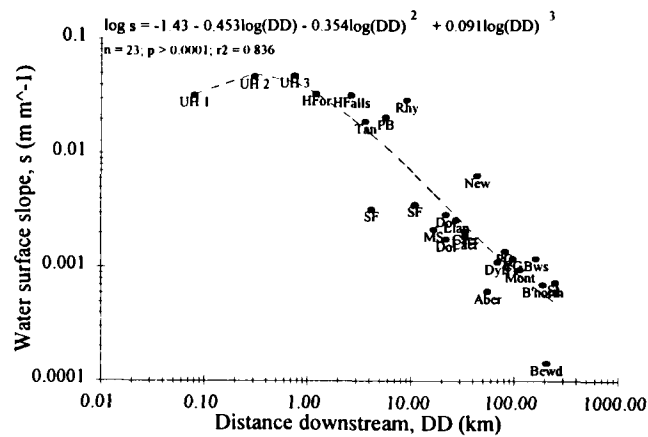


Figure 4.25 The spatial variation of water surface slope along the Severn at a high-flow level, including the best-fit trend line and equation.

at Crew Green, which is consistent with the medium-flow results (Figure 4.15). Therefore, this suggests that either the timing of flow measurement was in error or the gauging station was prone to inaccurate readings at high flows; the magnitude of abstractions is likely to be insignificant at high flow levels.

#### 4.5.4 Water surface slope

The downstream decline of water surface slope was dominated by two almost discrete distributions (Figure 4.25). The log-log polynomial best-fit line ( $\log(s) = -1.43 - 0.45\log(DD) - 0.35\log(DD)^2 + 0.09\log(DD)^3$ ;  $n = 23$ ;  $p < 0.001$ ;  $r^2 = 0.84$ ) indicates that the division between the upper and lower catchment is marked by a rapid decline of slope (Figure 4.25). In the upper reaches, slope was almost constant at a value of between  $0.02 - 0.03 \text{ m m}^{-1}$ , and, following this, declined abruptly between Rhydyronnen (9 km) and Severn Ford (11 km). Downstream from Severn Ford to Saxons Lode, the reduction in slope was more gradual. This trend is considerably different to the low- and medium-flow trends (Figures 4.7 & 4.14), primarily because of: a) the enhanced slopes further downstream from the headwaters; and b) an increase of slopes in the lower catchment by an order of magnitude. These two factors perhaps indicate that topographical controls are 'drowned out' by increasing stage, allowing the water surface slope to adjust to the valley slope.

#### 4.5.5 Flow resistance

Figures 4.26 and 4.27 show that flow resistance ( $n$  and  $f$ ) generally decreased with distance downstream at high-flows. In the headwaters,  $n$ -values exceeded 0.1 ( $f > 1$ ), but further downstream the distribution was practically uniform, except for minor peaks at Rhydyronnen and Montford (Figure 4.26); this contradicts the theoretical distribution of a continual downstream decrease proposed by Knighton (1987). Also, the magnitude of the roughness coefficients are almost the same as for the medium-flows (Figure 4.17). The uniformity of this distribution suggests that in the lower reaches, the high-flow roughness coefficients do not decrease as rapidly with stage as in the upper reaches because enhanced boundary roughness (shrubs, trees) at high stage counteracts the reduced relative roughness: in the upper reaches, the banks are generally free from vegetation and thus resistance would decrease with stage.

#### 4.5.6 Total and unit stream power

Total stream power increased with distance downstream, reaching a slight peak in the middle reaches (Figure 4.28); this trend is best described by the log-log quadratic function:  $\log(Q) = 2.50 + 0.63\log(DD) - 0.17\log(DD)^2$ ;  $n = 23$ ;  $p > 0.001$ ,  $r^2 = 0.58$ ). The lower and upper envelope curves indicate the possible range of total stream powers for a given reach along the channel. In this zone, the magnitude of total stream powers ( $\Omega > 4000 \text{ W m}^{-1}$ ) embrace the stream powers estimated by Lewin (1982; 1983) and Brown (1987) in studies of the Severn. In the upper reaches, high water surface slopes and low discharges impose a confined limit on the range of possible total stream powers. Further downstream, slope and discharge were more variable over time and space, thus widening the upper and lower limits of the distribution. The location of the mid-basin peak coincides with the region of high channel activity, which Lewin (1982; 1983; 1987) attributed to high stream powers despite considerable scatter in his results. Figure 4.28 demonstrates that the scatter was possibly the result of inter-reach scale variation in

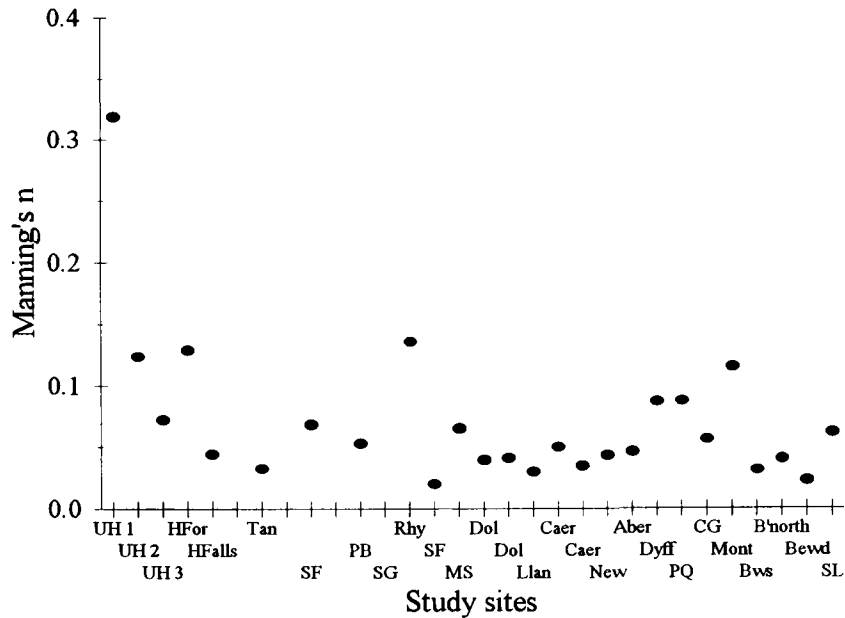


Figure 4.26 The spatial variation of Manning's  $n$  roughness coefficient along the Severn at a high-flow level.

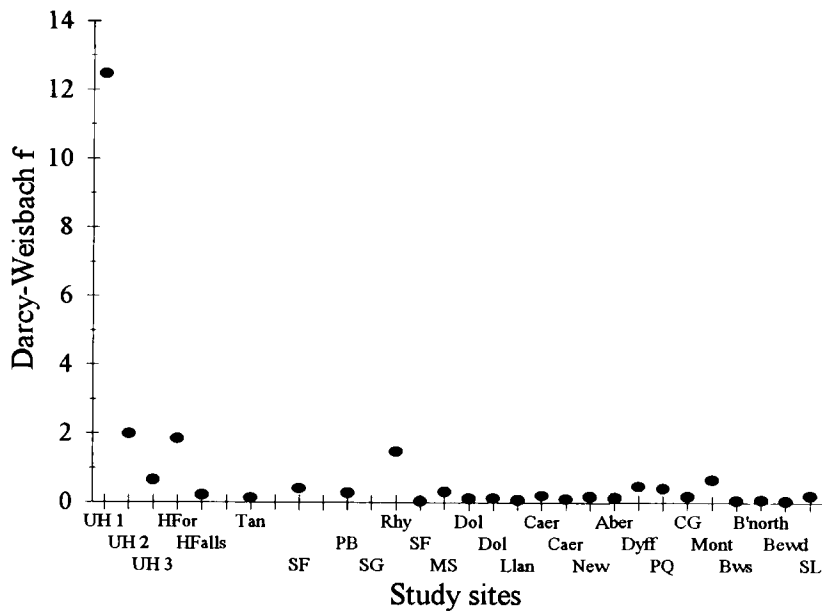


Figure 4.27 The spatial variation of the Darcy-Weisbach friction factor,  $f$ , along the Severn at a high-flow level.

stream power, which appears to form a mid-basin peak when represented at a catchment-scale in this study.

Unit stream power increased greatly downstream from the source to Rhydyronnen, then declined sharply between Rhydyronnen and Severn Ford and remained low at all sites further downstream (Figure 4.29). The envelope curves illustrate the spatial variation of minimum and maximum unit stream powers through the catchment. The upper limit increases downstream from the source, and peaks at 9 km (Rhydyronnen) ( $\omega > 400 \text{ W m}^{-2}$ ); thereafter, the upper limit is no greater than  $50 \text{ W m}^{-2}$ . These values agree with those estimated by Brown (1987) and Lewin (1987) on the Severn, and predicted by Magilligan (1992) in the Galena catchment, Wisconsin.

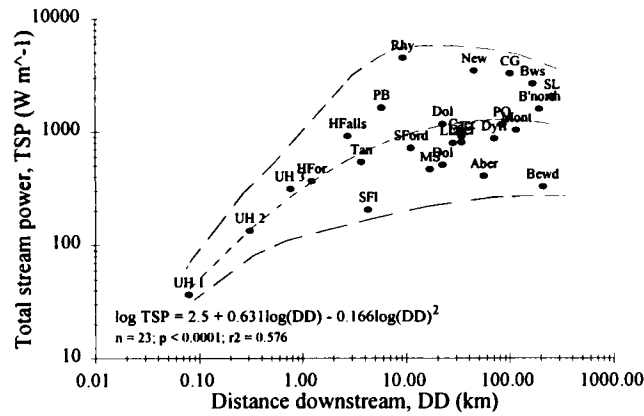


Figure 4.28 The spatial variation of total stream power along the Severn at a high-flow level, including the best-fit trend line and equation. The upper and lower limits of the distribution are bounded by an envelope curve.

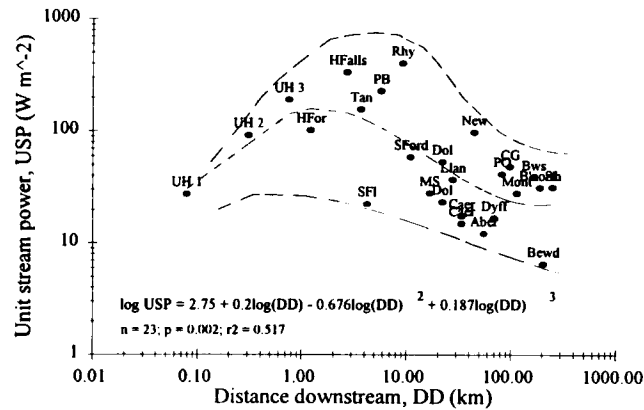


Figure 4.29 The spatial variation of unit stream power along the Severn at a high-flow level, including the best-fit trend line and equation. The upper and lower limits of the distribution are bounded by an envelope curve.

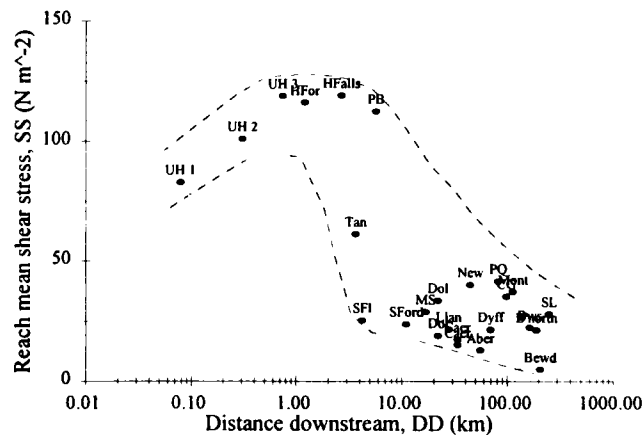


Figure 4.30 The spatial variation of reach mean shear stress along the Severn at a high-flow level, including the best-fit trend line and equation. The upper and lower limits of the distribution are bounded by an envelope curve.

#### *4.5.7 Reach mean shear stress*

Reach mean shear stress increased slightly downstream from the headwaters, but declined abruptly at Rhydyronnen and remained low at all sites downstream to Saxons Lode (Figure 4.30). Like the total and unit stream power trends (Figures 4.28 and 4.29, respectively), Rhydyronnen dominated this distribution, with a peak of  $> 250 \text{ N m}^{-2}$ . The sites upstream achieve shear stress values of between  $80 - 130 \text{ N m}^{-2}$ , except for Tanllwyth and Severn Flume which were considerably lower. Downstream from Severn Ford, shear stress values were confined between  $10 - 50 \text{ N m}^{-2}$ , reflecting the influence of longitudinal variation of water surface slope on these trends (Figure 4.25).

### **4.6 Inter-relationships between stage, channel form and channel hydraulics**

#### *4.6.1 Introduction*

The analysis of low-, medium- and high-flows on the downstream variation of channel hydraulics has revealed consistent trends emerging along the channel. This section will, therefore, analyse the significance of increasing flow levels on the spatial distributions of these hydraulic variables (see Table 4.1). It will also analyse the spatial relationships between the channel geometry parameters measured during flow measurement (section 3.4) to evaluate the impact of flow geometry on the channel hydraulics.

#### *4.6.2 Effect of stage on the downstream distribution of channel geometry*

Water width increased rapidly through the middle reaches of the Severn, but at a slower rate in the headwater and lower reaches (Figure 4.31). This non-linear distribution, described by log-log polynomial functions (Table 4.1), existed at each of the low-, medium and high-flow levels considered in this study. The significance of these congruous width distributions demonstrates how the river responds to an increase in stage along the channel by increasing the width at a constant relative magnitude: this suggests either that the channel form is similar along the entire Severn or that the site selection procedure has successfully identified similar channel forms. Two outliers exist at Caersws and Pool Quay. The former is a wide (Figure 4.1), meandering reach (Figure 4.3) where width rapidly increases with stage. Conversely, the latter is a deeply incised reach carved into post-glacial sediments (Figure 4.2) and thus compensates for a limited increase of width by rapidly increasing flow depth. The spatial variation of width implies that the headwaters and lower reaches are prevented from eroding laterally at comparable rates to the sites located in the middle reaches, and will be discussed further in Chapter 7.

Mean depth increases with distance downstream along the Severn, and stage (Figure 4.32 & Table 4.1). However, unlike the water width distribution (Figure 4.31), the rate of increase of mean depth between flow conditions is great, particularly in the headwaters and at sites between Abermule and Montford (Figure 3.1). In addition, slight floodplain inundation is indirectly represented by unusually low high-flow mean depths at Dolwen, Caersws, Newtown and Buildwas. These trends are replicated in the downstream distribution of hydraulic radius at the three flow conditions (Figures 4.33). The consistency between the upper, middle and lower Severn trends for width (Figure 4.31), mean depth (Figure 4.32)



and hydraulic radius (Figure 4.33) suggest that there is a downstream transition in the factors controlling lateral channel adjustment; such factors may include: channel hydraulics and available energy; valley confinement; bank composition, structure and resistance; and vegetation. These will be discussed in greater detail in Chapter 7, but first, the effect of stage on the spatial distribution of channel hydraulics will be reviewed.

#### 4.6.3 Effect of stage on the downstream distribution of channel hydraulics

A comparison of mean velocities measured at low-, medium- and high-flows reveals a distinct tendency for velocities to increase downstream at medium- and high-flows (Figure 4.34 & Table 4.1). This conforms with the results of hydraulic geometry studies (eg: Leopold & Maddock, 1953; Charlton *et al.*, 1978; Bray, 1982) and confirms the findings of Leopold (1953). However, these results present a more comprehensible illustration of the manner in which velocity changes downstream because only one river was analysed, and distance downstream was plotted on the ordinate axis, rather than discharge (Mackin, 1963) (section 2.4.4). Furthermore, the at-a-site magnitude of velocity increases with flow level, although considerable variability exists between sites. In particular, mean velocities in excess of  $2 \text{ m s}^{-1}$  were estimated in the upper reaches between Hafren Falls and Severn Ford (Figure 4.34).

Figure 4.35 and Table 4.1 demonstrate that the rate of increase of discharge downstream is comparable at low-, medium- and high-flow conditions. The magnitude of the recorded discharges flowing through the Severn were relatively low by world standards (maximum measured discharge on the Amazon of  $26\,600 \text{ m}^3 \text{ s}^{-1}$  (Richey *et al.*, 1986)), but represent a moderate flow for the UK (maximum mean daily discharge on the River Thames at Teddington Weir =  $475 \text{ m}^3 \text{ s}^{-1}$  over a four-year period (Shaw, 1988)). Figure 4.35 also reveals a measurement selection problem in the middle reaches between medium- and high-flows as the two distributions converge. Hence, it is likely that channel hydraulic variables measured at medium- and high-flows may be similar in these reaches, as indeed was the case for mean velocities (Figure 4.34). The significance of tributary inputs on the downstream trend is also apparent in the Mount Severn - Dolwen reach (Afon Clywedog), and the Pool Quay - Crew Green (Afon Vyrnwy).

The impact of stage on the water surface slope is relatively insignificant in the upper and middle reaches (upstream of Newtown), but causes a large increase of slope in the lower reaches (Figure 4.36); this is particularly pronounced between Abermule and Buildwas. The stage-invariant slope in the upper-middle reaches suggests that they approximate the steep valley slopes, and thus represent quasi-uniform slopes. This implies that in steep mountain streams, the channel slope may be used to represent the water surface slope (which is more difficult to measure).

Flow resistance decreases with stage in the reaches upstream of Mount Severn, but is more variable in the middle and lower reaches (Figures 4.37 and 4.38). Indeed, at study sites between Dolwen and Bridgnorth, flow resistance is equally likely to increase with stage. These latter trends suggest that the absence of large in-channel roughness components and bank-side vegetation results in reduced resistance at low-flow, but enhanced resistance at high-flow: hence, the reverse trend. Furthermore, there is a tendency for the location at which roughness declines to very low levels to migrate upstream as flow levels increase.

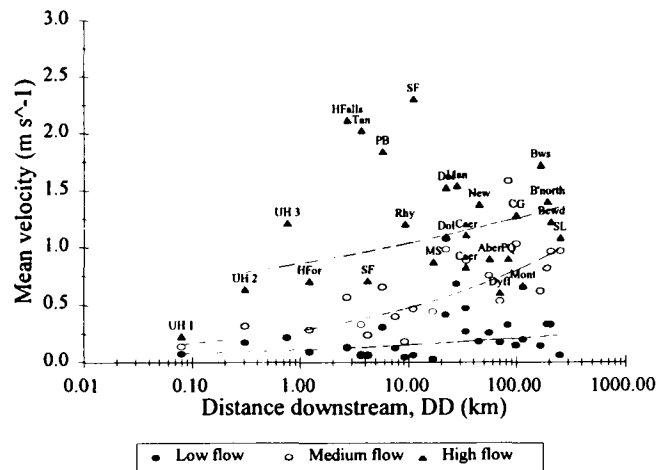


Figure 4.34 The spatial and temporal variation of mean velocity along the Severn, including the best-fit trend lines used in Figures 4.5, 4.14 and 4.23 and listed in Table 4.1.

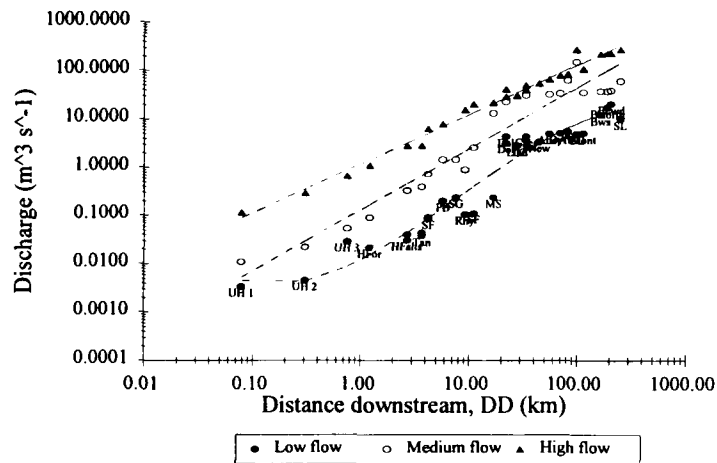


Figure 4.35 The spatial and temporal variation of discharge along the Severn, including the best-fit trend lines used in Figures 4.6, 4.15 and 4.24 and listed in Table 4.1.

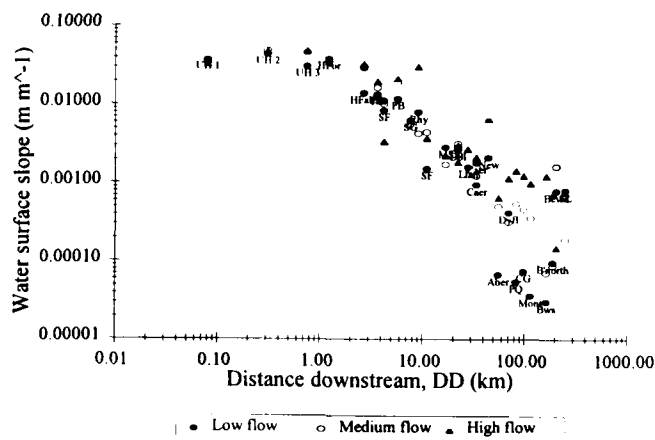


Figure 4.36 The spatial and temporal variation of water surface slope along the Severn.

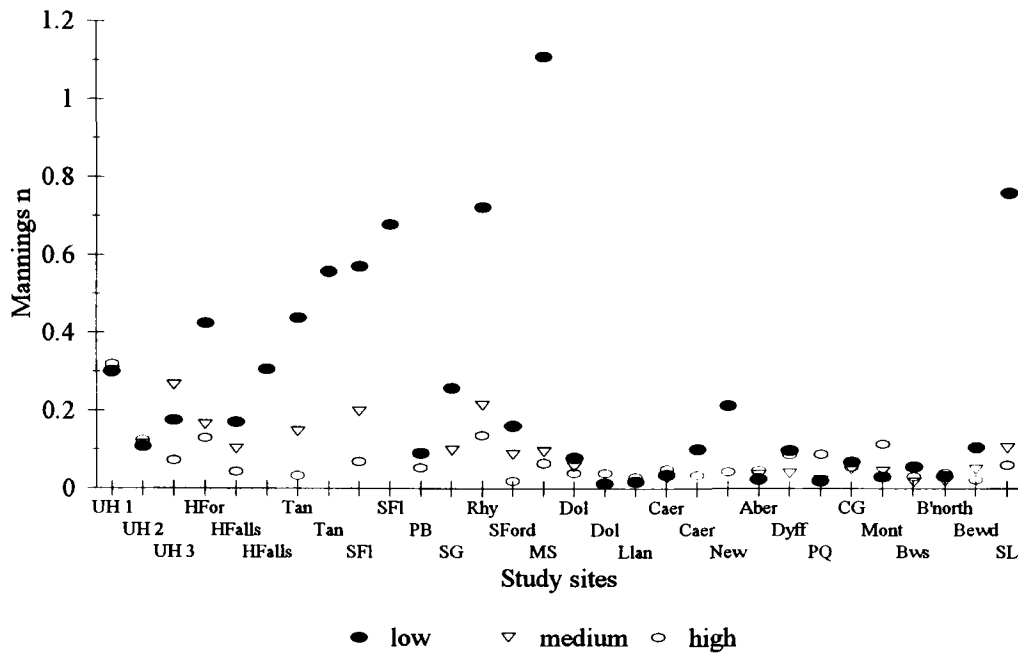


Figure 4.37 The spatial and temporal variation of Manning's  $n$  roughness coefficient along the Severn.

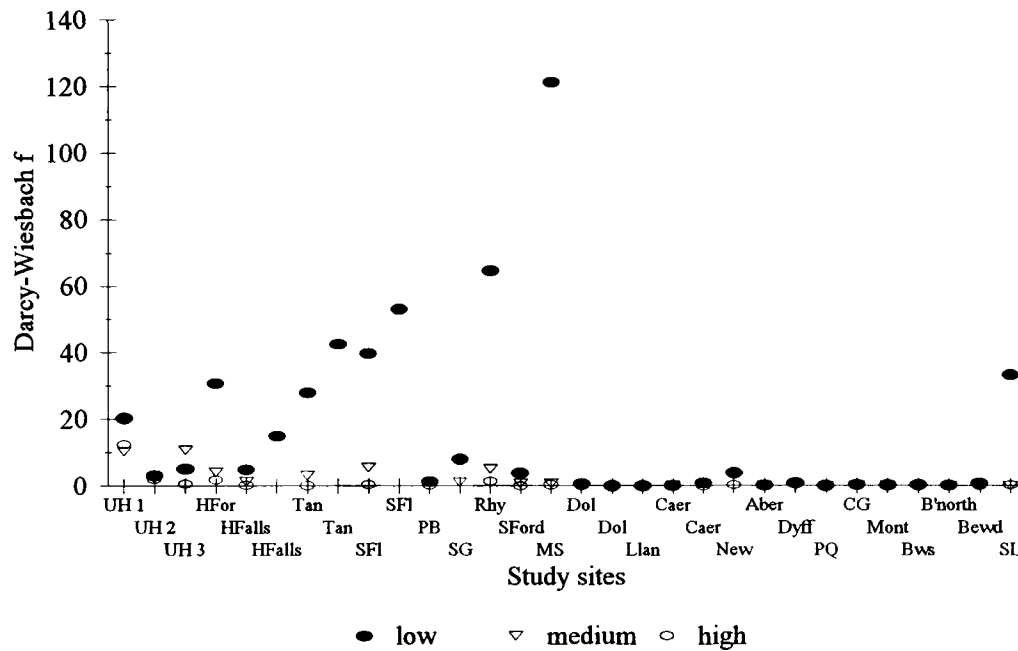


Figure 4.38 The spatial and temporal variation of the Darcy-Weisbach friction factor,  $f$ , along the Severn.

Total stream power increases with stage downstream along the Severn (Figure 4.39 & Table 4.1). The trend lines indicate that total stream power rises rapidly through the upper reaches, and remains relatively constant at approximately  $300 \text{ W m}^{-1}$  between 10 - 250 km downstream. Although some reach-scale variability exists in this distribution (particularly in the low-flow trends), the three flow conditions produce significantly different magnitudes of stream power. Similarly, the unit stream power distribution shows that stream powers are significantly different along the channel as flow levels rise (Figure 4.40). Indeed, this demonstrates convincing evidence for a upper-middle basin peak of almost  $400 \text{ W m}^{-2}$ , and strongly supports the theories of Graf (1982; 1983a), Lewin (1982; 1983; 1987), Lawler (1992) and Lecce (1993).

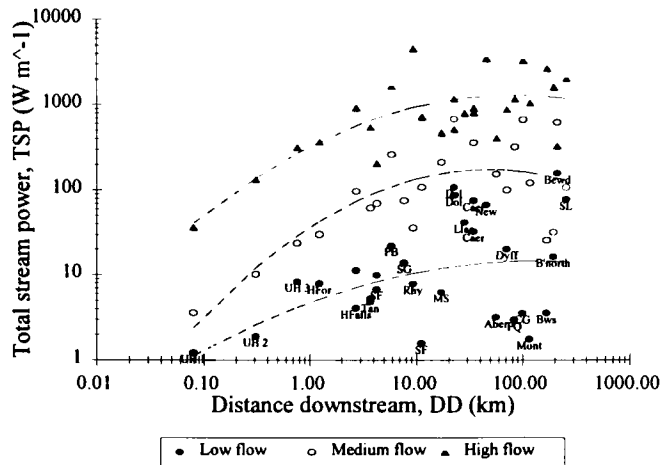


Figure 4.39 The spatial and temporal variation of total stream power along the Severn, including the best-fit trend lines used in Figures 4.10, 4.19 and 4.29 and listed in Table 4.1.

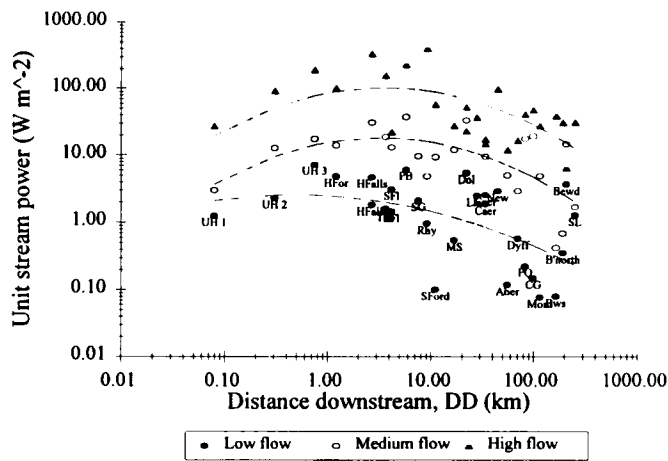


Figure 4.40 The spatial and temporal variation of unit stream power along the Severn, including the best-fit trend lines used in Figures 4.11, 4.20 and 4.30 and listed in Table 4.1.

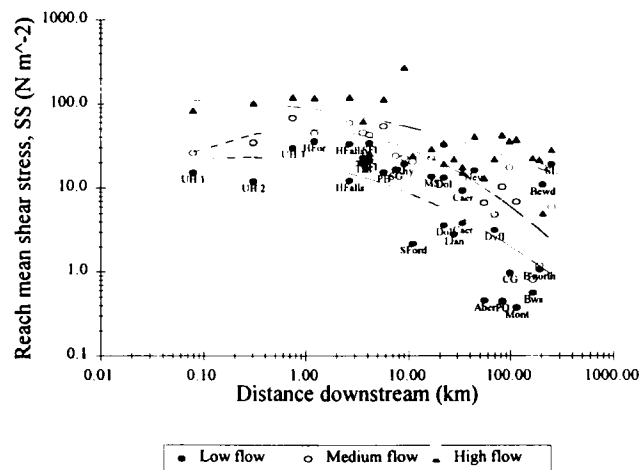


Figure 4.41 The spatial and temporal variation of reach mean shear stress along the Severn, including the best-fit trend lines used in Figures 4.12 and 4.21 and listed in Table 4.1.

Reach mean shear stress also exhibits a slight mid-basin peak ( $> 200 \text{ N m}^{-2}$ ), although the general trend at the three flow levels is of a downstream decline (Figure 4.41 & Table 4.1). In contrast to the total and unit stream power distributions, the magnitude of variation of shear stress with stage is poorly defined and results in more at-a-site variability, particularly between Dolwen and Newtown. However, this may be partly attributable to the discharge measurement selection errors (Figure 4.35) discussed earlier in this section. The inter-reach and at-a-site variation of stream power and shear stress potentially have important implications for the remobilisation of alluvial deposits and the diversity of ecological habitats in the channel. For example, locations of high shear stress and stream power are likely to be the foci of enhanced channel erosion (Graf, 1982, 1983a; Bull, 1979; Lewin, 1982, 1983, 1987) and conversely, low shear stress and stream power may induce sediment deposition. Hence, the longitudinal variation of available energy will lead to the uneven movement and storage of sediment in the channel (Graf, 1982). Correspondingly, the habitat preferences of in-channel species are likely to reflect the spatial variation of these hydraulic variables (Statzner & Higler, 1986), along the channel, and be affected by the magnitude of variation with stage. The implications of these results are discussed further in sections 7.6 - 7.8.

## 4.7 Spatial variation of channel hydraulic parameters

### 4.7.1 Introduction

The continuity of flow and processes within the fluvial system produces a variety of inter-related channel forms which are primarily controlled by the local climate, geology, land use and topography (Knighton, 1987). The nature of adjustment between channel geometry and channel hydraulics has been defined earlier in this chapter in relation to the River Severn. However, in this section the precise relationship between these parameters is discussed in the context of the hydraulic geometry theory (Leopold and Maddock, 1953). This theory is limited by its ability to define the determinacy of response and transient channel behaviour (Thornes, 1977) (section 2.3.3.2), but the nature of this study permits the functional relationships between hydraulic parameters to be cross-examined, both along the channel and for a range of flows. This section is important for understanding the nature of the relationship between hydraulic parameters, and the manner by which these relationships alter downstream.

### 4.7.2 Hydraulic geometry of the River Severn

The spatial variation of channel parameters along the Severn demonstrated systematic variation through the basin, particularly at the Vyrnwy confluence and through the Ironbridge Gorge. In this section, however, the general downstream trends are compared at low- ( $F \geq 70 \%$  flow frequency) and high- ( $F \leq 10 \%$ ) flow levels to compare the Severn data with other gravel-bed rivers and thereby test the validity of the hydraulic geometry theory, and in the following section (4.7.3) to evaluate the nature of adjustment of hydraulic parameters through the basin and under different flow frequencies. The best-fit hydraulic geometry relationships for width ( $w$ ), mean depth ( $\bar{d}$ ) and mean velocity ( $\bar{u}$ ) based on the data set for 25 study sites on the River Severn at low-flows (L) are as follows:

$$w_L = 12.27Q^{0.46} \quad [4.1]$$

$$d_L = 0.47Q^{0.40} \quad [4.2]$$

$$u_L = 0.18Q^{0.17} \quad [4.3]$$

and for high (H) flows are:

$$w_H = 2.81Q^{0.57} \quad [4.4]$$

$$d_H = 0.40Q^{0.33} \quad [4.5]$$

$$u_H = 0.19Q^{0.08} \quad [4.6]$$

The downstream variation of channel geometry is intimately associated with bankfull discharge through several orders of magnitude (Ferguson, 1986). The exponent values for width, mean depth, and mean velocity shown in Table 4.5 suggest a consistency between channel forms throughout temperate regions. The results from the Severn (at low-flow ( $F > 70\%$ ) and high-flow ( $F < 10\%$ )) generally agree with other estimates from gravel- and cobble-bed rivers (Table 4.5), and lie within the modal class of values for  $b$ ,  $f$  and  $m$  reported by Park (1977) from a study of 72 rivers from around the world (Figure 4.42). However, the two exponent values for low- and high-flow velocity are the highest and lowest  $m$ -values of the data set, respectively (Table 4.5); this demonstrates the significance of flow frequency on downstream trends which has been omitted from many previous studies. Furthermore, this indicates that the representativeness of the Severn may be questioned as the velocity and slope exponents differ greatly from other published data (Table 4.5). Indeed, the slope exponents indicate the large range of slope values between the headwaters and the lower reaches, the tendency for this gradient to decline as stage increases, and similarity with the momentum equation components, described later in section 7.4. It may therefore be concluded that the steep channel slopes in the upper channel reaches enhance the rate of change of hydraulic parameters in the Severn basin; furthermore, the measurement of hydraulic parameters over a range of flow frequencies provides an indication of how the water prism responds to a given stage, discharge and channel geometry along the channel.

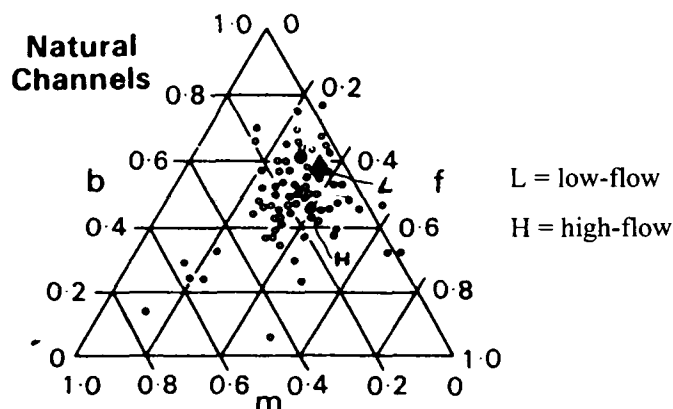


Figure 4.42 A tri-axial graph of downstream hydraulic geometry exponents (after Park, 1977) including the results from this study of the River Severn.

Table 4.5 Downstream hydraulic geometry relations for gravel-bed rivers and canals (after Knighton, 1987)

Data source	Channel location	Discharge	Exponents			
			width, $b$	depth, $f$	velocity, $m$	slope, $z$
Leopold & Maddock (1953)	Great Plains & South-West, USA	$Q_{ma}$	0.45 - 0.56 *	0.37 - 0.45 *	0.10	-0.19 - -0.50 *
Nixon (1959)	Britain	$Q_b$	0.49	0.33 *		-0.10 *
Brush (1961)	16 Appalachian streams	$Q_{2.33}$	0.55	0.36	0.09	
Simons & Albertson (1963)	Indian and USA canals	$\sim Q_b$	0.50	0.36		-0.24
Emmett (1972)	Upper Salmon River, Idaho	$Q_b$	0.54	0.34	0.12	
Emmett (1975)	17 Alaska rivers	$Q_b$	0.53	0.33	0.14	
Charlton <i>et al.</i> (1978)	23 Britain rivers	$Q_b$	0.45	0.40		-0.24
Dunne & Leopold (1978)	Upper Green River, Wyoming	$Q_{ma}$	0.55	0.35	0.10	
Griffiths (1980)	6 New Zealand rivers	$Q_b$	0.48	0.43	0.11	
Bray (1982)	70 Alberta rivers	$Q_2$	0.53	0.33	0.14	-0.34
Andrews (1984)	Colorado: thick bank vegetation	$Q_b$	0.48	0.37	0.14	-0.44
	thin bank vegetation	$Q_b$	0.48	0.38		-0.41
Hey and Thorne (1986)	62 British rivers	$Q_b$	0.52	0.39	0.10	-0.20
Parker (1979)	Theoretical-momentum diffusion	$Q_b$	0.50	0.42		-0.41
Chang (1980)	Theoretical-minimum stream power	$Q_b$	0.47	0.42		
<b>This study</b>	<b>River Severn: low flow conditions</b>	$< Q_b$	<b>0.46</b>	<b>0.40</b>	<b>0.17</b>	<b>-0.73</b>
	<b>high flow conditions</b>	$\sim Q_b$	<b>0.57</b>	<b>0.33</b>	<b>0.08</b>	<b>-0.66</b>

Discharge ( $Q$ ) defined as bankfull ( $Q_b$ ) a mean annual flow ( $Q_{ma}$ ), or with a recurrence interval of 2 ( $Q_2$ ) or 2.33 ( $Q_{2.33}$ ) years.

Symbols:  $w = aQ^b$ ,  $d = cQ^f$ ,  $u = kQ^m$ ,  $s = gQ^z$

\* Data from Yalin (1992)

### 4.7.3 Inter-relationships between channel hydraulic parameters, at-a-site and downstream

The data for the w-Q, d-Q and u-Q relationships under in-bank flow conditions are presented in Figure 4.43. The rate of change of width downstream increases slightly with flow magnitude (Figure 4.43a), but decreases for both mean depth (Figure 4.43b) and mean velocity (Figure 4.43c). The schematic predictions by Leopold and Maddock (1953) implied a constant rate of change downstream in these parameters with flow magnitude. However, this does not occur for most parameters in Figure 4.43, implying that channel roughness and the reference flow considered exert a considerable control on the channel hydraulics (Richards, 1982; Bathurst, 1992). For example, boulder drag and ponding in pools enhance resistance in the upper reaches (upstream of Llanidloes (Figure 3.1)) at low-flows, whereas further downstream resistance may depend mainly on bed material roughness. Hence, mean velocity would increase sharply at-a-site and downstream in response to changes in the dominance of channel resistance (Figure 4.43e). At high flows, boulder drag and ponding would be much reduced; this rate of decline is less downstream from Llanidloes where resistance is controlled more by channel form resistance (Figure 4.43e). Therefore, the mean velocity would increase downstream at a lower rate during high flows (Figure 4.43c). This control on mean velocity may also help in explaining the similar downstream trend for mean depth (Figure 4.43b).

In a study of 5 gravel-bed rivers in Western US, Prestegard (1983) found that water surface slope was most correlated with roughness elements, both at-a-site and downstream. The results from this study show that slope varies little with stage downstream (section 4.6.3), and changes at-a-site are low in the headwaters, but increase with discharge (and therefore distance downstream) (Figure 4.43d). The steep, confined headwater reaches prevent any significant change in slope with stage; this is possibly explained by the boulder-bed and step/riffle-pool sequences which dominate slope at low-flow (Prestegard, 1983), but are replaced in dominance by the valley slope as stage increases. Further downstream, the level of confinement and valley slope are reduced in places (eg. Vyrnwy confluence), allowing the channel to meander freely and inundate the floodplain. Therefore slope changes markedly with stage as irregularities in the bed and channel geometry are drowned out and the flow path shortens (Leopold *et al.*, 1964). In-channel and bank vegetation through the middle and lower reaches seasonally affects channel roughness at low-flow (Gurnell & Midgley, 1994), and also at high-flow as banktop trees and shrubs are submerged (Beven & Carling, 1992). Thus the interaction between the channel form, bed material, and seasonal variations in vegetation cover appears to control the spatial pattern of channel hydraulics along the Severn, and the temporal patterns during flood events.

## 4.8 Summary

This chapter has presented the results of the fieldwork programme. It has described how the channel geometry and channel hydraulic parameters are distributed spatially along the channel and with increasing flow level. It is evident from this analysis that definite trends are apparent along the river which are consistent with the hydraulic geometry theory, but local discontinuities are present in response to local and regional geomorphic and hydrological controls. The next chapter will discuss the methods adopted for simulating the same hydraulic parameters using the 1-D hydraulic model, MIKE11.

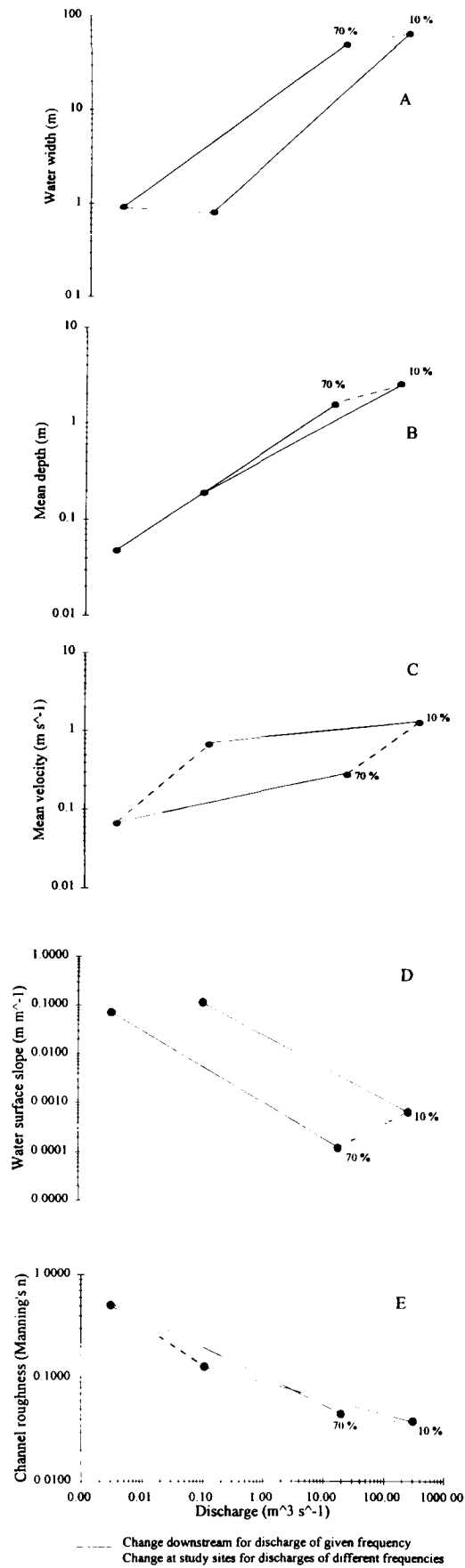


Figure 4.43 The spatial and temporal variation of the hydraulic geometry parameters: a) width; b) mean depth; c) mean velocity; d) water surface slope; and e) roughness, for the 25 study sites on the Severn, under low- ( $F \geq 70\%$ ) and high- flow conditions ( $F \leq 10\%$ ).

## CHAPTER 5

### MODELLING CHANNEL HYDRAULICS USING MIKE11

#### 5.1 Introduction

The previous two chapters have presented the methodology and results of the fieldwork programme. This chapter shall discuss how channel hydraulics may be simulated along the River Severn (Chapter 6 will describe the model results). The aim is to improve the spatial and temporal resolution of the measured channel hydraulic parameters along the Severn (Chapter 4), beyond the capabilities of traditional field techniques (Chapter 3). The procedure adopted for this modelling exercise is summarised in Figure 5.1; the sub-chapter headings in this flow diagram flow sequentially through the various stages discussed in Chapter 5. This chapter will begin with a review of the rationale behind modelling and the choice of the 1-D model, MIKE11 (Figure 5.1). Following this, the data input requirements, model computation schemes and the parameterization of roughness and floodplain storage are explained (Figure 5.1). The model is then used to simulate a large flow event which occurred in February 1989, primarily using topographical and flow boundary information supplied by the former NRA (Figure 5.1). Finally, this simulation is compared with flow data and measured channel hydraulic parameters to evaluate the representativeness and accuracy of the predictions (Figure 5.1).

#### 5.2 Computational modelling of channel hydraulics

##### *5.2.1 Introduction: Considerations behind modelling channel hydraulics*

The application of hydraulic models in river studies provides a valuable insight into the dynamics of the fluvial system at a variety of scales. Their main functions include the duplication, examination and investigation of known flow events / phenomena, with resultant predictions of likely scenarios (Przedwojski *et al.*, 1995). However, the success of computational hydraulic models relies upon the choice of an appropriate model (Warwick & Heim, 1995), together with the selection of suitable cross sections and their spacing (Samuels, 1990). A balance must be struck between having frequent sections and precise hydraulic representation, and the time and money spent on human and computational resources. Too much data can afford unnecessary expense in its collection, processing and simulation, whereas too little data can yield calculation instabilities and large errors (Samuels, 1990).

Three vital components of a successful modelling study, identified by Slade & Samuels (1990), are:

- a) consistent and reliable data. Cross sections should be representative of the channel, provide a comprehensive spatial coverage, include sites of specific interest, control structures and the model limits. If it is unfeasible to survey the cross sections personally, the choice of sections will depend primarily upon the availability of a data set, and secondly upon the accuracy and representativeness of the data.

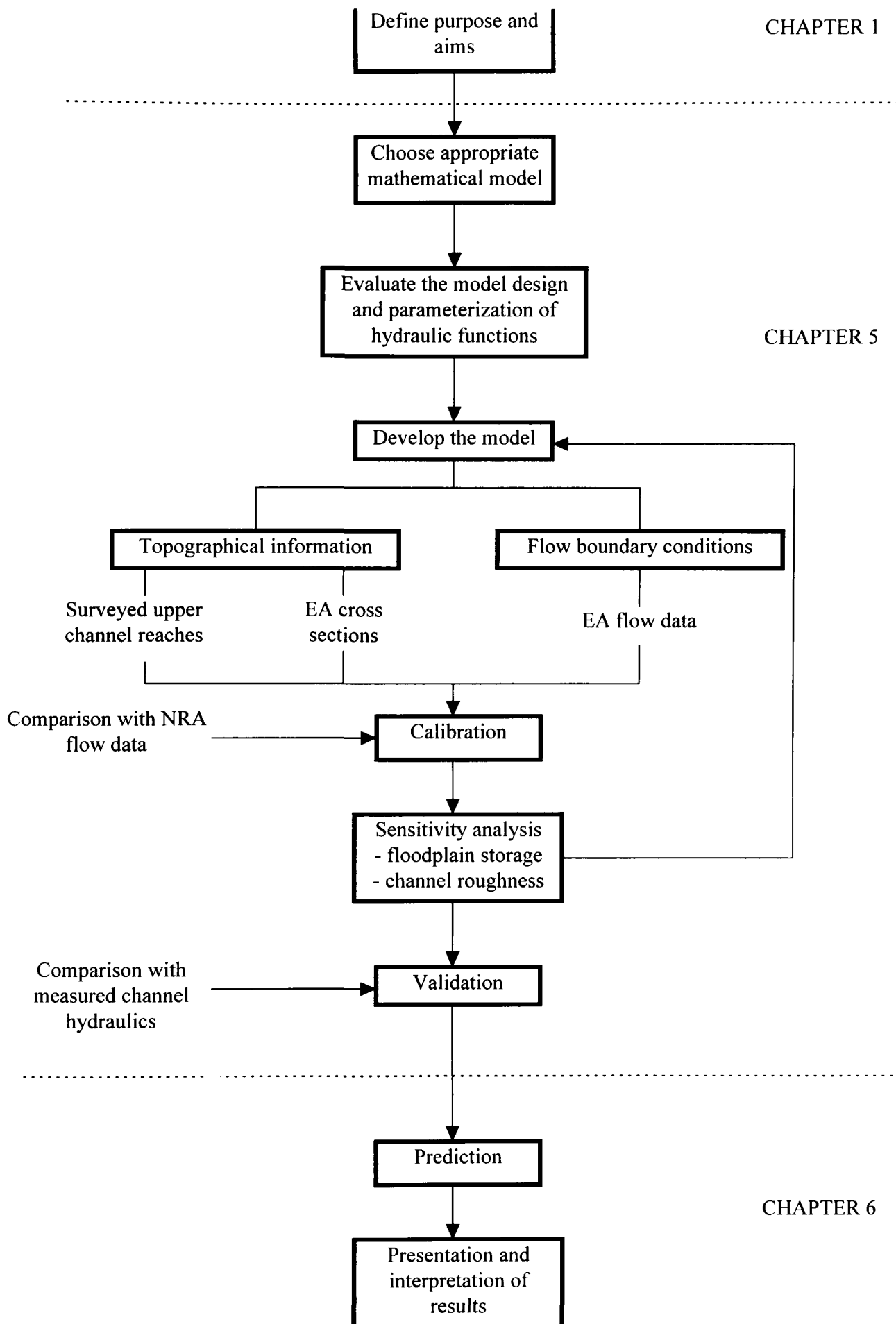


Figure 5.1 A simple representation of the modelling procedure adopted for this study. This chapter will focus on the development of the model and the evaluation of its predictive capabilities.

- b) correct calculation procedures. Friction factors must be correctly determined for the section (Knight & Demetriou, 1984; Beyer & Portner, 1994)); calibration and sensitivity analysis and validation techniques must be accurate (Woltemade & Potter, 1994) and suitable (Warwick & Heim, 1995); distance and time steps should be appropriate (Samuels, 1990).
- c) intelligent interpretation of results. The full consideration of model assumptions, the network design, the assessed inputs, and the assumed roughness and discharge coefficients is essential before the interpretation of results (Slade & Samuels, 1990).

### 5.2.2 The rationale for choosing MIKE11

This study of catchment scale channel hydraulics required a model which was available, user-friendly and suitable for use on a PC. It was important that it was sophisticated enough to simulate hydraulics at this scale, but not inefficient in terms of computational time and resources. The most suitable models to emerge from this selection criteria were MIKE11 and HEC-2, both of which are widely used by hydraulic engineers. MIKE11 is a 1-D hydraulic model produced by the Danish Institute of Hydraulics; it has the capability of supplementing the hydrodynamics with other modules, such as cohesive sediment transport, water quality and eutrophication. HEC-2 is a 1-D hydraulic model produced by the US Army Corps of Engineers. It has similar hydrodynamic capabilities as MIKE11, however, it does not have the potential to add other modules. MIKE11 was therefore chosen because of its greater potential flexibility, its availability within Civil Engineering, and a desire to extend present reach-scale analyses with the model (Beyer & Portner, 1994; Macilwaine *et al.*, 1994) to the catchment-scale.

The aims of this modelling study were therefore:

- to develop the hydrodynamic component of MIKE11 for simulating flows at a catchment-scale;
- to simulate the flow hydraulics along the Severn at a high spatial and temporal resolution;
- to evaluate the predictive capabilities of the model against field data.

The hydrodynamic module of MIKE11 can simulate both steady and unsteady flow through a pre-defined open channel network. This is based on the numerical resolution of the Saint Venant equation, using an implicit, unidirectional finite difference scheme (ie: flows travelling in only one direction and calculated by solving all points on the computational grid simultaneously at time  $t_{n+1}$ ). The calculations are performed within a computational grid consisting of Q-points and h-points, where discharge (Q) and stage (h) are computed, according to the time step ( $\Delta t$ ) and space steps ( $\Delta x$ ) selected by the user. The numerical scheme is a 6-point, centred Abbot-scheme (Figure 5.2) (see Danish Hydraulics Institute, 1990). The user may choose between a fully dynamic or diffusive wave equation which can calculate backwater effects, or the kinematic wave. The river morphology is defined by the geometry and network of the channel, and the boundaries as time varying stage or discharge. The effects of flow structures, flood plains, tides and wind may also be simulated.

### 5.2.3 Input requirements

The configuration of the channel network and the definition of flows must first be defined by the user. This is achieved through separate menu options. Data may be entered either manually, or by importing text-files in a format described by the MIKE11 User Manual (Danish Hydraulics Institute, 1990). The different elements required are: a) the channel geometry and resistance of each cross section; b) the channel network configuration; and c) the flow conditions at the boundary limits and any tributary inputs. Additional features, such as the configuration of control structures (ie: weirs) and specification of flood plains are optional, but were included in this study.

- a) Channel cross sections. Each cross section consists of a series of x-z co-ordinates to represent the dimensions of the channel, and Manning's  $n$  values to represent the resistance (Figure 5.3). The raw data are automatically processed in the model into a form used in the hydrodynamic computations, ie: cross sectional area, width and hydraulic radius. If water levels rise above the specified levels during computation, MIKE11 extends the river banks vertically to prevent the model crashing if an instability occurs; this also overcomes any lack of knowledge about the cross section.
- b) Network configuration. Each cross section is assigned a chainage value and a set of x-y co-ordinates from which the section can be located in space (Figure 5.3). The sections are connected by common reference names (Topological Identification names) to denote similar databases, and common channel names to distinguish between separate branches in the drainage network. A value for DX-MAX (maximum space step,  $\Delta x$ ) must be assigned to each river branch. MIKE11 always locates an h-point in the computational grid at the cross section locations. If the distance between cross sections is greater than DX-MAX, then MIKE11 inserts additional h-points. Q-points are spaced at equidistant intervals between h-points by the model.
- c) Boundary conditions. The boundary conditions to be specified for the model include:
  - a time series boundary of stage versus time (h-t), or discharge versus time (Q-t) at all upstream boundaries;
  - a time series boundary of stage versus time (h-t), or a stage-discharge relationship (h-Q) at the downstream boundary;
  - a times series boundary of discharge versus time (Q-t) for all tributary inputs.

Each condition must be entered manually by the user or imported from a text-file in a format defined by the MIKE11 User Manual (Danish Hydraulics Institute, 1990).

- d) Weirs. MIKE11 simulates flow over a weir as having either of three flow conditions (see section 5.4.3):

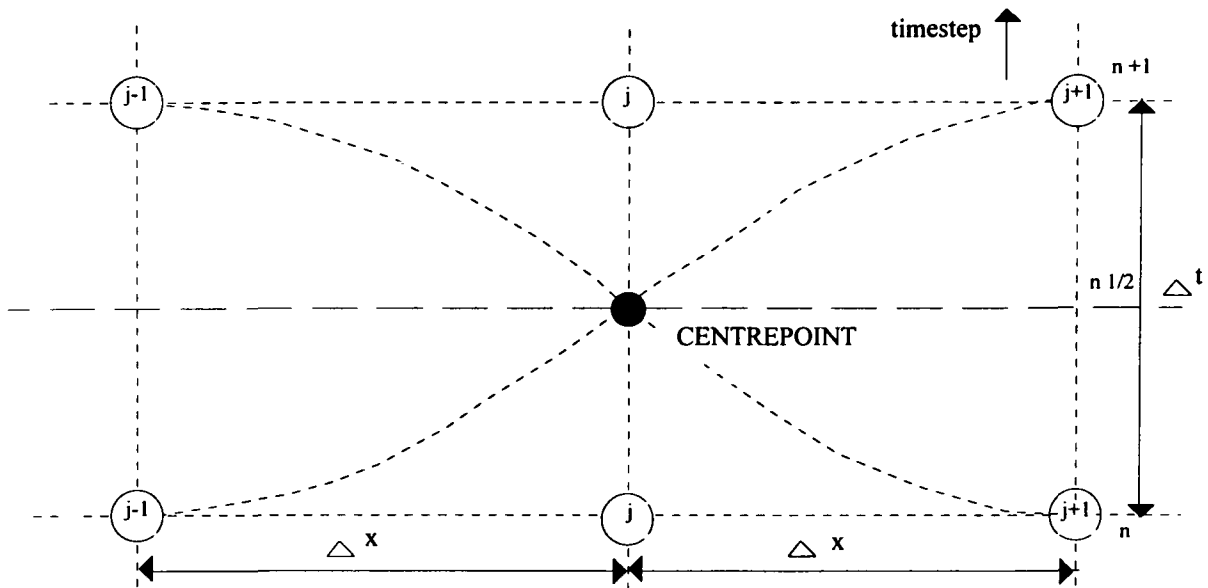


Figure 5.2 The centred 6-point Abbott scheme (Danish Hydraulics Institute, 1990)

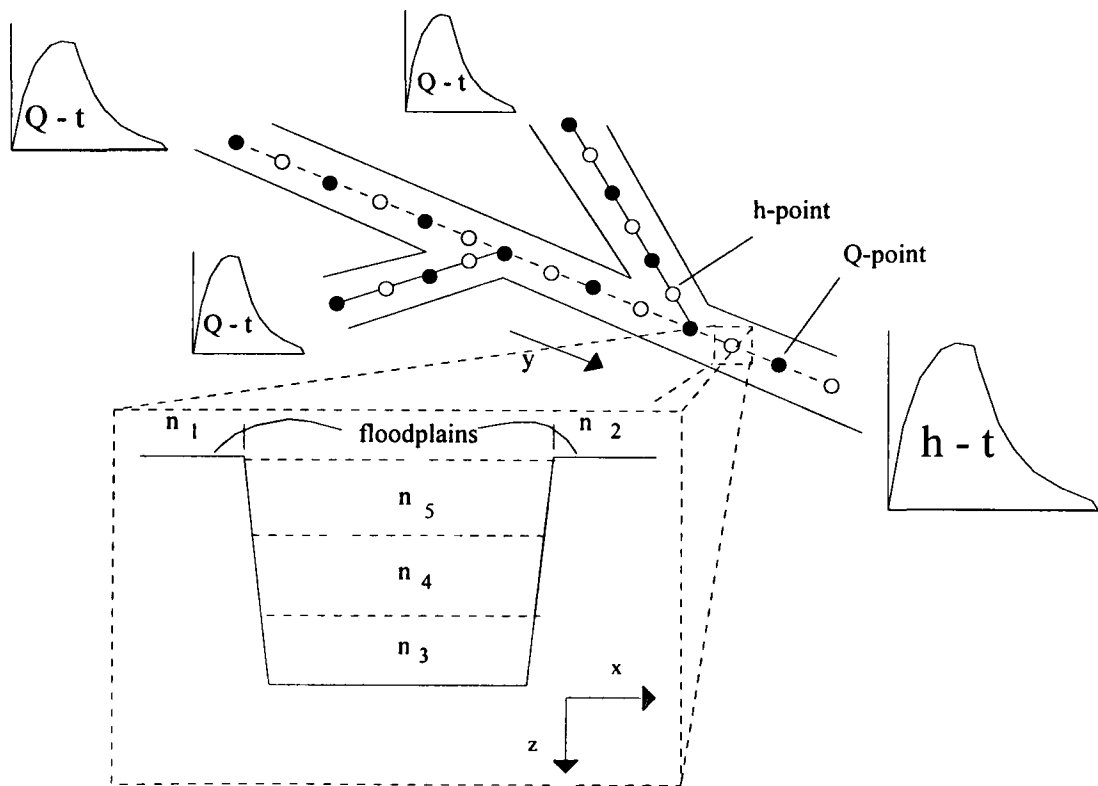


Figure 5.3 The schematization of the channel network topography and flow simulation requirements of MIKE11.

- zero flow - when water levels on the upstream and downstream side are below the crest level, or when the two levels are equal;
- drowned flow - when flow on both sides of the weir is in the same state as flow over the weir itself (eg: subcritical / supercritical);
- free overflow - water levels on either side are at such a level as to deliver the maximum discharge for a given head at the upstream side of the structure. Discharge, Q, is defined as,

$$Q = 1.705\alpha_c w_s H_s^{3/2} \quad [5.1]$$

where,  $Q$  = discharge ( $m^3 s^{-1}$ )  
 $\alpha_c$  = coefficient (accounting for energy losses in discharge and the upstream velocity head)  
 $w_s$  = structure width (m)  
 $H_s$  = available energy head above the weir crest (m)

Floodplain storage, or water detention basins, may be defined by the user according to water levels at each cross section (see section 5.4.3). As water depth reaches a level above the floodplain it is allowed to flow freely onto and along the floodplain. This results in the temporary loss of water from the channel, which is indicated by an attenuation of the flood peak ('storage') (Figure 5.4). When water levels fall in the channel, the stored water flows back into the channel ('release'), resulting in a long recession limb but no loss of volume.

#### 5.2.4 Model computation

The fully dynamic wave description in MIKE11 is solved by vertically integrating the equations for conservation of momentum and velocity (the Saint Venant equations).

Conservation of mass:

$$\frac{\partial(\rho dw)}{\partial t} = - \frac{\partial(\rho ds_c \bar{u})}{\partial x} \quad [5.2]$$

Conservation of momentum:

$$\frac{\partial(\rho dw \bar{u})}{\partial t} = - \frac{\partial\left(\alpha' \rho dw \bar{u}^2 + \frac{1}{2} \rho g w d^2\right)}{\partial x} \quad [5.3]$$

These assume that the water is incompressible and homogeneous, the bed slope is small, the flow is subcritical and the wave-lengths of the water are large compared to the water depth. The momentum equation must be altered to solve for unsteady flow through a heterogeneous channel topography. Terms are therefore added to represent the bottom slope ( $S_b$ ) and a variable width ( $w$ ). Depth ( $d$ ) is replaced by water level ( $h$ ). The equations are integrated across a section of any shape by dividing the section up

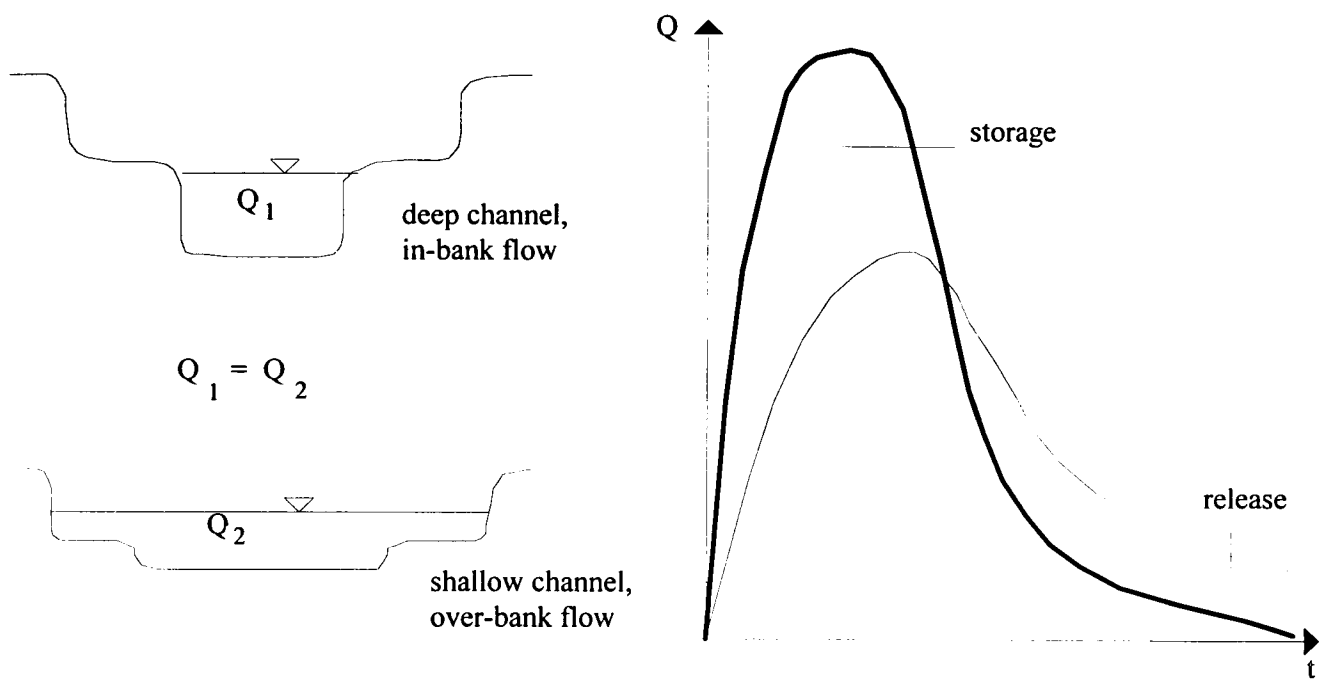


Figure 5.4 The significance of storage in MIKE11, demonstrated using in-channel (A) and over-bank (B) flow in two channels having the same discharge.

into a series of subsections (Figure 5.5). This scheme assumes no exchange of water between subsections, enabling area and discharge to be calculated, ie:

Area:

$$A = \int_0^w h dw \quad [5.4]$$

Discharge:

$$Q = \int_0^w h \bar{u} dw = \bar{u} A \quad [5.5]$$

By integration of the mass and momentum conservation equations (3.33 & 3.34), introducing equations (5.2 & 5.3) and including a term for hydraulic resistance (C), the basic equations used in MIKE11 are formulated, ie:

$$\frac{\partial Q}{\partial x} + \frac{\partial A}{\partial t} = q \quad [5.6]$$

$$\frac{\partial Q}{\partial t} + \frac{\partial \left( \alpha \frac{Q^2}{A} \right)}{\partial x} + gA \frac{\partial h}{\partial x} + \frac{gQ|Q|}{C^2 AR} = 0 \quad [5.7]$$

MIKE11 solves these equations using an implicit finite difference scheme and a computational grid, consisting of alternating h- and Q-points where stage and discharge are solved every time step (Figure 5.2). By default, the equations are solved twice for every time step to obtain a fully centred description, which involves starting the first iteration from the results of the previous time step and the second iteration using the centred values from this calculation.

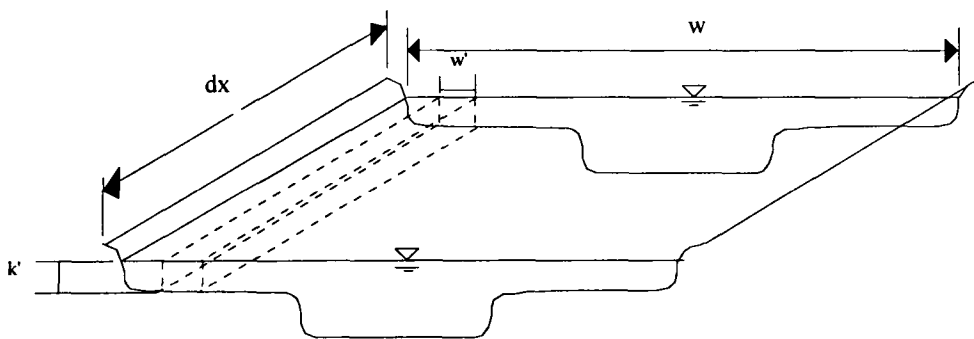


Figure 5.5 The cross section is divided into a series of rectangular channels by MIKE11 to cope with irregular channel morphologies (Danish Hydraulics Institute, 1990).

Stability may be ensured by defining suitable time ( $\Delta t$ ) and space ( $\Delta x$ ) steps, in order to satisfy the velocity condition (a variant of the Courant condition). This demands that both the topographic resolution be sufficiently fine that non-linearities in water levels and discharge are adequately resolved and that the time step ( $\Delta t$ ) is small enough to give an accurate representation of a wave, ie: that the water will not be transported more than one space step in one time step, and thus must not greatly exceed 1. It is defined as:

$$C_v = \frac{u\Delta t}{\Delta x} \leq 1 \text{ or } 2 \quad [5.8]$$

where,  $C_v$  = velocity condition  
 $\Delta t$  = time step (seconds)  
 $\Delta x$  = space step (m)

### 5.2.5 Model output

The output from MIKE11 consists of time series plots, or print-outs, of discharge, stage or velocity; these may be viewed on the screen or exported to disk as text-files. Stage results are given for each h-point, whilst the discharge and velocity are given for each Q-point (Danish Hydraulics Institute, 1990). These data alone were insufficient for this study, and therefore a FORTRAN program was written to calculate the appropriate hydraulic parameters (such as water surface slope, hydraulic radius, shear stress and stream power) by linking the model output to the channel cross section files (Appendix II).

### 5.2.6 Channel roughness sensitivity analysis

A sensitivity analysis of both floodplain storage and boundary roughness was undertaken to evaluate their response to variations in the flow. The response of the flow to varying values of floodplain storage and over a constant bed roughness was observed, by creating a simple, 10 km long, rectangular channel, with uniform slope ( $0.0003 \text{ m m}^{-1}$ ). This experiment was run by altering the area of storage on the floodplain (floodplain width times distance between cross sections) and calculating the volume of water ‘lost’ from the downstream hydrograph, and the reduction in stage at a cross section midway along the reach. Figure 5.6 illustrates that for unsteady flow, a simple linear relationship exists between the volume of water stored on the floodplain and the peak stage. An increase in storage area thus results in an increase in the volume of water stored on the floodplain (Figure 5.7); this represents only ‘temporary’ storage as  $\geq 99 \%$  of the flow was returned to the channel over time.

The impact of increasing the boundary roughness coefficient (Mannings  $n$ ) along a 10km rectangular reach of constant discharge was to increase the flow depth (Figure 5.8). Three flows were chosen to represent in-channel flow ( $50 \text{ m}^3 \text{ s}^{-1}$ ), over-bank flow ( $350 \text{ m}^3 \text{ s}^{-1}$ ), and a transitional flow between the two former conditions ( $150 \text{ m}^3 \text{ s}^{-1}$ ). The range of  $n$ -values was considered appropriate for the study of mountain and lowland channel reaches. The rate of increase of stage with roughness was consistent at all three levels, although the transition between in-bank and over-bank resulted in an abrupt decrease in slope (Figure 5.8). Furthermore, the use of narrow floodplains (50 m), with the same roughness values as the channel, caused the model to treat the section as a two stage channel with uniform conveyance over the floodplain. These two experiments therefore helped in the appreciation of how the model simulates floodplain flow.

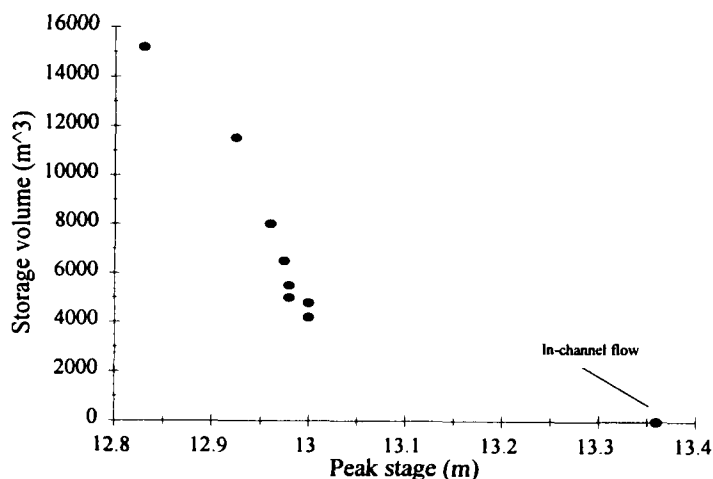


Figure 5.6 The effect of floodplain storage on the attenuation of the floodwave (represented by peak stage).

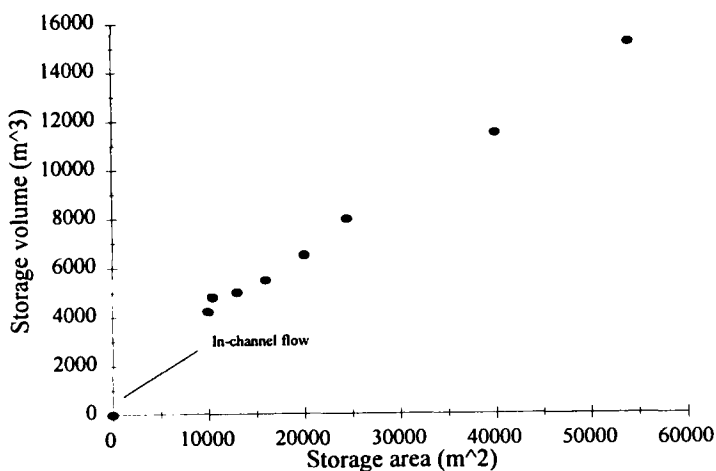


Figure 5.7 The effect of varying floodplain area on the volume of water stored on the floodplain.

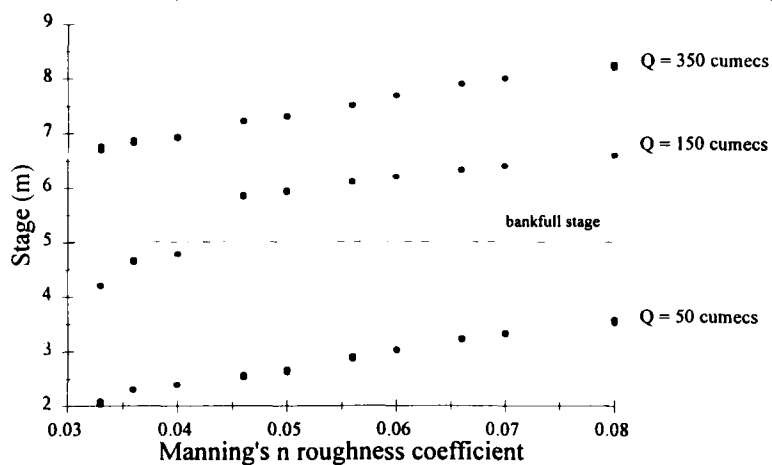


Figure 5.8 The significance of channel roughness on stage in a simple rectangular channel, for three constant flows ( $Q = 50, 150$  and  $350 \text{ m}^3 \text{ s}^{-1}$ ).

### 5.3 Flow event simulation: the February 1989 flow event

The mid-February 1989 flow event was caused by the passage of a warm front from the west between the 17 and 18 (Figure 5.9), preceded by a cold spell which left a snow layer on higher ground and a smaller flow event. The later event brought moderate - intense rainfall in the west of the UK, centred across the western margin of Wales (Figure 5.10). Indeed, the precipitation record at Tanllwyth showed that this was a persistent storm event (17-19 February), punctuated by short outbursts in excess of  $7.0 \text{ mm hr}^{-1}$  (Figure 5.11). At Trimpley, near Bewdley, only 9.5 mm fell, with a maximum of just  $2.0 \text{ mm hr}^{-1}$ . On preceding days (13th - 16th) (Figure 5.9), deep depressions over Iceland (968 mm) brought a sequence of fronts and cold westerlies, yielding heavy rain and some snow showers on high ground. The combination of wet antecedent conditions, some snowfall on higher ground (eg: Plynlimon), and rainfall over Wales and the borderlands meant that the moderate rainfall over wet ground produced a significant flow event along in the Severn basin.

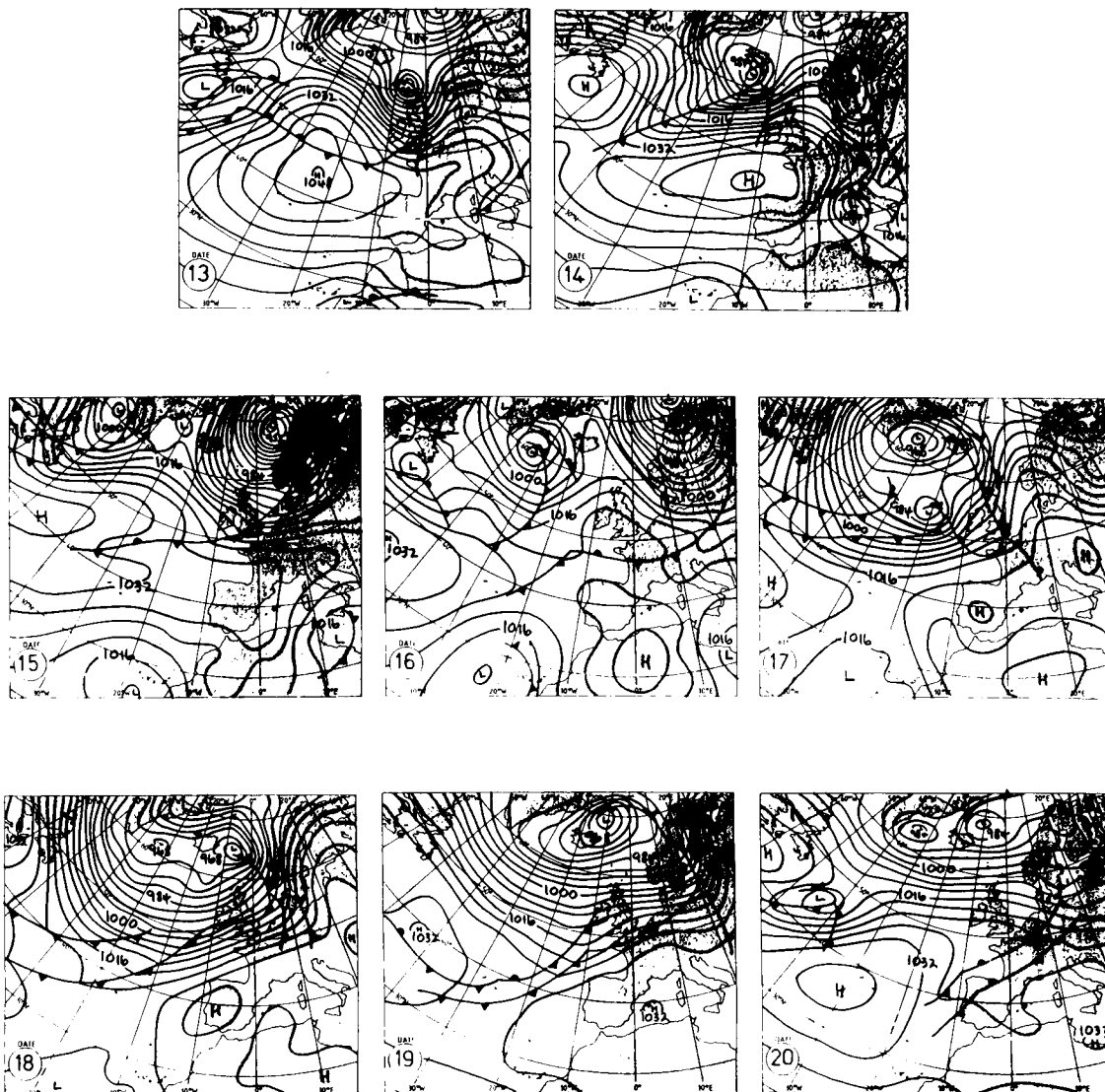


Figure 5.9 Daily weather maps (1200 GMT) from 13 - 20 February 1989, showing the synoptic weather conditions prior to and during the simulated flow event.

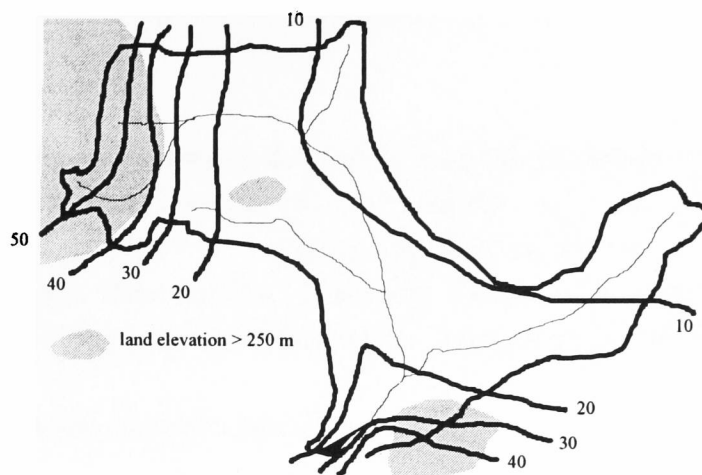


Figure 5.10 A isohyet distribution of the total precipitation (mm) recorded at 37 monitoring stations throughout the Severn basin during the rainstorm event (17 - 20 February 1989).

The flows recorded at Abermule and Bewdley during this event reached maxima of  $150 \text{ m}^3 \text{ s}^{-1}$  and  $250 \text{ m}^3 \text{ s}^{-1}$ , respectively. These correspond to an event with a return period of less than 2 yrs: a 2 yr event at Abermule is rated as  $195 \text{ m}^3 \text{ s}^{-1}$ , and at Bewdley as  $340 \text{ m}^3 \text{ s}^{-1}$  (defined using an EV1-moment analysis).

This event was chosen because it represents a fairly typical flow event along the Severn which reached an approximate bankfull limit in most parts of the catchment. This satisfied two of the project criteria. The third criterion was that the extent of inundation was minimised because of the recognised problems of simulating floodplain flow.

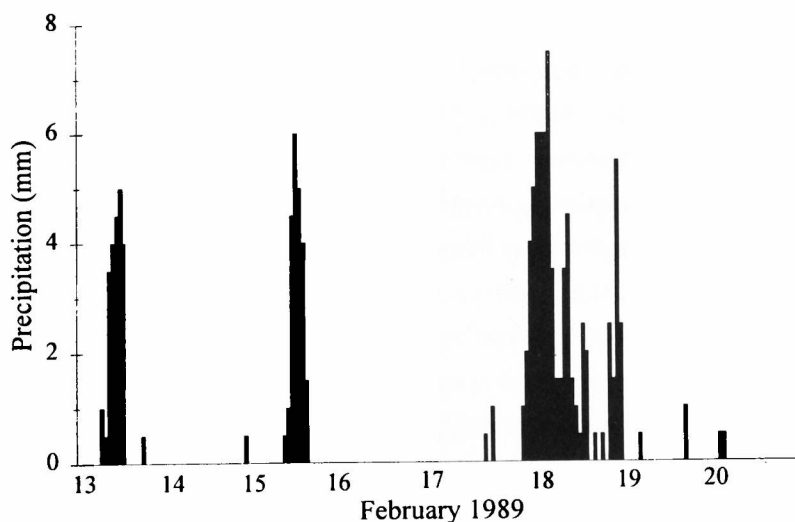


Figure 5.11 Precipitation recorded at hourly intervals at the Tanllwyth remote weather station in the Plynlimon catchment. The simulated event includes the minor precipitation event on 15 February 1989, and the prolonged event which occurred between 17 - 19 February 1989.

## 5.4 MODEL DESIGN AND PARAMETERIZATION

### 5.4.1 Introduction

The aim of the modelling exercise was to develop the model to successfully simulate a flow event along the River Severn. This section shall describe how the MIKE11 model was used to simulate the flow event described in the preceding section (5.3). It begins by outlining the various stages of model development (representation of channel form and flow conditions). This is followed by a series of tests designed to evaluate the accuracy of the model (ie: calibration; sensitivity analysis; validation) (Figure 5.1).

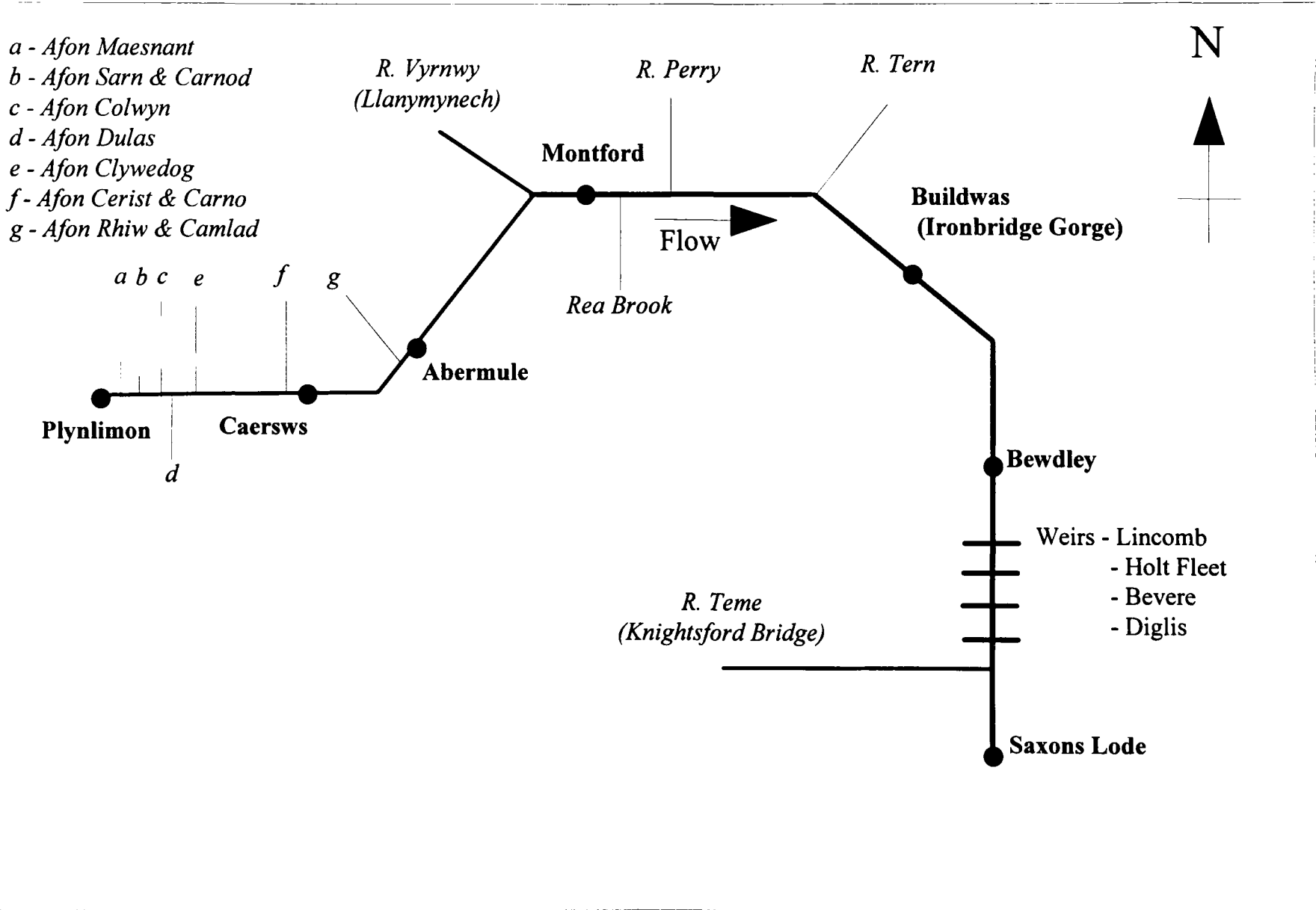
### 5.4.2 Channel network and cross section data

The topographical form of the Severn basin was represented by cross sectional information and the channel network pattern; this was the first step towards the development of the model (Figure 5.1). The channel reach included in the model simulation covered almost the entire non-tidal Severn, and thus the majority of the fieldwork sites described in Chapters 3 and 4. It extended from the first major gauging station in Plynlimon (Severn Flume, 4.26 km downstream from the source) to the last major gauging station before tidal effects dominate the hydraulic flow of the channel (Saxons Lode, 254.6 km) (Figure 5.12). The channel network and morphological form of the channel were largely represented by cross sectional data provided by the EA, between Abermule and Saxons Lode: the channel reach upstream of Abermule was represented by personally surveyed sections (Figure 5.12).

Chainage values on each EA cross section helped define the channel network for the reach downstream of Abermule (Figure 5.12). Upstream of Abermule, chainage values for the 20 sections were derived from a digitised map of the Severn. The location of tributary inputs was also estimated using annotated maps supplied by the EA and detailed Ordnance Survey maps (1:10 000) of the upper Severn.

The EA provided cross sectional data for the reach between Abermule (55 km downstream) and Saxons Lode (250 km downstream), including the Vyrnwy tributary from Llanymynech and the Teme tributary from Knightsford Bridge (Figure 5.12). These data were surveyed in 1976 by Mott MacDonald. Fieldwork data at a limited number of sites indicate that no significant changes to river channel have occurred during this period, although it is appreciated that the channel represented in the model will be slightly different to the Severn today (section 7.2). The spacing of the sections in the original data set was approximately 500 m. However, a subset of cross sections was chosen because of computational constraints imposed by the model. This subset was achieved by sampling every second section sequentially along the channel, thus increasing the longitudinal spacing ( $\Delta x$ ) to approximately 1000 m. The EA data split the channel section into five zones to represent composite channel roughness; these are shown in Figure 5.3. These roughness data were evaluated by Mott MacDonald during a flood simulation project of the Severn, using Hydro and Onda 1-D computer models. The reach between Severn Flume (4.26 km) and Abermule (55.91 km) was represented by 20 surveyed cross sections (Figure 5.12): ten sections were surveyed for the fieldwork programme and a further ten to increase the coverage of the reach between Llanidloes and Abermule. Composite channel roughness for the 20 manually surveyed sections used estimates of Manning's  $n$  values,

Figure 5.12 A schematic representation of the River Severn showing the simulated channel reach, major tributary inputs and weirs (not to scale).



primarily taken from fieldwork calculations (sections 4.3.5, 4.4.5, 4.5.5, 4.6.3), and supported by empirical data (Bathurst, 1992), and photographic evidence (Barnes, 1967).

The model included four broadcrested weirs in the reach between Bewdley and Saxons Lode, at Holt Fleet, Lincomb, Bevere and Diglis (Figure 5.12). The location, width and crest level of each was supplied by the EA (Table 5.1). MIKE11 simulation of flow over a weir was described in 5.2.4. On account of the coarse spatial resolution of the channel (260 cross sections covering 250 km of the Severn), bridges and all other hydraulic control structures were not included in the model.

Table 5.1 Location and dimensions of the broad-crested weirs included in the model simulation.

Name	Distance downstream from source, (km)	Width (m)	Crest level (a.s.l) (m)
Lincolmb	218.4	94.0	15.9
Holt Fleet	226.2	92.2	13.7
Bevere	231.4	107.9	11.9
Diglis	238.2	116.3	10.4

Table 5.2 The location of the upstream and downstream flow boundaries in each simulated reach. The performance of the simulation through each reach was evaluated against measured flow at a gauging station (control gauge) located approximately equidistant between the flow boundaries.

Reach number	Gauge name	Distance downstream from source (km)		
		Upstream	Control gauge	Downstream
Reach 1	Severn Flume	4.3		
	Caersws		34.1	
	Abermule			55.9
Reach 2	Abermule	55.9		
	Montford		115.5	
	Buildwas			166.4
Reach 3	Montford	115.5		
	Buildwas		166.4	
	Bewdley			207.9
Reach 4	Buildwas	166.4		
	Bewdley		207.9	
	Saxons Lode			254.6

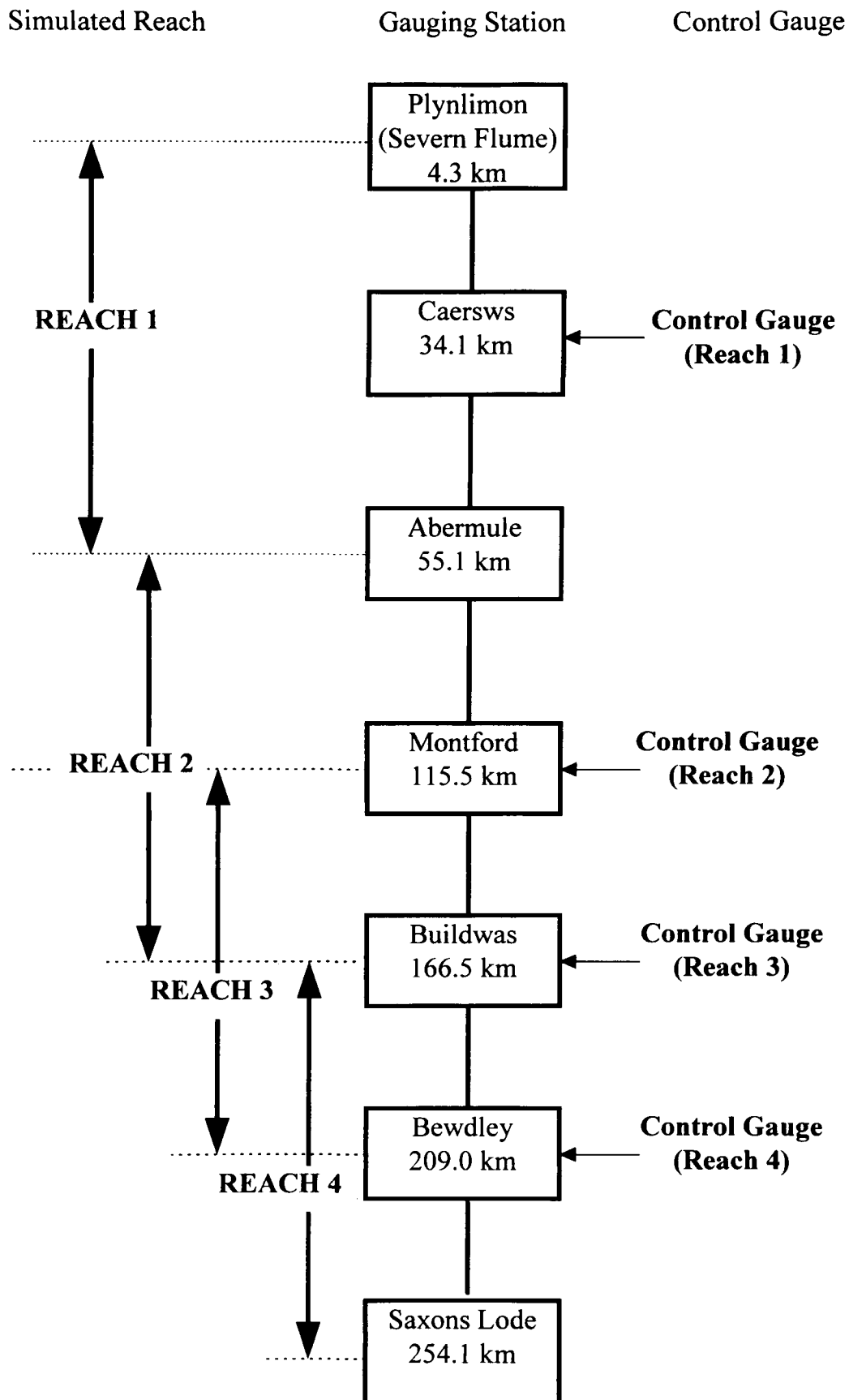


Figure 5.13 A schematic representation of the reaches simulated in the model. The cross section data for the reach between Plynlimon and Abermule were personally surveyed; the data for the reach between Abermule and Saxons Lode was provided by the EA.

### 5.4.3 Flow boundary conditions

The boundary conditions were included in the second stage of the model development (Figure 5.1): hence, this section will describe how spatially- and temporally-varying flows were represented in MIKE11. An ideal model simulation would route the flow through a complete and continuous reach. However, detail was lost because computational constraints restricted the number of cross sections or lateral inputs. By dividing the channel reach into the minimum number of possible units (controlled upstream and downstream by EA gauging stations and without omitting any of the 260 cross sections) three reaches remain. This produced reaches of disparate length. Therefore, a compromise was achieved between reach length, spatial coverage and study sections by using four reaches (Figure 5.13 & Table 5.2). It is recognised that there is a certain subjectiveness in this development and an argument could be made for slightly smaller reaches, but this would require a considerable reorganisation of the database.

The advantages of dividing the Severn channel into a series of discrete reaches are:

- a) error propagation was minimised by using four short reaches (approximately 50 km) rather than one long reach (250 km); for example, the reach between the Vyrnwy confluence and Montford is notoriously difficult to simulate because of the interaction between the Vyrnwy and Severn channels, the Morda gap and floodplain flow (Lindsay, 1995). The simulation of flow through a short reach which is prone to complex hydraulic behaviour restricts the inaccuracies of the model simulation to that reach;
- b) the specific design of the four reaches enabled flows to be routed between two EA gauging stations and have a third gauging station roughly half-way along the reach to compare the accuracy of the simulation runs (section 5.4.4);
- c) shorter reaches reduced computational time and expense, and produced smaller, more manageable data sets with a sufficient spatial resolution to yield reasonably accurate results.

The details of the four reaches are summarised in Table 5.2. Where overlap occurs between reaches, the data derived from the succeeding (downstream) reach was used in preference to the preceding (upstream) reach for the following reasons: a) possible errors generated at the Vyrnwy confluence (100 km) could be limited to the reach upstream of Montford (115 km), where the Montford - Bewdley reach began; and b) the upstream flow boundary would generate flow data of greater accuracy than flows that were routed along a channel reach of over 50 km in length.

The upstream flow boundaries and tributary inputs were represented by time-series discharge data (15 minute intervals), and the downstream flow boundaries by time-series stage data (15 minute intervals). The EA provided the flow and stage data for all the major gauging stations on the Severn and the Dulas, Vyrnwy, Tern and Teme tributaries (Figure 5.12). The discharge contributed from other significant tributaries (Figure 5.12) were represented by estimating the flow magnitude and time to peak from a

comparison between the flow in the main branch of the Severn, the location in the basin, catchment size, historical flow records and the gauged flows of adjacent tributaries. For example, the discharge,  $Q_{\text{ungauged}}^t$ , contributing to the Severn at any time in an ungauged catchment (drainage area,  $DA_{\text{ungauged}}$ ), was estimated from,

$$Q_{\text{ungauged}}^t = \left( \frac{DA_{\text{ungauged}}}{DA_{\text{gauged}}} \right) Q_{\text{gauged}}^t \quad [5.9]$$

where,  $Q_{\text{gauged}}^t$  = the discharge gauged at time,  $t$  ( $\text{m}^3 \text{s}^{-1}$ )  
 $DA_{\text{gauged}}$  = drainage area of the gauged catchment ( $\text{m}^2$ )

Hence, the time-varying discharge at all ungauged tributaries was calculated from the ratio of the ungauged drainage area and the gauged drainage area (estimated from 1:10 000 scale maps) multiplied by the 15-minute discharge data from the gauged catchment. The accuracy of the estimates were evaluated against previously measured flows from these basins.

#### 5.4.4 Model calibration

‘A model can be efficient only if it relies on field data and if its predictions can be verified by measurable data’ (Przedwojski *et al.*, 1995, p. 142). Thus, an obvious advantage of reach-division system was that at least one gauging station was present roughly half way along the subsections to evaluate the accuracy of the model. From this station, each simulation by MIKE11 was compared with ‘real’ EA data to calibrate the model (Figure 5.14), ie: the performance of each modelled reach was evaluated, and inconsistencies in the model simulations identified. Furthermore, these calibrations have ensured that floodplain storage problem was resolved (section 5.4.5).

Figure 5.14 (a-d) illustrates the accuracy of the model at simulating the February 1989 event. Between 15 - 24 February, two flow events occurred along the Severn. The first, and smaller, event (peak discharge (15 - 16 February) =  $70 \text{ m}^3 \text{ s}^{-1}$  at Bewdley) was simulated reasonably well. Slight discrepancies in the prediction of this first event suggests that at upstream sites there was insufficient time for the flood wave to travel to the gauging station. Caersws would have been similarly affected but because there was a lack of gauged tributaries between Severn Flume and Caersws, all inputs had to be estimated and the Caersws hydrograph was used for the calibration.

The second event (peak discharge (19 - 21 February) =  $215 \text{ m}^3 \text{ s}^{-1}$  at Bewdley) was simulated more accurately by the model (Figure 5.14a-d & Table 5.3). All four model hydrographs predict the steep rising limb very well and have reasonable success in simulating the recessional limb, although at Buildwas, the discharge was consistently overestimated. The simulation of peak flows was less successful. At Caersws, the primary peak was underestimated by  $5 \text{ m}^3 \text{ s}^{-1}$  and the secondary peak overestimated by  $10 \text{ m}^3 \text{ s}^{-1}$ . The EA-measured hydrograph at Montford had a ‘shoulder’ and peak characteristic of over-banking at this

site (McCartney & Naden, 1994). MIKE11 failed to simulate this, but under predicted discharge at the peak by only  $2 \text{ m}^3 \text{ s}^{-1}$  (Table 5.3). In contrast, the peak discharges at Buildwas and Bewdley over predicted the measured EA flows by  $\leq 20 \text{ m}^3 \text{ s}^{-1}$ . This represented an error margin for peak flow of  $\leq 10 \%$  at each of the four gauging station sites, which was within the error limits of most gauging stations (Table 5.3).

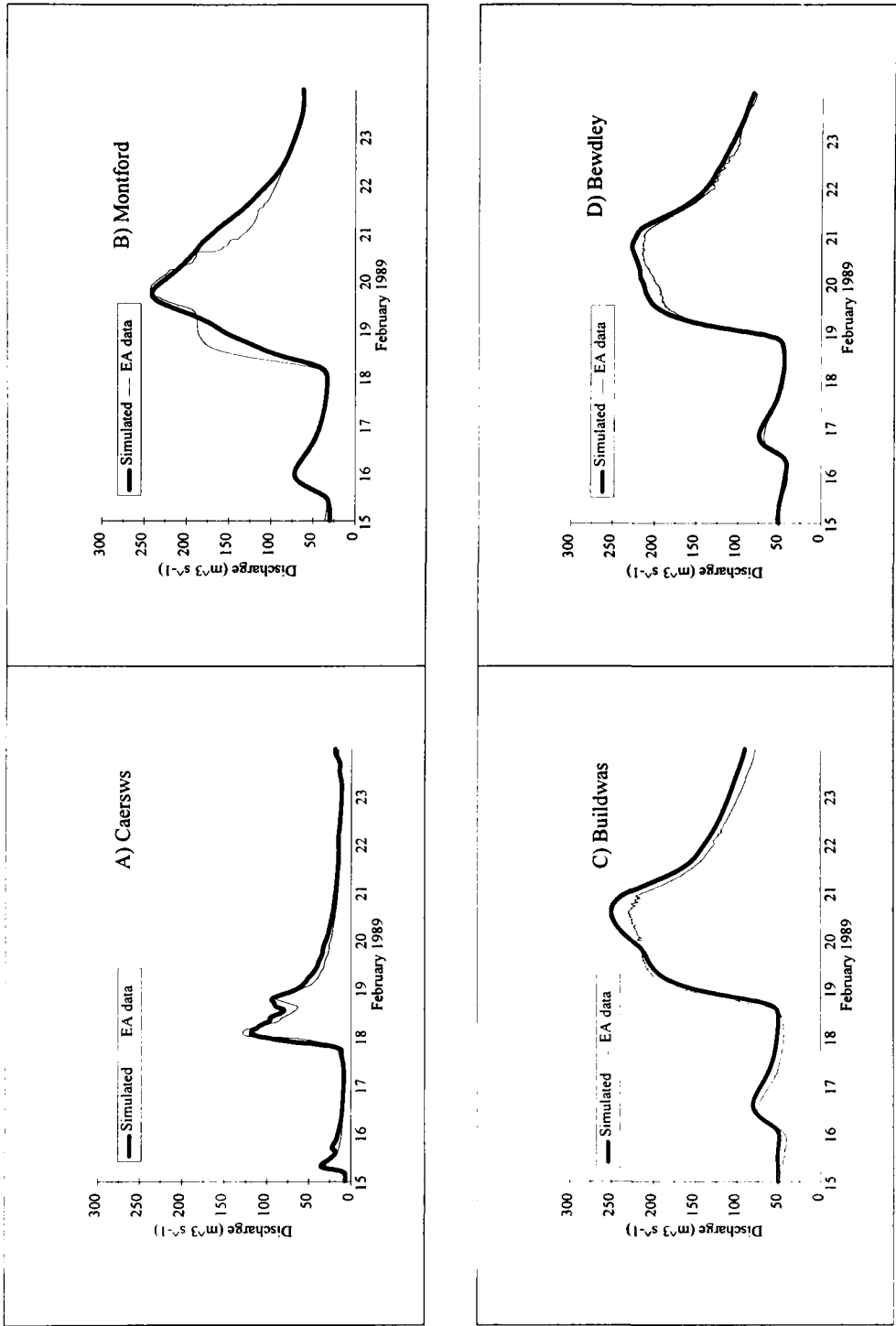


Figure 5.14 A comparison between flow hydrographs measured at EA gauging stations and simulated in the model, presented in upstream - downstream order, ie: A) Caersws; B) Montford; C) Buildwas; D) Bewdley.

Table 5.3 The performance of the MIKE11 simulation against measured flows at EA gauging stations.

Distance Downstream (km)	Gauging station	Volume (m <sup>3</sup> )				Peak discharge (m <sup>3</sup> s <sup>-1</sup> )			
		EA measured flow (1x10 <sup>6</sup> )	MIKE11 simulated flow (1x10 <sup>6</sup> )	Difference (EA - MIKE11) (1x10 <sup>6</sup> )	% difference	EA measured flow (1x10 <sup>6</sup> )	MIKE11 simulated flow (1x10 <sup>6</sup> )	Difference (EA - MIKE11) (1x10 <sup>6</sup> )	% difference
34.1	Caersws	18.8	21.9	-3.1	-16.1	128.2	118.7	9.5	7.4
115.5	Montford	79.0	79.5	-0.5	-0.7	242.6	240.8	1.8	0.7
166.5	Buildwas	87.7	93.4	-5.7	-6.5	230.3	250.2	-20.1	-8.0
207.9	Bewdley	86.9	86.9	< 0.01	< 0.01	215.3	227.3	-12.0	-5.3

Despite the errors incurred at peak flow levels by over-bank flow, the difference by volume at three of the four sites was low. Table 5.3 shows that the percentage difference between the volume of flow simulated by the model and measured by the EA was within 10 % at Montford, Buildwas and Bewdley. At Caersws, the difference of 16 % emphasises the difficulties encountered in estimating flows from ungauged reaches, and that only significant lateral inputs could be accounted for (no small tributaries and no diffuse sources).

#### *5.4.5 Sensitivity analysis: the problem of floodplain storage*

The calibration exercise demonstrated that the model could successfully simulate a range of flows reasonably accurately: however, after the flow inundated the floodplain, the simulation became inaccurate. This indicated that the natural process of floodplain flow, storage and recharge was being simulated as simple flow conveyance on the floodplain (ie: no storage occurred, resulting in an enhanced peak discharge and greater discharges on the falling limb of the hydrograph) (Danish Hydraulics Institute, 1990). As discussed in 5.2.7, MIKE11 has the capability of simulating floodplain flow by a variety of means. Here, it was represented by adding an additional flooded area into the cross sectional information before a model run: this took the form of a stage - width relationship that allowed the water to flow over the floodplain, but at a reduced rate because of enhanced boundary roughness ( $n_1$  &  $n_2$ ) (Figure 5.3).

Figure 5.15 illustrates the effect of adding flooded areas to the sections prone to flooding upstream of Montford. In summary, the effect of adding storage area was to flatten the shape of the hydrograph, and thereby, a) decrease the flood peak, b) delay the flood peak; and c) increase discharge on the falling limb, by the rapid recharge of water from the floodplain into the channel. Depending on antecedent conditions, recharge would normally occur gradually over the course of several days in response to the temporary storage of water in depressions and the time taken for water to seep back into the main channel (as through flow and groundwater). The outcome of this sensitivity analysis was that floodplain widths of 200 m were added to all cross sections where over-bank flow occurred (Vyrnwy confluence; upstream of Buildwas): this is felt to be justified on the basis of similar floodplain size and topographies at sites prone to flooding. As Figure 5.14 shows, following this analysis, the model design was altered by changing the floodplain storage areas and running the calibration exercise again. The model hydrograph at Montford clearly demonstrates that this solution does not solve the problem of floodplain storage, but, it provides a simple approximation to the problem without the need for extensive land surveys or DTM mapping.

#### *5.4.6 Model validation against field observations*

The purpose of the model development, described in sections 5.2 and 5.4.2-4, was to simulate the February 1989 event as accurately and efficiently as possible. Ideally, the model should be validated against: a) a secondary data set consisting of another event along this river; or b) another river and event using a similar cross sectional data set, to test whether the parameterization of the model was correct. Alternatively, a fieldwork programme could have been devised to complement the model development through the calibration and validation stages. However, the former was not possible because of the difficulty of obtaining another similar data set, and the latter was difficult because the format of the fieldwork

programme did not permit a spatial and temporal comparison of the hydraulic parameters at the resolution defined in the model. The model and field estimates of reach mean shear stress,  $\tau$ , and unit stream power,  $\omega$ , were therefore compared at a number of study site locations with the aim of testing the predictive capabilities of the model at these sites.

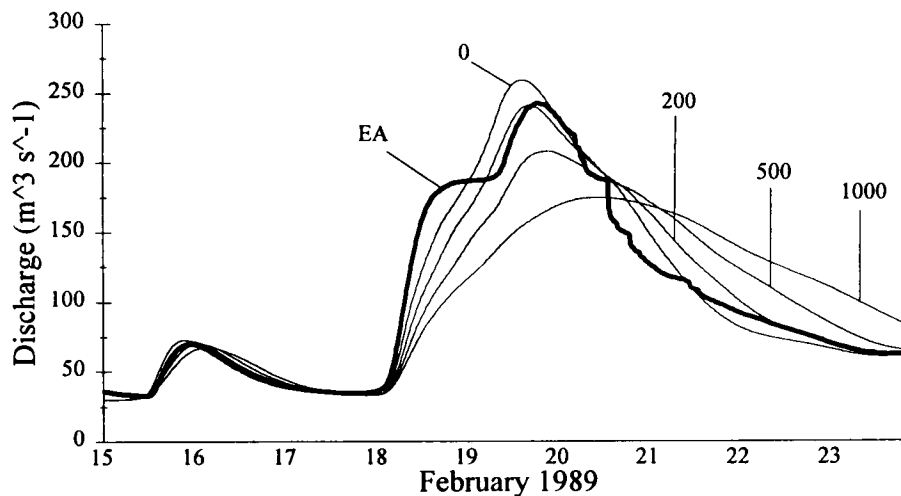


Figure 5.15 The simulation of floodplain storage at Montford, using total floodplain widths varying from 0 - 1000 m.

Figures 5.16 - 5.19 show how the field measurements of  $\tau$  and  $\omega$  compare with simulated at-a-site variations during the flood event. Not all the study sites were included in this comparison because, a) the simulated channel does not extend upstream from Severn Flume (4.26 km downstream), and b) some study sites do not contain data for all three flow levels (low, medium and high). However, these data clearly show a number of interesting features of the two data sets,

- a) discharge (and therefore  $\tau$  and  $\omega$ ) measured under low flow conditions in the field was lower than the discharge simulated by the model (Figures 5.16 - 5.19). Field measurements of  $\tau$  and  $\omega$  appear to correspond with the predicted if the predicted trends are extended to lower discharges.
- b) in the upper reaches (sites Severn Flume to Mount Severn), the model predictions of  $\tau$  and  $\omega$  are generally greater than field measurements, whereas in the lower reaches (Pool Quay to Saxons Lode) the model predictions are generally less than the field measurements (Figures 5.16 - 5.19).
- c) the agreement between the measured and predicted  $\tau$  and  $\omega$  for a range of flows is good at only some sites (Figures 5.16 - 5.19) - predominantly those in the middle reaches, ie: Dolwen, Caersws, Abermule and Dyffryn.

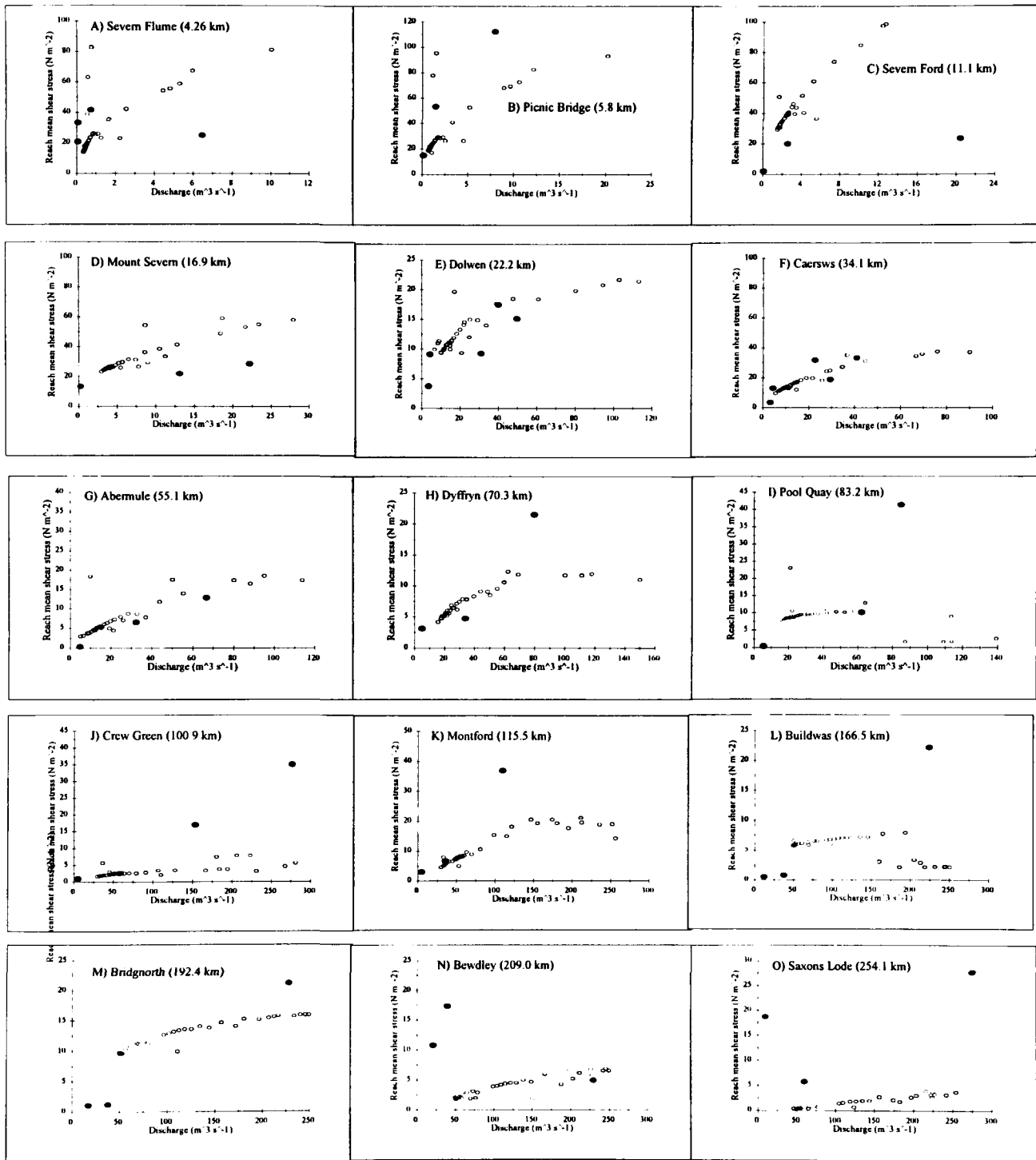


Figure 5.16 A comparison between measurements of reach mean shear stress (●) made at 15 field sites under a range of flows with estimates of shear stress (○) simulated by MIKE11 during a flow event in February 1989.

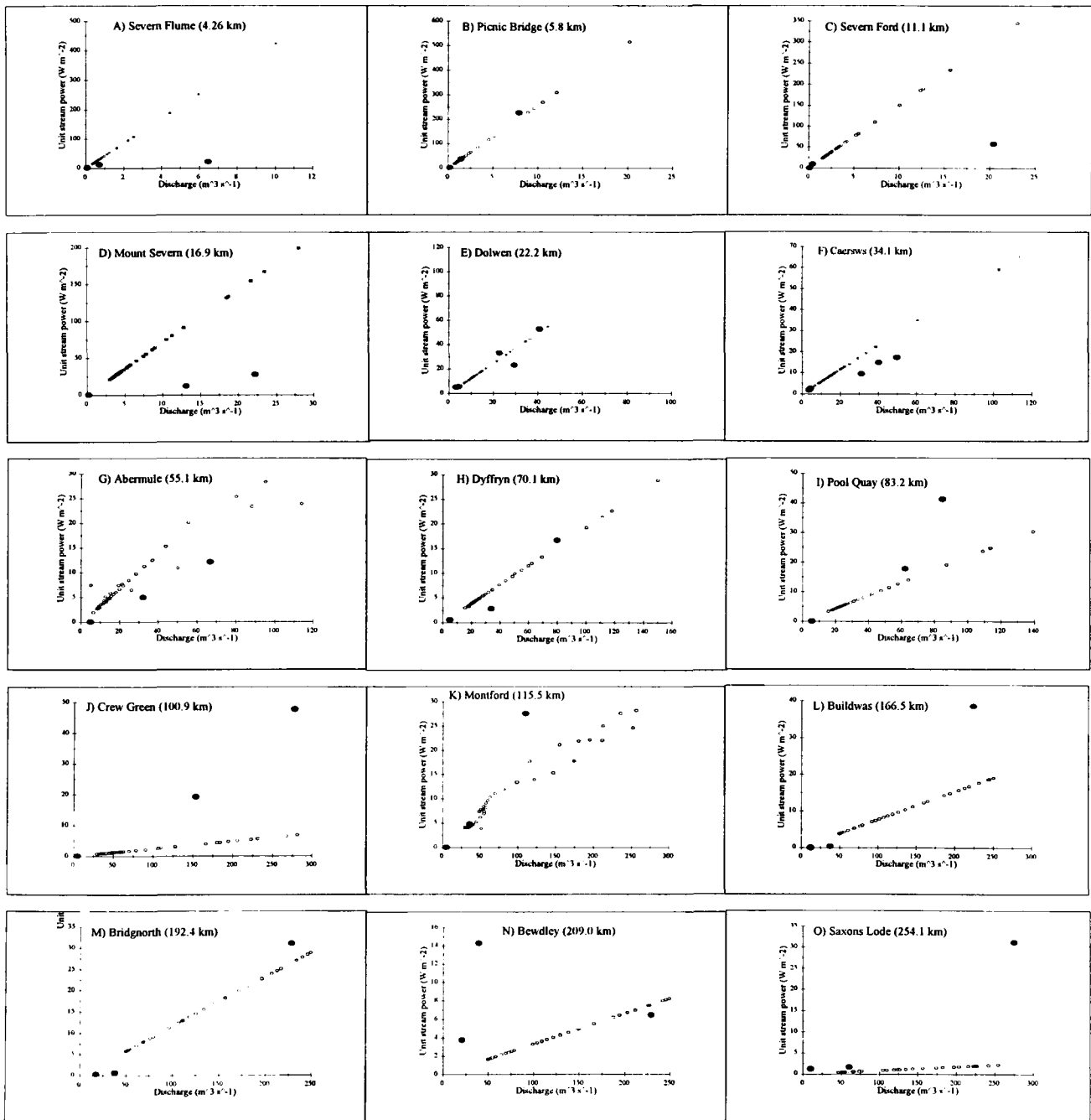


Figure 5.17 A comparison between measurements of unit stream power (●) made at 15 field sites under a range of flows with estimates of unit stream power (○) simulated by MIKE11 during a flow event in February 1989.

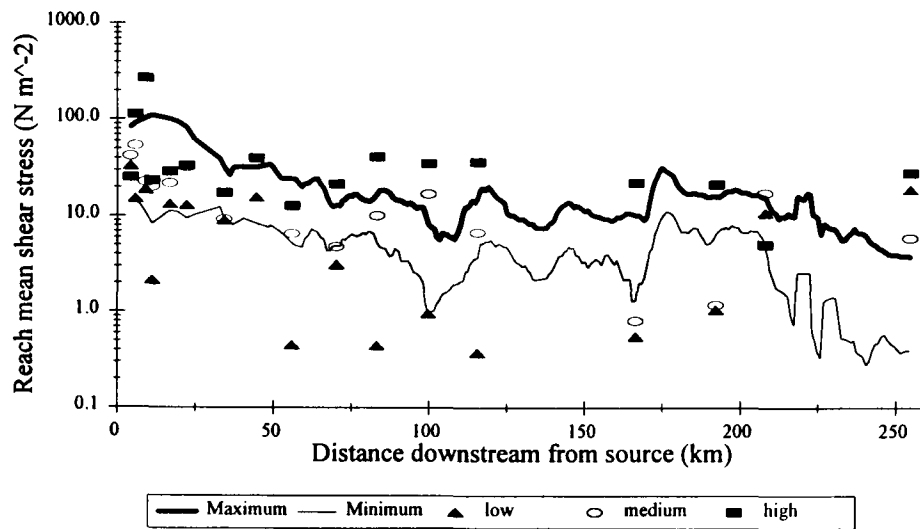


Figure 5.18 A comparison between modelled reach mean shear stress (maximum and minimum) and measured shear stress at low, medium and high flows.

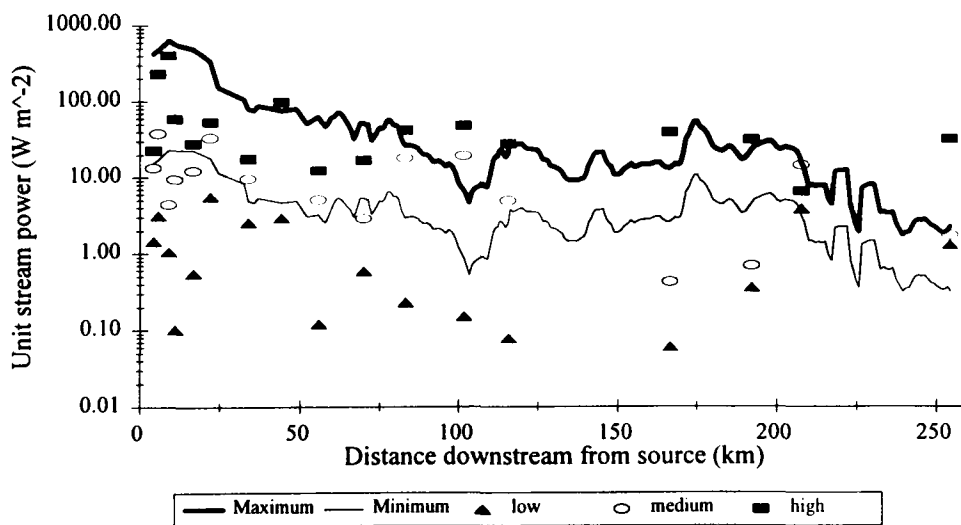


Figure 5.19 A comparison between modelled unit stream power (maximum and minimum) and measured unit stream power at low, medium and high flows.

- d) several anomalous trends are apparent in these data sets: a) the field measurements of  $\tau_{\text{peak}}$  at Dyffryn and Pool Quay were measured at bankfull flows. However, the model failed to predict their values, either because the time period selected for the model results did not include bankfull stage, or the morphometry of the channel reach in the model does not conform with reality; b) unusually high  $\tau$  and  $\omega$  at low and medium flows at Bewdley and Saxons Lode suggest that additional hydraulic features (eg: riffles, bridges, meander bends) exert a control on the flow before being ‘drowned out’ at higher flows; c)  $\omega$  varies almost linearly with discharge until the bankfull level is exceeded and thereafter the relationship becomes more complex.

The downstream variation of the predicted - measured relationship is perhaps the result of scale exerting a control on the estimation of water surface slope, and thus also on  $\tau$  and  $\omega$ . For example, slope in the upper reaches was measured over approximately 50 - 100 m (10 channel widths), and in the model over approximately 2000 m (distance between 3 cross sections). Hence, the simulated slope will be greater than the measured, because the valley slope will exceed the reach slope. Thus the predicted values of  $\tau$  and  $\omega$  will exceed those measured. Slope was measured in the lower reaches over approximately 1000 m, and in the model over 2000 m. Therefore, as riffles and bars are exposed at low flows, the reach slope will exceed the overall valley slope. This will give low flow  $\tau$  and  $\omega$  values greater than the predicted values at the downstream sites. Alternatively, the representation of channel roughness (resulting from the natural variability of bed grain sizes, channel geometry and planform variations) may be inaccurate, and thus may produce unrealistic estimates of  $\tau$  and  $\omega$ . This is a critical factor in the validation of the model and will therefore be analysed in greater detail in section 7.3.

These trends indicate that despite the influence of scale on the two measurement procedures and the difficulty of channel roughness representation the model results closely approximate field results at a range of flows. This suggests that the model can be used to extrapolate downstream trends in channel hydraulic parameters at a greater spatial and temporal resolution than is reasonably achievable in the field.

## 5.5 Summary

This chapter has described how the 1-D model, MIKE11, can be used to simulate a flow event at a catchment-scale. It has demonstrated that the form of the River Severn can be represented at a fairly high spatial resolution using a simple, PC-driven model. Furthermore, the model can be partitioned into a series of discrete reaches to achieve successful results without any loss of accuracy, or representativeness. The validation tests have shown that the model can predict measured reach mean shear stress and unit stream power precisely at the majority of sites: however, the influence of unsteady flow in a natural channel on boundary roughness and floodplain flow is not sufficiently understood to accurately simulate over-bank flow in a 1-D model (see Chapter 7). Notwithstanding this shortcoming in the model parameterization, the potential of the model for evaluating the spatial and temporal variation of flows and channel hydraulics is evident and will be the focus of the following Chapter (6).

## CHAPTER 6

### DOWNSTREAM VARIATION OF CHANNEL HYDRAULICS ALONG THE RIVER SEVERN: MODEL RESULTS

#### 6.1 Introduction

This chapter will present the results from the 1-D simulation of a flow event along the River Severn. It will examine each of the channel hydraulic parameters discussed in Chapter 4, but individually, rather than in terms of flow frequency. Thus it will be possible to reveal both the at-a-site temporal variation at three reference locations, and the spatial distribution of each parameter along the channel; these are simulated at a high space and time resolution by the MIKE11 model, as described in Chapter 5. It will begin with a review of the channel geometry parameters and be followed by the channel hydraulic parameters, including mean velocity, discharge, stream power and shear stress. Flow resistance is omitted from this analysis because roughness coefficients for each section were already specified in the model.

The three reference sites were selected because they were characteristic of particularly distinctive reaches in the upper, middle and lower Severn; the morphological and hydrological features of these sites are presented in Table 6.1. The temporal variation of each parameter at these sites used data saved at six hour intervals from the model; this was plotted against time-varying discharge at that site to examine the impact of the event on each hydraulic parameter. Also, the maximum and minimum values of each parameter at all cross sections along the simulated reach were plotted against distance downstream on a linear scale to examine the detailed spatial variation of channel hydraulics during the flow event, particularly in the middle and lower reaches.

Table 6.1 The location and characteristics of the three sites chosen to represent the simulated temporal variation of channel hydraulics.

Site name	Basin location	Distance downstream (km)	Site description
Dolwen	Upper	34.1	Straight, relatively confined, moderate slope, bank vegetation
Crew Green	Middle	100.9	Sinuous, wide floodplain on left bank, low slope
Buildwas	Lower	166.4	Straight, relatively confined, moderate slope, bank vegetation, upstream of Ironbridge Gorge

## 6.2 Downstream distribution of channel geometry during the flow event

### 6.2.1 Temporal variation of water prism geometry parameters

Water width rose to a maximum at the peak level of discharge during the flood event (Figure 6.1). At Dolwen and Buildwas the rate of increase was moderate (50 % and 100 % rise, respectively), but, at Crew Green discharge exceeded the bankfull limit, resulting in a rapid rise in width from 50 m to 210 m (500 %). The non-linear response in water width between the rising and falling limbs (hysteresis) of the hydrographs was less evident at the two former sites, but pronounced at Crew Green; on the falling limb at Crew Green the width was approximately 150 m greater than the preceding rising limb for the same discharge value, suggesting residual flow or temporary storage, occurred on the floodplain. Furthermore, this anti-clockwise loop is consistent with the trend observed at Buildwas, possibly in response to the attenuation of the floodwave in the middle-lower catchment.

Hydraulic radius reached a maximum with peak discharge at Dolwen and Buildwas (Figure 6.2). At Crew Green, where the peak flow exceeded the bankfull limit (Figure 6.2), hydraulic radius fell from a peak of almost 4 m at bankfull to < 2 m as the flow remained overbank. Like the water width hysteresis loops, the in-bank flows at Dolwen and Buildwas produced little variation in hydraulic radius at a given discharge; similarly, the direction of the loops opposed one another. The temporal trend was more complex at Crew Green although the flow - hydraulic radius relationship corresponded to the other sites up to a bankfull limit. Thereafter, a large increase in the wetted perimeter (demonstrated in the water width trend (Figure 6.1)) caused a rapid decline as discharge continued to rise. The consequences of floodplain inundation at Crew Green will be discussed throughout this chapter, and in Chapter 7.

### 6.2.2 Spatial variation of water prism geometry parameters

The minimum and maximum water widths increased downstream along the Severn during the event (Figure 6.3). However, whilst the minimum width increased downstream with little inter-reach variation, the maximum width distribution was dominated by a sequence of sharp peaks between 75 km and 230 km, which reached a highest value of > 600 m just upstream of the Buildwas reach. These peaks define the location of floodplain inundation during the flood event, and in part, the level of confinement of the channel geometry. The peaks occurred at Dyffryn (70 km), upstream and downstream of the Vyrnwy confluence (100 km), and in the reaches: Shrewsbury - Buildwas (120 - 170 km); and Bewdley - Worcester (210 - 230 km). This agrees well with published accounts of flooding in the Severn catchment (eg: McCartney & Naden, 1992) and highlights the degree of inundation possible from only a moderate flow event. Clearly, the occurrence of over-banking at particular reaches along the river will significantly affect the spatial and temporal variation of channel hydraulics discussed in this study (section 7.4).

The minimum and maximum hydraulic radii increased by similar magnitudes downstream between the source and Saxons Lode (Figure 6.4). Notwithstanding the great variability between reaches, there exist three separate distributions superimposed on the general rising trend. From the source downstream to approximately 75 km, hydraulic radius increased from a maximum of 0.7 m to almost 2.0 m; between 75

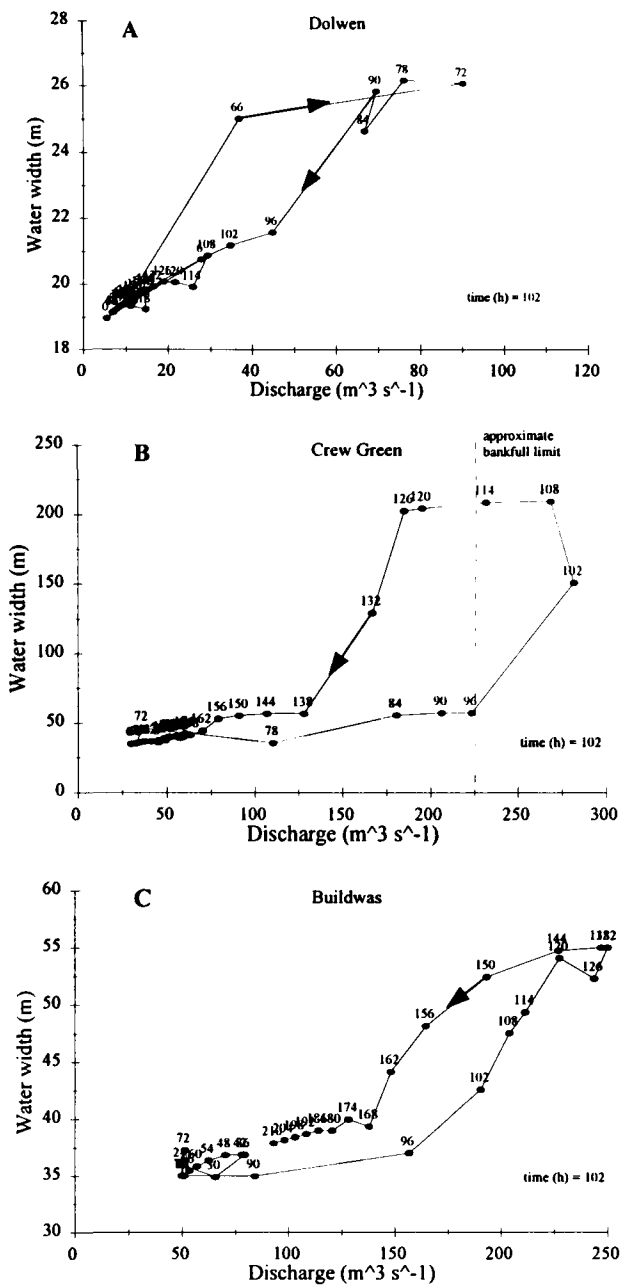


Figure 6.1 The temporal variation of water width at: a) Dolwen; b) Crew Green; and c) Buildwas.

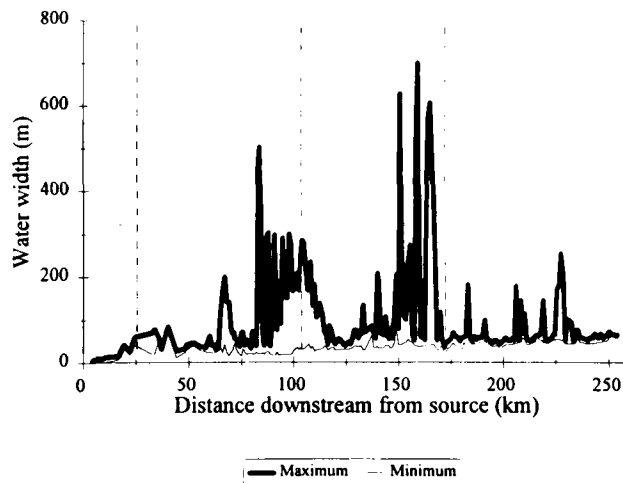


Figure 6.2 The spatial variation of water width along the Severn, expressed as a maximum and minimum of the data series at each cross section; the dashed lines indicate the locations of Dolwen, Crew Green and Buildwas, respectively.

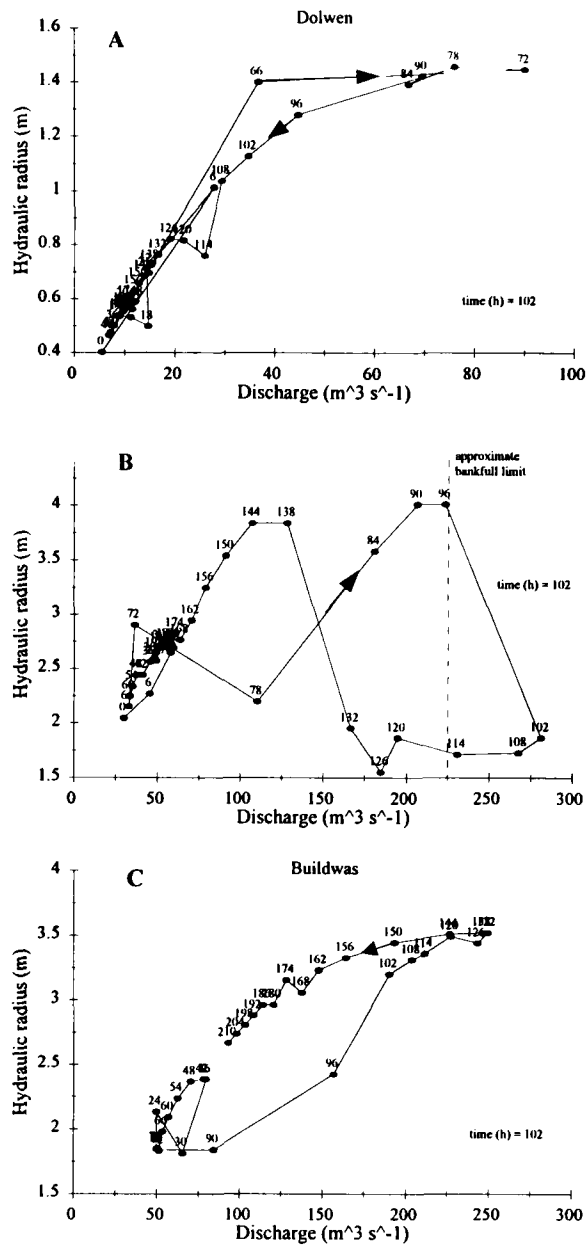


Figure 6.3 The temporal variation of hydraulic radius at: a) Dolwen; b) Crew Green; and c) Buildwas.

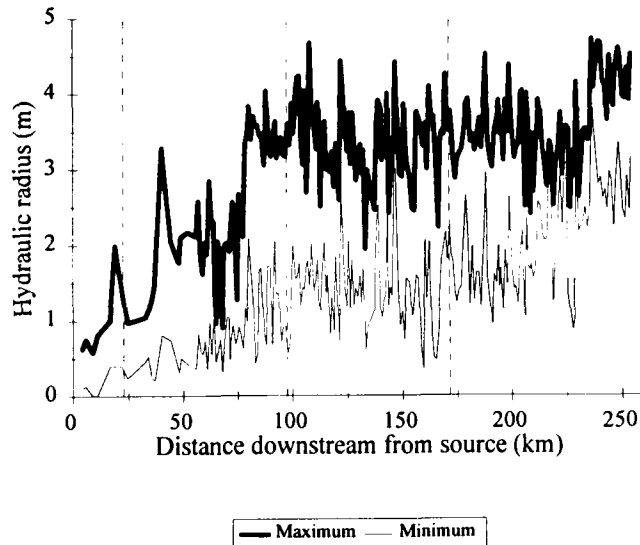


Figure 6.4 The spatial variation of hydraulic radius along the Severn, expressed as a maximum and minimum of the data series at each cross section; the dashed lines indicate the locations of Dolwen, Crew Green and Buildwas, respectively.

km and 230 km it remained relatively constant at a mean maximum value of almost 3.5 m (with a mean minimum of 1.5 m); thereafter, downstream of the Teme confluence, both the minimum and maximum appear to increase abruptly to 2.8 m and 4.5 m respectively. This sequence of transitions along the channel relate to modifications of the channel form which could potentially influence the spatial (and temporal) distribution of the channel hydraulic parameters. Unlike the maximum water width spatial distribution, the maximum hydraulic radii are likely to correspond to bankfull hydraulic radii (and approximate mean depth): conversely, the minimum hydraulic radii may relate to overbank conditions in the reaches as demonstrated by Figure 6.4, or low-flow conditions.

### 6.3 Downstream distribution of mean velocity during the flow event

#### 6.3.1 Temporal variation of mean velocity

Mean velocity generally increased with stage, but the maximum did not correspond to peak discharge at all sites (Figure 6.5). At Dolwen, mean velocity rose from approximately  $0.8 \text{ m s}^{-1}$  to  $2.2 \text{ m s}^{-1}$ ; velocities decreased at a lesser rate as discharge declined, and therefore, velocities were greater on the falling limb than on the rising limb, for a given discharge. Conversely, at Crew Green and Buildwas, mean velocity reached a maximum as discharge increased ( $1.4 \text{ m s}^{-1}$  and  $2.0 \text{ m s}^{-1}$ , respectively) and declined at the peak: velocities continued to decline as the discharge fell. The clockwise hysteresis loops found at Crew Green and Buildwas are consistent with trends observed by Leopold *et al.* (1964) on the San Juan River, Utah. They concluded that modifications in the bed configuration and patterns of turbulence decreased the flow resistance and hydraulic radius (mean depth); thus, mean velocity would increase to satisfy the continuity equation. However, as MIKE11 is a fixed-bed model, a peak in mean velocity before maximum discharge must be attributable to the geometry of the cross section and the steep rising limb of the floodwave. It is possible that greater boundary roughness on the upper banks and floodplain, and high turbulent shear between in-bank and over-bank states, may reduce the mean velocity (Beven & Carling, 1992) (see section 7.4). Furthermore, the model parameterization of flow conveyance over the floodplain assumes in-channel and floodplain flow components have equal velocities, but in reality, the in-channel mean velocity generally exceeds the floodplain flow velocity (Bhowmik & Demissie, 1982). Hence, the simulated mean velocity for overbank flow may be lower than the true mean velocity.

#### 6.3.2 Spatial variation of mean velocity

Figure 6.6 indicates that the minimum mean velocity tended to increase slightly downstream, whilst the maximum mean velocity gradually decreased. Despite considerable reach-scale variability, including a major peak between 60 - 80 km downstream in the maximum velocity ( $u = 6.8 \text{ m s}^{-1}$ ), the best-fit lines clearly demonstrate contrasting downstream trends between the maximum and minimum distributions.

Maximum:  $u_{\text{fit}} = 5.42 DD^{-0.25}$ ,  $(n = 225; p < 0.0001; r^2 = 0.23)$

Minimum:  $u_{\text{fit}} = 0.22 DD^{0.10}$ ,  $(n = 225; p = 0.029; r^2 = 0.021)$

It is probable that the maximum mean velocities relate to the velocity of the flood wave peak, and such high magnitudes are not unusual for these reaches of the river, as discussed in section 7.4. Furthermore, the location of the peak velocities in the mid-basin (60 - 80 km) coincide with the sharp increase in hydraulic radius (Figure 6.4); these were attained as a bankfull level was reached. Together, these results suggest that the unusually high maximum velocities were achieved by the flood wave travelling through the reach whilst it remained in-bank. The low maximum velocities at 100 km downstream are the result of the low valley slope, the unconfined channel and floodplain inundation. Conversely, the peaks in the headwaters and the Ironbridge Gorge are the result of high valley and water surface slopes and the confined channel reaches. The reversal of the downstream trend with stage highlights earlier uncertainty in work by Leopold (1953), Leopold and Maddock (1953), Mackin (1963) and Carlston (1969) which indicated that mean velocity may decrease downstream (section 2.4.4). The implications of these results are that reaches along the channel respond differently to increasing discharge, because of variations in channel topography, slope, boundary and channel resistance, and flow regime: this subject will be the source of further discussion in Chapter 7.

## 6.4 Downstream distribution of discharge during the flow event

### 6.4.1 Temporal variation of discharge

The floodwave simulated from the February 1989 flow event was accentuated by flows from the Afon Vyrnwy and attenuated further downstream through the Shropshire plains (Figure 6.7). Figure 6.7 illustrates the temporal variation of discharge at Dolwen, Crew Green and Buildwas between 15 - 24 February 1989. This shows how two flow events were simulated (see also Figure 5.15). The first occurred at the beginning of the simulation period and was relatively minor compared to the second event. The latter event attained a peak discharge of almost  $90 \text{ m}^3 \text{ s}^{-1}$  at Dolwen on 18 February; the hydrograph was double-peaked and the recessional limb was initially steep. The peak discharge at Crew Green was  $275 \text{ m}^3 \text{ s}^{-1}$  and occurred at 1500 h, 19 February; as the Afon Vyrnwy is the only major tributary along the Dolwen - Crew Green reach, this implies a major contribution from the tributary, of an equal or greater magnitude than the flow on the Severn itself. The discharge hydrograph at Buildwas was reduced in magnitude and modified in shape. Whilst the discharge rose and fell rapidly at Crew Green (except for two small 'shoulders' on the rising and falling limbs, representing the topographic influence of the section geometry as over-banking occurred), at Buildwas the rising limb was initially as steep up to  $200 \text{ m}^3 \text{ s}^{-1}$  but more gradual approaching the peak discharge ( $250 \text{ m}^3 \text{ s}^{-1}$ ), with a recessional limb comparable to that at Crew Green. The broader hydrograph at Buildwas suggests some attenuation of the floodwave through the catchment as suggested earlier, although flow abstraction was not unfeasible. The wave took approximately 54 h to travel 144 km between Dolwen and Buildwas, representing an average wave speed of  $0.74 \text{ m s}^{-1}$ ; this was marginally greater through the Dolwen - Crew Green reach ( $0.90 \text{ m s}^{-1}$  compared with  $0.61 \text{ m s}^{-1}$ ), perhaps in response to greater levels of channel confinement (see section 7.4).

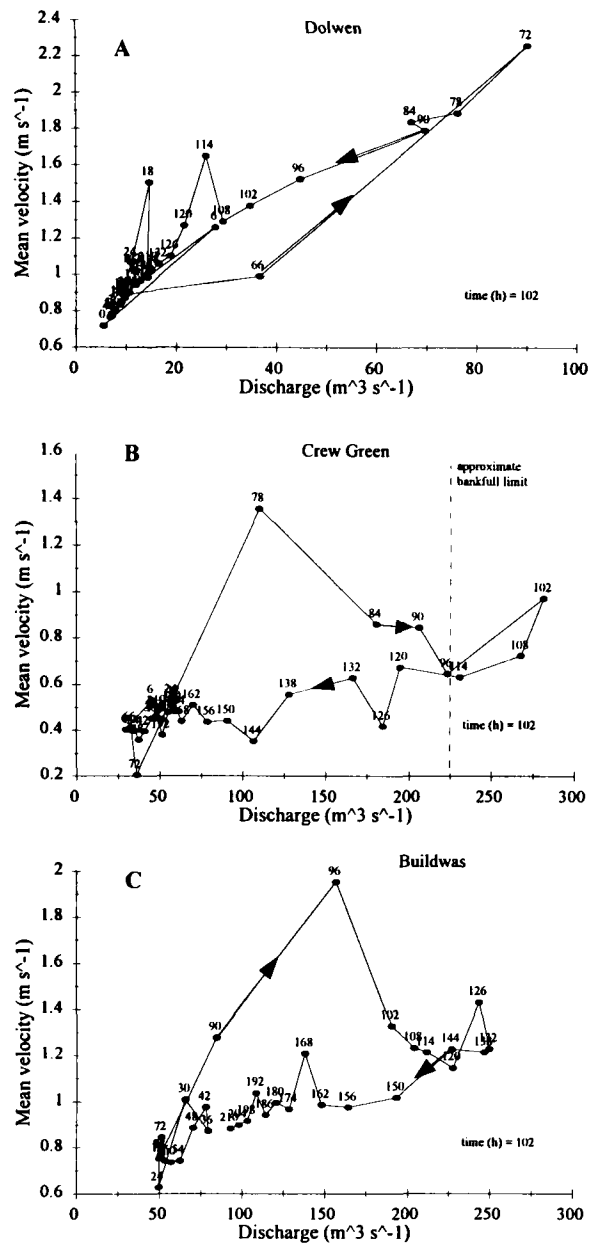


Figure 6.5 The temporal variation of mean velocity at: a) Dolwen; b) Crew Green; and c) Buildwas.

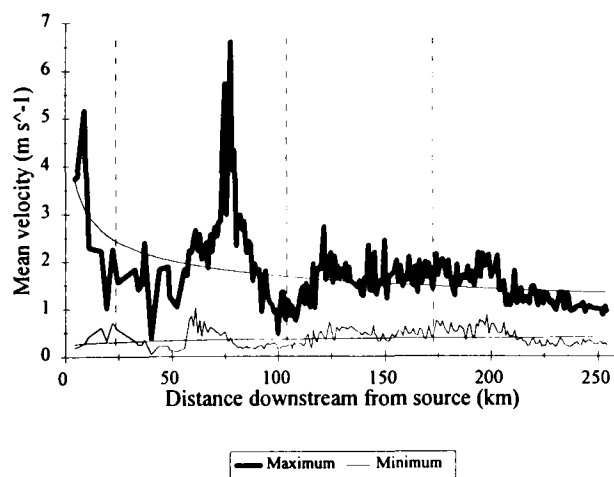


Figure 6.6 The spatial variation of mean velocity along the Severn, expressed as a maximum and minimum of the data series at each cross section; the dashed lines indicate the locations of Dolwen, Crew Green and Buildwas, respectively.

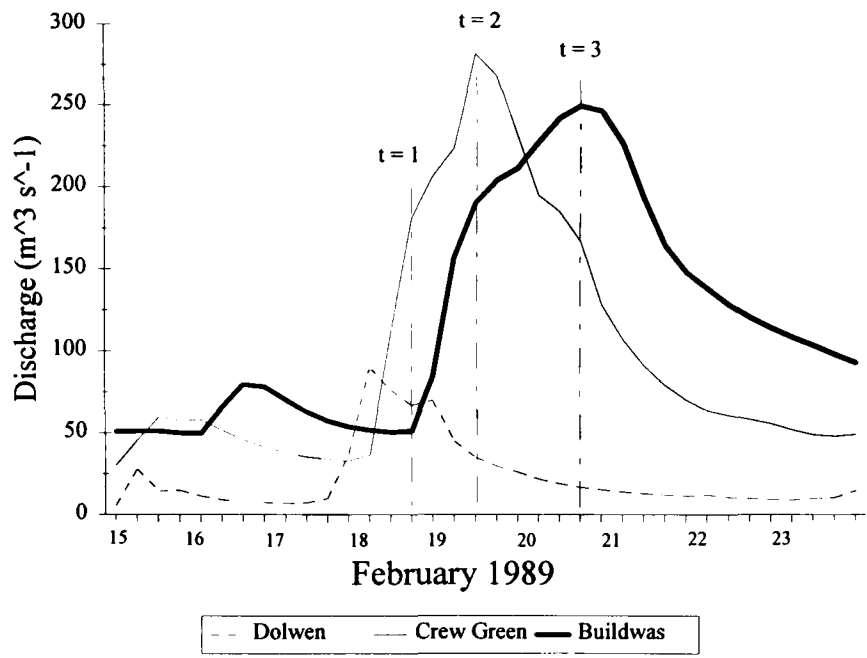


Figure 6.7 The temporal variation of discharge at Dolwen, Crew Green and Buildwas. The peak flow at each site is defined in Figure 6.8 as an instantaneous spatial distribution along the channel at three time intervals.

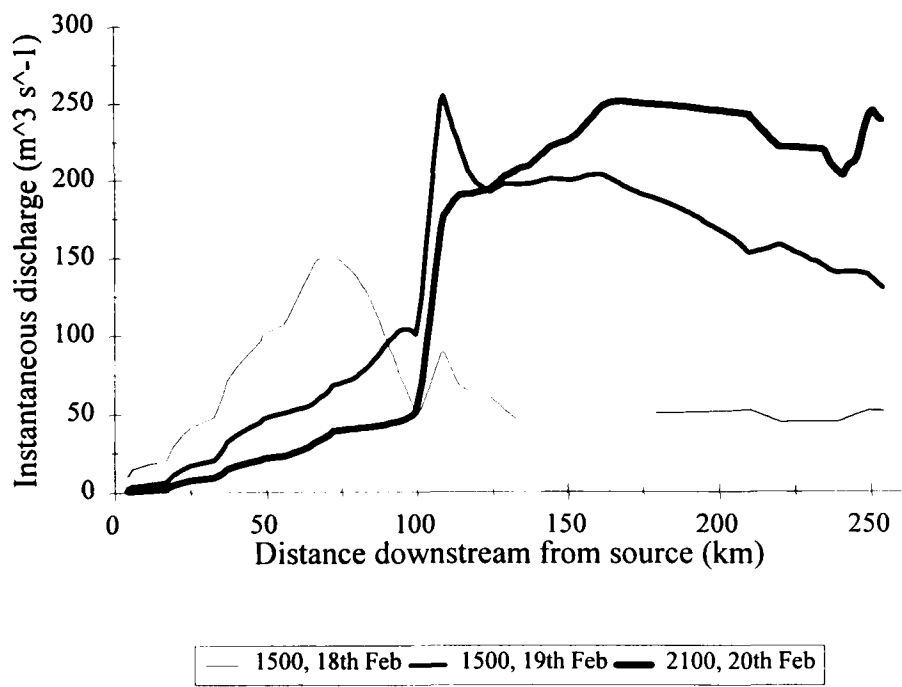


Figure 6.8 The spatial distribution of instantaneous discharge along the Severn, defined at three time periods: a) 1500, 18 February; b) 1500, 19 February; c) 2100, 20 February.

### 6.4.2 Spatial variation of discharge

The translation of the floodwave along the Severn channel was significantly altered by the Afon Vyrnwy, which greatly increased the flow magnitude in the lower 150 km of the simulated reach (Figure 6.8). The three time periods ( $t_p = 1, 2 \text{ \& } 3$ ) represent the approximate time of peak discharge at Dolwen, Crew Green and Buildwas, respectively. Hence, Figure 6.8 illustrates the instantaneous discharge along the channel at three separate time instants. At 1500, 18 February, the discharge peak at 75 km represents the downstream location of the floodwave; the secondary peak downstream of the Vyrnwy confluence demonstrates the disparate timing of flows from the Severn and Vyrnwy channels. Similarly, the two other time instants (1500, 19 February; 2100, 20 February) illustrate the non-synchronicity between flows from the Severn and Vyrnwy, the progressive reduction of flows in the upstream reaches, and the translation of the floodwave to the lower reaches (Figure 6.8). Thus it is evident that the precipitation event between the 17 - 20 February was not located centrally on the Plynlimon massif, but also produced significant rainfall on higher ground in the headwaters of the Vyrnwy catchment as mentioned in section 5.3 (Figure 5.10). Furthermore, the discontinuity in the flow regime between the upper and lower Severn catchment at the Vyrnwy confluence, may create a significant division between the hydraulic characteristics of the two reaches; this was indeed evident from the spatially varied mean velocities (Figure 6.6) which increased markedly between the Vyrnwy confluence and Bewdley, 210 km downstream.

## 6.5 Downstream distribution of water surface slope during the flow event

### 6.5.1 Temporal variation of water surface slope

Slope increased with rising stage during the flow event, and reached a maximum at peak discharge (Figure 6.9). This relationship holds for all three sites, although the magnitude of slopes and the direction of hysteresis differs. The water surface slope was relatively steep at Dolwen ( $0.0024 \text{ m m}^{-1}$ ), and only changed by  $0.0002 \text{ m m}^{-1}$  as the floodwave passed. At Crew Green and Buildwas, the slopes were an order of magnitude lower, although Buildwas was slightly greater at peak discharge ( $0.00085 \text{ m m}^{-1}$  at Buildwas;  $0.0003 \text{ m m}^{-1}$  at Crew Green). Despite these lower slopes and the different hydraulic conditions described in sections 6.3 and 6.4, the range of slopes at both sites was only  $0.0002 \text{ m m}^{-1}$ . It is also interesting to note that slopes were greater on the rising limb of the hydrograph for a given discharge at Dolwen and Crew Green, but lower at Buildwas. The former instance is consistent with observations by Leopold *et al.* (1964), which they attributed to 'a slight shortening of the course taken by water as discharge increases' (p. 247). However, the spatial resolution of this simulation did not permit this eventuality. Instead, it is perhaps the result of the reach-scale differences in the longitudinal channel gradient. For example, a negative break of slope at Buildwas may have induced a backwater effect which would reduce the rate of increase of slope with discharge; conversely, relatively constant downstream slopes at Dolwen and Crew Green perhaps permitted the slope to increase as the relative roughness decreased and the energy gradient steepened. The effect of over-banking at Crew Green had little effect on the water surface slope. Indeed, it is apparent that the slope steepened following the inundation of the floodplain, but retained the same temporal pattern as discharge fell. This suggests that an external

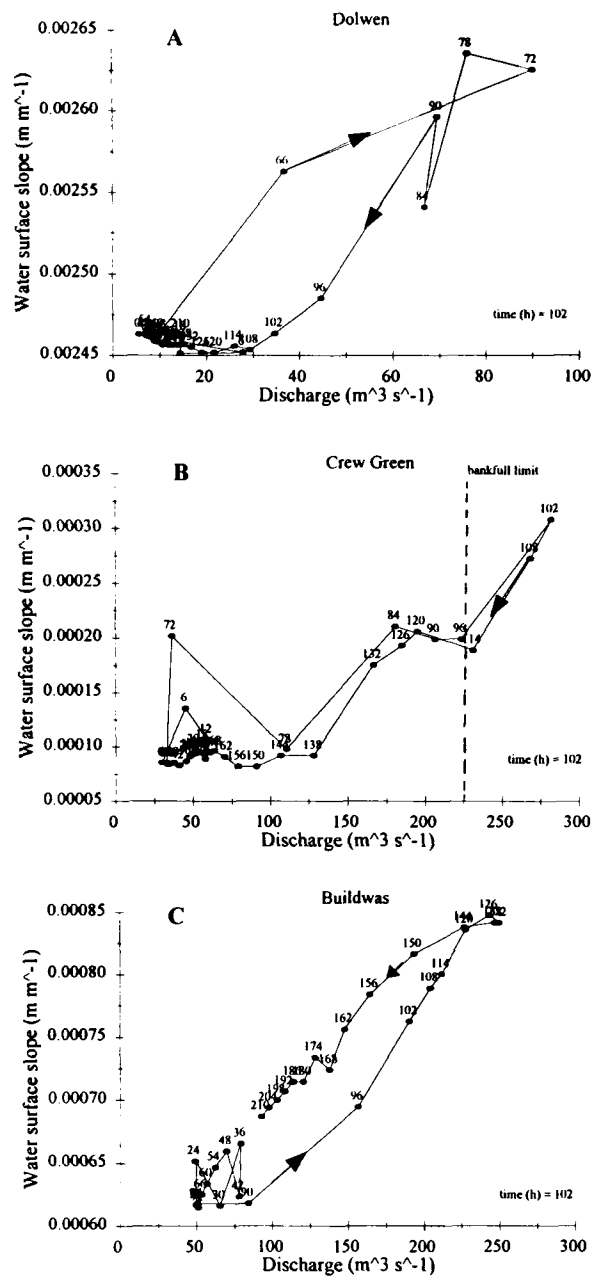


Figure 6.9 The temporal variation of water surface slope at: a) Dolwen; b) Crew Green; and c) Buildwas.

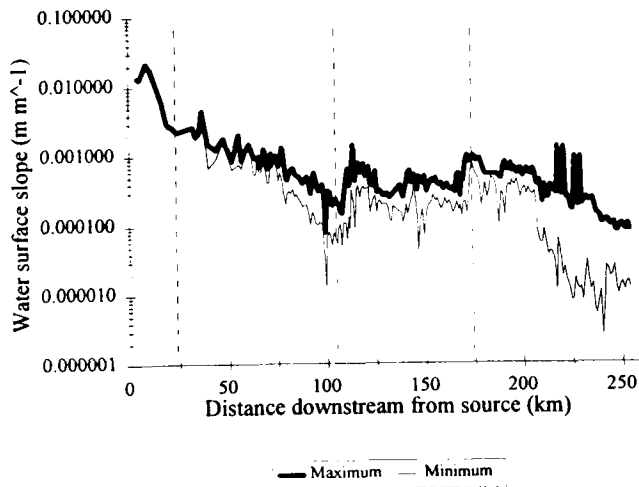


Figure 6.10 The spatial variation of water surface slope along the Severn, expressed as a maximum and minimum of the data series at each cross section; the dashed lines indicate the locations of Dolwen, Crew Green and Buildwas, respectively.

influence, such as the upstream Vyrnwy tributary or a local topographic feature, acts as a hydraulic control.

### 6.5.2 Spatial variation of water surface slope

Water surface slope decreased with distance downstream along the Severn to the Vyrnwy confluence: thereafter, it became more variable, with secondary peaks close to Montford and at the Ironbridge Gorge (Figure 6.10). The difference between the minimum and maximum trends was low in the reaches upstream of 75 km and at the Ironbridge Gorge, but more exaggerated in the reach 75 - 165 km, and downstream from the Gorge (210 km - 255 km). Hence, it was clear that slope varied little with stage in relatively steep channel reaches. The peaks in maximum slope are located where bedrock outcropped in the channel; however, the four peaks between 215 - 230 km downstream are attributable to sharp breaks of slope over the broad-crested weirs, near Worcester. Also, the weirs were partly responsible for the marked reduction in minimum slopes downstream from the Gorge by their regulation of stage, and thus the flattening of the water surface profile: a similar effect occurred at the Vyrnwy confluence by flow on the Severn backing up upstream of the tributary confluence. The reach-scale variability of these trends are perhaps the result of inconsistencies in: a) the location of the cross section; b) planform variations along the channel; and c) changes in the boundary resistance. The water slope will vary at a local scale as a result of variations in channel characteristics (Leopold & Wolman, 1957; Prestegard, 1983); thus, downstream changes in channel geometry, planform, and bed and bank roughness will produce a spatially varied representation of slope. However, as Figure 6.10 illustrated, by accumulating the reach-scale variations over a sufficiently large spatial scale a clear distribution of slope is discernible.

## 6.6 Downstream distribution of total and unit stream power

### 6.6.1 Temporal variation of total and unit stream power

Discharge is excluded from the temporal analysis of total and unit stream power as it is a component variable of the two parameters; instead, time (expressed in hours) is adopted as the independent variable in Figures 6.11 and 6.13. These trends indicate that stream power reached a maximum as discharge peaked. Indeed, a comparison between the discharge hydrographs in Figure 6.7 and the stream power hydrographs (Figures 6.11 and 6.13) reveals that the shape and timing of the hydrographs are similar. For example, the double-peaked discharge hydrograph at Dolwen and the 'shoulders' on the rising and falling limbs at Crew Green (Figure 6.7) are reflected in the total and unit stream power hydrographs at Dolwen and Crew Green (Figure 6.11 and 6.13). However, the magnitude of the discharge and stream power hydrographs are not directly related: at Dolwen, the lowest peak discharge produced the highest peak total and unit stream power, whereas at Crew Green, the opposite was the case. Thus it is apparent that where discharge dominates the *temporal* distribution of total and unit stream power, the longitudinal variability of the channel slope and form (eg: width) along the Severn channel is influential in defining the stream power *magnitude*. This conclusion is consistent with the findings of Graf (1983) in the Utah mountains and Magilligan (1992) in the Galena watershed; they showed that small variations in the channel geometry downstream were sufficient to determine how stream power varied spatially along the channel.

## 6.6.2 Spatial variation of total and unit stream power

The maximum stream power peaked within the first 10 km ( $\Omega = 4300 \text{ W m}^{-1}$ ,  $\omega = 1000 \text{ W m}^{-2}$ ) and declined gradually to a low of  $\Omega = 300 \text{ W m}^{-1}$  ( $\omega = 1 \text{ W m}^{-2}$ ) close to the Vyrnwy confluence; thereafter, stream power increased to a secondary peak of  $\Omega = 2000 \text{ W m}^{-1}$  ( $\omega = 80 \text{ W m}^{-2}$ ) at the Ironbridge Gorge (Figures 6.12 & 6.14). The magnitude of these stream powers are in the upper limits of values recorded by Ferguson (1981) in rivers at a bankfull level throughout the UK. Despite considerable variability it is clear that the general downstream distribution has the form of the polynomial least-squares best-fit line plotted in Figure 6.13.

$$\text{Maximum: } \text{TSP}_{\text{fit}} = 3628.95 - 55.16 \text{ DD} + 0.21 \text{ DD}^2 + 9\text{E-}04 \text{ DD}^3 - 4.6\text{E-}06 \text{ DD}^4 \quad (n = 225; p < 0.0001; r^2 = 0.16)$$

$$\text{Minimum: } \text{TSP}_{\text{fit}} = 264.41 \text{ DD}^{-0.26} \quad (n = 225; p < 0.0001; r^2 = 0.16)$$

This trend line indicates that stream power does not decrease downstream from the source, as suggested by Knighton (1987), but that the lithological control exerted by the Ironbridge Gorge constrains the channel and elevates stream powers - a theory postulated by Magilligan (1992) using a similar methodological approach. This example also highlights the reach-scale variability of stream power over the general catchment-scale distribution. Furthermore, the departure of the maximum stream power from the minimum is perhaps indicative of the level of confinement of the channel throughout the catchment: in the upper reaches and through the Ironbridge Gorge, the channel is largely confined by the bedrock, whereas in the Vyrnwy confluence reach and downstream from Worcester, the channel is unconfined and the bankfull level is frequently exceeded. Thus the range of stream power values is maximised in confined reaches where channel capacity and mean flow velocity are high (Figure 6.6), and the threshold of entrainment of bank material (bedrock) is sufficient to prevent significant lateral erosion, and hence maintain low water widths (Figure 6.3). These issues are discussed at greater depth in sections 7.6 - 7.8.

## 6.7 Downstream distribution of reach mean shear stress

### 6.7.1 Temporal variation of reach mean shear stress

Shear stress increased with discharge, and peaked at the maximum flow level if the flow remained within bank (Figure 6.15). At Dolwen and Buildwas, shear stress peaked at  $36 \text{ N m}^{-2}$  and  $28 \text{ N m}^{-2}$ , respectively, and the hysteresis loop was narrow (Figure 6.15). However, at Crew Green, shear stress peaked before the maximum discharge at almost  $8 \text{ N m}^{-2}$  and declined rapidly as the flow inundated the floodplain, creating a broad hysteresis loop (Figure 6.15). An examination of the two component variables (hydraulic radius (Figure 6.2) and water surface slope (Figure 6.9)) reveals that the shape and size of the channel strongly influenced the peak magnitude and temporal variation (hysteresis loop shape and direction) (Mishra & Seth, 1996): shear stress increases rapidly with flow if the channel is confined and varies little on the rising and falling limbs of the hydrograph; however if the flow over-tops the bank, the reach mean shear stress is maximised at a bankfull level and thereafter decreases because energy dissipation is enhanced as the water flows over the floodplain. The magnitude of shear stress at the three sites is comparable with the stream power trends, for example: Dolwen > Buildwas >> Crew Green.

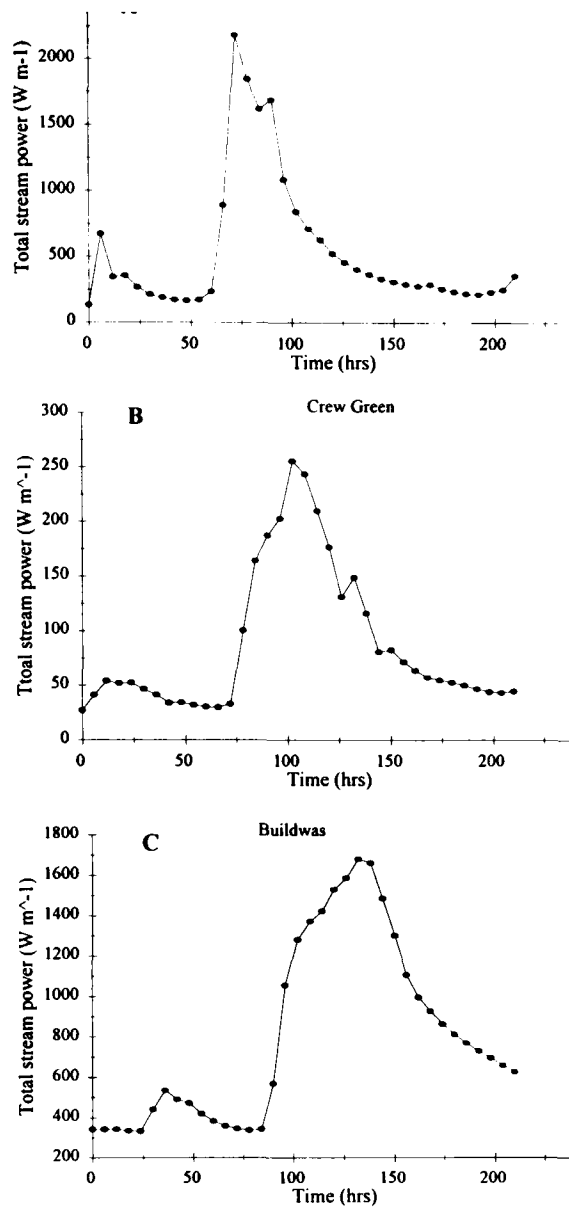


Figure 6.11 The temporal variation of total stream power at: a) Dolwen; b) Crew Green; and c) Buildwas.

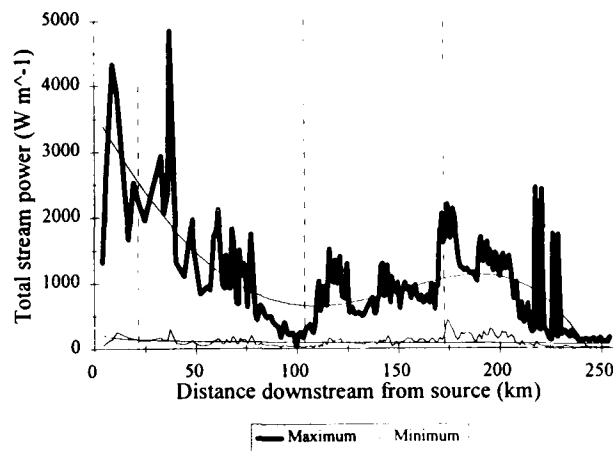


Figure 6.12 The spatial variation of total stream power along the Severn, expressed as a maximum and minimum of the data series at each cross section; the dashed lines indicate the locations of Dolwen, Crew Green and Buildwas, respectively. The trend lines represent lines of best-fit by least-squares regression.

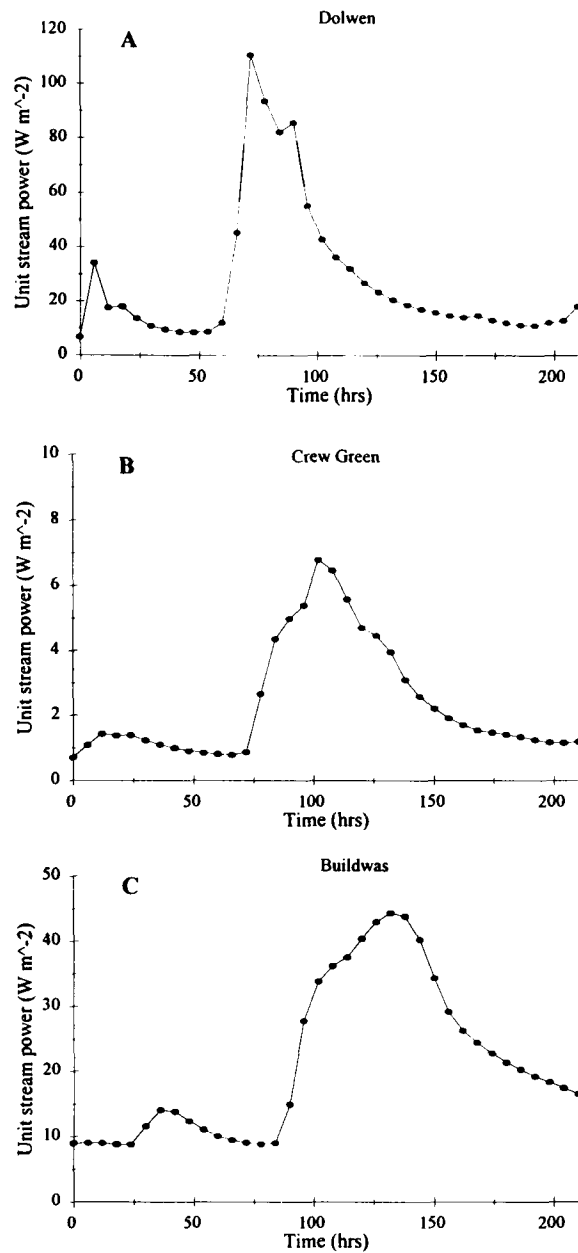


Figure 6.13 The temporal variation of unit stream power at: a) Dolwen; b) Crew Green; and c) Buildwas.

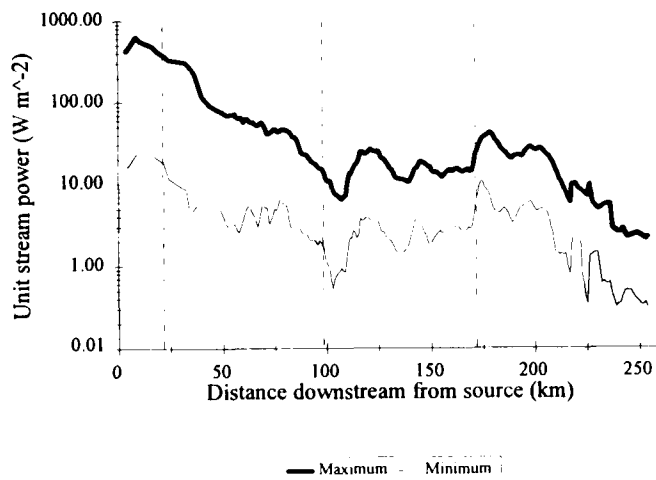


Figure 6.14 The spatial variation of unit stream power along the Severn, expressed as a maximum and minimum of the data series at each cross section; the dashed lines indicate the locations of Dolwen, Crew Green and Buildwas, respectively.

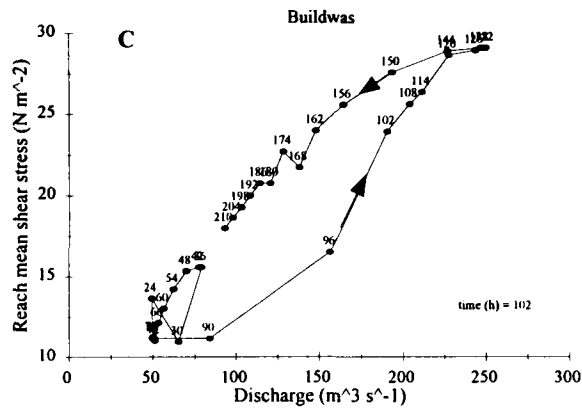
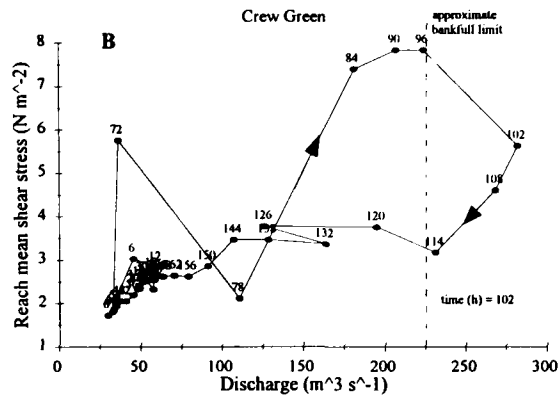
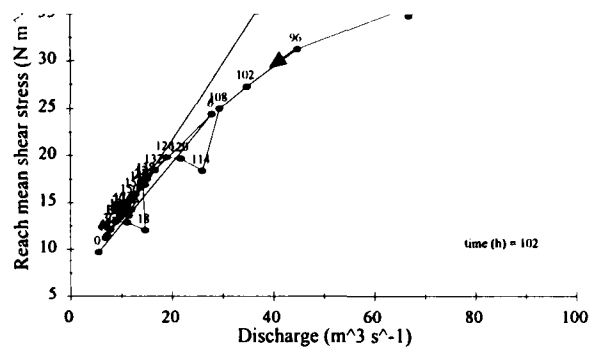


Figure 6.15 The temporal variation of reach mean shear stress at: a) Dolwen; b) Crew Green; and c) Buildwas.

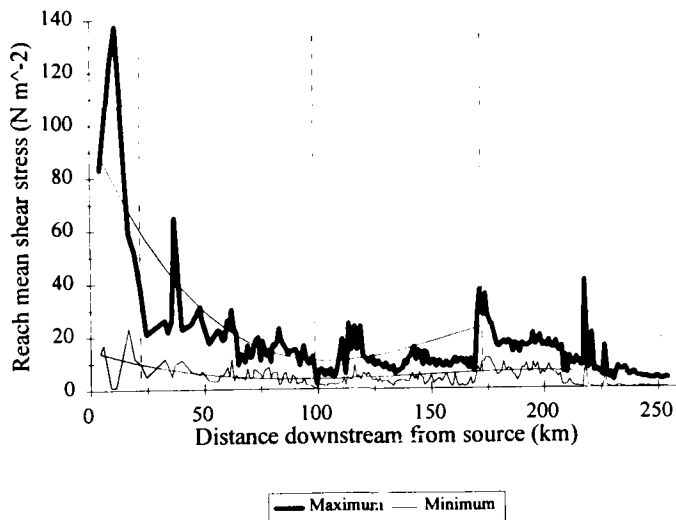


Figure 6.16 The spatial variation of reach mean shear stress along the Severn, expressed as a maximum and minimum of the data series at each cross section; the dashed lines indicate the locations of Dolwen, Crew Green and Buildwas, respectively. The trend lines represent lines of best-fit by least-squares regression.

This is consistent with the difference between water surface slope magnitudes at these sites, implying that slope exerts an effective control over the magnitude of stream power and shear stress in a reach.

### 6.7.2 Spatial variation of reach mean shear stress

Maximum reach mean shear stresses fell rapidly from a peak close to the source ( $140 \text{ N m}^{-2}$ ), but remained greater than  $20 \text{ N m}^{-2}$  as far as 60 km downstream: minor peaks also occurred at 115 km, 170 km and 215 km downstream (Figure 6.16). The least-squares best-fit line highlights the general decline of shear stress from the source region, although it fails to predict the considerable variation through the catchment, particularly in the elevated values through the Ironbridge Gorge (Figure 6.16).

$$\text{Maximum: } SS_{\text{fit}} = 97.50 - 1.99 DD + 0.01 DD^2 - 3E-05 DD^3 \quad (n = 225; p < 0.0001; r^2 = 0.70)$$

$$\text{Minimum: } SS_{\text{fit}} = 15.11 - 0.28 DD + 0.002 DD^2 - 5E-06 DD^3 \quad (n = 225; p < 0.0001; r^2 = 0.358)$$

This tendency for multiple shear stress peaks along the channel conforms with the findings of Magilligan (1992), although the overall magnitude of shear stresses in the Severn catchment are much greater. The incidence of floodplain inundation at the Vyrnwy confluence reach and upstream of the Ironbridge Gorge (150 - 170 km downstream) clearly resulted in a reduction of maximum levels of reach mean shear stress (as discussed above (section 6.8.1)) (Figure 6.16); this is also depicted by the reduced difference between the maximum and minimum values. Indeed, the minimum values vary more conservatively than the maximum, although the general trends are replicated to some degree. As discussed in section 6.7.2, the range of shear stresses at-a-site are perhaps indicative of channel confinement: this at-a-site range, and the spatial variation longitudinally along the channel, have important implications for the instream aquatic flora and fauna, lateral channel stability and the transport of sediment and pollutants along the channel, which will be discussed in the following chapter (7).

## 6.8 Summary

This chapter has presented the results from the 1-D simulation of a flow event along the Severn channel. The results have demonstrated both the considerable variability of channel hydraulics at-a-site and downstream, and the consistency of trends when analysed at a high spatial and temporal resolution. These trends are predominantly controlled by the spatial variation of the channel form, slope and discharge through the catchment. They have shown that the incidence of floodplain inundation has considerable impact on the temporally varied hydraulics, and that channel confinement will enhance reach-scale shear stresses and stream power. The following chapter will discuss these results and the fieldwork results presented in Chapter 4, and highlight the wider implications of this research.

## CHAPTER 7

### CONTROLS AND IMPLICATIONS OF DOWNSTREAM CHANGES IN CHANNEL HYDRAULICS

#### 7.1 Introduction

The fieldwork and modelling simulation of previous chapters identified distinct patterns of longitudinal change in channel hydraulics. This chapter has 4 main objectives: (i) to discuss the representativeness of the form and fluvial processes of the River Severn; (ii) to appraise the strengths and limitations of the modelling procedure, and gauge the applicability of the model results; (iii) to explain the spatial and temporal variation of hydraulic parameters described in Chapters 4 and 6; and (iv) to examine the implications of the results, with a particular focus on the related issues of lateral channel change, sediment transport, and stream ecology.

#### 7.2 The representativeness of hydraulic measurements in the Severn catchment

##### 7.2.1 Introduction

Before the results are discussed in later sections it is appropriate to determine: a) whether the study river was representative of other rivers in the UK and world (section 7.3.2); and b) whether the fieldwork methods (section 7.3.3) and the model design and computation scheme (section 7.3.3) were sufficiently accurate to define the ‘real’ trends and variations of hydraulic parameters along the Severn.

##### 7.2.2 The River Severn

The River Severn was originally chosen for several reasons:

- a) it is the longest river in the UK, making it ideal for examining catchment-scale downstream trends;
- b) it is comprehensively monitored in the headwaters by the IH and along the length by EA gauging stations (Figure 3.1), thereby providing both historical and ‘real time’ data throughout the catchment;
- c) previous investigations in various research areas have generated detailed information regarding the historical development, channel activity and geometry of the channel (Table 3.1);
- d) it lies close to Birmingham for rapid fieldwork reconnaissance (Figure 3.1).

However, the Severn is strongly concave by UK standards, possibly as a result of the glacial legacy which diverted the course of the river (Wheeler, 1979) (Figure 7.1). The Ironbridge Gorge also exerts a strong regional control over the channel slope and confines the channel between Ironbridge and Bewdley (Figure 6.3). Together these topographical controls appear to be significant in the spatial variation of channel hydraulics (eg: Figure 6.15): thus the question of the representativeness of the channel is appropriate.

Furthermore, intensive channel management schemes throughout this century, such as channelisation, regulation and abstraction, have had a significant impact on the river (Wood, 1987; Douglas, 1988; Higgs & Petts, 1988). The channelisation of the Severn through the middle and lower reaches (Brookes, 1982; cited in Gregory, 1987) has had a major effect on the size and geometry of the channel through ‘improvement’ schemes (ie: resectioning, realignment, regrading and tree clearance (Gregory, 1987; Lindsay, 1995)), which impact on the channel by enhancing mean stream power magnitudes by approximately 35 % and destabilising the bank material (Brown, 1987). Similarly, the Vyrnwy and Clywedog reservoirs regulate the Severn by maintaining flow levels in the lower reaches by compensation releases (Douglas, 1988). Although their combined catchment area (144.3 km<sup>2</sup>) is small in comparison with the total basin area at Saxons Lode (6850.0 km<sup>2</sup>), their effect on flow regime is significant (Higgs, 1987; Higgs & Petts, 1988).

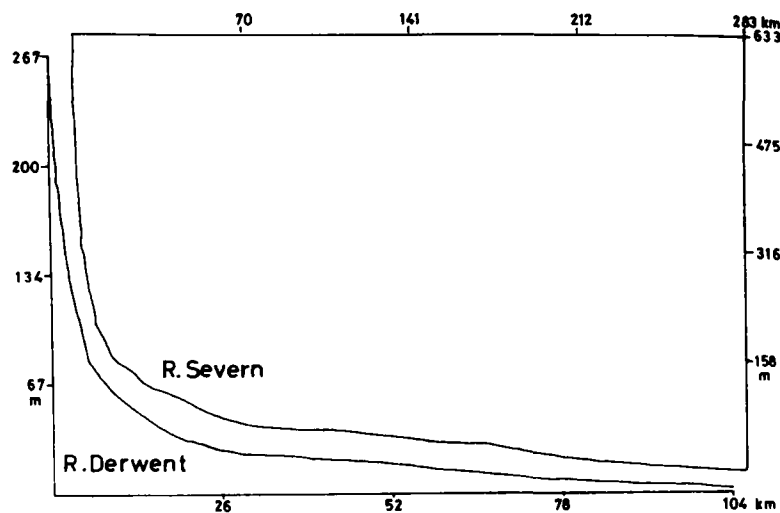


Figure 7.1 The longitudinal profile of the River Severn, and comparison with a similar longitudinal profile from the River Derwent (Wheeler, 1979, p. 252).

By concentrating on a large river at a catchment-scale, it is clear that evidence of anthropogenic interaction will be prevalent. It is believed that the advantages of comprehensive flow monitoring, previous research and proximity out-weigh the impact of flow regulation and channelisation in the middle and lower reaches. Therefore, the results from this study do not represent a wholly natural system, but given the difficulties of finding a large natural basin within the UK, they are considered suitable for this downstream analysis of channel hydraulic parameters.

### 7.2.3 Fieldwork study: techniques and results

The number and spacing of study sites and the frequency of visits were limited by time, resources and safety constraints; hence, sufficient sites were chosen to offer a complete coverage of the catchment at an adequate spatial resolution. Some scatter associated with spatial hydraulic variability may therefore be

attributable to the complexities of site selection, such as the location within the pool-riffle unit. Also, straight, uniform reaches possibly underestimate the actual magnitude and variability of flow variables in meandering and irregular reaches. The flow categorisation scheme covered a range of flows comparable in magnitude along the channel, up to the limits of the flow measurement capabilities. The variety of measurement techniques selected demonstrate that a balance between the resources, access, safety, flow magnitudes and the spatial extent of the study was difficult to achieve.

The field and modelling results (Chapters 4 and 6) revealed that some sites were not representative because of their close proximity to hydraulic jumps (eg: Upper Hafren 3 (Plate 7.1)) or pools (eg: Tanllwyth (Plate 7.2)). Bathurst (1977, 1982, 1988) and Hey (1979) highlight the difficulty of measuring discharge and other hydraulic parameters in headwater channels where turbulent flow and the irregular channels develop from high channel slopes, low relative depths and large obstacles. Similarly, Hey (1979), Beven and Carling (1992), Carling and Wood (1994) showed that flow hydraulics vary both within and between pool - riffle units, in response to the changing topography and roughness of the bed. Indeed, Carling and Wood (1994, p. 330) observed that ‘slight change in the location of any test section within a pool-riffle reach may induce a notable change in form of the shear velocity - discharge function and consequently in the delineation of any threshold discharge competent to move sediment’ The reach-scale variation of hydraulic parameters was measured at Tanllwyth under a low-flow condition. Figure 7.2 illustrates how the topographic control of the riffles, at 12 m and 35 m downstream, increase the local slope and shear stress and decrease the hydraulic radius and width. The position of the study section clearly produced different hydraulic results in the pool than over the riffle. These issues have clear implications for the representation of flow hydraulics in a reach and the associated magnitude of error.

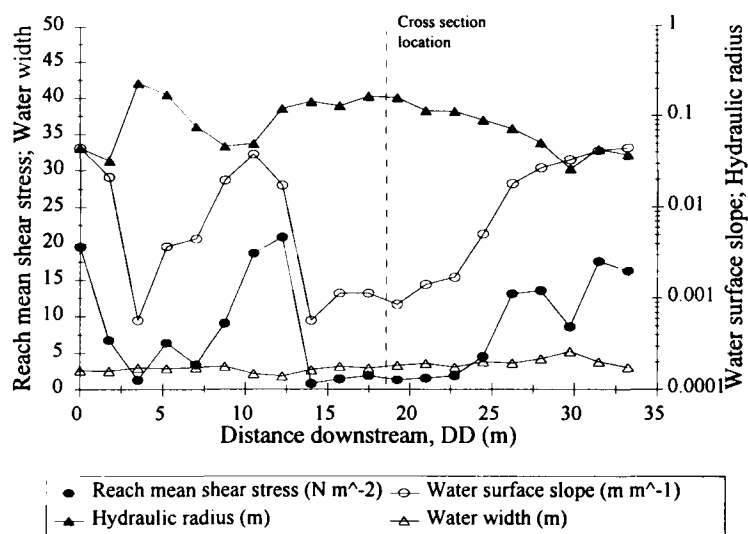


Figure 7.2 The reach-scale variation of several hydraulic parameters along the study reach at Tanllwyth ( $Q = 0.009 \text{ m}^3 \text{ s}^{-1}$ ). This illustrates the significance of the cross section location within the pool-riffle unit.

#### 7.2.4 Model simulation: techniques and results

MIKE11 successfully simulated channel hydraulics along the Severn, although the accuracy of the simulation was restricted by the topographic representation of the channel (space step = 1 km), the 1-D computation, validation by a single flow event, and the omission of bridges and bars. The 1 km space step was a convenient solution to computational constraints in the model and the representation of an irregular channel geometry. The topographic scheme in the model assumed each section was representative of the reach. However, Figure 7.2 demonstrates that no section may be truly representative of a reach, though a multiple-section approach (eg: Jarrett, 1984) may reduce inaccuracies inherent in the single-section technique. Similar applications of spatial sampling exist in bed material sampling (Church *et al.*, 1987), bank erosion monitoring (Lawler, 1993) and terrain analysis (Lane *et al.*, 1994), where consideration of local point-scale inaccuracies are balanced against the scale of the analysis in order to achieve a suitable measurement resolution.

Channel adjustment following the 1976 survey of the Severn may explain some deviation between the model results and the 1994-6 field results. Nevertheless, a comparison with two surveyed study sections at Abermule and Bewdley revealed little change over time at these sites (Figure 7.3). Indeed, the most active reach of the Severn (Llanidloes - Newtown (Lewin, 1987)) was surveyed in 1996 for this study; this included 14 sections surveyed along the 30 km reach between Llanidloes and Abermule.

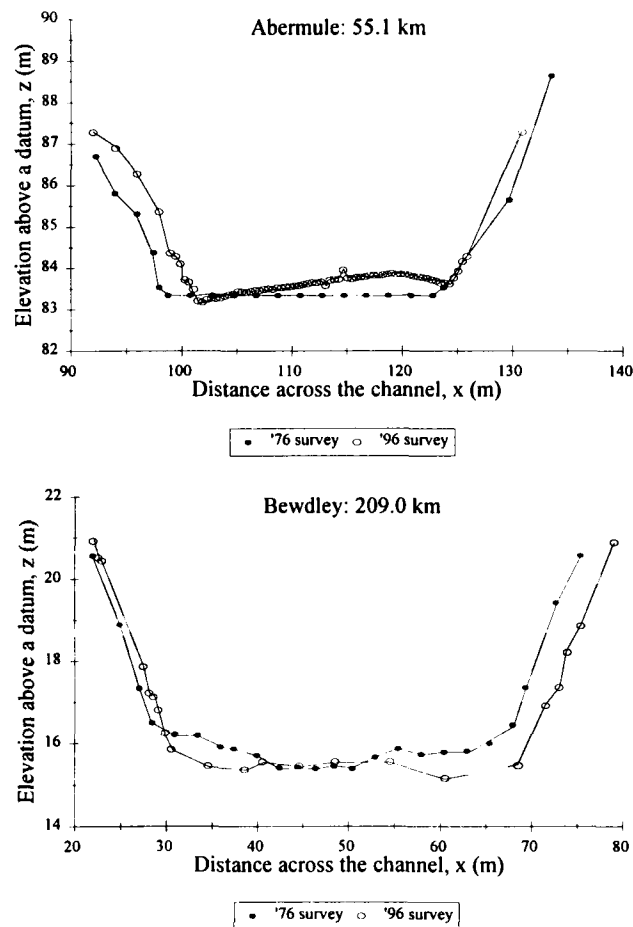


Figure 7.3 A comparison between the EA cross section data (surveyed in 1976) and the field survey (1995) at: a) Abermule; and b) Bewdley.



Plate 7.1 A hydraulic jump situated upstream of the study section at Upper Hafren 3.



Plate 7.2 The study section at Tanllwyth, located centrally over a pool.

The 1-D simulation excluded secondary flow effects. Thus the longitudinal variation of vertical and lateral components in flow velocity which are important in the selective erosion, transport and deposition processes were not represented. Instead, the intra- and inter-reach-scale hydraulic variations were represented by section mean velocity and flow resistance, and reach mean shear stress and stream power. This was believed to be a satisfactory compromise at this scale of enquiry provided the water surface slope were accurately simulated, and the geometry and spacing of sections was precise (eg: Bridge & Jarvis, 1977; Magilligan, 1992). However, as section 5.4.6 highlighted, there was some inconsistency between reach lengths in the field study and thus in the model: the potential effect of this error is discussed further in the following section (7.3).

The February 1989 flow event simulated was generally typical of events along the Severn in terms of origin (Bull, 1996) and form (McCarthy & Naden, 1995). The magnitude was comparable to the flows examined in the field study and attained an approximate bankfull limit throughout most of the catchment. A bankfull flow is commonly assumed to represent a flow which achieves the most work in terms of sediment transport and channel erosion (Wolman & Miller, 1960); hence, though only one event was simulated, it was considered a suitable example for the more detailed study of downstream change of channel hydraulic parameters. Other Severn events are compared in section 7.4.

### **7.3 Issues of model validation**

#### *7.3.1 Introduction*

The aim of the model design and parameterization stages discussed in Chapter 5 was to replicate the channel topography and hydraulic variability of the Severn and complement the field results measured at a limited number of sites and flow levels. This section will compare the methodologies of these studies, and discuss the relative success of the validation experiment (section 5.4.6). Two possible reasons for simulation inaccuracies were: a) the reach lengths differed between the field and model calculations (section 7.3.2); and b) the model failed to adequately represent the variability of channel roughness in space and time (section 7.3.3). An understanding of these issues is critical before the model results can be correctly interpreted.

#### *7.3.2 Disparity between field and model reach lengths*

Reach mean estimates of flow resistance, shear stress and stream power were calculated from water surface slopes measured along a reach, defined by 5 - 10 channel widths (pool-riffle unit (Keller & Melhorn, 1978)). Simulated slopes at the section ( $y = x$  km downstream) were calculated from the difference between the water elevation at the adjacent sections ( $y = (x - 1$  space step) and  $y = (x + 1$  space step)). A section spacing of 1 km therefore generated a simulated reach length of 2 km. In the upper reaches, the simulated slope (reach length  $\leq 2$  km) greatly exceeded the measured slope (10 - 50 m). The predicted shear stress and stream power values in Figures 5.18 and 5.15 were therefore larger than those measured in the field, as the valley slope greatly exceeds the reach slope. Further downstream, the difference between the measured and simulated reach lengths declined as channel width increased, corresponding to a greater agreement between field and model results. However, this theory fails to fully explain the anomalous results at

Bewdley and Saxons Lode at low flow, and considerable under-prediction at sites between Pool Quay and Buildwas under high flows (section 5.4.6); this will be discussed in the following section.

The lateral (eg: meanders) and longitudinal (eg: pool-riffle) variations in the water elevation generated by bed irregularities modify the large-scale topographical control exerted by the valley slope. In order to appreciate this control which varies in dominance through the system, the elevation of the bed was calculated using measured water surface slopes at each study site and the elevation of the channel at the source.

$$\text{Elevdiff}_1 = - \left[ S_w \cdot \left( \frac{y_1 + y_2}{2} - \frac{y_0 + y_1}{2} \right) \cdot 1000 \right] \quad [7.1]$$

$$\text{Elev}_{y+1} = \text{Elev}_0 + \text{Elevdiff}_1 \quad [7.2]$$

where,  $\text{Elevdiff}_y$  = Difference in water surface elevation between the study sections,  $y_0$  and  $y_1$   
 (km downstream)  
 $\text{Elev}_0$  = Water surface elevation at the first study section (m)  
 $\text{Elev}_1$  = Water surface elevation (m)  
 $y_1$  = Chainage at study section number 1 (km)

Figure 7.4a shows that the actual and predicted longitudinal profiles differ greatly, and a comparison between the residuals in Figure 7.4b reveals 3 distinct zones along the channel. In the headwaters (A), the water surface slope roughly approximates the valley slope (Figure 7.4a), yielding a residual elevation of < 20 m (Figure 7.4b). Through the steep upper-middle reaches (Plynlimon - Newtown) (B), the reach slope is reduced at the study sections as sites are positioned predominantly over pools (Figure 7.2); this thereby increases the difference between water surface slope estimates of elevation and the actual elevation, and yields greater simulated reach mean shear stresses (Figure 7.4b). Further downstream (C), the water surface slope exceeds the low-gradient valley slope because pool-riffle units and form roughness increase the reach slope, and therefore the simulated parameters more closely approximate the field measured parameters (Figure 7.4b). This example raises an important question for future investigations regarding the reach length over which the water surface slope and hydraulic conditions can be accurately measured.

### 7.3.3 Representation of roughness in the model

The EA dataset contained composite Manning's  $n$  values for each section which were carefully calibrated against measured flows and define the channel bed, bank and floodplain roughness separately (Section 5.4.2). Figure 7.5 demonstrates that the inter-reach variability is low, but large-scale changes in roughness, and therefore channel form, are well represented, particularly between 70 km to 115 km and around the Ironbridge Gorge (160 - 210 km). It also appears that bed, bank and floodplain  $n$ -values at-a-site are similar. However, a comparison between field measurements of roughness and model bed roughness from sites containing a complete low-, medium - and high-flow dataset in Figure 7.6 reveals that roughness varies by up to one order of magnitude with stage in natural channels, and therefore only the measured high-flow  $n$ -values closely correlate with the model  $n$ -values. The actual difference between the measured mean  $n$ -values and the simulated bed mean  $n$ -value is only 0.005 and the magnitude of one standard

deviation is comparable. These results suggest that the EA  $n$ -values are a fair approximation of reality, although the limited variation with stage (Figure 7.5) suggests that their calibration exercise was perhaps made against flood flows and not against a range of flows. Consequently, incorrect roughness approximations, which are particularly difficult to evaluate in the upper reaches at low-flows, may limit the representation of stage simulated in the model.

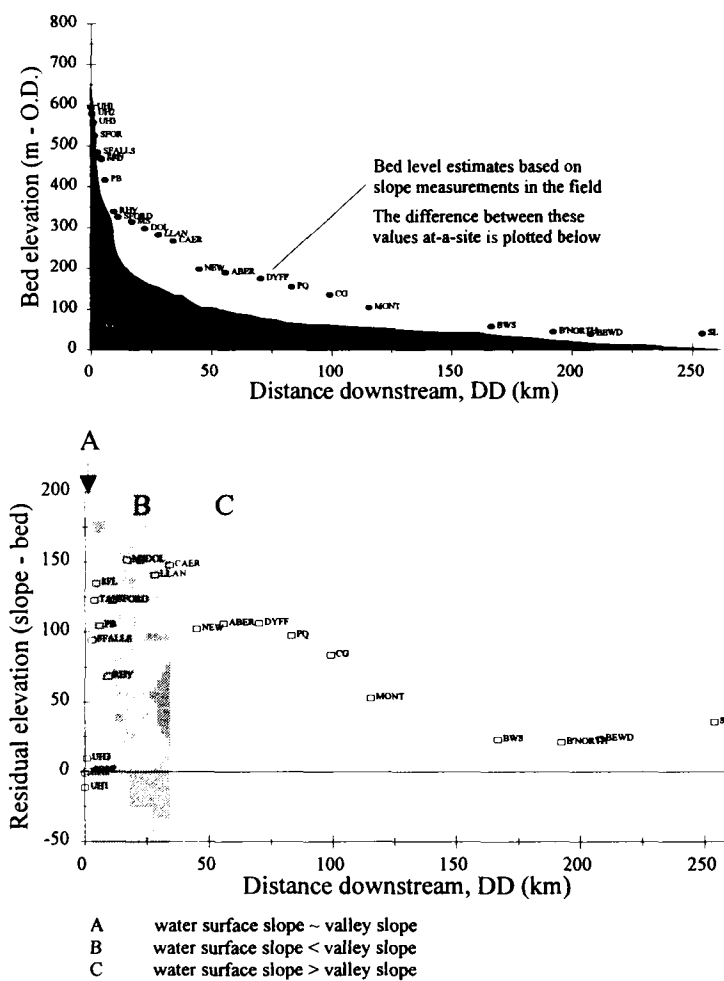


Figure 7.4 An evaluation of the influence of reach length on the determination of water surface slope, showing a) the difference between bed elevations and elevation derived from slope calculations, and b) the residual slope elevation. This shows a distinct spatial trend in the representation of slope along the channel.

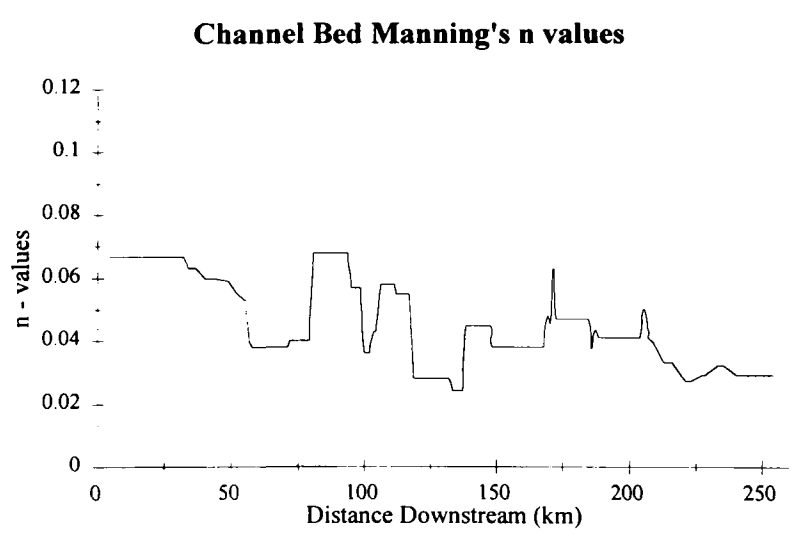
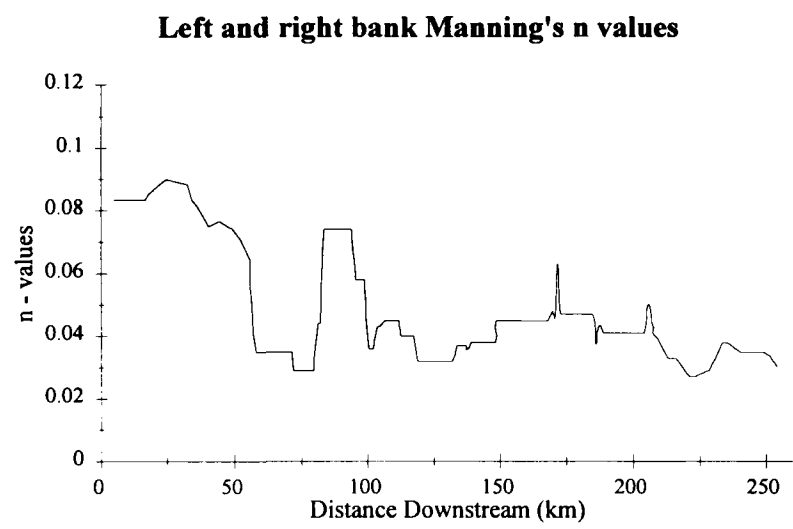
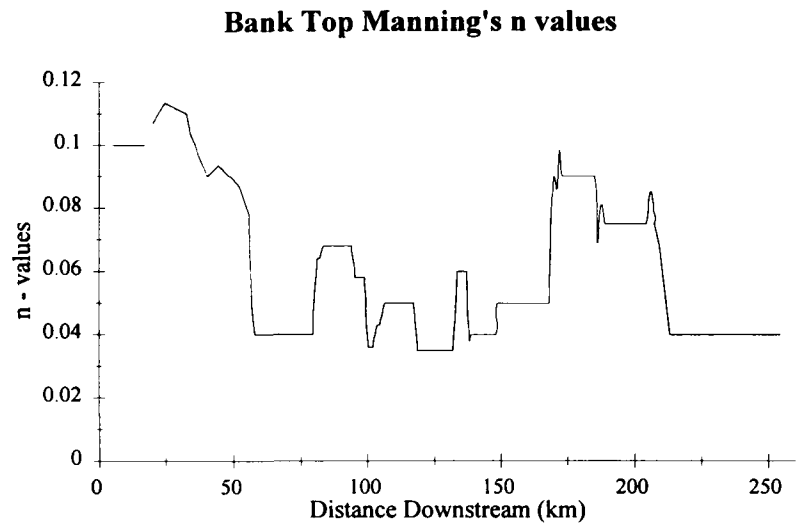


Figure 7.5 The downstream variation of Manning's  $n$ -values used in the model to simulate the bank top, bank and bed roughness.

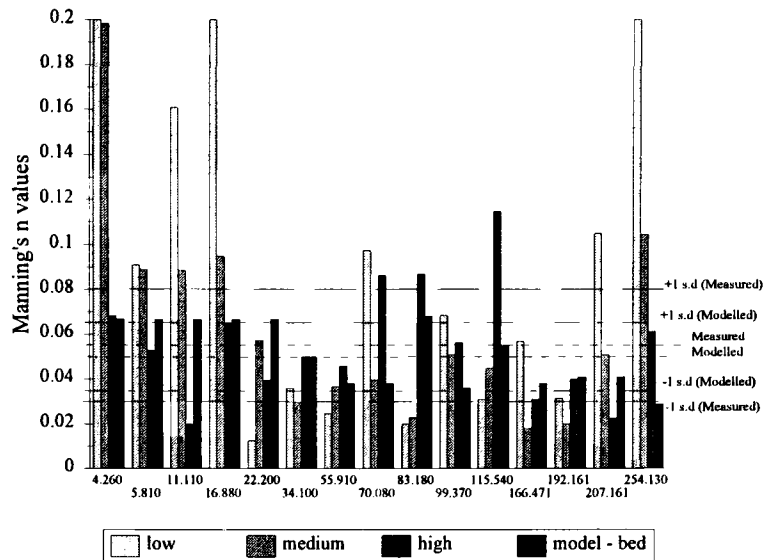


Figure 7.6 A comparison between roughness coefficients measured in the field and simulated in the model at complementary sites which have a complete low-, medium- and high-flow record. The mean and standard deviations of the two datasets are included

MIKE11 does not simulate stage-varying roughness at a section. In reality, the interaction between flow and the channel boundary components (sand, pebbles and boulders; vegetation; irregular bank surfaces; non-uniform planform) results in a complex downstream variation of roughness with stage (Bathurst, 1993). This has important implications for the prediction of sediment transport in natural channels, ie: 'efficiency in the entrainment process is related not only to the over-all channel geometry and distribution of roughness type across the active bed but also varies as a function of discharge as the proportion of various bank roughness elements submerged in the flow alters' (Carling, 1983; p. 16).

In Figure 7.7a, roughness is inversely proportional to stage at the sites indicated. This relationship is typical of most channels where large bed roughness elements are drowned out as stage increases, thus reducing the roughness and turbulent energy dissipation (Bathurst, 1993). For most of the channel (70 %), however, the high-flow roughness component increases significantly (Figure 7.7b), representing the traditional stage-roughness relationship (Figure 7.7a) (Chow, 1959). It is possible, therefore, that enhanced roughness at high flows in the middle reaches of the Severn are caused by a combination of high channel sinuosity (Figure 4.3) and the presence of bank vegetation (Plate 7.3). The former may be attributable to increased energy dissipation rates as the channel follows a tortuous flow path and impacts upon oblique and irregular channel banks (eg: Caersws & Pool Quay) (Plate 4.4). The latter may be the result of drag exerted by trees and bushes, which increase turbulent mixing in the water through the interaction between laterally varied flow velocities between the thalweg and backwater pools (Knight, 1989; Beven & Carling, 1992; Carling & Wood, 1994). These examples demonstrate the importance of representing the channel roughness accurately and recognising the significance of stage.

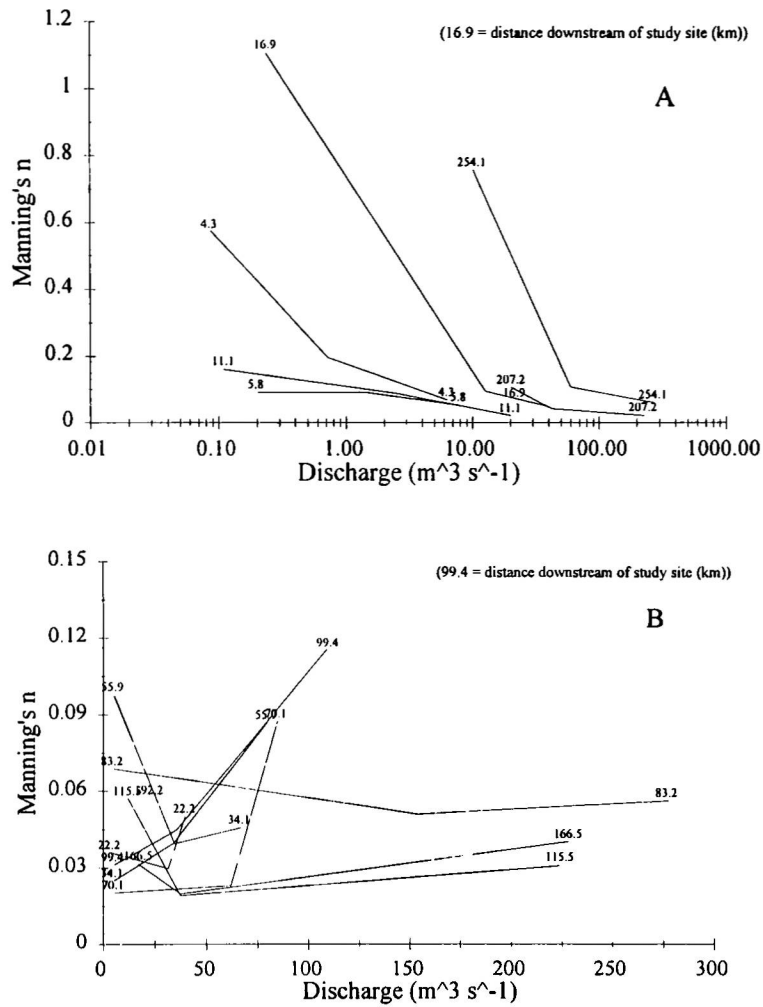


Figure 7.7 The relationship between roughness and discharge. (a) represents sites which exhibit an inverse relationship, and b) represents those sites where a positive or unclear relationship holds.

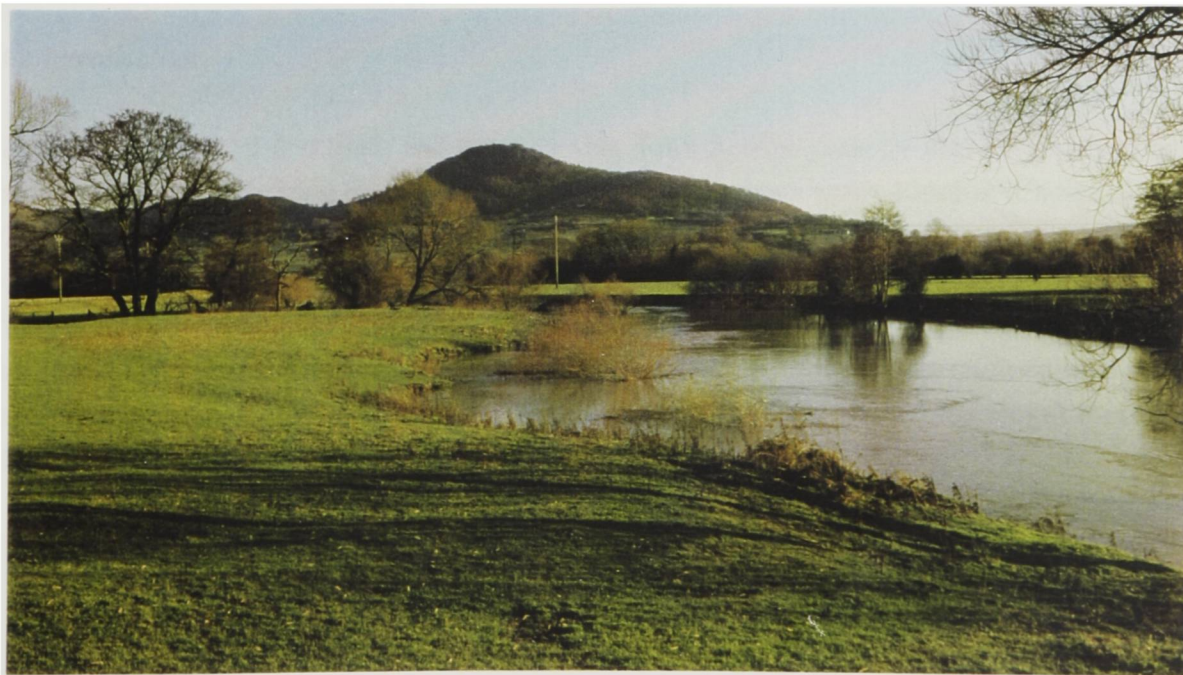


Plate 7.3 The presence of vegetation on the upper bank acts as an additional roughness element at high flows.

### *7.3.4 Accuracy of the model simulation*

It has been proposed that the non-compatibility of the reach lengths and the inaccurate representation of roughness may explain some inconsistencies between the two data-sets at high flows (section 5.4.6). Over-bank flow was poorly simulated in the model calibration and therefore the accuracy of floodplain storage and the attenuation of the floodwave at peak flow was reduced (peak discharge simulated to within  $20 \text{ m}^3 \text{ s}^{-1}$  (section 5.4.5)). Furthermore, the lack of understanding of mechanisms of floodplain flow in 1-D, 2-D and 3-D models, and known complications in the flow routing at the Vyrnwy confluence (Lindsay, 1995) restricts the parameterization of such flows (Knight & Demetriou, 1983; Knight, 1989; Wolff & Burges, 1994). Hence, the flow event adopted in this study was considered a sufficient magnitude to represent a significant flow, but which minimised the scale of floodplain inundation.

Notwithstanding these limitations, the results indicate that the model can accurately route flows along the Severn up to a bankfull limit: above bankfull, the model requires detailed floodplain geometry and boundary roughness information which is not available in an adequate form at present. Furthermore, the field and model trends described in Chapter 6 demonstrate the possibility for delineating geomorphic controls on downstream hydraulics. The magnitude of the predicted channel hydraulic parameters was generally accurate to within a factor of 2 and were achieved at a spatial scale far greater than field reconnaissance would permit. This is less accurate than reach-scale analyses by Carling and Wood (1994), for example, but it demonstrates the predictive capability of the model. The high temporal resolution also enables hydraulic processes associated with unsteady flows and floodwave movement to be analysed (section 7.4). Hence, the advantages of the detailed spatial and temporal data complement the more reliable field data; moreover, the similarity between the two data-sets, spatially and temporally, reinforces the confidence which may be given to the interpretation of the results.

## **7.4 Dynamics of floodwave propagation**

### *7.4.1 Introduction*

It is generally accepted that time- and space-varying flows in river channels may be greatly simplified in terms of mean flow velocities, depths and storage in one downstream space direction (Chow, 1959; Abbott, 1979). This section will examine the dynamics of floodwaves in natural channels and compare the manner by which these processes are simulated in 1-D models. For this investigation, the results from the modelling of the February 1989 event are analysed together with a selection of flow events of varying magnitude from the Severn. The purpose of this section is therefore to: a) examine the controls on floodwave velocity and shape; b) explain the spatial variations of hydraulics (eg: mean velocity and discharge) measured in the field; and c) demonstrate the representativeness of the February 1989 flow event.

#### 7.4.2 Mechanisms of floodwave propagation

The spatial variability of runoff in a catchment, and floodwave development, results from the non-uniform distribution of precipitation, relief, network topography and antecedent conditions (Calver *et al.*, 1972; Beven & Kirkby, 1979). The wave is transported downstream under the influence of gravity, at a velocity (or wave velocity) which generally exceeds the mean flow velocity of the channel (Chow, 1959). Although the form of the wave is dependent upon the timing and magnitude of inputs, channel and floodplain form, and roughness (boundary and channel) (Wolff & Burges, 1994), little attention has been paid to the detailed variation of hydraulic parameters associated with these controls, both spatially and temporally, in the channel.

The temporal transformation of the four components of the momentum equation (equation 7.3) during the February 1989 event are represented in Figure 7.8.

$$S_0 = S_f^{(1)} + \frac{\partial h^{(2)}}{\partial y} + \frac{u}{g} \frac{\partial u^{(3)}}{\partial x} + \frac{1}{g} \frac{\partial u^{(4)}}{\partial t} \quad [7.3]$$

where,

- $S_0$  = bed slope ( $\text{m m}^{-1}$ )
- $S_f$  = friction slope ( $\text{m m}^{-1}$ )
- $\partial h$  = difference in elevation between adjacent cross sections (km)
- $\partial y$  = distance between adjacent cross sections (m)
- $\partial u$  = difference in mean velocity between adjacent cross sections ( $\text{m s}^{-1}$ )
- $\partial t$  = time difference between model computation (s)

Figure 7.8 illustrates the spatial variation of each component over four time periods during the event. The high spatial resolution shows how the friction slope <sup>(1)</sup> and bed slope gradient <sup>(2)</sup> terms have consistent distributions and magnitude for the six example time periods: ( 1) 0900, 16 February; 2) 0900, 18 February; 3) 1500, 18 February; 4) 2100, 18 February; 5) 0900, 19 February; 6) 2100, 20 February) and appear to control the transport and shape of the wave through the upper reaches (Figure 7.8a & b), where the channel is steep and confined (note the difference in scale); here the kinematic wave would provide an approximation to the wave solution. The weirs at Worcester increase the slope of the bed and friction slope as the floodwave flows over them. The Flood Studies Report, volume 3, by NERC (1975, p. 4) stated that the advection <sup>(3)</sup> and acceleration <sup>(4)</sup> terms may be ignored unless the channel was steep. These results show that the advection <sup>(3)</sup> and acceleration <sup>(4)</sup> terms are an order of magnitude smaller than the friction <sup>(1)</sup> and bed <sup>(2)</sup> slopes, in agreement with NERC (1975). The results demonstrate that the acceleration term appears to reflect the interaction between the wave and the irregular channel geometry (Figure 7.8c), particularly through the vertically incised channel between Dyffryn (70 km) and Pool Quay (85 km) which experiences exaggerated flow acceleration and deceleration; this is possibly caused by greater channel conveyance efficiency (Wyzga, 1996). Downstream changes in slope and channel size have little impact on the magnitude of acceleration, although this may reflect the comparability in scale between the flow magnitude and channel size in any reach through the catchment. The advection term is more variable between sections (Figure 7.8d), resulting from changes in the acceleration of the water between reaches, caused by irregularities in the channel topography, and hence flow velocity, downstream, as discussed in

section 6.2 and 6.3. The magnitude of the variability is greater through confined reaches (eg: Ironbridge Gorge, 160 - 210 km), possibly caused by enhanced mean velocities through these reaches.

Friction induced by a non-uniform channel geometry and planform, and floodplain inundation modifies the hydrograph shape and peak discharge (Burkham, 1976; Hughes, 1980; Archer, 1989; Wolff & Burges, 1994; Woltemade & Porter, 1994; Wyzga, 1996). In-channel flow is dominated by topographic and roughness variations which induce some flow retardation and wave attenuation, although lateral inputs dominate wave transformations (Reid *et al.*, 1989). However, an example of a floodwave on the Severn from September 1994 (Figure 7.9a) shows how the wave form may remain fairly constant whilst travelling downstream, despite considerable inputs from tributaries if: a) the precipitation event is isolated in one region of the basin; b) the event is uniform throughout the basin; or c) no storage, or temporary retention, occurs on the floodplain. These hydrographs were derived from discharge data recorded at six gauging stations along the Severn at 15-minute intervals; they represent a range of event magnitudes which occurred during the study period.

As the flow over-banks, floodplain conveyance simulation becomes a significant problem (Knight & Demetriou, 1983) (section 5.4.5). Rashid and Chaudry (1995) suggest that 2-stage flow modelling must therefore limit conveyance on the floodplain by increasing storage and roughness. A comparison between their data (Figure 7.10a) and the model calibration curve for Bewdley (Figure 7.10b) shows that when storage and recharge of flow are poorly represented, momentum flux over the section distorts the simulated hydrograph. Hence, the peak discharge is accentuated (Archer, 1989; Rashid & Chaudry, 1995) and the flow velocity on the floodplain is increased. In natural systems, this effect is limited by the dissipation of kinetic energy at the zone of mass transfer on the channel-floodplain boundary (Bhowmik & Demissie, 1984; Knight, 1989) which at present cannot be represented in 1-D models. In the following section, the manner in which the channel hydraulics respond to the spatially varied topographic controls and lateral inputs, under temporally-varied flow conditions, is discussed. This begins with an analysis of channel form and roughness on the propagation of the floodwave (section 7.4.3), and is followed by an examination of the influence of flow magnitude on these trends (section 7.4.4). This represents an important link between channel hydraulics, sediment transport, channel stability and flood events.

#### 7.4.3 Impact of channel form and roughness on floodwave properties

In the following discussion, the mean wave peak velocity (defined here as the mean velocity of the discharge peak between continuously monitoring gauging stations on the Severn) and peak discharge are used to define the hydraulic properties of the wave. Mean wave peak velocity,  $U_{wp}$  is calculated from the distance between gauging stations,  $\delta y$  and the time difference between peak discharges,  $T_p$ .

$$U_{wp} = \frac{\delta y}{\delta T_p} \quad [7.4]$$

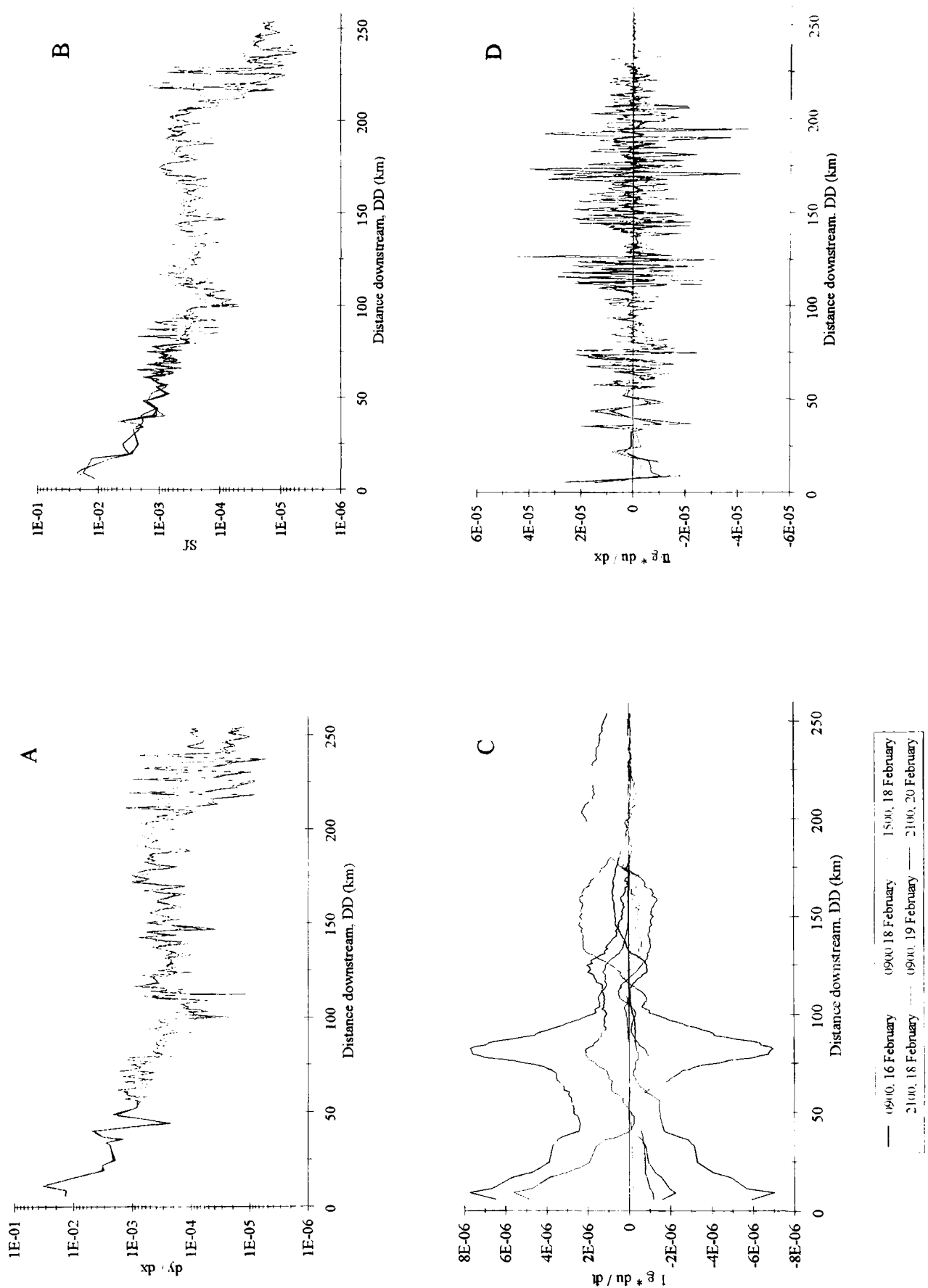


Figure 7.8 The spatial pattern of the momentum equation components at selected period during the simulated February 1989 event (at 1) 0900, 16 February; 2) 0900, 18 February; 3) 1500, 18 February; 4) 2100, 18 February; 5) 0900, 19 February; 6) 2100, 20 February); these represent the downstream variation of: a) the water surface slope,  $\partial y / \partial x$ ; b) the friction slope,  $S_f$ ; c) the acceleration of the wave,  $1/g \partial u / \partial t$ ; and d) the advection of the wave,  $\bar{u} / g \partial u / \partial x$ .

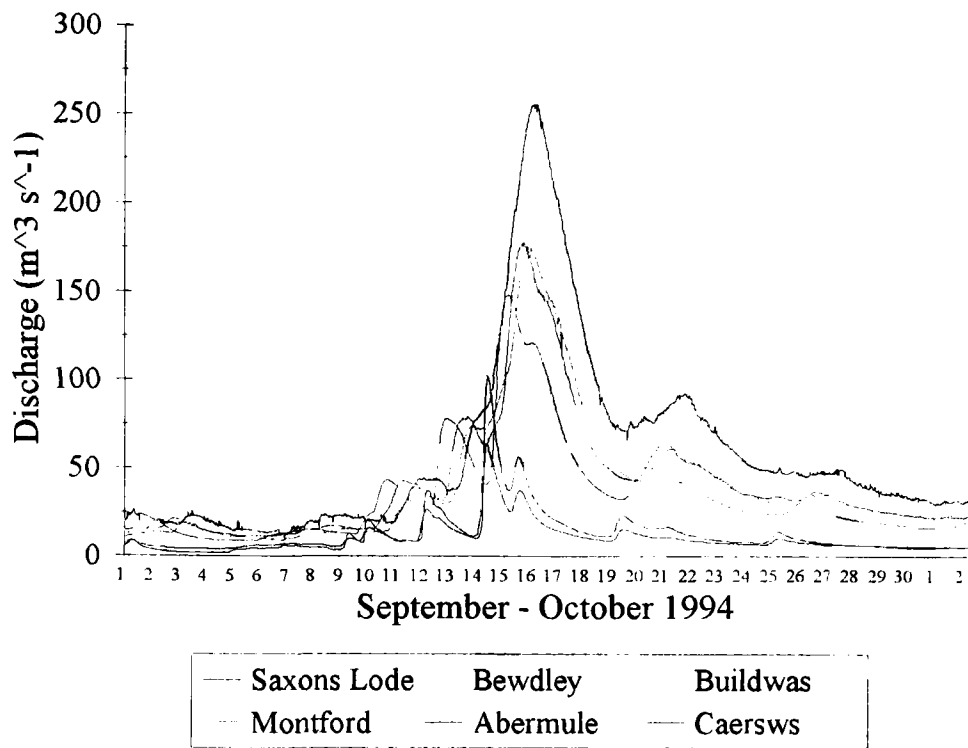


Figure 7.9a The downstream transformation of a flow event along the Severn channel in September 1994.

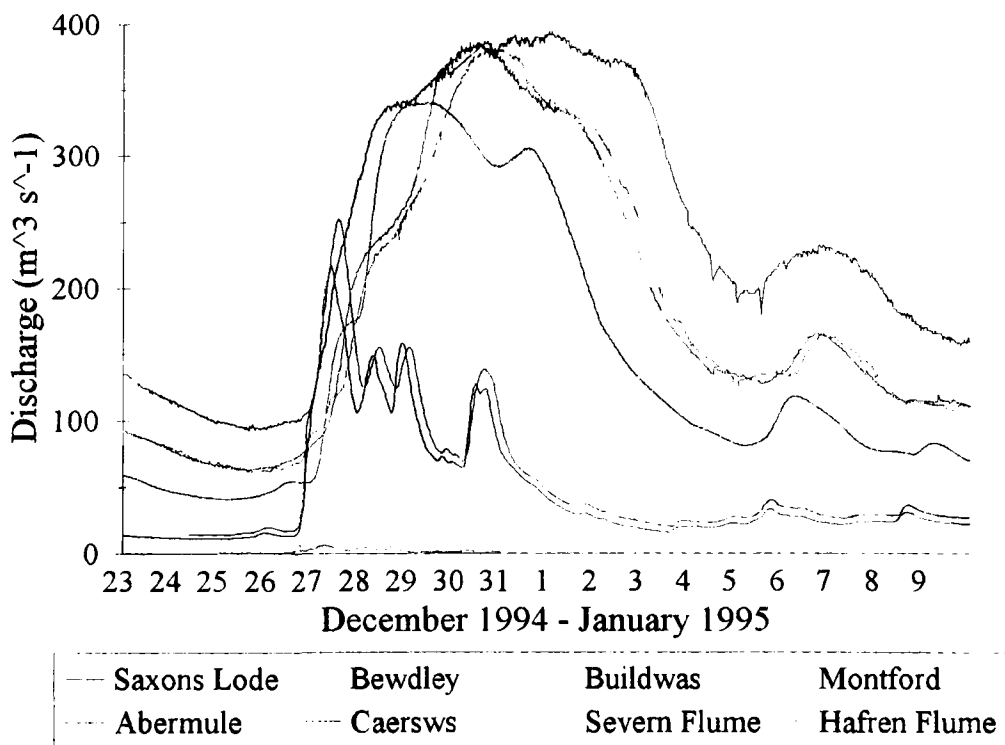


Figure 7.9b The downstream transformation of a flow event along the Severn channel in December 1994

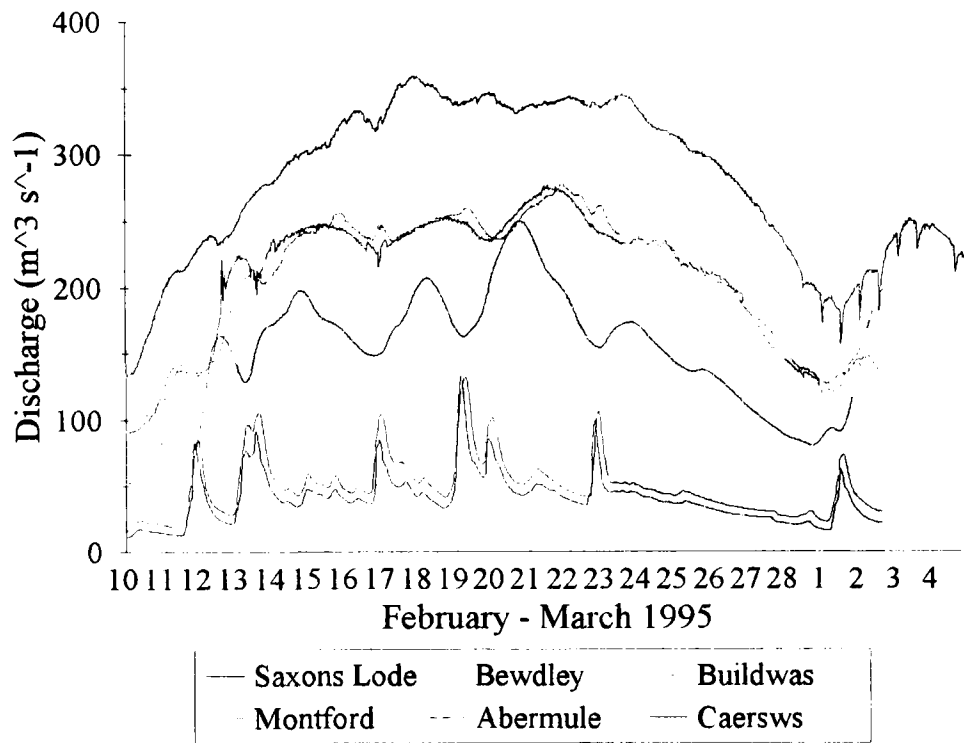


Figure 7.9c The downstream transformation of a flow event along the Severn channel in February 1995.

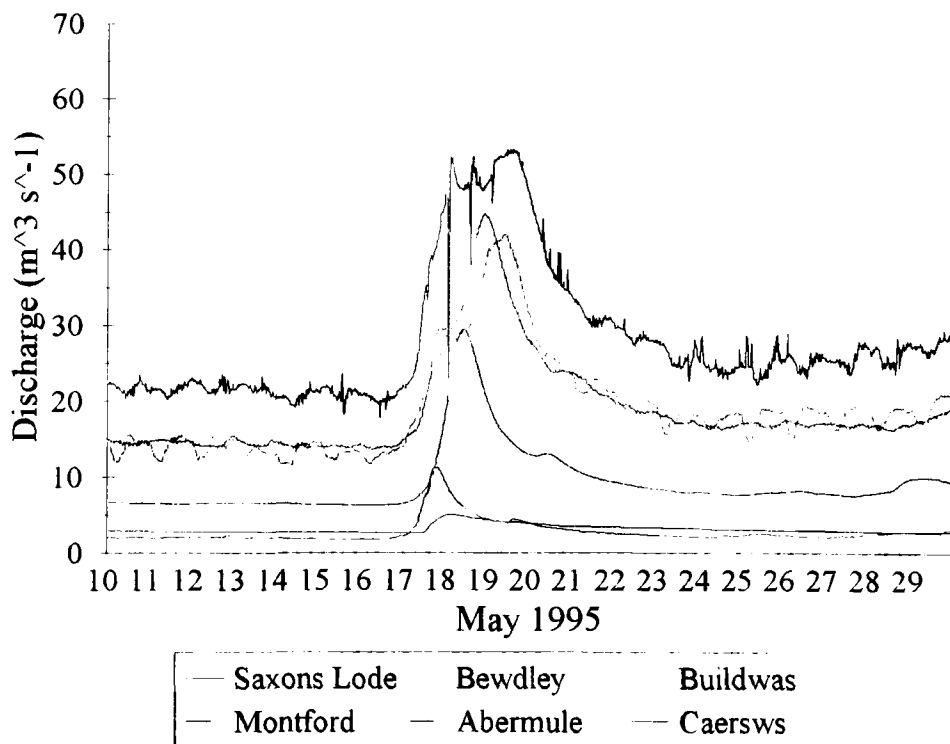


Figure 7.9d The downstream transformation of a flow event along the Severn channel in May 1995.

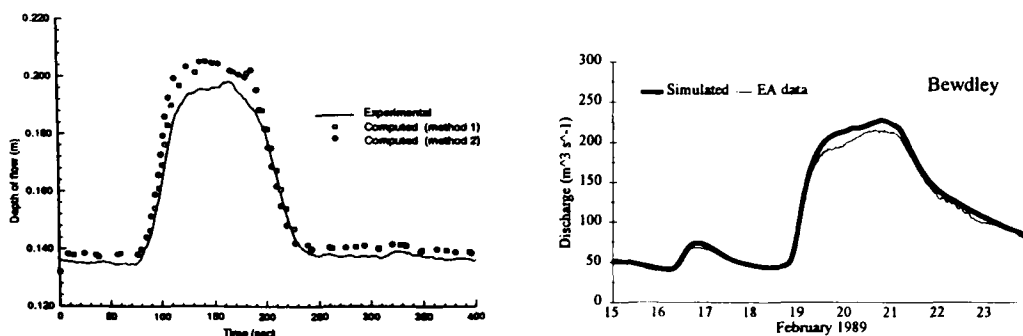


Figure 7.10 A comparison between a) the Rashid and Chaudry (1995) laboratory study of over-bank flow and b) the calibration curve for Bewdley (model simulation vs. EA measured flow). The model simulation in both cases over-predicts the depth and magnitude of flow, caused by the inadequate representation of roughness and storage on the floodplain. Note the difference between the time scales and parameters on the x- and y-axes.

The velocity of the wave falls to a minimum (approximately  $0.5 - 1.0 \text{ m s}^{-1}$ ) through the Abermule - Montford and Montford - Buildwas reaches for all the selected 9 flood flows (Figure 7.11). This coincides with reaches prone to floodplain inundation close to Pool Quay (Hey, 1979), at the Vyrnwy confluence (Lewin, 1989; Lindsay, 1995) and upstream of Buildwas (Brown, 1987) as discussed in sections 6.4.1 and 6.4.2; furthermore, channel sinuosity is high in these particular reaches (Figure 4.3). Therefore, as the flow begins to over-top the banks, the floodplain flow component travels at a lower mean velocity on account of high boundary roughness (Bhowmik & Demissie, 1982; Wolff & Burges, 1994; Wyzga, 1996), as described in sections 6.6.1. Also, lateral momentum transfer from the main channel component (Knight, 1989), reduces the overall mean velocity of the flow and peak discharge, and temporary storage on the floodplain will attenuate the hydrograph (Figure 7.9d) as observed at Montford (section 6.4.1). The consistency of this downstream trend (Figure 7.11), and the enhanced wave peak velocities through the steeper and more confined channel reaches (Caersws - Abermule; Buildwas - Bewdley) emphasise the relationship between floodwave attenuation and roughness, caused by either: a) floodplain flow; or b) high channel roughness induced by vegetation and / or channel sinuosity (Wyzga, 1996). When the flow remains in-bank the wave retains the kinematic, or uniformly progressive (Burkham, 1976), wave form of the September - October 1994 event (Figure 7.9a) and flows at higher flow velocities than the over-bank flow of December 1994 - January 1995 (Figure 7.9b), or February 1995 (Figure 7.9c).

These results have important implications for channel stability and sediment transport. The former is influenced by variations in the period of wetting by the flow as the wave attenuates downstream (Lawler, 1992) and the changing magnitude of hydraulic stress induced by the flow through different channel geometries (Carling, 1983). Similarly, changes in the velocity of the wave may affect the velocity of the sediment wave (Bull, pers comm.) and therefore, the redistribution of sediment in the catchment.

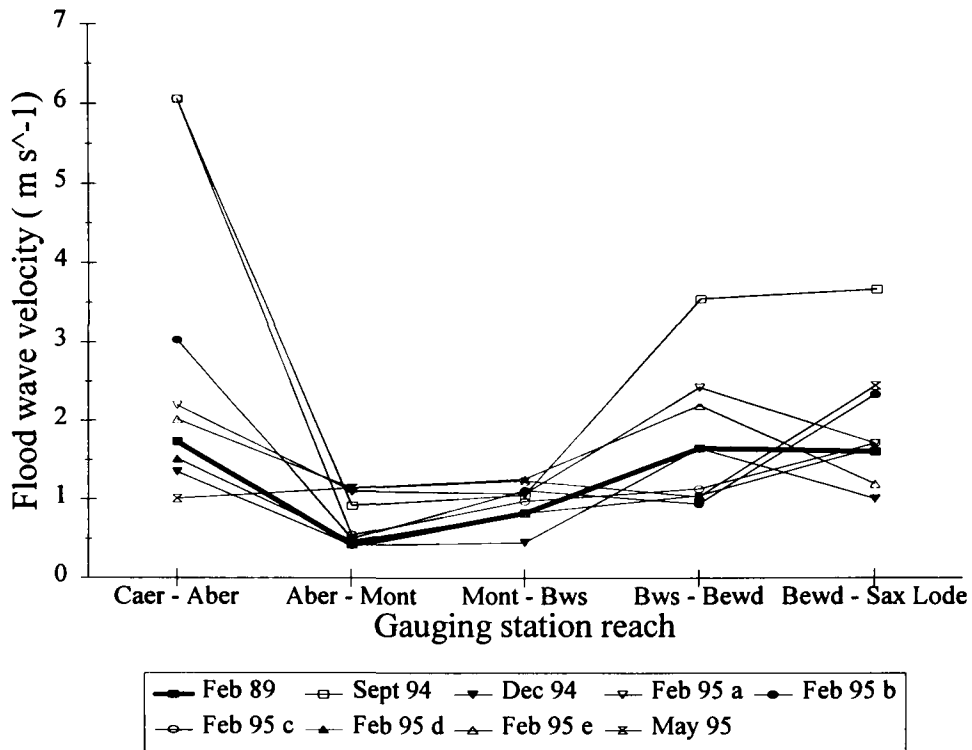


Figure 7.11 Downstream variation in the mean wave peak velocity of the floodwave between EA gauging stations for 9 events between 1989 - 1995.

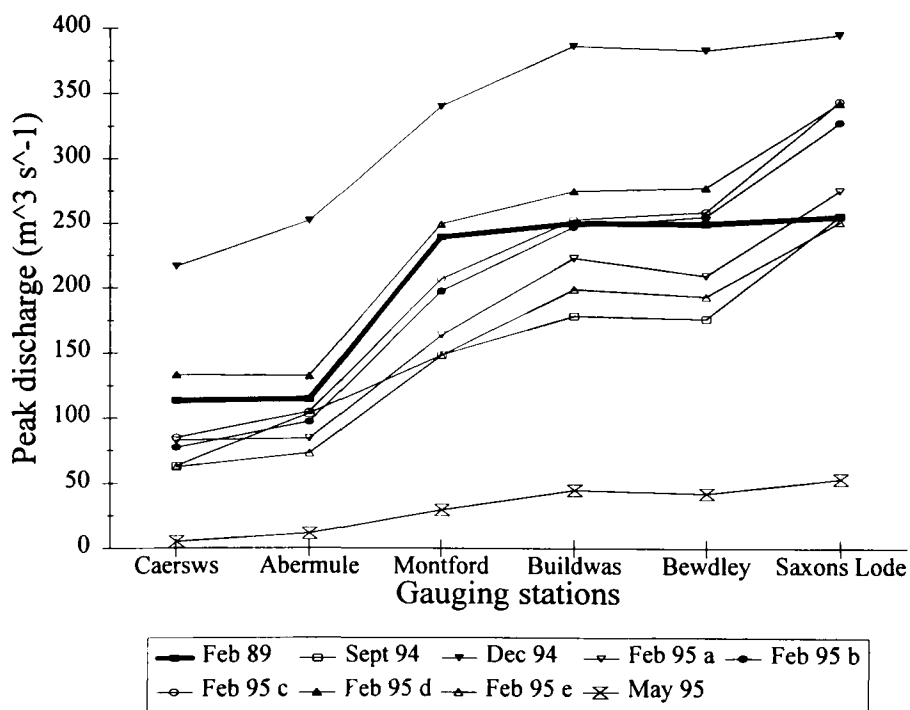


Figure 7.12 Downstream variation of peak discharge measured at EA gauging stations for 9 events between 1989 - 1995.

#### *7.4.4 Impact of flow magnitude on floodwave properties*

Figure 7.12 demonstrates how events of lower peak discharge (and magnitude) (eg: September 1994) tend to produce greater wave peak velocities (Figure 7.11). Conversely, the December 1994 event generated lower than average wave peak velocities (Figure 7.9b) along the Severn, despite having a greater magnitude (Figure 7.12). This illustrates how the magnitude of the event may modify the velocity of the wave through the interaction between the channel and floodplain. This may also provide some empirical justification for the magnitude-frequency argument, as higher magnitude events generate lower wave speeds and lower shear stresses (section 6.7.1) than moderate-sized events which remain in-bank and occur more frequently.

Figures 7.11 and 7.12 also offer some indication of how the February 1989 event was representative of flows during the study period. The spatial variation of discharge was similar for most events, although the Teme basin input was small in comparison to the other flows. Furthermore, downstream variation of mean wave peak velocity was comparable with other events. These trends also confirm the discharge field results by demonstrating the significance of the Afon Vyrnwy on the spatial variation of discharge (Figure 4.6) and highlight the lack of variability through the Caersws-Abermule and Montford-Bewdley reaches, caused by few major tributaries (Figure 4.6). The influence of tides, or periodic flood releases from the Vyrnwy and Clywedog reservoirs, on flows in the lower catchment is also evident from Figure 7.9d

In summary, flows routed through river channels are influenced by spatially varied controls which modify the wave magnitude and shape. Model parameterization of such flows may simplify such controls and thus limit the accuracy of the predictions. This study has attempted to avoid such problems by examining an event which was both significant in terms of the channel-forming potential, and representative of other events in recent years. It has shown that the level of confinement and sinuosity of a channel appear to be important in defining the velocity and shape of the floodwave.

### **7.5 Spatial variation of channel transport parameters: stream power and shear stress**

#### *7.5.1 Introduction*

The previous sections have quantified the considerable variation of channel hydraulics downstream along the channel, with flow magnitude and during an individual event. Accordingly, the distributions of channel transport parameters are affected by these semi-dependent controls and themselves influence the form of the channel through the alluvial reaches of the basin. This section will explore the factors controlling these distributions of stream power and shear stress in the context of previous research, and attempt to expand this analysis of the Severn to the wider context of fluvial geomorphology. The implications of this analysis are important for determining the possible location of channel instability (section 7.6) and the source of sediment supply in fluvial systems (section 7.7) which both impact upon the stability and diversity of the stream ecosystems downstream (section 7.8).

### 7.5.2 Evidence for a stream power peak in river basin studies

The field results (Chapter 4) showed a slight peak in shear stress and unit stream power within 10 km of the source, and how total stream power increased gradually downstream but became more variable in the middle and lower reaches. The results from the model simulation (Chapter 6) were generally in good agreement (section 5.4.6 & Chapter 6), but did not produce a similar distribution for total stream power. Evidence from previous research (sections 2.3.3.4 and 2.3.3.5) suggests that values of shear stress and unit stream power should reach a maximum close to the source (Lecce, 1993). For example, the study by Graf (1982) in the Henry mountains showed a distinct peak within the upper 100 km<sup>2</sup> of a 5000 km<sup>2</sup> basin (Figure 2.10); similar work by Baker & Costa (1987) on a variety of rivers throughout the US demonstrated that the presence and location of this peak was consistent between basins. However, these studies and later ones by Magilligan (1992), Lawler (1992) and Lecce (1993) did not attempt to examine these trends and the related hydraulic parameters at a sufficient scale and resolution to understand the detailed spatial variations between the channel hydraulics and channel geometry.

A comparison between the medium- and high-flow total and unit stream power trends from this study with similar bankfull estimates by Lecce (1993) for four reaches in the Blue River basin is shown in Figure 7.13; the best-fit lines were generated using section-averaged data from the Severn and from the Lecce study. The results by Lecce cover a smaller spatial range, but include between 18 and 28 sections in each reach. Both the total and unit stream power from his study increase to a peak within a basin area of 50-60 km<sup>2</sup> and thereafter decline rapidly downstream. In contrast, the high-flow Severn results are less variable through the catchment and do not create a discernible peak, although the magnitude of the results are comparable within the upper 100 km<sup>2</sup> of the basin. The medium-flow trends demonstrate that a mid-basin peak does occur at a lower flow magnitude, and at a similar basin size (50-100 km<sup>2</sup>) to the four Blue River basin tributaries; although the scatter in both datasets is large. Both the medium- and high-flow results highlight that the peak in stream power (total and unit) is partly controlled by flow frequency. In addition, the configuration of the basin, and differences in the channel geometry and characteristics of flow inputs appear to be significant in defining an energy peak.

At a larger scale, data from a study of US rivers by Leopold and Wolman (1957) shows that the shear stress and unit stream power peaks are present in the headwaters of river basins (Figure 7.14a & b). Total stream power increases with drainage area, as the field results suggest (Figure 7.14b), and does not peak as close to the source as Lawler (1992) predicted. Similarly, mean velocity generally increases with drainage area (Figure 7.14c), in agreement with the field measurements in sections 4.6.3 and 6.3, and confirming the predictions of Leopold (1953). The potential for high energy reaches to be located further downstream is demonstrated using the Clark Fork River; this highlights how multiple peaks of flow energy may be present in the lower reaches of rivers (section 6.8.2) (Figure 7.14b). The scatter in these plots is likely to result from the collective nature of this analysis which is consistent with many previous attempts to derive empirical downstream relationships from multiple basin studies, rather than from a single channel (eg: Leopold & Maddock, 1953).

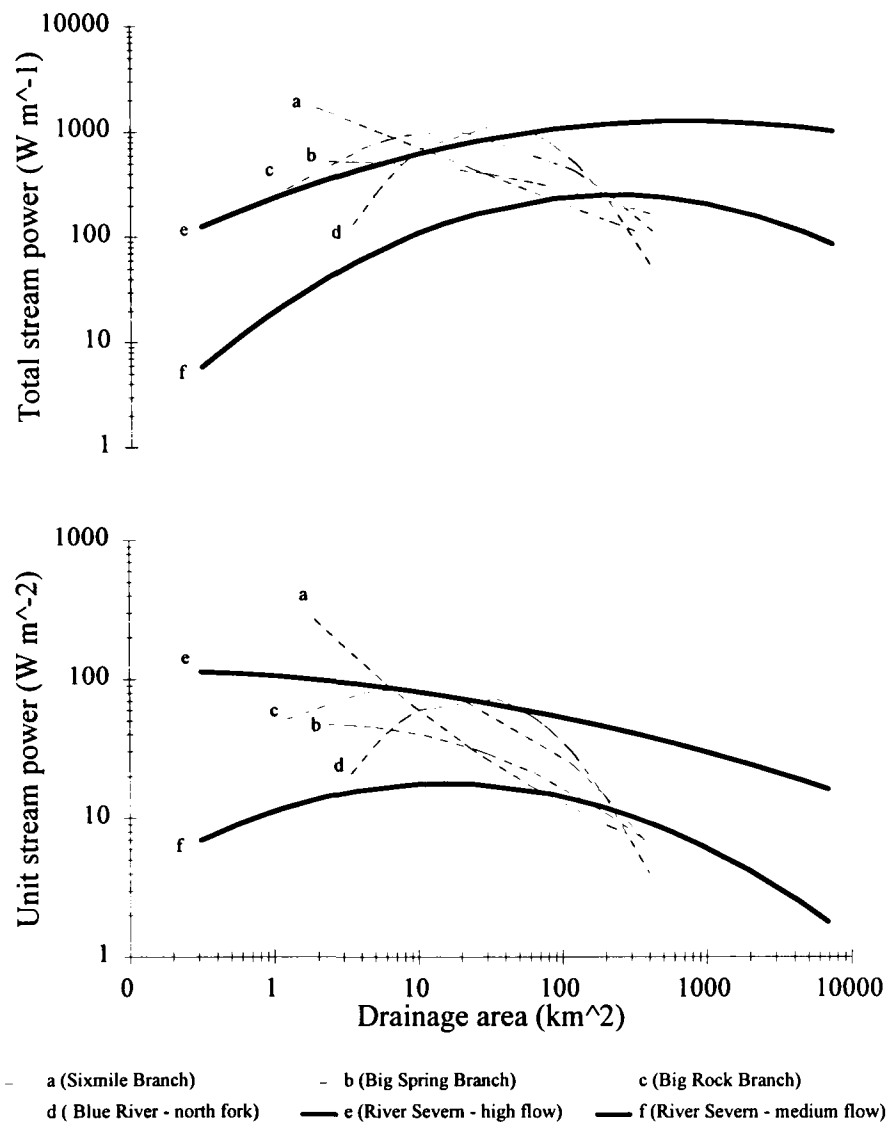


Figure 7.13 A comparison between measured a) total, and b) unit stream power values from this study and from the Lecce (1993) study of 4 channels in the Blue River basin, Wisconsin.

The Lawler (1992) conceptual model of longitudinal total and unit stream power distribution provides a theoretical approach for defining the link between hydraulic controls and stream power variation. This is based on the mathematical formulation of total and unit stream power from hydraulic information regarding the downstream change in discharge, slope and width in a temperate fluvial basin. Figure 7.15a shows how the hydraulic parameters: discharge; slope; and width, differ between the original model (1992) and the predicted trends from the high-flow field results. The total (Figure 7.15b) and unit stream power (Figure 7.15c) field-estimated trends again illustrate that a power peak does not form along the channel at this flow magnitude. However, by comparing these trends with the component trends it is clear that discharge will dominate the overall magnitude of the stream power predictions (Baker & Costa, 1987). Furthermore, the significant departure between the two slope components in Figure 7.15a is believed to be responsible for the shape of the distribution, and hence, the presence / absence of a power peak in the upper reaches (Magilligan, 1992; Lecce, 1993), as discussed in section 6.7.1. Therefore, in an over-concave basin (Wheeler, 1979) like the Severn, the stream power peak will be less pronounced (Figure 7.15b), and is less likely to conform to the theoretical predictions by Lawler (1992) and field measurements by Graf (1982) and Lecce (1993).

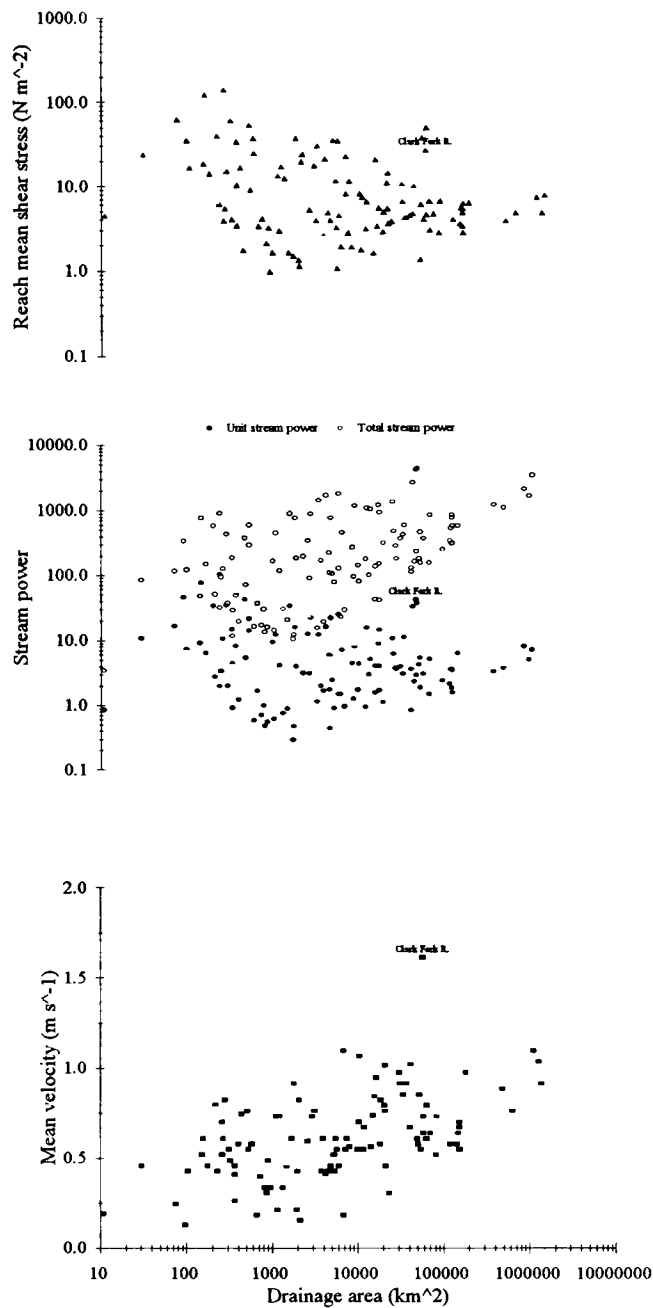


Figure 7.14 Trends for a) reach mean shear stress, b) total and unit stream power, and c) mean velocity, against drainage area for sites within the USA (Leopold & Wolman, 1957); flows are estimated from the mean annual discharge. Note the anomalously high values for the Clark Fork River.

### 7.5.3 Geomorphic control over stream power and shear stress variability

Local variations in shear stress and stream power generally develop in response to changes in the degree and form of geological control through the catchment (Graf, 1982); these controls are related to past flow and sediment regimes, and the geomorphic evolution of the system. The model simulation by Magilligan (1992) of the Galena watershed observed that the degree of channel and valley confinement controlled the downstream pattern of channel energy. Resistant lithologies generate steeper channel slopes and a more confined channel geometry (Figure 7.16), and enhance the rate of increase of stream power with stage (section 6.7.2). Thus, the upper reaches of the Severn and the Ironbridge Gorge are characterised by anomalously high levels of shear stress and stream power. Conversely, less resistant lithologies have gentler channel slopes, wider channels and floodplains which reduce the rate of change of shear stress and stream power with stage (and discharge) (Figure 7.16).

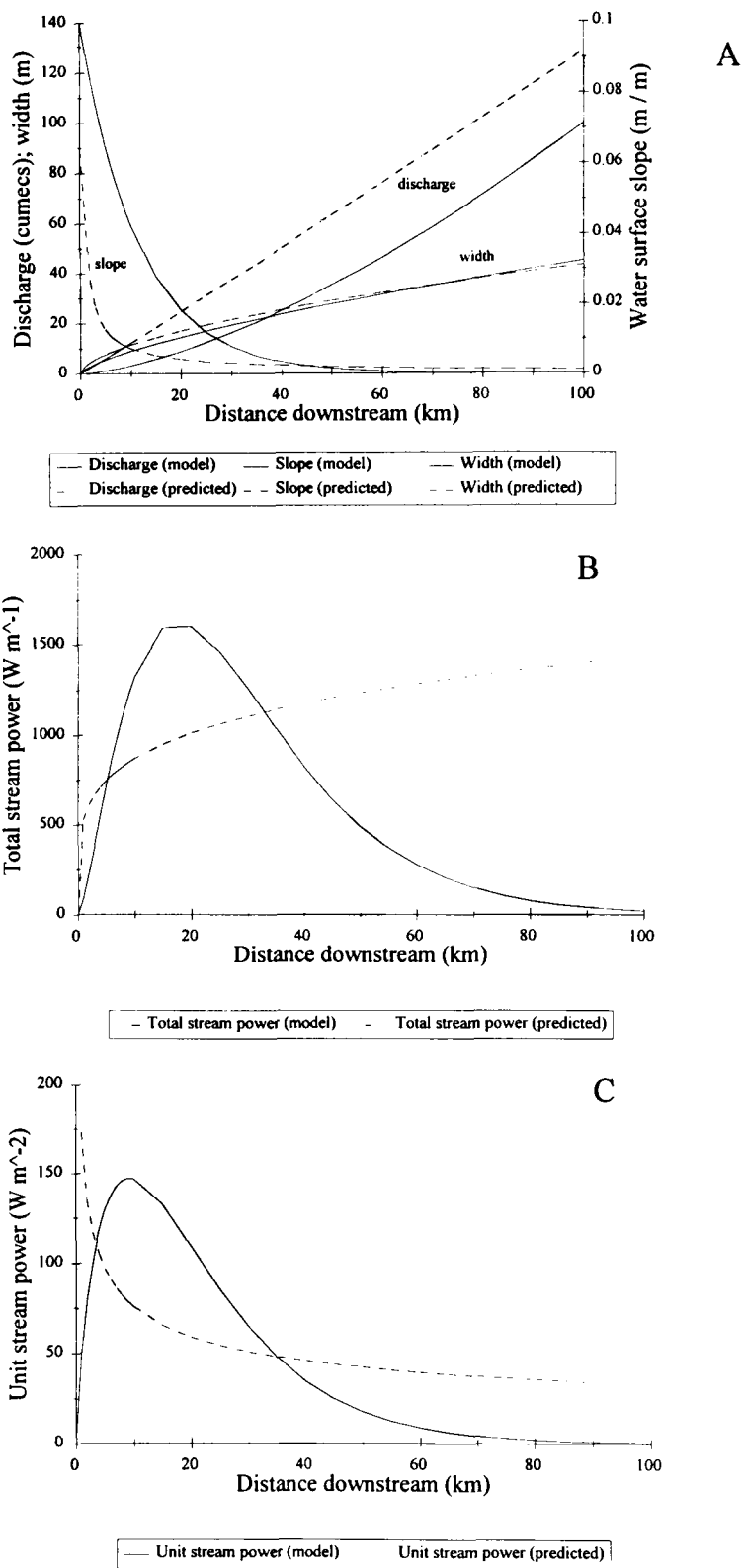


Figure 7.15 A comparison between the modelled hydraulic parameters (Lawler, 1992) and predicted downstream trends from the field study for high-flows (approximate bankfull flow). This includes a downstream comparison of: a) discharge, width and slope; b) total stream power; and c) unit stream power.

On the Severn, such areas are clearly defined by floodplain inundation from Pool Quay - Montford and upstream of Buildwas with correspondingly low levels of channel energy. Figure 7.17a demonstrates this relationship using maximum width and shear stress values, approximating to a bankfull stage, simulated from the February 1989 event. This clearly depicts the regions of inundation and high energy along the channel, reflecting differences in the level of channel confinement. A direct comparison between width and shear stress in Figure 7.17b produces a good agreement. The performance of the model may be questioned for the outliers highlighted; these relate to sections simulated between 235 - 254 km and may be produced by errors in the design of the stage boundary at Saxons Lode. Alternatively, channel embankment in the lowland flood-prone reaches may reduce water widths and increase simulated shear stresses (Wyzga, 1996).

The controls on shear stress and stream power are not continuous downstream, but vary according to the local and regional geological boundaries, tributary inputs and anthropogenic influences (Graf, 1982). Thus, the distribution of these parameters and other hydraulic variables are influenced at a variety of scales by spatially-varied controls. For example, the glacial legacy of the Severn at the Ironbridge reach affects the channel geometry and hydraulics through enhanced slopes and a constrained channel path. Similarly, the channel geometry downstream of the Vyrnwy confluence is adjusted to accommodate the rapid increase of discharge and sediment load from the Afon Vyrnwy. Between these discontinuities in external controls, the channel form and hydraulics are not constant, but vary about an approximate mean; this is consistent with the stochastic changes in channel width between tributary junctions observed by Richards (1980). Therefore, the downstream pattern of channel hydraulics along the Severn is a complex response to external controls which are not spatially continuous along a channel (Bull, 1979; Knighton, 1987).

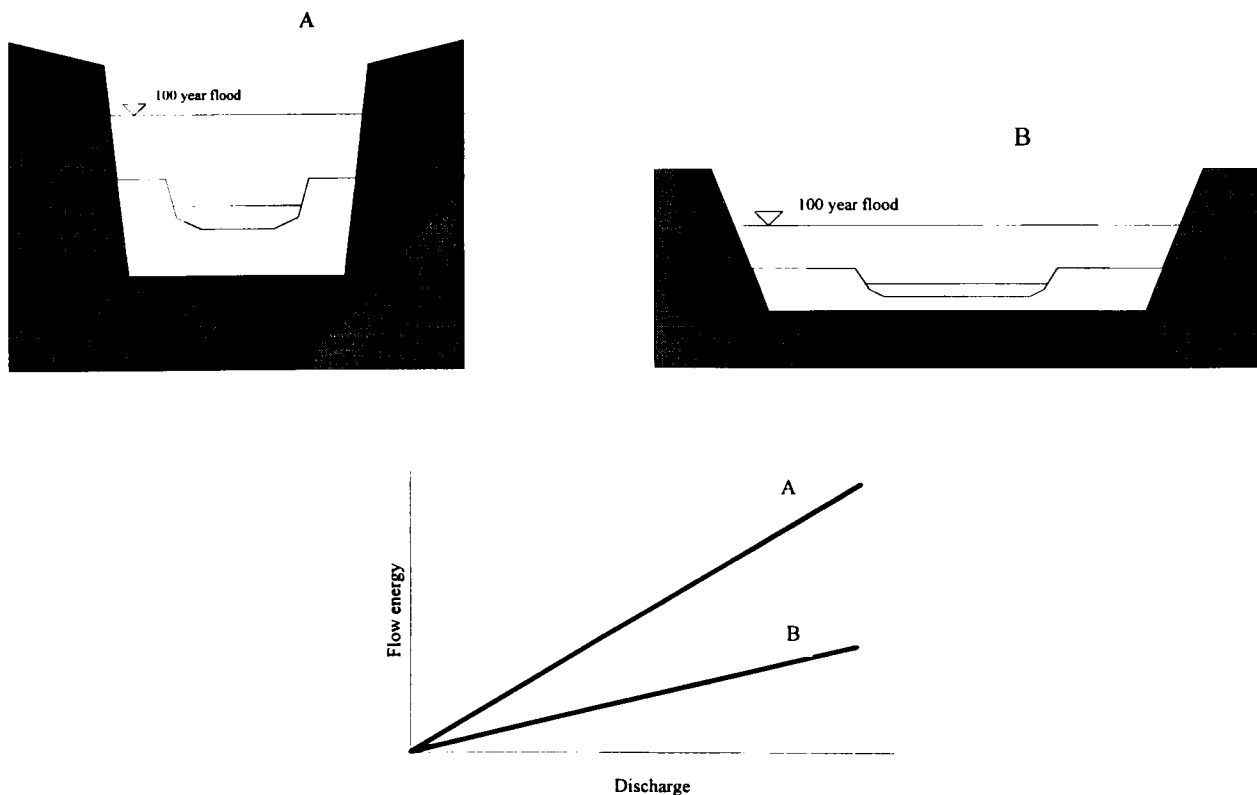


Figure 7.16 The theoretical control of channel morphology on the temporal variability of flow energy (after Magilligan, 1992).

## 7.6 Channel hydraulics and lateral channel adjustment

### 7.6.1 Introduction

The impact of spatially varied channel hydraulics on the downstream pattern of erosion along the Severn is analysed in this section. Despite considerable attention to reach-scale processes in this field, comparatively few studies (Lewin, 1983, 1987; Lawler, 1992; Bull, 1996) have examined in detail the controls on erosion processes at this scale. Therefore, the results from this study have the potential to examine the conclusions made by Lewin (1983; 1987) about erosion rates along the Severn, the conceptual model of bank erosion process domains developed by Lawler (1992) and the significance of bank resistance on bank erosion trends downstream along rivers.

### 7.6.2 Interaction between channel hydraulics and bank erosion processes along the Severn

Lateral channel adjustment occurs when the boundary shear stress imposed by the flow exceeds the critical entrainment threshold of the boundary material (Bull, 1979). The mechanism of erosion is dependent on such factors as: micro-climate; boundary material size and composition; antecedent hydrological conditions; bank height; flood wave attenuation; and vegetation. At a catchment-scale, the mode and magnitude of bank erosion is conditioned by the variety of controls exerted through different process domains (Lawler, 1992). These domains reflect the downstream change in dominance of controls affecting bank erosion processes.

The conceptual model constructed by Lawler (1992) predicts subaerial activity (needle-ice; freeze-thaw activity; desiccation) to be the dominant erosion process in the headwaters of a basin, where stream power is low (Figure 7.18) and bank height is insufficient to induce mass failure. Within 2 km from the source, the slope and discharge are sufficiently low to prevent high stream powers and it is likely that subaerial activity will exceed hydraulic activity. However, evidence from this study suggests that unit stream power and shear stress are high in the headwaters and decline downstream from approximately 10 km ( $100 \text{ km}^2$ ).

Further downstream in the 'piedmont' zone (Newson, 1981), stream power is predicted to peak (Figure 7.18) and hence the potential for hydraulic entrainment of sediment from the boundary is high; the preparation processes are predicted to remain constant at a low level and mass failure be negligible owing to the shallow height of the banks. This theory is based upon observations by Newson (1981) that the middle reaches of many gravel-bed rivers are highly active, and supported by historical bank erosion estimates by Lewin (1987); this, he believed, was largely attributable to a stream power peak. Figure 7.19 represents the estimates by Lewin (1987) of bank erosion rates along the Severn superimposed onto the results for unit stream power at a high-flow (approximate bankfull) level. Notwithstanding the limited spatial extent of the Lewin estimates and the lack of hydraulic measurements at the erosion sites, it is clear that the unit stream power peak and erosion rate peak do not coincide. Indeed, the magnitude of unit stream power at the location of maximum erosion rates is much lower than elsewhere along the channel ( $< 50 \text{ W m}^{-2}$ ). Furthermore, spatially-averaged bank erosion rates measured over a 2-year period by Bull (1996) illustrate how erosion rates increase between Tanllwyth and Caersws from  $1.29 \text{ cm yr}^{-1}$  to  $46.0 \text{ cm yr}^{-1}$  as unit stream power rises to a peak and declines (Couperthwaite *et al.*, 1996) (Figure 7.20). Together, these

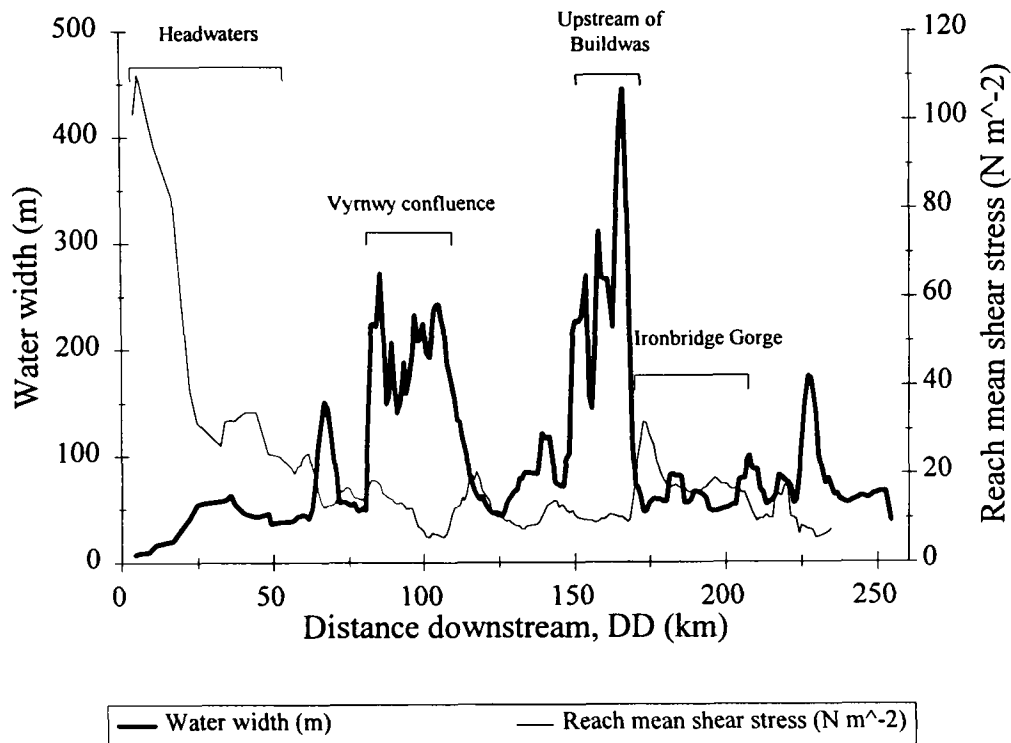


Figure 7.17a The downstream pattern of water width and reach mean shear stress, using a moving average (5 space steps). This highlights both the variability in the hydraulic trends, and also the consistency between these variables, particularly at the Vyrnwy confluence and upstream of Buildwas where floodplain inundation is pronounced, and in the headwaters and the Ironbridge Gorge where the channel is steep and constrained.

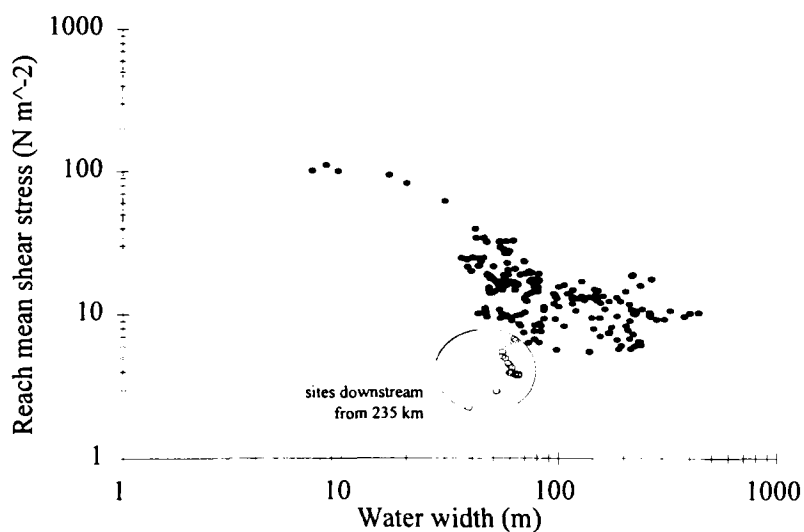


Figure 7.17b The inverse relationship between water width and reach mean shear stress, calculated from the maximum simulated at-a-site values. The outlier from this distribution (circled) are all located downstream of 235 km. This suggests that either channel embankments exert a significant control through these reaches, or the model downstream boundary was in error.

results imply either that additional factors are important in the consideration of bank erosion, or that the methods used to measure erosion or unit stream power are in error. The latter cannot be ruled out with any certainty, but the former may possibly be caused by downstream variations in the magnitude of bank resistance (eg: bank material size and composition; land use; vegetation) (section 7.6.3).

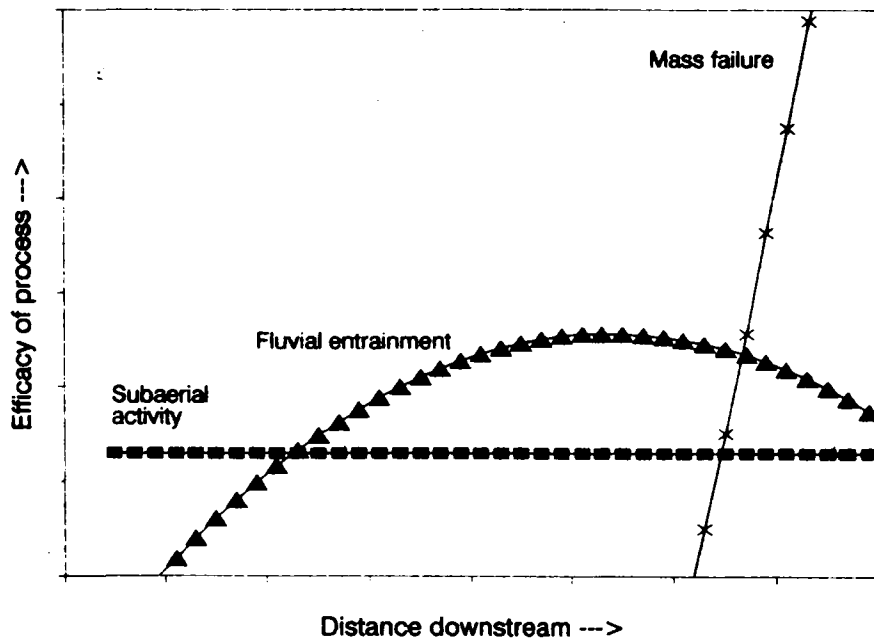


Figure 7.18 A conceptual model for the downstream change in the dominance of bank erosion processes (from Lawler, 1992; p. 137).

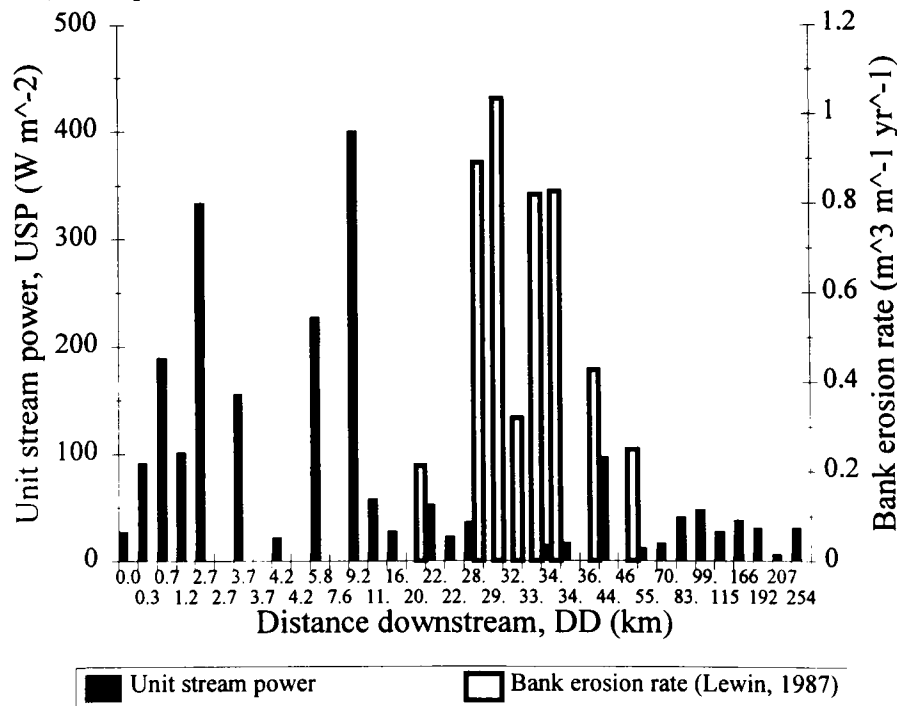


Figure 7.19 A comparison between unit stream power measured at a high-flow level with estimates of bank erosion rates (Lewin, 1987) along the upper Severn. Note the disparity between the peaks of the two distributions.

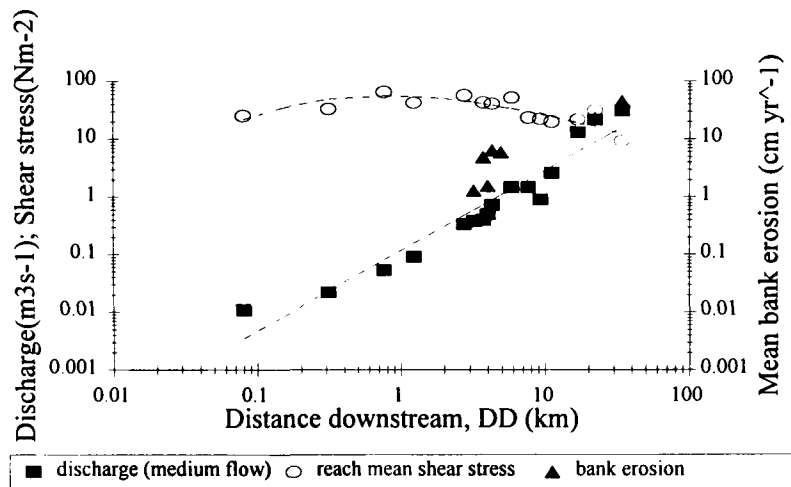


Figure 7.20 The downstream distribution between reach mean shear stress, discharge and bank erosion in the upper reaches of the Severn at a medium-flow level (Couperthwaite *et al.*, 1996). Predicted trend lines are marked as dashed lines.

In the middle-lower reaches, Lawler's model (1992; 1995) predicts bank erosion by mass failure to dominate as channel banks reach a critical height at which slumping-, slab-, or cantilever-failure are possible (Figure 7.18). Erosion by fluvial entrainment is expected to decline in response to decreasing channel slopes, whilst preparation processes remain low, but constant (Figure 7.18). However, the field results and model simulation show that shear stress and stream power do not decrease in a systematic manner downstream (eg: Figure 7.17a). Discontinuities in the spatial distribution of fluvial energy and channel geometry, generated by lateral inputs and variations in the rates of weathering between geological units, control the erosive potential of the flow, and hence, produce a variable downstream trend. Furthermore, the high rates of bank erosion in the 'piedmont' zone of the Severn are believed to be the result of mass failure (Couperthwaite *et al.*, 1996). Thus, it may not be possible to simplify the efficacy of erosion by hydraulic entrainment into a simple model, as a consideration must be made for variations in the hydraulics and bank composition along the channel.

### 7.6.3 Significance of boundary and planform resistance on channel form and processes

The downstream distribution of bank resistance is poorly understood (Knighton, 1987). Like channel hydraulics, consideration of bank erosion processes in fluvial geomorphology has diverted from large-scale perspectives to micro- and meso-scale studies in an attempt to define the processes and mechanisms. Hence, studies which consider the relationship between the channel hydraulics, bank resistance and bank erosion are scarce (eg: Lapointe & Carson, 1986). In the previous section it was indicated that bank resistance may be a significant factor in the elucidation of downstream trends in bank erosion. A recent study of bank erosion processes by Harris (1997) on the River Severn (source to Newtown) has examined

one measure of resistance which enables some conclusions to be made relating to the earlier unit stream power - bank erosion relationship defined in Figure 7.17.

Harris (1997) measured the silt-clay content of both channel banks at approximately equidistant locations along the Severn (Schumm & Khan (1972) used width-depth ratio); the lower and upper bank were sampled to represent any possible stratification of the bank-face. The distribution of the silt-clay content is shown in Figure 7.21. The upper and lower silt-clay content increases at a similar rate to 20 km downstream; thereafter, the upper component continues to rise, reflecting the increase in bank cohesion along the channel (80 %), but also possibly enhancing the potential for rotational failure as pore water pressure is more likely to build up and the residual angle of shearing resistance to reduce. The lower bank component falls markedly downstream from 20 km, indicating a coarsening of the basal layer. The development of a gravel basal layer is likely to promote bank erosion by mass failure (Thorne & Lewin, 1979; Lawler, 1992; Hooke, 1995) and may explain the high rates of bank erosion in the reach between 20 - 50 km downstream on the Severn (Figure 7.19 & 7.20) (Couperthwaite *et al.*, 1996).

This example offers an insight into the significance of the geological boundary at Llanidloes. Upstream of Llanidloes, the steep and laterally-confined channel and river valley enhance the rate of change of shear stress and stream power with discharge (Figure 7.16). Downstream from Llanidloes, the more erodible floodplain deposits (described above) and gentler valley slopes generate wider channels which reduce the rate of increase of shear stress and stream power with discharge (Figure 7.16) (Magilligan, 1992). The boundary between these non-alluvial and alluvial fluvial environments also coincides with a major break of slope (Figure 4.36). Hence, in the upper reaches, the fluvial energy appears to be sufficient to erode the banks, but the banks are probably too resistant. However, further downstream fluvial energy in the channel is lower, but the reduced resistance in the basal layer weakens the bank and enhances the erosion by hydraulic entrainment.

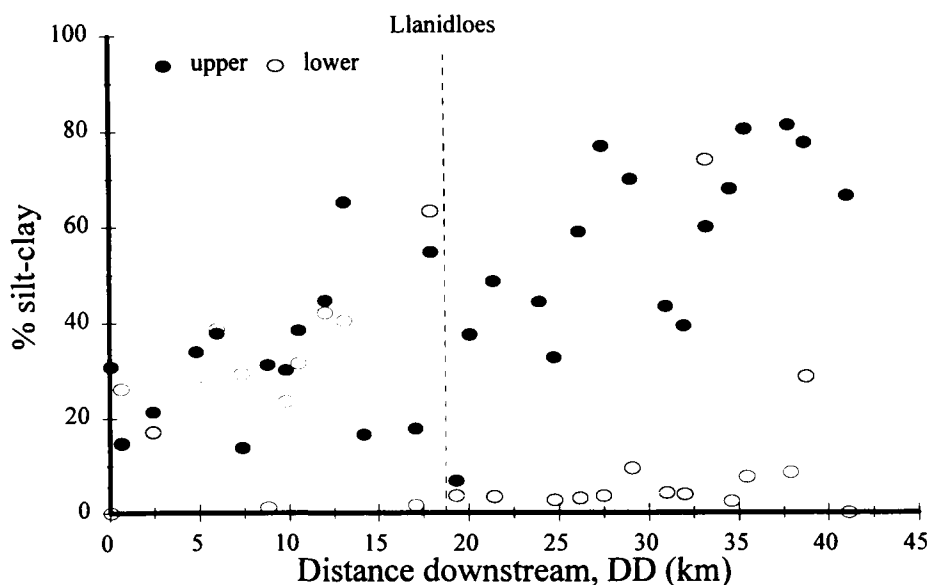


Figure 7.21 The downstream variation in the lower and upper bank silt-clay content (% weight) in the upper Severn (Couperthwaite *et al.*, 1996; Harris, 1997). Note the deviation between the upper and lower bank components close to Llanidloes.

Channel form adjustment is also dependent upon spatial and temporal variations of the growth and structure of in-channel or bank vegetation (Thorne, 1990; Watson, 1987; Gurnell & Midgley, 1994). It may induce aggradation by the deposition of suspended sediment in response to flow retardation by aquatic flora (Watson, 1987; McKenney *et al.*, 1995), or by the suppression of turbulent eddies responsible for the entrainment and transport of sediment from the channel boundary (Thorne, 1990). Alternatively, localised scour may result from changes in the magnitude and direction of flow (Pitlo & Dawson, 1980), according to the age of the vegetation (McKenney *et al.*, 1995), or variations along the bank in the stabilising properties of plant roots (Charlton *et al.*, 1978). Indeed, the stabilising potential of bank vegetation is dependent upon the vegetation weight, stem flexure, and the rooting depth and density (Kouwen & Unny, 1973; Thorne, 1990).

## **7.7 Channel hydraulics and sediment transport**

### *7.7.1 Introduction*

‘The drainage basin, as an integral part of global sedimentary and geochemical cycles, involves erosional, transportational and sedimentary or storage processes’ (Brown, 1987; p. 307). These processes are controlled, in part, by the spatial variation of channel hydraulics through the basin, which operate at a variety of temporal and spatial scales. This study has considered a large catchment-scale, at a short temporal perspective, in order to appreciate the general inter-relationships between hydraulic and geomorphic variables in a basin at an approximate steady-state equilibrium. The dynamic adjustment between the hydraulics and the channel form (at-a-site and downstream) is determined by the local storage and transfer of sediment. This section will therefore examine this relationship using the field data, and other published data from the Severn. The aim is to demonstrate that an appreciation of the spatial and temporal variation of channel hydraulics may provide an important insight into the dynamics of sediment and contaminant supply, storage and remobilisation in fluvial systems.

### *7.7.2 The potential of stream power for evaluating sediment storage in fluvial systems*

Bull (1979) outlined the significance of channel hydraulics, and particularly stream power, in defining the critical threshold which separates modes of erosion and deposition in streams. Later work by Graf (1982, 1983a, 1983b), Lewin (1983, 1987), Nanson and Croke (1992) and Lecce (1993) have extended this concept to interpret the adjustment of natural channels to local hydraulic conditions. Indeed, from the study of sediment removal in the Henry mountains, Utah, Graf (1982; p. 210) concluded, ‘the most important consequences of the spatial variation in fluvial energy is the uneven movement and temporary storage of sediment’. This suggests that at times in reaches of high stream power, the transport and removal of sediment will exceed the rate of deposition, whereas sedimentation will be more likely to occur in reaches of low stream power. Sediment deposition in a reach may reduce the channel capacity (Hey, 1975, cited in Lewin, 1987) or trigger the adjustment of another flow variable (eg: width or velocity) to compensate for the alteration of depth (Andrews, 1979). Such modification of the channel geometry is akin to the theoretical system adjustment discussed by Graf (1982), whereby a threshold may be crossed following a steady-state condition, and thus trigger an adjustment to the distribution of fluvial energy, and hence, the patterns of sediment transport and deposition.

The field evaluation of channel hydraulics and differential sediment transport has largely concentrated upon reach-scale studies of braided (eg: Ashworth & Ferguson, 1989; Ashmore, 1991; Ashworth *et al.*, 1992) and meandering reaches (eg: Hooke, 1974, 1975; Bridge, 1977; Lapointe & Carson, 1986), or examined the sediment budget of channels with limited hydraulic information (eg: Lewin, 1987; Walling & Webb, 1987; Ashmore & Day, 1988). The study by Walling and Quine (1993) in the Severn basin investigated the spatial distribution of fluvial deposits using Caesium-134 ( $^{134}\text{Cs}$ ) from Chernobyl fallout. They established a sediment budget for the basin, and thereby, identified zones of sediment transport and deposition along the main channel. The methodological approach adopted for their study is described in Lambert and Walling (1988); Rowan *et al.* (1992), and Walling and Quine (1993). The recent nature (1986-9) and location of this research (River Severn: Mount Severn - Gloucester) make it ideal for a comparison between the hydraulic data and their estimates of in-channel and floodplain storage measured at 32 sites along the channel, to determine the significance of stream power, and channel hydraulics, on the redistribution of sediment in river basins.

Four zones along the channel are identified in Figure 7.22 for the purpose of highlighting hydraulic-sedimentary processes along the channel:

- a) The 'piedmont' zone is a highly active reach between Llanidloes and Newtown where the rate of channel and floodplain reworking is high (Thorne & Lewin, 1979; Lewin, 1982, 1983, 1987) and the floodplain is frequently inundated. This corresponds to a peak in the inventory ( $^{134}\text{Cs}$  level per unit square metre of fine sediment stored on the channel/floodplain floor) of channel and floodplain deposits (Figure 7.22b). Although stream power is declining (Figure 7.22a), the energy of the flow is sufficient to overcome the resistance of the bed deposits and bank material (Figure 7.21) and rework and deposit the mountain-derived sediments (Newson, 1981), but insufficient to transport sediment through the reach.
- b) The peak in the floodplain  $^{134}\text{Cs}$  inventory at the Vyrnwy confluence (Figure 7.22b) coincides with a well-developed and frequently inundated floodplain. However, despite low stream powers through the reach (Figure 7.22a), generated by low channel slopes and a high width-depth ratio, the storage of sediment in the channel is low. This may be caused by either: a) a limited supply of sediment; b) a transport capacity (and stream power) sufficient to carry the sediment load through the reach; or c) an error in the estimation of the sediment store.
- c) Through the Ironbridge Gorge, high levels of stream power prevent the deposition of fine sediment in the channel (Figure 7.22c); hence, the amount of  $^{134}\text{Cs}$  in the inventory is low compared with the background activity (level of  $^{134}\text{Cs}$  measured in a fine sediment sample) (Figure 7.22b). The effect of channel confinement through the Gorge prevents the flow from exceeding the bankfull capacity, and therefore the floodplain inventory level is almost zero.
- d) Downstream from Bewdley, the  $^{134}\text{Cs}$  originated from headwater sources is heavily diluted by local sources and declines sharply (Figure 7.22b). This coincides with a marked increase in the level of

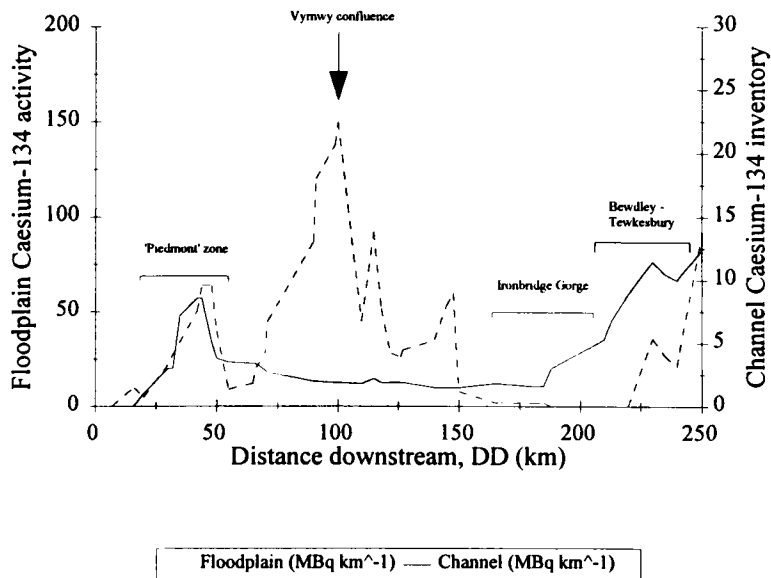
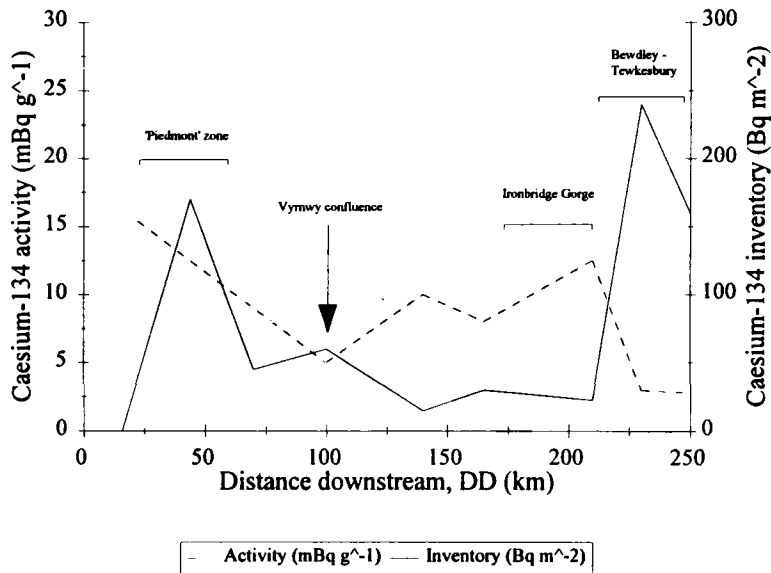
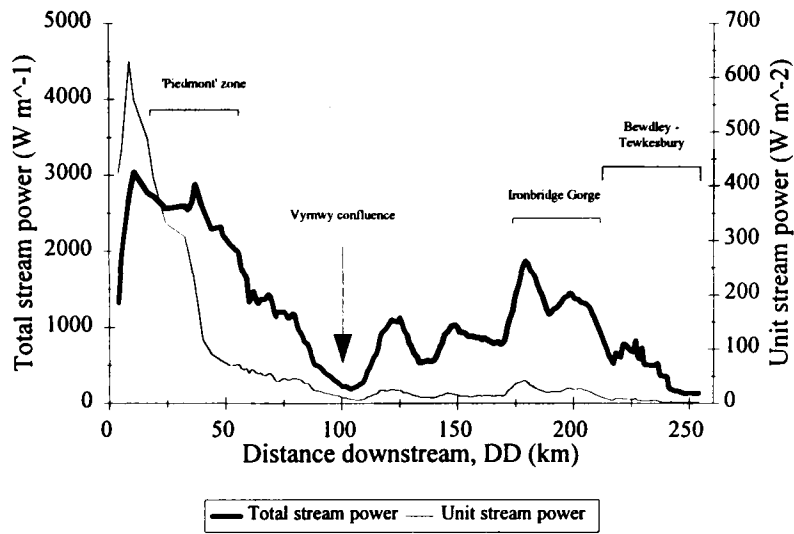


Figure 7.22 The downstream variation of stream power and sediment storage along the Severn, using sediment data from Walling and Quine (1993). This demonstrates that regions of high stream power strongly coincide with zones of sediment transport, and conversely, regions of low stream power coincide with zones of sediment storage.

$^{134}\text{Cs}$  stored in-channel and on the floodplain (Figure 7.22c), which mirrors the declining stream power distribution through this reach (Figure 7.22a).

In summary, the zones of sediment deposition and transport through the Severn basin appear to be related to bankfull estimates of stream power. This implies that the potential redistribution and accumulation of contaminants and pollutants from agricultural and industrial waste may be elucidated with reference to the spatial distribution of channel hydraulics, and particularly stream power.

## 7.8 Channel hydraulics and the zonation of macro-habitats

### 7.8.1 Introduction

The physical flow parameters are important for determining the structure and composition of communities in lotic ecosystems (Statzner, 1981). Since flow hydraulics and stream temperature change downstream from the headwaters, a zonation of species assemblages are expected along the longitudinal profile of a channel. The River Continuum Concept (RCC) (Vannote *et al.*, 1980) provides a theoretical justification for the down-channel relationship between stream communities and flow hydraulics. In practice, the natural variability of external system controls does not create a smooth continua between the physical variables, but discontinuities which redefine the distribution of the biota (Statzner & Higler, 1986). The Serial Discontinuity Concept (SDC) is an example from the study of river regulation (Ward & Stanford, 1983; 1995); this conceptualises the relative impact of impoundment at various positions along the river on the ecological character of the system. This section will examine how the results from this research may influence the practical application of these and other theories, and discuss the importance of channel hydraulics for an overall understanding of the river ecosystem.

### 7.8.2 The river continuum concept (RCC)

A central theory of the RCC is that the adjustment toward a dynamic equilibrium in natural channels will create a continua of inter-related biological communities (Statzner & Higler, 1985). This implies that the variance of total and unit stream power would be minimised throughout the catchment, and would lead to a dynamic equilibrium of the river basin (Leopold *et al.*, 1964; Kapoor, 1990). In their review of the RCC, Statzner & Higler (1985) found no evidence for a reduction in the variability of energy, as proposed by Vannote *et al.* (1980), based on the study of 16 RCC stations in the US by Minshall *et al.* (1983). Therefore, Statzner and Higler (1985) predict a downstream sequence of biota assemblages defined by transitions in the physical character (hydraulics and channel geometry) of the channel. In a study of Jumpingpound Creek, Alberta, Hiebert (1996) observed transitions in regions of hydraulic stress, although the general sequence of transitions differed from the Statzner and Higler (1985) hypothesis according to variations in slope between study sites. This is consistent with the spatially varied distribution of channel hydraulics measured in this study. The pattern of stream power (Figure 6.15) simulated at a high spatial resolution reveals a number of peaks and troughs, corresponding to changes in the slope, geometry and flow regime of the channel. Similarly, Statzner and Higler (1986) and Milner and Petts (1994) argue that microscale variations in basin topology, caused by lakes and additional baselevels, would disrupt the continuous gradient of hydraulic variables and ecological conditions downstream. Hence the longitudinal

profile of aquatic communities would produce a complex mosaic containing interdigitating patches of different ecosystems, or species assemblages (Naiman *et al.*, 1988). The applicability of this tenet of the RCC is therefore limited in large river basins where system controls are randomly distributed (section 4.6). The channel will adjust to a dynamic equilibrium according to these spatial and temporal controls, and is unlikely develop a smooth continuum of energy and hydraulics.

The RCC also proposes that biological diversity will peak in the mid-reaches in response to maximum diel temperature variations in the mid-basin region and the convergence between headwater and estuarine communities (Statzner & Higler, 1985). Accordingly, the authors state 'in systems with a highly stable physical structure, biotic diversity may be low and yet total stability of the stream ecosystem still be maintained. In contrast, systems with a high degree of physical variation may have species diversity or at least high complexity in species function which acts to maintain stability' (Vannote *et al.*, 1980; p. 134). The stability of the physical environment is defined by the relative frequency of bed material movement, lateral channel migration and channel avulsion; ecological stability is more difficult to define but commonly refers to the resilience or speed of recovery by a community to disturbance. The RCC therefore assumes that streams in the middle reaches are the most dynamic, as found by Graf (1982) in the Henry Mountains, and Lewin (1983, 1987) and Bull (1996) on the Severn. However, the Llanidloes - Newtown reach is only one of several reaches along the Severn which exhibit a high degree of physical variation, in terms of both channel form and channel hydraulics. Other examples include: Dyffryn - Vyrnwy confluence; Montford - Shrewsbury; Buildwas - Bewdley. As Statzner & Higler (1986; p. 137) state: '...high species richness is found in zones of transition of hydraulic stress...In these transition zones species assemblages overlap and a relatively large number of species live near the limits of their ecological tolerance. Thus in these zones of major hydraulic and faunistic change (transition zones) the potentials of community stability and resilience must be different from those in zones upstream and downstream'. The presence of these zones may also agree with the Intermediate Disturbance Hypothesis (IDH), which states that diversity will be maximised at intermediate levels of disturbance, with competitive exclusion and physical elimination causing species loss at the limits of the disturbance continuum (Death & Winterbourn, 1995). Thus the potential biological diversity along the Severn, and in other rivers in general, may be serially distributed longitudinally downstream in response to physical and hydrological factors. Additional controls on species diversity and abundance will vary according to climate, water quality and species colonising position.

### 7.8.3 *The serial discontinuity concept (SDC)*

The impact of impoundment on a river channel has consequent effects on the ecological and physical stability of the system. This is manifest through changes in the flow, sediment, and thermal regime, and upon the habitat of the river, both upstream and downstream of the dam (Petts, 1984). The theoretical background to the SDC (Ward and Stanford, 1983; 1995) is a simple conceptualisation of these factors built upon the RCC; hence, the gradient of physical conditions along a channel produces a distribution of stream biota which abruptly changes, or 'resets', at an impoundment, and thence continues downstream. Figure 7.24a illustrates a hypothetical channel based upon the SDC model. Channel instability falls to a minimum through the steep, bedrock reaches in the headwaters of the channel, and subsequently increases as the bedrock control lessens, a floodplain forms and the channel is free to migrate laterally and rework coarse alluvial deposits. In this 'piedmont' zone, the channel slope is still steep (Figure 7.24b) and therefore

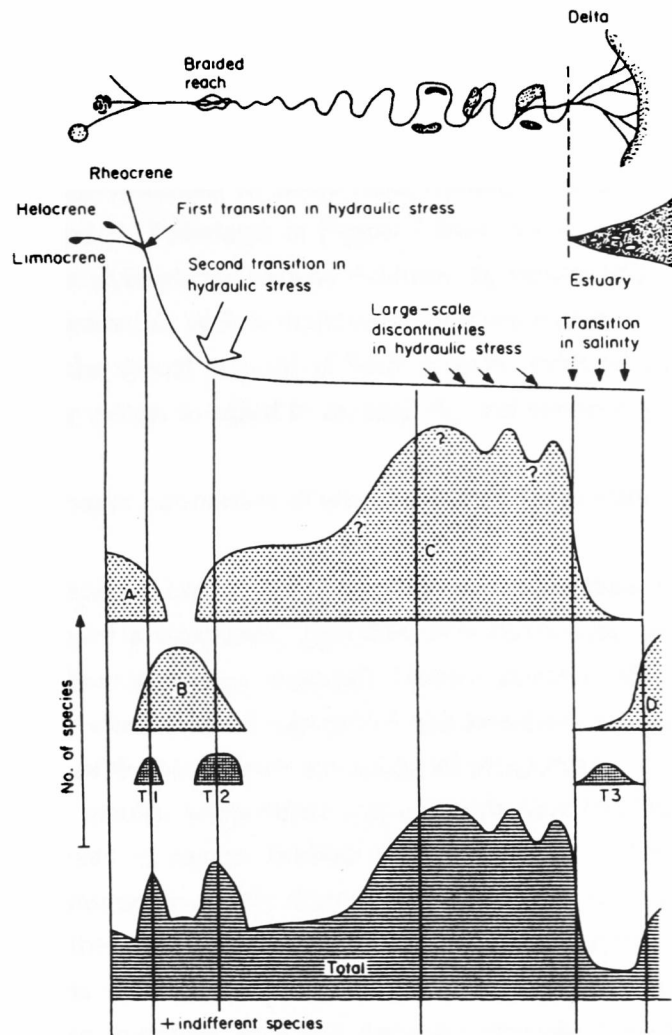


Figure 7.23 A conceptual model for the faunistic zonation pattern in natural stream associated with the longitudinal gradient of hydraulic processes in river basins (from Statzner & Higl, 1986; p. 136).

for a given flow the energy available to rework and transport boundary deposits is high (Figure 7.24c). Further bedrock or artificial constraints downstream along the channel would reduce the potential instability of the channel by preventing lateral expansion; however, this also straightens the flow path, thus steepening the channel (Figure 7.24b). This results in secondary energy peaks, such as at the Ironbridge Gorge on the Severn (Figure 7.24c). Tributary inputs (Figure 7.24a) may have the opposite effect on the stability of the channel, by increasing the magnitude of flow, sediment load and possibly gradient in the downstream reaches. The consequent adjustment of the channel geometry and form will determine whether the stream power through the reach alters. For example, an increase in width would reduce the unit stream power, but not total stream power; however, an increase in slope would increase both stream power parameters. Along the Severn, a reduction in slope at the confluence of the Severn and Vyrnwy (Figure 7.24b) causes stream power to decline (Figure 7.24c); this is enhanced by an increased frequency of

overbank events produced by a greater magnitude of flow and a resistance from the boundary to accommodate the flow within bank which further reduces the energy of the flow in the reach.

Based upon this discussion, it is hypothesised that serial discontinuities may result from the natural variation of the channel topography, generated by 'physical discontinuities' along a channel (Figure 7.24). These physical discontinuities may develop from long-term structural adjustments to the river basin (eg: channel diversion or capture) as found at the Ironbridge Gorge, short-term adjustments caused by channelization, or by temporal variations in flows from tributaries such as the Clywedog and Vyrnwy (symbolised by G (Gorge) and T (Tributary) in Figure 7.24a). Each of these controls affects the slope, roughness and geometry of the channel, and thereby modifies the pattern of channel hydraulics through the system. In turn, the channel hydraulics seek to maintain an efficient transport of sediment load by adjusting the channel boundary. Thus the spatial patterns of bank erosion, sediment transport and storage, are the dynamic responses of the river system to adjust to the spatially and temporally varied channel hydraulics.

#### *7.8.4 The importance of hydraulic parameters in ecological habitat assessment*

'Connectivity in the fluvial system means that repercussions of any man-induced change at any given location can be transmitted over a wide area, especially in a downstream direction' (Brookes, 1988; p. 164). Though specifically directed toward managed channel systems, this cautionary note is equally applicable to natural systems where channel adjustment and hydrological change, for example, may alter the flow and sediment regime of the river. From an ecological perspective, the relationship between channel hydraulics and stream water quality, temperature and sediment load has important implications for the ecological stability and diversity of aquatic habitats (Milner and Petts, 1994). For example, it has been demonstrated that sediment storage is closely related with the spatial variation of stream power (section 7.8). Sedimentation reduces the range of substrate material, and with it the diversity and productivity of species; it may also fill pools and dead-zones which act as refugia for many fish species, and degrade riffles, thereby de-oxygenating important salmonid spawning grounds. Similarly, the interaction between hydraulics and bank vegetation affects the physical stability of the bank material (Thorne, 1990) (section 7.6) and therefore the contribution of fine sediment from bank to the water course (Bull, 1996). Furthermore, vegetation alters the degree of shading and local diel temperature variations, and also contributes organic matter to benthic communities. Together these examples suggest that a more informed appreciation of the hydraulic variability at a reach- and catchment-scale may improve our present understanding of the factors controlling the zonation and diversity of stream habitats and their associated communities.

### **7.9 Summary**

The downstream pattern of channel hydraulics in the Severn basin appears to be strongly influenced by spatially discontinuous controls. By considering a single channel reach at a high spatial and temporal resolution, the measured and simulated distribution of hydraulics is shown to reflect regional variations in the geological composition of the catchment and the localised impact of tributaries. Comparison with similar studies on the Severn (eg: Lewin, 1987) and in the US (eg: Graf, 1982; Magilligan, 1992; Lecce, 1993) indicates that the spatial pattern of flow energy (reach mean shear stress, and total and unit stream

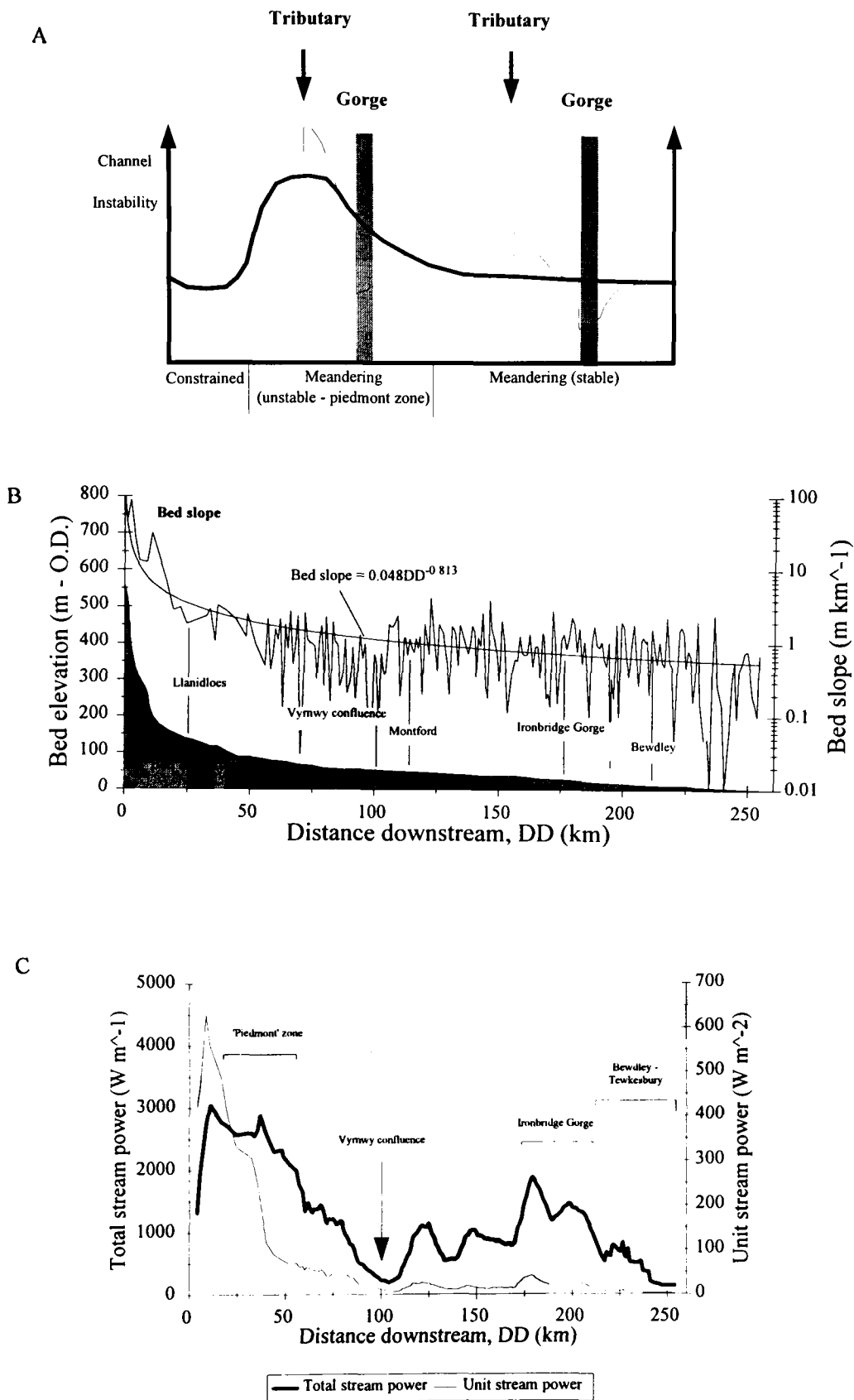


Figure 7.24 A comparison between, a) the conceptualisation of the Serial Discontinuity Concept based upon physical discontinuities, b) the downstream distribution of bed slope and bed elevation, and c) the downstream distribution of total and unit stream power. This highlights the importance of natural external controls on the downstream variation of channel stability and channel processes and hence for the zonation of macro-habitats in a river basin.

power) is dominated by the distribution of slope through the catchment. Furthermore, it is suggested that stream power may be used to explain the longitudinal distribution of sediment storage through the catchment, although bank resistance appears to act as a control upon the location and magnitude of lateral channel adjustment. The analysis of these parameters, using a complementary field and modelling approach, has illustrated the importance of scale in fluvial geomorphology, in terms of both the connectivity of the system at the basin-scale and the practical difficulty of representation.

## CHAPTER 8 CONCLUSIONS

### 8.1 Introduction

This chapter summarises the results of the research undertaken along the non-tidal Severn between 1993 and 1996. The principle aim was to understand the mechanisms controlling the spatial and temporal variation of channel hydraulics parameters at a basin scale. The conclusions to this project are presented in section 8.2; these address the research objectives, which can be summarised as:

1. To examine how channel hydraulic parameters are distributed downstream under steady and unsteady flow conditions.
2. To define the spatial distribution of stream power and shear stress in the Severn basin.
3. To develop a model which may complement traditional flow measurement techniques by accurately simulating unsteady flow along the entire non-tidal Severn.
4. To evaluate how downstream change in channel size, shape and slope affects the propagation of floodwaves along the Severn.
5. To consider the effect of the spatial variation in channel hydraulic parameters on lateral channel adjustment, sediment transport and the zonation of aquatic habitats.

In the final section (8.3), the potential for future studies in this research area are discussed.

### 8.2 Summary of study results

#### *8.2.1 Downstream distribution of channel hydraulic parameters*

Chapters 4 and 6 demonstrated how the basin-scale distribution of both the measured and modelled channel hydraulic parameters were found to be highly variable in space and time. Comparison between these datasets suggests that the limited number of field sites and the potential lack of accuracy in the 1-D model simulation were not significant, as the results obtained for each hydraulic parameter were comparable. Thus the model provides the opportunity to expand the potential of field measurements to the calibration and validation of high resolution model simulations at the basin- and event-scale. The results indicate that the random distribution of geological units, basin topology and land use appears to alter the perceived continuum of hydraulic forms and processes, as proposed by Knighton (1987). The hydraulic adjustment to changes in slope, roughness, flow or boundary resistance at these transitional zones are complex, but amenable to prediction when analysed at the scale and resolution achieved by the field measurements and model simulation. Along the Severn, such transitional zones were identified at

the following locations: Llanidloes; Newtown; Dyffryn; Vyrnwy confluence; Montford; Ironbridge; and Bewdley. The nature of the adjustment by individual parameters is now reviewed.

The downstream increase in water width and mean depth was dominated by flow inputs, such as the Clywedog and Vyrnwy tributaries, as predicted by Richards (1980) (Figure 4.31). Lateral confinement upstream of Llanidloes and through the Ironbridge Gorge limited natural adjustment (eg: Caersws (Plate 4.4)), and thereby developed a channel adapted to the flow regime (Figure 4.31) but with little variation in planform geometry (Figure 4.33); the transition to an alluvial channel at Llanidloes allowed greater freedom for the channel form to adjust to local differences in flow hydraulics (eg: Caersws and Pool Quay). Non-linear responses by flow variables to unsteady flow were dominated by channel form: for example, the model showed that confined reaches at Dolwen and Buildwas experienced 50 - 100 % increase in water width between rising / falling stage; the unconfined reach at Crew Green experienced an increase of greater than 500 %, with the direction and form of the loop dependent upon upstream and downstream hydraulic controls and floodplain inundation (Figure 6.1). The discontinuous increase of maximum hydraulic radius downstream from Dyffryn (Figure 6.4) indicates the enhanced incision by the channel into the floodplain alluvium, as observed by Hey (1975, cited in Lewin, 1987). Maximum hydraulic radius remains relatively constant at 3 - 4 m between Dyffryn (75 km downstream) and Bewdley (210 km), perhaps reflecting channelisation schemes designed to enhance channel capacity, maintain stability and form, and aid navigation in the middle and lower reaches. Therefore the detailed downstream predictions from the model could offer the engineer the opportunity to study the impact of management schemes, in terms both the hydrological impact (flood risk) and the effect of a change of flow regime and / or channel form on the channel hydraulics (channel instability risk).

At a constant flow frequency, mean velocity increased downstream from 0.2 - 1.5 m s<sup>-1</sup> under high flow conditions, confirming earlier trends defined by Leopold (1953). However, the reach-scale variability was great, particularly downstream from Llanidloes where mean velocity varied by up to 1.0 m s<sup>-1</sup> between reaches (eg: Montford - Buildwas) (Figure 4.34). This implies that the downstream increase in discharge and decline in roughness are sufficient to overcome the sharp reduction in slope. However, confinement and steep valley slopes in the upper reaches elevate unsteady flow velocities, resulting in a downstream decline in maximum flow velocity during a flow event (Figure 6.6), as Carlston (1969) observed on the Mississippi. This is consistent with wave simulation analysis results which indicate that floodwaves attenuate less and travel faster through confined channels (section 7.4). The peaks in mean velocity in advance of the flood peak, perhaps caused by enhanced water surface slopes and lower channel roughness at higher stages, may be responsible for peak sediment concentrations on the rising limb of floodwaves (Bull, 1996). This analysis of the event simulation conforms with previous theoretical and simulated models of the longitudinal behaviour of wave hydraulics (Woltemade, 1993; Mishra & Seth, 1996) , but also provides supportive evidence to theories by Burkham (1976) and Wolfe and Burges (1994) that the morphological form of the channel (ie: constrictions, expansions and tributaries) plays a significant role in modifying the wave velocity and attenuation. However, the present lack of information concerning reach-scale approximations of flow resistance is illustrated by the excessive mean velocities simulated near Dyffryn (Figure 6.6) ( $u = 6.5 \text{ m s}^{-1}$ ) which indicate that the

hydraulics through that reach and perhaps other reaches may not be representative of actual flow conditions by a factor of two (Figure 4.34).

The Afon Vyrnwy alters the flow regime of the Severn downstream from the confluence (Figure 6.9), and in turn dominates the spatial distribution of discharge and other channel hydraulic parameters for up to 100 km downstream. The rapid increase in discharge at the headwaters ( $0.003 - 20 \text{ m}^3 \text{ s}^{-1}$  from Upper Hafren 1 to Mount Severn at low flow conditions) is generated by efficient flow routing through the dense network of tributaries and artificial agricultural drains in Plynlimon. The downstream rate of increase in discharge,  $Q_{\text{high}} = 1.17 DD^{1.02}$ , was similar at all three flow frequencies (low,  $F \geq 70 \%$ ; medium,  $10 \leq F \leq 70 \%$ ; high,  $F \leq 10 \%$ ) (Figure 4.35), although flow abstraction (Douglas, 1988) and uncertainties in field calculations may explain the comparable medium- and high-flow discharges in the lower reaches.

Peaks in water surface slope occurred through laterally-constrained reaches (eg: Upper Hafren 2 =  $0.047 \text{ m m}^{-1}$ ), or at bedrock outcrops (eg: Newtown =  $0.0063 \text{ m m}^{-1}$ ). High water surface slopes near the source, between Upper Hafren 1 and Severn Ford (Figure 4.36), and through the Ironbridge Gorge varied little with stage (Figure 6.10), reflecting the lithological control over the magnitude and spatial adjustment of hydraulic parameters (Magilligan, 1992). Downstream from Llanidloes, slopes became more variable spatially and temporally (Figure 4.36) as a result of enhanced reach-scale adjustment in the channel geometry, planform and roughness through the alluvial floodplain. Slopes were more variable at low flows, and more difficult to measure accurately, because flow obstructions (eg: riffles, boulders and vegetation) disrupt the water surface profile by enhancing the boundary and channel roughness (Bathurst, 1993). The temporal response to unsteady flow was small (temporal change  $< 0.0002 \text{ m m}^{-1}$ ) in the three selected reaches (section 6.5), although inundation of the floodplain at Crew Green caused a small rise in slope from  $0.0002$  to  $0.00031 \text{ m m}^{-1}$ . This was perhaps attributable to an upstream hydraulic control, such as the Vyrnwy confluence, which increased the gradient of the water in the downstream reach. However, the difference in length of reaches used to calculate water surface slopes in the field and model inevitably generates inaccuracies between the two datasets, and measures to reduce the long reach length in the model were resisted to optimise computer memory. Small differences in water surface slopes therefore between field and model datasets may thus be created.

Flow resistance generally declined downstream from the source, although at low- and medium-flow levels resistance increased from  $n = 0.3$  to  $1.1$  downstream to Llanidloes. Resistance decreased with stage from  $n = 0.11$  to  $0.02$  at Bewdley (Figure 4.37), in response to a decline in the effectiveness of bed and form roughness elements as discharge increased (Bathurst, 1993). This decline was accentuated at Llanidloes where the channel form is transformed rapidly between non-alluvial and alluvial states (section 7.7). However, between Dolwen and Bridgnorth (Figure 7.7), resistance was equally likely to *increase* with stage because bank-side roughness components (planform, vegetation) became submerged at higher stages (as observed by Beven & Carling (1992) also on the Severn). There was also a tendency for the location at which roughness declined to very low levels to advance *upstream* with increasing flow frequency (Figures 4.37 & 4.38). Peaks in resistance along the Severn of  $n > 0.2$  coincided with regions

of channel and valley confinement where bedrock outcrops and boulder deposits impart exaggerated resistance to the flow; these occurred at Plynlimon, Newtown and Dyffryn (Figure 4.37). Nevertheless, the Ironbridge Gorge did not exhibit unusually high values of Manning's  $n$  or Darcy-Weisbach  $f$  ( $n = 0.03 - 0.20$ ), although this may be caused by the rapid change of depth with stage resulting in a decreased effectiveness of the roughness elements on the channel bed.

### *8.2.2 Downstream distribution of stream power and shear stress*

Unit stream power and reach mean shear stress were found to peak within 10 km of the source of the Severn ( $\tau = 119 \text{ N m}^{-2}$ ), whereas total stream power increased with distance downstream as far as Buildwas ( $\Omega = 2600 \text{ W m}^{-1}$ ). The distribution of boundary shear stress differed greatly from reach mean shear stress, in terms of magnitude and downstream trend, although the measurement strategy in coarse gravel channels was difficult to accomplish. The presence of an energy peak is consistent with the findings of Graf (1982; 1983a), Lewin (1982; 1983; 1987), Baker and Costa (1987), Lawler (1992), Magilligan (1992) and Lecce (1993). However, the peak is closer to the source than previously anticipated by Lewin (1987) (Figure 7.21), it is less localised than for the tributaries of the Blue River, Wisconsin (Lecce, 1993) or the Henry Mountains basins (Graf, 1982; 1983a) (Figure 7.15), and it is serially reproduced elsewhere in the catchment in both the field and model results, most notably at the lithologically controlled zones of hydraulic transition (Figure 7.24). Furthermore, the variable downstream trend is inconsistent with the gradual downstream change conceptualised by Knighton (1987) and the spatial uniformity hypothesised by Kapour (1990).

Local channel lithology appears to dominate the spatial variation of stream power and shear stress in the Severn basin: high energy levels in laterally-confined channels and valleys are created by enhanced valley slopes and constrained water widths (Magilligan, 1992; Lecce, 1993); conversely, wide, low-gradient channels which are free to inundate the floodplain generate lower energy levels (Magilligan, 1992). These results are consistent with the study on the Allt Dubhaig by Ferguson and Ashworth (1991) in which the downstream adjustment of channel form was believed to be induced by slopes inherited from the deglacial period. Flow magnitude dominates the variation of stream energy with stage, resulting in greater variability through laterally-confined reaches, such as the Severn headwaters and the Ironbridge Gorge (Figure 6.12). Inter-reach variability was high from local variations in water elevation and channel topography through pool-riffle sequences and meanders. At low-flows these dominate the downstream distribution, although at higher flows and at the resolution achieved in this study, a series of peaks and troughs in fluvial energy were evident (Figure 6.12). This reflects the discontinuous impact of external controls, especially at Llanidloes, the Vyrnwy confluence and Ironbridge (Figure 3.1), on the hydraulic processes operating along the Severn.

### *8.2.3 The potential for 1-D modelling of channel hydraulics at a catchment-scale*

Chapters 5 and 6 demonstrated how the 1-D MIKE11 model parameterised the Severn channel geometry and simulated the variation of channel hydraulic parameters during an individual event. The high model resolution in space (1 km) and time (15 min) enabled the distribution of the hydraulic parameters to be

analysed in greater detail than previously possible (Magilligan, 1992). The similarity between the modelled and measured field data (peak discharge predicted to within  $20 \text{ m}^3 \text{ s}^{-1}$  (section 5.4.4)) indicated the relative accuracy of the simulation, even given the computational constraints imposed by the 1-D representation of 3-D processes over the 250 km channel length. Such constraints included the parameterization of over-bank flow using 1-D approximations (section 5.4.5), the non-linear response of flow resistance to temporal variations in stage in a reach during a flood event (section 7.3.3), the simulation of flow in steep, hydraulically rough channels and the definition of a reach length for the computation of reach-averaged hydraulic parameters (section 7.3.2). These factors demonstrate the need for further investigation.

The EA database provided cross-section information which both coincided with field study sites (Figure 5.12), and covered the majority of the fluvial Severn downstream from Abermule, at a spacing of only 500 m. The unsteady flow event reached a similar magnitude to the measured steady high-flow (at Bewdley, maximum discharge simulated =  $220 \text{ m}^3 \text{ s}^{-1}$ , and measured =  $230 \text{ m}^3 \text{ s}^{-1}$ ). Partitioning of the Severn channel into four reaches (Figure 5.13) enabled hydraulics to be simulated over reach lengths of approximately 50 km; the calibration experiment (section 5.4.4) highlighted that little accuracy was lost, for a gain in spatial resolution and computational efficiency. However, the model validation showed that although reach mean shear stress and unit stream power were simulated to within an order of magnitude at most sites (section 5.4.6), differences between the section geometries and roughness in the field and the model were sufficient to alter the channel hydraulics, particularly at higher stages (section 7.3). Furthermore, the bankfull level attained in most reaches generated hydraulic information which may be cross-correlated with studies in other rivers and fluvial environments; it also limited the difficult representation of floodplain inundation, storage and flow to isolated regions in the catchment (Vyrnwy confluence and upstream of Buildwas) (Figure 6.2).

The model simulation of hydraulics along the Severn provides a simple tool for evaluating the geomorphological, hydrological and lithological controls which dominate the transfer of water and sediment through river basins. It has highlighted the significance of scale and resolution in the representation of reach-scale hydraulic processes, and the limitations of traditional field techniques. It has the potential to complement, but not replace, field methods through the interpolation of hydraulics through ungauged reaches and improve our understanding of the mechanisms behind floodwave generation and propagation, river channel adjustment, floodplain inundation, and sediment transport.

#### *8.2.4 Downstream propagation of floodwaves*

The simulated flow event (February 1989) and other events in the hydrological years, 1994-5, which occurred during the field programme demonstrated the significance of downstream variations in channel form and event magnitude on floodwave propagation. Channel confinement enhanced mean wave peak velocities from  $1.0$  to  $3.8 \text{ m s}^{-1}$  between Buildwas and Saxons Lode (September 1994) (Figure 7.13) by increasing the conveyance capacity of the channel and limiting the attenuation of the wave form. Through incised (Pool Quay) or laterally-confined reaches (Plynlimon, Dyffyn, Ironbridge Gorge), mean wave peak velocity was high (eg:  $3 \text{ m s}^{-1}$  between Caersws - Abermule, February 1995) and attenuation

was minimised; at Dolwen and Buildwas (both laterally-confined), the passage of the floodwave resulted in little or no change in the channel hydraulic parameters between the rising and falling limbs of the hydrograph (Figure 6.9 a and c). In wide channel reaches, mean wave peak velocity was lower and the wave form attenuated because the high relative roughness of weakly inundated floodplains restricted wave speeds, and enhanced lateral momentum diffusion and storage. Non-linear response to the rising and falling limbs of the hydrograph in the channel hydraulic parameters was also pronounced (Figure 6.9 b), although the direction differed between parameters. The model simulation results agree with Mishra and Seth (1996) who found that changes in the physical character of a channel reach alter the form of the wave (dynamic or kinematic) and velocity, shape and at-a-section hysteresis. The results from this study suggest that mean wave peak velocity for in-channel flow events exceed velocities for moderate over-bank flow events; however for extreme magnitude events, mean wave peak velocity is expected to be positively related to event magnitude. Interaction between channel form and mean wave peak velocity demonstrates that sediment transport (Meigh, 1987) and bank erosion studies (Bull, 1996) should examine the hydraulic characteristics of the wave, as the geometry and location of study reaches within the catchment play a significant role in the propagation and development of a flow event.

#### *8.2.5 Downstream interaction between channel hydraulics, bank erosion and sediment transport*

Peak shear stresses and stream powers occur in the upper 10 km of the Severn basin (< 100 km<sup>2</sup>) and therefore do not occur in reaches of maximum channel mobility, as defined by Lewin (1987) (section 7.7; Figure 7.21). It is suggested that this is caused by bank resistance controlling the entrainment of sediment from the bed and banks (Harris, in prep). Along the Severn, maximum channel mobility occurs where the energy levels of the flow are sufficient to overcome the resistance of the banks; this coincides with the development of a coarse gravel sublayer at Caersws (Couperthwaite *et al.*, 1996; Harris, in prep). The relationship between the stream power peak and maximum channel mobility inferred by Newson (1981), Lewin (1983; 1987) for the Severn may therefore be misleading. The energy peaks indicate where lateral adjustment may be *potentially* maximised, although these peaks are most likely to occur in regions of lateral constraint in response to a confined flow path which increases the energy gradient and prevents over-bank flow.

The location of points of sediment removal and storage along the Severn appear to be related to the transport parameters, total and unit stream power (section 7.8). A comparison with the study by Walling and Quine (1993) on the Severn (Figure 7.24), who investigated the spatial distribution of fluvial deposits using Caesium-134 from Chernobyl fallout, demonstrates that an inverse relationship may exist between fluvial energy and channel storage in the reaches examined. This study has indicated that in zones of moderate to high unit stream power (eg: the 'piedmont' zone and Ironbridge Gorge), the rate of sediment reworking is high, storage is low and the volume of deposit is small. Whereas, in low energy zones (eg: Vyrnwy confluence, and between Bewdley and Worcester) the transport capacity of the flow is reduced, selective deposition is enhanced and the volume of sediment deposited increases.

Discontinuities in the spatial distribution of channel hydraulics potentially impact upon the zonation of stream habitats (Statzner & Higler, 1986). Zones of hydraulic transition, represented by abrupt changes

in reach-scale hydraulics, produce 'hot-spots' for species diversity as ecological habitats overlap and competition for limited resources increases (Statzner *et al.*, 1988; Hiebert, 1996). The presence of these hydraulic transition zones along the Severn in the reaches: Llanidloes - Newtown; Dyffryn - Montford; and Buildwas - Bewdley, is consistent with the theory proposed by Statzner and Higler (1986). Moreover, these physical discontinuities (Figure 7.26), and lakes (Milner & Petts, 1994), in the fluvial system extend the Serial Discontinuity Concept (Ward and Stanford, 1983; 1995), from a view-point based solely upon the ecological impact of single and multiple impoundments in river basins to an appreciation of natural variability in river basins. Hence, this detailed analysis of basin-scale hydraulics has assisted in the identification of the hypothesised hydraulic transitions (Statzner & Higler, 1986) and boundaries (Naiman *et al.*, 1988) proposed in the ecological sciences.

### **8.3 Potential for further research**

This final section will consider the outstanding problems raised by this research project and provide some suggestions for future initiatives to explore this field of hydraulic research.

1. This study has concentrated on examining a single river channel in considerable detail, albeit one of the largest in the UK. A less detailed, but more extensive, approach may be adopted to the field and model analysis of several channels of different sizes in similar, and diverse, fluvial environments. Therefore, the impact of scale, flow regime, geology and land use on the spatial variation of hydraulic processes could be tested more thoroughly.
2. The field study was prevented from analysing individual flood events by time, financial and logistical constraints. Such an investigation, carried out synchronously at several locations in an intensively monitored basin using Advanced Doppler Velocity Profiling (ADVP) equipment, would provide important information regarding the downstream change in floodwave hydraulics and channel adjustment, the temporal variation of channel roughness and point boundary shear stresses, the inter-relationship between sediment transport and hydraulics at the event time-scale, and a complementary analysis of the February 1989 model fixed-bed simulation.
3. A lack of understanding concerning the temporal variation of roughness in natural channels, and mechanisms governing the transport and storage of flow over floodplains has restricted their parameterization and simulation in the MIKE11 model. Further field investigation is necessary before these important hydraulic factors are simulated correctly in current hydraulic models.
4. Results from this study suggest that mean boundary shear stress and reach mean shear stress are poorly correlated. An accurate estimation of the energy gradient, and therefore reach mean shear stress, is dependent upon the section geometry and length of the channel reach selected. The inappropriateness of reach mean shear stress (and stream power) in non-uniform, sinuous reaches limits the potential usefulness of understanding active fluvial processes in meander bends and braided reaches using simple hydraulic parameter estimation techniques; hence, this may perhaps explain the weak relationship between bank erosion and stream power found by Lewin (1987) and in

this study. Therefore, a closer examination of the shear stress / stream power peak and the boundary shear stress distribution in the upper Severn basin (and other basins) and at the zone of maximum channel activity (Llandinam - Newtown) may help evaluate the relationship between reach-averaged and point measurements of shear stress and bank erosion activity.

5. The MIKE11 model representation of the Severn channel successfully simulated the unsteady flow of an event at a 1 km resolution along the 250 km reach. However, it was limited by computer memory problems which prevented all EA cross sections from being included, and a complete model run being performed between the headwaters and Saxons Lode. Also, the channel geometry was less well represented in the upper Severn basin, between the source and Llanidloes. Furthermore, bridges, abstractions, complex flow paths (eg: Morda Gap flow (Lindsay, 1995)) and floodplain storage nodes were omitted. The model simulation would be greatly improved if each of these issues were resolved.
6. The model simulation concentrated on a single flow event (18 - 24 February 1989), although this was believed to be representative as it achieved a bankfull level in most parts of the catchment and therefore makes the results comparable with other geomorphological studies (eg: Lewin, 1987; McEwen, 1994). Further examination of other events in the catchment would assist in the validation of the model, and the evaluation of temporal changes in channel hydraulic distributions along the channel for events of varying magnitude, origin and character.

#### **8.4 Summary**

This study has extended our understanding of the downstream distribution of channel hydraulic parameters at a basin-scale, through the application of conventional fieldwork methods and a 1-D model simulation. The analysis of individual parameters over steady and unsteady flows has revealed that longstream patterns are spatially discontinuous, in response to external hydrological and geological controls. Furthermore, the detailed spatial and temporal variation of fluvial energy through a basin has not been evaluated previously. Hence, this study has important implications for evaluating the distribution of fluvial deposits which are found to be related to total and unit stream power. Nevertheless, bank erosion activity is found to be only weakly related to fluvial energy, because of the control exerted by longstream variations in bank resistance. The spatial variability of channel geometry, slope and degree of valley confinement also appear to affect floodwave propagation, particularly the velocity of the wave peak and wave attenuation. This study has therefore provided some insight into the exploration of this research area and several specific ideas for future initiatives in the field of fluvial geomorphology.

## REFERENCES

- Abbott, M. B. 1979. *Computational Hydraulics: Elements of the Theory of Free Surface Flow*, Pitman Press, Bath, 324 pp.
- Alabyan, A. 1996. 'A computer model of bank erosion based on secondary flow simulation', in Ashworth, P. J., Bennett, S. J., Best, J. L. and McLelland, S. J. (Eds) *Coherent Flow Structures in Open Channels*, John Wiley & Sons, Chichester, 567-580.
- Allen, J. R. L. 1977. 'Changeable rivers: some aspects of their mechanics and sedimentation', in Gregory, K. J. (Ed), *River Channel Changes*, John Wiley & Sons, Chichester, 15-45.
- Andrews, E. D. 1979. 'Hydraulic adjustment of the East Fork River, Wyoming to the supply of sediment', in Rhodes, D. D. and Williams, G. P. (Eds), *Adjustments of the Fluvial System*, Kendall/Hunt, Dubuque, Iowa, 69-94.
- Andrews, E. D. 1983. 'Entrainment of gravel from naturally sorted riverbed material', *Geological Society of America Bulletin*, **94**, 1225-1231.
- Andrews, E. D. 1984. 'Bed-material entrainment and hydraulic geometry of gravel-bed rivers in Colorado', *Geological Society of America Bulletin*, **95**, 371-378.
- ASCE 1963. 'Friction factors in open channels', (Task Force Report), *Journal of the Hydraulics Division*, **89**, 97-143.
- Archer, D. R. 1989. 'Flood wave attenuation due to channel and floodplain storage and effects on flood frequency', in Beven, K. and Carling, P. (Eds), *Floods: Hydrological, Sedimentological and Geomorphological Implications*, John Wiley & Sons, Chichester, 37 - 46.
- Ashmore, P. E. 1991. 'How do gravel-bed rivers braid?', *Canadian Journal of Earth Sciences*, **28**, 326-341.
- Ashmore, P. E. and Day, T. J. 1988. 'Spatial and temporal patterns of suspended-sediment yield in the Saskatchewan River basin', *Canadian Journal of Earth Sciences*, **25**, 1450-1463.
- Ashworth, P. J. and Ferguson, R. I. 1986. 'Intrrelationships of channel processes, changes and sediments in a proglacial river', *Geographiska Annaler*, **68A**, 361-371.
- Ashworth, P. J. and Ferguson, R. I. 1989. 'Size-selective entrainment of bedload in gravel-bed streams', *Water Resources Research*, **25**, 627-634.

- Ashworth, P. J., Ferguson, R. I., Ashmore, P. E., Paola, C., Powell, D M. and Prestegard, K. L. 1992. 'Measurements in a braided river chute and lobe II: sorting of bedload during entrainment, transport and deposition', *Water Resources Research*, **28**, 1887-1896.
- Bagnold, R.A. 1960. 'Sediment discharge and stream power: a preliminary announcement', *Circular: U.S. Geological Survey*, **421**.
- Bagnold, R. A. 1966. 'An approach to the sediment transport problem from general physics', *U.S. Geological Survey Profesional Paper*, **422-I**.
- Baker, V. R. and Ritter, D. F. 1975. 'Competence of rivers to transport coarse bedload material', *Geological Society of America Bulletin*, **86**, 975-978.
- Baker, V. R. and Costa, J. E. 1987. 'Flood power', in Mayer, L. and Nash D. (Eds), *Catastrophic Flooding*, Allen and Unwin, Boston, 1-21.
- Baker, V. R. and Kochel, R. C. 1988. 'Flood sedimentation in bedrock fluvial systems', in Baker, V. R., Kochel, R. C. and Patten, P. C. (Eds) *Flood Geomorphology*, John Wiley & Sons, New York, 123-137.
- Barnes, H. H. 1967. 'Roughness characteristics of natural streams', *U.S. Geological Survey Water Supply Paper*, **1849**.
- Bathurst, J. C. 1977. *Resistance to Flow in Rivers with Stoney Beds*, Unpublished Ph.D thesis, University of East Anglia.
- Bathurst J. C. 1979. 'Distribution of boundary shear stress in rivers', in Rhodes, D.D. and Williams, G.P. (Eds) *Adjustments of the Fluvial System*, Kendall/Hunt, Dubuque, Iowa, 95-116.
- Bathurst, J. C. 1982. 'Theoretical aspects of flow resistance', in Hey, R. D., Bathurst, J. C. and Thorne, C. R. (Eds), *Gravel-Bed Rivers*, John Wiley & Sons, Chichester, 83-108.
- Bathurst, J. C. 1985. 'Flow resistance estimation in mountain rivers', *Journal of the Hydraulics Division*, **111**, 625-643.
- Bathurst, J. C. 1988. 'Flow resistance of large scale roughness', *Journal of the Hydraulics Division*, **104**, 1587-1603.
- Bathurst, J. C. 1993. 'Flow resistance through the channel network', in Beven, K. and Kirkby, M.J. (Eds), *Channel Network Hydrology*, John Wiley & Sons, Chichester, 69-98.

- Bathurst, J. C., Thorne, C. R. and Hey, R. D. 1977. 'Direct measurements of secondary currents in river bends', *Nature*, **269**, 504-506.
- Bathurst, J. C., Thorne, C. R. and Hey, R. D. 1979. 'Secondary flow and shear stress at river bends', *Journal of the Hydraulics Division*, **105**, 1277-1295.
- Beckinsale, R. P. and Richardson, L. 1964. 'Recent findings on the physical development of the Lower Severn valley', *Geographical Journal*, **130**, 87-105.
- Begin, Z. B. 1981. 'The relationship between flow-shear stress and stream pattern', *Journal of Hydrology*, **52**, 307-319.
- Best, J. L. 1992. 'On the entrainment of sediment and initiation of bed defects: insights from recent developments within turbulent boundary layer research', *Sedimentology*, **39**, 737-752.
- Beven, K. and Kirkby, M. J. 1979. 'A physically-based variable contributing-area model of catchment hydrology', *Hydrological Sciences Bulletin*, **24**, 43-69.
- Beven, K., Kirkby, M. J., Schofield, N. and Tagg, A. F. 1984. 'Testing a physically-based flood forecasting model (TOPMODEL) for three UK catchments', *Journal of Hydrology*, **69**, 119-143.
- Beven, K. and Carling, P. A. 1992. 'Velocities, roughness and dispersion in the lowland River Severn', in Carling, P. A. and Petts, G. E. (Eds), *Lowland Floodplain Rivers: Geomorphological Perspectives*, John Wiley & Sons, Chichester, 71-93.
- Beven, K. and Wood, E. F. 1993. 'Flow routing and hydrological response of channel networks', in Beven, K. and Kirkby, M. J. (Eds), *Channel Network Hydrology*, John Wiley & Sons, Chichester, 99-129.
- Bethess, R. and White, W. R. 1987. 'Extremal hypotheses applied to river regime', in Thorne, C.R., Bathurst, J.C. and Hey, R.D. (Eds) *Sediment Transport in Gravel Bed Rivers*, John Wiley & Sons, Chichester, 767-789.
- Beyer, N. A. and Portner, C. 1994. 'MIKE11: Hydrodynamic simulation of flood protection systems', *Hydroinformatics '94*, Rotterdam, Brookfield, 407-414.
- Bhowmik, N. G. 1982. 'Shear stress distribution and secondary currents in straight open channels', in Hey, R.D., Bathurst, J.C. and Thorne, C.R. (Eds), *Gravel-Bed Rivers*, John Wiley & Sons, Chichester, 31-61.
- Bhowmik, N. G. 1984. 'Hydraulic geometry of floodplains', *Journal of Hydrology*, **68**, 369-401.

- Bhowmik, N. G. and Demissie, M. 1982. 'Carrying capacity of flood plains', *Journal of the Hydraulics Division*, **108**, 443-452.
- Billi, P., Hey, R. D., Thorne, C. R. and Tacconi, P. (Eds) 1990. *Dynamics of Gravel-Bed Rivers*, John Wiley & Sons, Chichester, 673pp.
- Bonnett, P. J. P., Leeks, G. J. L. and Cambray, R. S. 1989. 'Transport processes for Chernobyl labelled sediment: preliminary evidence from upland Mid Wales', *Land Degradation and Rehabilitation*, **11**, 39-50.
- Bray, D. I. 1982. 'Flow resistance in gravel bed rivers', in Hey, R.D., Bathurst, J.C. and Thorne, C.R. (Eds), *Gravel-Bed Rivers*, John Wiley & Sons, Chichester, 109-138.
- Brayshaw, A. C., Frostick, L. E. and Reid, I. 1983. 'The hydrodynamics of particle clusters and sediment entrainment in coarse alluvial channels', *Sedimentology*, **30**, 137-143.
- Brebner, A. and Wilson, K. C. 1967. 'Derivation of the regime equation from relationships for pressurized flows', *Proceedings of the Institute of Civil Engineers*, **36**, 47-62.
- Bridge, J. S. 1977. 'Flow, bed topography, grain size and sedimentary structure in open channel bends: a three dimensional model', *Earth Surface Processes*, **2**, 401-416.
- Bridge, J. S. and Jarvis, J. 1976. 'Flow and sedimentary processes in the meandering River Soth Esk, Glen Cova, Scotland', *Earth Surface Processes*, **1**, 303-337.
- Bridge, J. S. and Jarvis, J. 1977. 'Velocity profiles and bed shear stress over various bed configurations in a river bend', *Earth Surface Processes*, **2**, 281-297.
- Bridge, J. S. and Jarvis, J. 1982. 'The dynamics of a river bend: a study in flow and sedimentary processes', *Sedimentology*, **5**, 499-540.
- Brierley, G. J. and Hickin, E. J. 1985. 'The downstream gradation of particle sizes in the Squamish River, British Columbia', *Earth Surface Processes and Landforms*, **10**, 597-606.
- British Standards Institution 3680, 1980. *Measurement of Liquid Flow in Open Channels: Velocity-Area Methods*, Part 3A, 9 pp.
- Brookes, A. 1988. *Channelized Rivers: Perspectives for Environmental Management*, John Wiley & Sons, Chichester, 326pp.
- Brown, A. G. 1987. 'Holocene floodplain sedimentation and channel response of the lower River Severn, United Kingdom', *Zeitschrift fur Geomorphologie*, **31**, 293-310.

- Brush, L. M. 1961. 'Drainage basins, channels, and flow characteristics of selected streams in Central Pennsylvania', *U. S. Geological Survey Professional Paper*, **282-F**, 145-181.
- Bull, W. B. 1979. 'Threshold of critical power in stream', *Geological Society of America Bulletin*, **90**, 453-464.
- Bull, L. J., Lawler, D. M., Leeks, G. J. L. and Marks, S. 1995. 'Downstream changes in suspended sediment fluxes in the River Severn, UK', in Osterkamp, W. R. (Ed) *Effects of Scale on Interpretation and Management of Sediment and Water Quality*, IAHS, **226**, 27-36.
- Bull, L. J. 1996. *Dynamics of Fluvial Sediment Transport and River-Bank Sediment Supply*, Unpublished Ph.D thesis, University of Birmingham.
- Burkham, D. E. 1970. 'Channel changes of the Gila River of Safford Valley, Arizona, 1846-1970', , *U. S. Geological Survey Professional Paper*, **655-G**, 24pp.
- Burkham, D. E. 1976. 'Effects of changes in an alluvial channel on the timing, magnitude and transformation of flood waves, southeastern Arizona', *U. S. Geological Survey Professional Paper*, **655-K**, 25pp.
- Burkham, D. E. and Dawdy, D. R. 1976. 'Resistance equation for alluvial-channel flow', *Journal of the Hydraulics Division*, **102**, 1479-1489.
- Burrin, P. J. 1980. 'A review of valley fill sediments and floor morphology in the Severn valley', in *Palaeohydrology of the Temperate Zone: Previous Research and Research Objectives*, May 1981, IGCP Project 158.
- Calver, A., Kirkby, M. J. and Weyman, D. R. 1972. 'Modelling hillslope and channel flows', in Chorley, R. J. (Ed), *Spatial Analysis in Geomorphology*, Methuen, London, 197-220.
- Carling, P. A. 1983. 'Threshold of coarse sediment transport in broad and narrow natural streams', *Earth Surface Processes and Landforms*, **8**, 1-18.
- Carling, P. A. 1988. 'Channel change and sediment transport in regulated UK rivers', *Regulated Rivers: Research and Management*, **2**, 369-387.
- Carling, P. A. 1991. 'An appraisal of the velocity-reversal hypothesis for stable pool-riffle sequences in the River Severn, England', *Earth Surface Processes and Landforms*, **16**, 19-31.

- Carling, P. A. 1992. 'The nature of the fluid boundary layer and the selection of parameters for benthic ecology', *Freshwater Biology*, **28**, 273-284.
- Carling, P. A. 1995. 'Implications of sediment transport for instream flow modelling of aquatic habitat', in Harper, D. M. and Ferguson, A. J. D. (Eds) *The Ecological Basis for River Management*, John Wiley & Sons, Chichester, 17-31.
- Carling, P. A. and Glaister, M. S. 1988. 'Reconstruction of a flood resulting from a moraine dam failure using geomorphological evidence and dam-break modelling', in Baker, V. R., Kochel, R. C. and Patten, P. C. (Eds) *Flood Geomorphology*, John Wiley & Sons, New York, 181-200.
- Carling, P. A. and Wood, N. 1994. 'Simulation of flow over pool-riffle topography: a consideration of the velocity reversal hypothesis', *Earth Surface Processes and Landforms*, **19**, 319-332.
- Carlston, C. W. 1969. 'Downstream variations in the hydraulic geometry of streams: special emphasis on mean velocity', *American Journal of Science*, **267**, 499-599.
- Cebeci, T. and Bradshaw, P. 1977. *Momentum Transfer in Boundary Layers*, McGraw-Hill, New York.
- Chadwick, A. and Morfett, J. 1986. *Hydraulics in Civil Engineering*, Allen and Unwin, London, 492pp.
- Chang, H. H. 1979. 'Minimum stream power and river channel patterns', *Journal of Hydrology*, **41**, 303-327.
- Chang, H. H. 1980. 'Geometry of gravel streams', *Journal of the Hydraulics Division*, **106**, 1443-1456.
- Charlton, F. W., Brown, P. M. and Benson, R. W. 1978. *The hydraulic geometry of some gravel bed rivers in Britain*, Hydraulics Research Station Report, IT 180.
- Chow, V. T. 1959. *Open-Channel Hydraulics*, McGraw-Hill Book Co., 680pp.
- Church, M. A., McLean, D. G. and Wolcott, J. F. 1987. 'River bed gravels: sampling and analysis', in Thorne, C. R., Bathurst, J. C. and Hey, R. D. (Eds), *Sediment Transport in Gravel-bed Rivers*, John Wiley & Sons, Chichester, 43-88.
- Clifford, N. J. and Richards, K. S. 1992. 'The reversal hypothesis and the maintenance of riffle-pool sequences: a review and field appraisal', in Carling, P. A. and Petts, G. E. (Eds), *Lowland Floodplain Rivers: Geomorphological Perspectives*, John Wiley & Sons, Chichester, 43-70.
- Coles, D. 1968. 'The law of the wake in the turbulent boundary layer', *Journal of Fluid Mechanics*, **1**, 191-226.

- Coleman, N. L. 1981. 'Velocity profiles with suspended sediment', *Journal of Hydraulic Research*, **19**, 211-229.
- Coleman, N. L. 1986. 'Effects of suspended sediment on the open-channel velocity distribution', *Water Resources Research*, **22**, 1377-1384.
- Costa, J. E. 1983. 'Palaeohydraulic reconstruction of flash-flood peaks from boulder deposits in the Colorado Front Range', *Geological Society of America Bulletin*, **94**, 986-1004.
- Costa, J. E. 1988. 'Rheologic, geomorphic and sedimentologic differentiation of water floods, Hyperconcentrated flows, and debris flows', in Baker, V.R., Kochel, R.C. and Patton, P.C. (Eds) *Flood Geomorphology*, John Wiley & Sons, New York, 113-122.
- Couperthwaite, J. S., Lawler, D. M., Bull, L. J. and Harris, N. M. 1996. 'Downstream change in channel hydraulics and river bank erosion rates in the Upper Severn, UK', *Proceedings of the Interceltic Colloquium on Hydrology and Water Management*, Brittany, France, 93-101.
- Cowan, W. L. 1956. 'Estimating hydraulic roughness coefficients', *Agricultural Engineering*, **37**, 473-475.
- Culling, W. E. 1988. 'A new view of the landscape', *Transactions of the Institute of British Geographers*, **13**, 345-360.
- Cunge, J. A., Holly, F. M. and Verwey, A. 1980. *Practical Aspects of Computational River Hydraulics*, Pitman Press, Bath, 420pp.
- Danish Hydraulics Institute 1990. *MIKE11 User Manual*, Danish Hydraulics Institute.
- Davidson, D. A. 1978. *Science for Physical Geographers*, Arnold, London.
- Davies, T. R. H. 1987. 'Channel boundary shape - evolution and equilibrium', in Richards, K. (Ed), *River Channels: Environment and Process*, Methuen, 228-248.
- Davies, T. R. H. and Sutherland, A. J. 1983. 'Extremal hypotheses for river behaviour', *Water Resources Research*, **19**, 141-148.
- Davies, T. R. H. and Sutherland, A. J. 1984. Reply to comment, *Water Resources Research*, **20**, 741-742.
- Davy, B. W. and Davies, T. R. H. 1979. 'Entropy concepts in fluvial geomorphology: a reevaluation', *Water Resources Research*, **15**, 103-106.

- Dawson, F. H. 1978. 'The seasonal affects of aquatic plant growth on the flow of water in a stream', *Proc. EWRS 5th Symposium on Aquatic Weeds*, 71-78.
- Dawson, M. R. and Gardner, V. 1987. 'River terraces: a general model and a palaeohydrological and sedimentological examination of the Late Devensian terraces of the Lower Severn basin', in Gregory, K. J., Lewin, J. and Thornes, J. B. (Eds) *Palaeohydrology in Practice*, John Wiley & Sons, Chichester.
- Death, R. G. and Winterbourn, M. J. 1995. 'Diversity patterns in stream benthic invertebrate communities: the influence of habitat stability', *Ecology*, **76**, 1446-1460.
- Dietrich, W. E. 1987. 'Mechanics of flow and sediment transport in river bends', in Richards, K. S. (Ed) *River Channel: Environment and Process*, Basil Blackwell, England, 179-217.
- Dietrich, W. E. and Whiting, P. 1989 'Boundary shear stress and sediment transport in river meanders of sand gravel', in Ikeda, S. and Parker, G. (Eds), *River Meandering*, American Geophysical Union (Water Resources Monograph no. 12), Washington, 1-50.
- Douglas, J. R. 1988. 'Regulating the River Severn', *Regulated Rivers: Research and Management*, **2**, 309-322.
- Dunne, T and Leopold, L. B. 1978. *Water in Environmental Planning*, San Francisco: Freeman.
- Dury, G. H. 1983. 'Osage-type underfitness on the River Severn near Shrewsbury, Shropshire, England', in Gregory, K. S. (Ed) *Background to Palaeohydrology*, John Wiley & Sons, Chichester.
- Dury, G. H. 1984. 'Abrupt variation in channel width along part of the River Severn near Shrewsbury, Shropshire, England', *Earth Surface Processes and Landforms*, **9**, 485-492.
- Dury, G. H., Sinker, G. A. and Pannett, D. J. 1972. 'Climate change and arrested meander development on the River Severn', *Area*, **4**, 81-85.
- Elfick, M., Fryer, J., Brinker, R. and Wolf, P. 1994. *Elementary Surveying*, Harper Collins, UK, 510pp.
- Emmett, W. W. 1972. 'The hydraulic geometry of some Alaskan streams south of the Yukon River', *Open-File Report, U. S. Geological Survey, Water Resources Division, Alaska District*.
- Emmett, W. W. 1975. 'The channels and waters of the upper Salmon River area, Idaho', *U. S. Geological Survey Professional Paper*, **870A**.
- English Nature 1994. 'Scientific aspects of the River Severn at Montford', *English Nature*, 5pp.

- Fenton, J. D. and Abbott, J. E. 1977. 'Initial movement of grains on a stream bed: the effect of relative protrusion', *Proceedings of the Royal Society of London, Series A*, **352**, 523-537.
- Ferguson, R. I. 1973. 'Channel pattern and sediment type', *Area*, **5**, 38-41.
- Ferguson, R. I. 1981. 'Channel form and channel changes', in Lewin, J. (Ed) *British Rivers*, Allen and Unwin, London, 90-125.
- Ferguson, R. I. 1986. 'Hydraulics and hydraulic geometry', *Progress in Physical Geography*, **10**, 1-31.
- Ferguson, R. I., Prestegard, K. L. and Ashworth, P. J. 1989. 'Influence of sand on hydraulics and gravel transport in a braided gravel-bed river', *Water Resources Research*, **25**, 635-643.
- Ferguson, R. I. and Ashworth, P. J. 1992. 'Spatial patterns of bedload transport and channel change in braided and near-braided rivers', in: Billi, P., Hey, R. D., Thorne, C. R. and Tacconi, P. (Eds), *Dynamics of Gravel-Bed Rivers*, John Wiley & Sons, Chichester, 477-496.
- Ferguson, R. I. and Ashworth, P. J. 1991. 'Slope-induced changes in channel character along a gravel-bed stream: the Allt Dubhaig, Scotland', *Earth Surface Processes and Landforms*, **16**, 65-82.
- Ferguson, R. I. and Paola, C. in press. 'Grain size distribution of gravel-river bedload: the sample size effect'.
- Feuro, V. and Baiamonte, G. 1994. 'Flow velocity profiles in gravel bed rivers', *Journal of Hydraulic Engineering*, **120**, 60-80.
- Fripp, J. B. and Diplas, P. 1993. 'Surface sampling in gravel streams', *Journal of Hydraulic Engineering*, **119**, 473-490.
- Ghosh, S. N. and Roy, N. 1970. 'Boundary shear distribution in open channel flow', *Journal of the Hydraulics Division*, **96**, 967-993.
- Gilbert, G. K. 1880. 'Land sculpture: geology of the Henry Mountains', *U. S. Geographical and Geological Survey of the Rocky Mountains Region*, 93-97, 100-108, 117-125, 137-144.
- Gilbert, G. K. 1914. 'The transportation of debris by running water', *U. S. Geological Survey Professional Paper*, **86**.
- Gomez, B. 1983. 'Temporal variations in bedload transport rates: the effect of progressive bed armouring', *Earth Surface Processes and Landforms*, **8**, 41-54.

- Graf, W. L. 1982. 'Spatial variations of fluvial processes in semi-arid lands', in Thorne, C. E. (Ed), *Space and Time in Geomorphology*, Allen and Unwin, Boston, 193-217.
- Graf, W. L. 1983a. 'Downstream changes in stream power in the Henry Mountains, Utah', *Annales of the Association of American Geographers*, **73**, 373-387.
- Graf, W. L. 1983b. 'Variability of sediment removal in a semi-arid watershed', *Water Resources Research*, **19**, 643-652.
- Gregory, K. J. and Walling, D. E. 1973. *Drainage Basin Form and Process: a Geomorphological Approach*, Edward Arnold Ltd, 458 pp.
- Gregory, K. J. 1987. 'Introduction', in Gregory, K. J., Lewin, J. and Thornes, J. B. (Eds), *Palaeohydrology in Practice*, John Wiley & Sons, Chichester, 1-15.
- Gregory, K. J. and Lewin, J. 1987. 'Conclusions: palaeohydrological synthesis and application', in Gregory, K. J., Lewin, J. and Thornes, J. B. (Eds), *Palaeohydrology in Practice*, John Wiley & Sons, Chichester, 341-363.
- Griffiths, G. A. 1980. 'Hydraulic geometry relationships of some New Zealand gravel bed rivers', *New Zealand Journal of Hydrology*, **19**, 106-118.
- Gupta, A. 1983. 'High-magnitude floods and stream channel response', *Special Publication of the International Association of Sedimentology*, **6**, 219-227.
- Gurnell, A. M. and Midgley, P. 1994. 'Aquatic weed growth and flow resistance: influence on the relationship between discharge and stage over a 25 year river gauging station record', *Hydrological Processes*, **8**, 63-73.
- Hack, J. T. 1957. 'Studies of longitudinal profile in Virginia and Maryland', *U. S. Geological Survey Professional Paper*, **294-B**.
- Harris, N. M. (1997). *The Influence of Scale on River Bank Processes*, Unpublished MSc. thesis, University of Birmingham.
- Harvey, A. M. 1969. 'Channel capacity and the adjustment of streams to hydrological regime', *Journal of Hydrology*, **8**, 82-96.
- Helley, E. J. and Smith, W. 1971. 'Development and calibration of a pressure difference bedload sampler', *Open File Report 73-108*, U. S. Geological Survey, Washington D. C.
- Henderson, F. M. 1966. *Open Channel Flow*, The MacMillan Co., New York.

- Herschy, R. W. (Ed) 1978. *Hydrometry: Principles and Practice*, John Wiley & Sons, Chichester, UK.
- Herschy, R. W. 1985. *Streamflow Measurement*, Elsevier Applied Science, London, 553pp.
- Hey, R. D. 1975. 'Response of alluvial channels to river regulation', *Proceedings of the 2nd World Congress*, **5**, International Water Resources Association, 183-188.
- Hey, R. D. 1978. 'Determinate hydraulic geometry of river channels', *Journal of the Hydraulics Division*, **104**, 869-885.
- Hey, R. D. 1979. 'Flow resistance in gravel-bed rivers', *Journal of the Hydraulics Division*, **105**, 365-379.
- Hey, R. D. and Thorne, C. R. 1975. 'Secondary flows in river channels', *Area*, **7**, 191-195.
- Hey, R. D., Bathurst, J. C. and Thorne, C. R. (Eds) 1982. *Gravel-Bed Rivers*, John Wiley & Sons, Chichester, 875pp.
- Hey, R. D. and Thorne, C. R. 1983. 'Accuracy of surface sediment samples from gravel-bed material', *Journal of Hydraulic Engineering*, **109**, 842-851.
- Hey, R. D. and Thorne, C. R. 1984. 'Flow processes and river channel morphology', In Burt, T.P. and Walling, D.E. (Eds), *Catchment Experiments in Fluvial Geomorphology, Proc. IGU Commission on Field Experiments in Geomorphology*, Exeter and Huddersfield, UK, 16-24 Aug 1981, Geo Books, Norwich, 489-514.
- Hey, R. D. and Thorne, C. R. 1986. 'Stable channels with mobile gravel beds', *Journal of Hydraulic Engineering*, **112**, 671-689.
- Hickin, E. J. 1983. 'River channel changes: retrospect and prospect', *Special Publication of the International Association of Sedimentology*, **6**, 61-83.
- Hiebert, J. 1996. 'Testing the stream hydraulics hypothesis: longitudinal patterns in flow variables', *North American Benthological Society*, 44th Meeting, Montana, U.S., 1-3.
- Higgs, G. and Petts, G. E. 1988. 'Hydrological changes and river regulation in the UK', *Regulated Rivers: Research and Management*, **2**, 349-368.
- Higgs, G. 1987. 'Environmental change and hydrological response: flooding in the upper Severn catchment', in Gregory, K. J., Lewin, J. and Thornes, J. B. (Eds). *Palaeohydrology in Practice*, John Wiley & Sons, Chichester, 133-161.

- Hinze, J. O. 1975. *Turbulence*, 2nd, edition, McGraw-Hill Book Co., New York.
- Hjulstrom, F. 1935. 'Studies of the morphological activity of rivers as illustrated by the River Fyris', *Bulletin of the Geological Institute, University of Uppsala*, **25**, 221-527.
- Hooke, R. L. B. 1974. 'Shear stress and sediment distribution in a meander bend', *Journal of Geology*, **83**,
- Hooke, R. L. B. 1975. 'Distribution of sediment transport and shear stress in a meander bend', *Journal of Geology*, **83**, 543-565.
- Hooke, J. M. 1995. 'Processes of channel planform change on meandering channels in the UK', in Gurnell, A. M. and Petts, G. E. (Eds) *Changing River Channels*, John Wiley & Sons, London, 87-115.
- Howard, A. D. 1992. 'Modelling channel migration and floodplain sedimentation in meandering streams', in Carling, P. A. and Petts, G. E. (Eds), *Lowland Floodplain Rivers: Geomorphological Perspectives*, John Wiley & Sons, Chichester, 1-41.
- Howe, G. M., Slaymaker, H. O. and Harding, D. M. 1967. 'Some aspects of the flood hydrology of the upper catchments of the Severn and Wye', *Transactions of the Institute of British Geographers*, **41**, 33-58.
- Hudson, J. A. and Gilman, K. 1993. 'Longterm variability in the water balances of the Plynlimon catchments', *Journal of Hydrology*, **143**, 355-380.
- Hughes, D. A. 1980. 'Floodplain inundation: processes and relationships with channel discharge', *Earth Surface Processes*, **5**, 297-304.
- Institute of Hydrology, 1975. *Flood Studies Report*, NERC, Wallingford.
- Ippen, A. T., Drinker, P. A., Jobin, W.R. and Shendin, O. H. 1962. 'Stream dynamics and boundary shear distributions for curved trapezoidal channels', *Massachusetts Institute of Technology, Hydrodynamics Lab. Report*, **46**, 81pp.
- Jackson, P. S. 1981. 'On the displacement height in the logarithmic velocity profile', *Journal of Fluid Mechanics*, **111**, 15-25.
- Jarrett, R. D. 1984. 'Hydraulics of high-gradient streams', *Journal of Hydraulic Engineering*, **110**, 1519-1539.

- Jarrett, R. D. 1990. 'Hydrologic and hydraulic research in mountain rivers', *Water Resources Bulletin*, **26**, 419-429.
- Jarrett, R. D. 1991. 'Wading measurements of vertical velocity profiles', *Geomorphology*, **4**, 243-247.
- Jolley, T. J. and Wheeler, H. S. 1993. 'Macromodelling of the River Severn', in *Macromodelling of the Hydrosphere*, IAHS, 214, 91-103.
- Kapoor, V. 1990. 'Spatial uniformity of power and altitudinal geometry of river networks', *Water Resources Research*, **26**, 2303-2310.
- Karim, M. F. and Kennedy, J. F. 1986. 'Velocity and sediment-concentration profiles in river flows', *Journal of Hydraulic Engineering*, **113**, 159-178.
- Kirby, C., Newson, M. D. and Gilman, K. 1990. 'Plynlimon research: the first two decades', *Institute of Hydrology Report*, **109**.
- Keller, E. A. and Melhorn, W. N. 1978. 'Rhythmic spacing and origin of pools and riffles', *Geological Society of America Bulletin*, **89**, 723-730.
- Kellerhals, R. and Bray, D. I. 1971. 'Sampling procedures for coarse fluvial sediments', *Journal of the Hydraulics Division*, **97**, 1165-1180.
- Kirkby, M. J. 1972. 'Alluvial and non-alluvial meanders', *Area*, **4**, 284-288.
- Kirkby, M. J. 1977. 'Maximum sediment efficiency as a criterion for alluvial changes', in Gregory, K. J. (Ed), *River Channel Changes*, John Wiley & Sons, 429-442.
- Kirkgoz, M. S. 1989. 'Turbulent velocity profiles for smooth and rough open channels', *Journal of Hydraulic Engineering*, **115**, 1543-1561.
- Knight, D. W. 1981. 'Boundary shear in smooth and rough channels', *Journal of the Hydraulics Division*, **107**, 839-851.
- Knight, D. W. 1989. 'Hydraulics of flood channels', in Beven, K. and Carling, P. (Eds), *Floods: Hydrological, Sedimentological and Geomorphological Implications*, John Wiley & Sons, Chichester, 83 - 106.
- Knight, D. W. and Demetriou, J. D. 1983. 'Flood plain and main channel flow interaction', *Journal of Hydraulic Engineering*, **109**, 1073-1092.

- Knight, D. W., Yuen, K. W. H. and Al-Hamid, A. A. I. 1994. 'Boundary shear stress distributions in open channel flows', in Beven, K.J., Chatwin, P.C. and Millbank, J.H. (Eds), *Mixing and Transport in the Environment*, John Wiley & Sons,
- Knighton, D. 1975. 'Variations in at-a-station hydraulic geometry', *American Journal of Science*, **275**, 186-218.
- Knighton, D. 1984. *Fluvial Forms and Processes*, Edward Arnold, 218pp.
- Knighton, D. 1987. 'River channel adjustment: the downstream dimension', in Richards, K. S. (Ed), *River Channels: Environment and Process*, Blackwell, Oxford, 95-128.
- Kochel, R. C. 1988. 'Geomorphic impact of large floods: review and new perspectives on magnitude and frequency', in Baker, V. R., Kochel, R. C. and Patten, P. C. (Eds) *Flood Geomorphology*, John Wiley & Sons, New York, 169-187.
- Komar, P. D. 1987. 'Selective gravel entrainment and the empirical evaluation of flow competence', *Sedimentology*, **34**, 1165-1176.
- Kouwen, N and Li, R. M. 1980. 'Biomechanics of vegetative channel linings', *Journal of the Hydraulics Division*, **106**, 1085-1103.
- Kouwen, N and Unny, T. E. 1973. 'Flexible roughness in open channels', *Journal of the Hydraulics Division*, **99**, 713-728.
- Kuhnle, R. A. 1992. 'Bedload transport during rising and falling stages of two small streams', *Earth Surface Processes and Landforms*, **17**, 191-197.
- Lacey, G. 1946-1947. 'A theory of flow in alluvium', *Journal of the Institute of Civil Engineers*, **27**, 16-47.
- Lambert, C. P. and Walling, D. E. 1988. 'Measurement of channel storage of suspended sediment in a gravel bed river', *Catena*, **15**, 65-80.
- Lane, E. W. 1955. 'The importance of fluvial morphology in hydraulic engineering', *Proceedings of the American Society of Civil Engineers*, **81**, 1-17.
- Lane, S. N., Chandler, J. H. and Richards, K. S. 1994. 'Developments in monitoring and modelling small-scale river bed topography', *Earth Surface Processes and Landforms*, **19**, 349-368.
- Langbein, W. B. 1964. 'Geometry of river channels', *Journal of the Hydraulics Division*, **90**, 301-311.

- Lapointe, M. F. and Carson, M. A. 1986. 'Migration patterns of an asymmetric meandering river: the Rouge River, Quebec', *Water Resources Research*, **22**, 731-743.
- Lawler, D. M. 1987. 'Spatial variability in the climate of the Severn basin: a palaeohydrological perspective', in Gregory, K. J., Lewin, J. and Thornes, J. B. (Eds), *Palaeohydrology in Practice*, John Wiley & Sons, Chichester, 49-78.
- Lawler, D. M. 1992. 'Process dominance in bank erosion systems', in Carling, P. A. and Petts G. E. (Eds), *Lowland Floodplain Rivers: Geomorphological Perspectives*, John Wiley & Sons, Chichester, 117-143.
- Lawler, D. M. 1993. 'The measurement of river bank erosion and lateral channel change: a review', *Earth Surf. Processes and Landforms Technical and Software Bull* **18**, 777-821.
- Lawler, D. M. 1994. 'Temporal variability in streambank response to individual flow events: the River Arrow, Warwickshire, UK', in Olive, L. J., Loughran, R. J. and Kesby, J. A. (Eds) *Variability in Stream Erosion and Sediment Transport*, IAHS, **224**, 171-180.
- Lawler, D. M. 1995. 'The impact of scale on the processes of channel side sediment supply: a conceptual model', in Osterkamp, W. R. (Ed) *Effects of Scale on the Interpretation and Management of Sediment and Water Quality*, IAHS, **226**, 175-185.
- Lecce, S. A. 1993. *Fluvial Response to Spatial and Temporal Variations of Stream Power, Blue River, Washington*, Unpublished Ph.D thesis, University of Wisconsin.
- Leopold, L. B. 1953. 'Downstream change of velocity in rivers', *American Journal of Science* **251**, 606-624.
- Leopold, L. B. 1970. 'An improved method for size distribution of stream bed gravel', *Water Resources Research*, **6**, 1357-1366.
- Leopold, L. B. 1973. 'River channel change with time: an example', *Geological Society of America Bulletin*, **84**, 1845-1860.
- Leopold, L. B. and Maddock, T. 1953. 'The hydraulic geometry of stream channels and some physiographic implications', *U. S. Geological Survey Professional Paper*, **252**, 57pp.
- Leopold, L. B. and Wolman, M. G. 1957. 'River channel patterns: braided, meandering and straight', *U. S. Geological Survey Professional Paper*, **282-B**, 85 pp.
- Leopold, L. B. and Skiltbitzke, H. E. 1967. 'Observations on unmeasured rivers', *Geografiska Annaler*, **49**, 247-285.

- Leopold, L. B., Wolman, M. G. and Miller, J. P. 1964. *Fluvial Processes in Geomorphology*, San Francisco, Freeman and Co., 522pp.
- Leopold, L. B. and Bull, W. B. 1979. 'Base level, aggradation and grade', *Proceedings of the American Philosophical Society*, **123**, 168-202.
- Lewin, J. 1982. 'British floodplains', in Adlam, B. H., Fenn, C. R. and Morris, L. (Eds), *Papers in Earth Studies*, Geo Books, Norwich, UK, 21-37.
- Lewin, J. 1983. 'Changes of channel patterns and floodplains', in Gregory, K. J. (Ed), *Background to Palaeohydrology*, John Wiley & Sons, Chichester, 303-319.
- Lewin, J. 1987. 'Historical river channel changes', in Gregory, K. J., Lewin, J., and Thornes, J. B. (Eds), *Palaeohydrology in Practice*, John Wiley & Sons, Chichester, 161-175.
- Lewis, G. W. and Lewin, J. 1983. 'Alluvial cutoffs in Wales and the Borderlands', *Special Publication of the International Association of Sedimentology*, **6**, 145-154.
- Li, Z. and Komar, P. D. 1986. 'Laboratory measurements of pivoting angles for applications to selective entrainment of gravel in a current', *Sedimentology*, **33**, 413-423.
- Limerinos, J. T. 1970. 'Determination of the Manning coefficient from measured bed roughness in natural channels', *U. S. Geological Survey Water Supply Papers*, **1898-B**, 47pp.
- Lindsay, D. A. 1995. *Flood Forecasting in the Severn-Vyrnwy Confluence*, Unpublished MSc. dissertation, University of Birmingham.
- Lisle, T. E. 1995. 'Particle size variations between bed load and bed material in natural gravel bed channels', *Water Resources Research*, **31**, 1107-1118.
- Livesey, J. R. 1996. *Flow Structure, Bedform Development and Sediment Transport in Mixed Sand and Gravel*, Unpublished Ph.D. thesis, University of Leeds.
- Macilwaine, R. V., Flew, N. W. J. and Cooper, J. N. M. 1994. 'Sankey Brook Catchment Study', *Journal of the Institute of Water and Environmental Management*, **8**, 576-584.
- Mackin, J. H. 1963. 'Rational and empirical methods of investigation in geology', in Albritton, C. C., Jr. (Ed), *The Fabric of Geology*, Addison-Wesley Publ. Co., 135-163.
- Magilligan, F. J. 1992. 'Thresholds and the spatial variability of flood power during extreme events', *Geomorphology* **5**, 373-390.

- Marchand, J. P., Jarrett, R. D. and Jones, L. L. 1984. 'Velocity profile, water-surface slope, and bed material size for selected streams in Colorado', *U. S. Geological Survey Open File Rep.*, **84-733**, 82pp.
- Marcus, W. A., Roberts, K., Harvey, L. and Tackman, G. 1992. 'An evaluation of methods for estimating Manning's n in small mountain streams', *Mountain Research and Development*, **12**, 227-239.
- Marcus, W. A., Ladd, S. C., Stoughton, J. A. and Stock, J. W. 1994. 'Pebble counts and the role of user-dependent bias in documenting sediment size distributions', *Water Resources Research*, **31**, 2625-2631.
- Marriott, S. 1992. 'Textural analysis and modelling of a flood deposit: River Severn, UK', *Earth Surfaces Processes and Landforms*, **17**, 687-697.
- McCartney, M. P. and Naden, P. S. 1994. 'A semi-empirical investigation of the influence of flood-plain storage on flood flow', *Journal of the Institute of Water and Environmental Management*, **9**, 236-246.
- McEwen, L. J. 1994. 'Channel planform adjustment and stream power variations on the middle River Coe, Western Grampian Highlands, Scotland', *Catena*, **21**, 357-374.
- McKenney, R., Jacobsen, R. B. and Wertheimer, R. C. 1995. 'Woody vegetation and channel morphogenesis in low-gradient, gravel-bed streams in the Ozark Plateaus, Missouri and Arkansas', *Geomorphology*, **13**, 175-198.
- Meigh, J. R. 1987. *Transport of bed material in a gravel-bed river*. Unpublished Ph.D. thesis, University of East Anglia.
- Meyer-Peter E. and Muller, R. 1948. 'Formulas for bed-load transport', *Proceedings of the second meeting of the International Association for hydraulic Structures Research, Stockholm, Sweden*, 39-64.
- Milner, A. M. and Petts, G. E. 1994. 'Glacial rivers: physical habitat and ecology', *Freshwater Ecology*, **32**, 295-307.
- Minshall, G. W., Peterson, R. C., Cummins, K. W., Bott, T. L., Sedell, J. R., Cushing, C. E. and Vannote, R. L. 1983. 'Interbiome comparison of stream ecosystem dynamics', *Ecological Monographs*, **53**, 1-25.
- Mishra, S. K. and Seth, S. M. 1996. 'Use of hysteresis for defining the nature of flood wave propagation in natural channels', *Hydrological Sciences*, **41**, 153-170.

- Mitchell, D. J. and Gerrard, A. J. 1987. 'Morphological responses and sediment patterns', in Gregory, K. S., Lewin, J. and Thornes, J. B. (Eds) *Palaeohydrology in Practice*, John Wiley & Sons, 177-199.
- Murgatroyd, A. L. and Ternan, J. L. 1983. 'The impact of afforestation on stream bank erosion and channel form', *Earth Surface Processes and Landforms*, **8**, 357-369.
- Naiman, R. J., Decamps, H., Pastor, J. and Johnston, C. A. 1988. 'The potential importance of boundaries to fluvial ecosystems', *Journal of the North American Benthological Society*, **7**, 289-306.
- Nanson, G. C. and Croke, J. C. 1992. 'A genetic classification of floodplains', *Geomorphology*, **4**, 459-486.
- National River Authority, Severn-Trent Region 1992. *Hydrological Report and Catalogue 1992*, 32pp.
- Newson, A. J. 1976. *Some aspects of the rainfall of Plynlimon, Mid Wales*, Report no. 34, Institute of Hydrology, Wallingford, Oxfordshire, UK.
- Newson, M. D. 1976. *The physiography, deposits and vegetation of Plynlimon catchment*. Report no. 47, Institute of Hydrology, Wallingford, Oxfordshire, UK.
- Newson, M. D. 1981. 'Mountain streams', in Lewin, J. (Ed), *British Rivers*, Allen and Unwin, London, 59-89.
- Newson, M. D. and Harrison, J. G. 1978. 'Channel studies in the Plynlimon experimental catchments', *Institute of Hydrology Report*, **47**, 61pp.
- Newson, M. D. and Leeks, G. J. L. 1987. 'Transport processes at a catchment scale', in Thorne, C. R., Bathurst, J. C. and Hey, R. D. (Eds) *Sediment Transport in Gravel-Bed Rivers*, John Wiley & Sons, 187-223.
- Nezu, I and Rodi, W. 1986. 'Open channel flow measurements with a laser doppler anemometer', *Journal of Hydraulic Engineering*, **112**, 335-354.
- Nikuradse, J. 1933. *Stromungsgesetze in rauhen Roeren, Verhein deutscher Ingenieure Forschungscheft No. 361*, Berlin. (English translation in National Advisory Committee for Aeronautics Technical Manual 1292 (1959), 62pp.
- Nixon, M. 1959. 'A study of the bankfull discharges of rivers in England and Wales', *Proceedings of the Institution of Civil Engineers*, **12**, 157-175.
- O'Connor, J. E. and Webb, R. H. 1988. 'Hydraulic modelling for palaeoflood analysis', in Baker, V.R., Kochel, R.C. and Patton, P.C. (Eds) *Flood Geomorphology*, John Wiley & Sons, New York, 393-402.

- Painter, R. B., Blyth, K., Mosedale, J. C. and Kelly, M. 1974. 'The effect of afforestation on erosion processes and sediment yield', *IAHS* **113**, 62-67.
- Paola, C. and Seal, R. 1995. 'Grain size patchiness as a cause of selective deposition and downstream fining', *Water Resources Research*, **31**, 1395-1407.
- Park, C. C. 1975. 'The relationship of slope and stream channel form in the River Dart, Devon', *Journal of Hydrology*, **29**, 139-147.
- Park, C. C. 1977. 'World-wide variations in hydraulic geometry exponents of stream channels: an analysis and some observations', *Journal of Hydrology*, **33**, 133-146.
- Parker, G. 1979. 'Hydraulic geometry of active gravel rivers', *Journal of the Hydraulics Division*, **105**, 1185-1201.
- Parker, G., Klingeman, P. C. and McLean, D. G. 1982. 'Bedload and size distribution in paved gravel-bed streams', *Journal of the Hydraulics Division*, **108**, 544-571.
- Patel, H. 1965. 'Calibration of the Preston tube and the limitations on its use in pressure gradients', *Journal of Fluid Mechanics*, **23**.
- Petryck, S. and Bosmajian, G. 1975. 'Analysis of flow through vegetation', *Journal of the Hydraulics Division*, **101**, 871-884.
- Petts, G. E. 1984. *Impounded Rivers: Perspectives for Ecological Management*, John Wiley & Sons, Chichester, 326pp.
- Petts, G. E. and Foster, I. 1990. *Rivers and Landscape*, Edward Arnold, 3rd edition, 274pp.
- Pickup, G. 1976. 'Adjustment of stream-channel shape to hydrologic regime', *Journal of Hydrology*, **30**, 365-373.
- Pickup, G. and Reiger, W. A. 1979. 'A conceptual model of the relationship between channel characteristics and discharge', *Earth Surface Processes*, **4**, 37-42.
- Pitlo, R. H. and Dawson, F. H. 1980. 'Flow resistance of aquatic weeds', in Pieterse, A. H. and Murphy, K. J. (Eds), *Aquatic Weeds: The Ecology and Management of Nuisance Aquatic Vegetation*, Oxford University Press, Oxford, 74-85.
- Powell, K. E. C. 1978. 'Weed growth - a factor of channel roughness', in Herschy, R. W. (Ed), *Hydrometry: Principles and Practices*, John Wiley & Sons-Interscience, 327-352.

- Prandtl, L. 1952. *Essentials of Fluid Dynamics*, Hafner, New York and Blackie, London, 452pp.
- Prestegard, K. L. 1983. 'Variables influencing water-surface slopes in gravel-bed streams at bankfull stage', *Geological Society of America Bulletin*, **94**, 673-678.
- Przedwojski, B., Blazejewski, R. and Pilarczyk, K. W. 1995. *River Training Techniques: Fundamentals, Design and Applications*, Balkema, Netherlands, 625pp.
- Pugh, J. C. 1975. *Surveying for Field Scientists*, Methuen, London, 230pp.
- Rashid, R. S. M. and Chaudry, M. H. 1995. 'Flood routing in channels with flood plains', *Journal of Hydrology*, **171**, 75-91.
- Reid, I., Frostick, L. E. and Layman, J. T. 1985. 'The incidence and nature of bedload transport during flood flows in coarse-grained alluvial channels', *Earth Surface Processes and Landforms*, **10**, 33-44.
- Reid, I. and Frostick, L. E. 1986. 'Dynamics of bedload transport in Turkey Brook, a coarse-grained alluvial channel', *Earth Surface Processes and Landforms*, **11**, 143-155.
- Reid, I., Best, J. L. and Frostick, L. E. 1989. 'Floods and flood sediments at river confluences', in Beven, K. and Carling, P. A. (Eds), *Floods: Hydrological, Sedimentological and Geomorphological Implications*, John Wiley & Sons, Chichester, 135 - 150.
- Reynolds, C. S., Carling, P. A. and Beven, K. 1991. 'Flow in river channels: new insights into hydraulic retention', *Archiv für Hydrobiologie*, **121**, 171-179.
- Rhoads, B. L. 1987. 'Stream power terminology', *Professional Geographer*, **39**, 189-195.
- Richards, K. S. 1972. 'Meanders and valley slope', *Area*, **4**, 288-290.
- Richards, K. S. 1973. 'Hydraulic geometry and channel roughness - a non-linear system', *American Journal of Science*, **273**, 877-896.
- Richards, K. S. 1976. 'The morphology of riffle-pool sequences', *Earth Surface Processes*, **1**, 71-88.
- Richards, K. S. 1977. 'Channel and flow geometry: a geomorphological perspective', *Progress in Physical Geography*, **1**, 65-102.
- Richards, K. S. 1980. 'A note on changes of channel geometry at tributary junctions', *Water Resources Research*, **16**, 241-244.

- Richards, K. S. 1982. *Rivers, Form and Process in Alluvial Channels*, Methuen, London, 361pp.
- Richards, K. S. 1990a. River channel form, in Goudie, A. (Ed) *Geomorphological Techniques*, Unwin Hyman Ltd., 82-91.
- Richards, K. S. 1990b. 'Fluvial geomorphology: initial motion of bed material in gravel-bed rivers', *Progress in Physical Geography*, **14**, 395-415.
- Richey, J. E., Meade, R. H., Salati, E., Devol, A. H., Nordin, C. F. and Dos Santos, U. 1986. 'Water discharge and suspended sediment concentrations in the Amazon River: 1982-1984', *Water Resources Research*, **22**, 756-764.
- Robert, A. 1990. 'Boundary roughness in coarse-grained channels', *Progress in Physical Geography*, **14**.
- Rowan, J. S., Bradley, S. B. and Walling, D. E. 1992. 'Fluvial redistribution of Chernobyl fallout: reservoir evidence in the Severn basin', *Journal of the Institute of Water and Environmental Management*, **6**, 659-666.
- Rudeforth, C. C. 1970. *Soils of North Cardiganshire*, Soil Survey, England and Wales. Harpenden, Herts, UK.
- Samuels, P. G. 1990. 'Cross-section location in 1-D models', in White, W. R. and Bettess, R. (Eds), *International Conference on River Flood Hydraulics*, John Wiley & Sons, Chichester, 439-450.
- Savini, J. and Bodhaine, G. L. 1969. 'Analysis of current-meter data at Columbia River gauging stations, Washington and Oregon', *U. S. Geological Survey Professional Paper*, **1869-F**, 31pp.
- Schlichting, H. 1979. *Boundary-layer Theory*, 7th edition, New York, McGraw-Hill, 817pp.
- Schumm, S. A. 1960. 'The shape of alluvial channels in relation to sediment type', *U. S. Geological Survey Professional Paper*, **352-B**, 17-30.
- Schumm, S. A. 1973. 'Geomorphic thresholds and complex response of drainage systems', in Morisawa, M. E. (Ed), *Fluvial Geomorphology*, Publ. in Geomorphology, State Uni. of New York, Binghamton, 335-346.
- Schumm, S. A. 1977. *The Fluvial System*, New York, John Wiley & Sons-Interscience, 338pp.
- Schumm, S. A. and Lichty, R. W. 1963. 'Channel widening and flood plain construction along Cimarron river in south-western Kansas', *U. S. Geological Survey Professional Paper*, **352-D**, 71-88.

- Schumm, S. A. and Khan, H. R. 1972. 'Experimental study of channel patterns', *Geol. Soc. Amer., Bull.*, **83**, 1755-1770.
- Shaw, E. 1988. *Hydrology in Practise*, 2nd Edition, Van Nostrand Reinhold (International), London, 539 pp.
- Shields, A. 1936. *Anwendung der Aehnlichkeitsmechanik und der turbulenzforschung auf die geschiebebewegung*, *Mitteilung der Preussischen versuchsanstalt fuer Wasserbau und Schiffbau*, Heft 26, Berlin.
- Simons, D. B. and Akbertson, M. L. 1963. 'Uniform water conveyance channels in alluvial material', *American Society of Civil Engineers Transaction*, **128**, 65-107.
- Slade, J. E. and Samuels, P. G. 1990. 'Modelling complex river networks', in White, W. R. and Bettess, R. (Eds), *International Conference on River Flood Hydraulics*, John Wiley & Sons, Chichester, 451-458.
- Statzner, B. 1981. 'The relation between 'hydraulic stress' and microdistribution of benthic macroinvertebrates in a lowland running water system, the Schierenseebrooks (North Germany)', *Archive fur Hydrobiologie*, **91**, 192-218.
- Statzner, B. and Higler, B. 1985. 'Questions and comments on the river continuum concept', *Canadian Journal of Fisheries and Aquatic Science*, **42**, 1038-1044.
- Statzner, B. and Higler, B. 1986. 'Stream hydraulics as a major determinant of benthic invertebrate zonation patterns', *Freshwater Biology*, **16**, 127-139.
- Statzner, B., Gore, J. A. and Resh, V. H. 1988. 'Hydraulic stream ecology: observed patterns and potential applications', *Journal of the North American Benthological Society*, **7**, 307-360.
- Stevens, M. A., Simons, D. B. and Richardson, E. V. 1975. 'Non-equilibrium river form', *Journal of the Hydraulics Division*, **101**, 557-566.
- Thorne, C. R. 1990. 'Effects of vegetation on riverbank erosion and stability', in Thornes, J. B. (Ed), *Vegetation and Erosion*, John Wiley & Sons, Chichester, 125-144.
- Thorne, C. R. and Lewin, J. 1979. 'Bank processes, bed material movement and planform development in a meandering river', in Rhodes, D.D. and Williams, G.P. (Eds) *Adjustments of the Fluvial System*, Kendall/Hunt, Dubuque, Iowa, 117-137.
- Thorne, C.R., Bathurst, J.C. and Hey, R.D. (Eds) 1987. *Sediment Transport in Gravel Bed Rivers*, John Wiley & Sons, Chichester, 995pp.

- Thornes, J. B. 1977. 'Hydraulic geometry and channel change', in Gregory, K. J. (Ed), *River Channel Changes*, John Wiley & Sons, Chichester, 91-100.
- Toghill, P. 1990. *Geology in Shropshire*, Swan Hill Press, Shrewsbury.
- Vannote, R. L., Minshall, G. W., Cummins, K. W., Sedell, J. R. and Cushing, C. C. 1980. 'The river continuum concept', *Canadian Journal of Fisheries and Aquatic Science*, **37**, 130-137.
- Vanoni, V. A. 1946. 'Transportation of suspended sediment by water', *Transactions of the American Society of Civil Engineers*, **111**.
- Vanoni, V. A. and Nomicos, G. N. 1959. 'Resistance properties of sediment-laden streams', *Journal of the Hydraulics Division*, **85**, 77-107.
- Vedula, S. and Achanta, R. R. 1985. 'Bed shear from velocity profiles: a new approach', *Journal of the Hydraulics Division*, **111**, 131-143.
- von Karman, T. 1934. 'Turbulence and skin friction', *J. Aeronautical Society*, **1**, 1.
- Walling, D. E. and Webb, B. W. 1987. 'Suspended load in gravel-bed rivers: UK experience', in Thorne, C. R., Bathurst, J. C. and Hey, R. D. (Eds), *Sediment Transport in Gravel-bed Rivers*, John Wiley & Sons, Chichester, 691-732.
- Walling, D. E. and Quine, T. A. 1993. 'Using Chernobyl-derived fallout radionuclides to investigate the role of downstream conveyance losses in the suspended sediment budget of the River Severn, United Kingdom', *Physical Geography*, **14**, 239-253.
- Wang, S. 1981. 'Variation of the von Karman constant in sediment-laden flow', *Journal of the Hydraulics Division*, **107**, 407-417.
- Ward, J. V. and Stanford, J. A. 1983. 'The serial discontinuity concept of lotic ecosystems', in Bartell, S. M. and Fontaine, T. D. (Eds), *The Dynamics of the Lotic Ecosystem*, Ann. Arbor. Science, 29-42.
- Ward, J. V. and Stanford, J. A. 1995. 'The serial discontinuity concept: extending the model to floodplain rivers', *Regulated Rivers: Research and Management*, **10**, 159-168.
- Warwick, J. J. and Heim, K. J. 1995. 'Hydrodynamic modelling of the Carson River and Lahontan Reservoir, Nevada', *Water Resources Bulletin*, **31**, 67-77.
- Watson, D. 1987. 'Hydraulic effects of aquatic weeds in UK rivers', *Regulated Rivers: Research and Management*, **1**, 211-227.

- Wheeler, D. A. 1979. 'The overall shape of longitudinal profiles of stream', in Pitty, A. F. (Ed), *Geographical Approaches to Fluvial Processes*, Geo books, Norwich, UK, 241-260.
- Whiting, P. J. and Dietrich, W. E. 1989. 'Boundary shear stress and roughness over mobile alluvial beds', *Journal of Hydraulic Engineering*, **116**, 1495-1511.
- Whittaker, J. G. and Jaeggi, M. N. R. 1982. 'Origin of step-pool systems in mountain streams', *Journal of the Hydraulics Division*, **108**, 758-773.
- Wiberg, P. L. and Smith, J. D. 1987. 'Initial motion of coarse sediment in streams of high gradient', *Erosion and Sedimentation in the Pacific Rim* (Proc. Corvallis Symp., August, 1987), IAHS Publ. no. 165, 299-308.
- Wiberg, P. L. and Smith, J. D. 1991. 'Velocity distribution and bed roughness in high-gradient streams', *Water Resources Research*, **27**, 825-838.
- Wilkinson, R. H. 1984. 'A method for evaluating statistical errors associated with logarithmic velocity profiles', *Geo-Marine Letters*, **3**, 49-52.
- Williams, G. P. 1978. 'Bankfull discharge of rivers', *Water Resources Research*, , 1141-1158.
- Wills, J. L. 1924. 'The development of the Severn valley in the neighbourhood of Iron-Bridge and Bridgnorth', *Quarterly Journal of the Geological Society of London*, **80**, 274-314.
- Wills, J. L. 1938. 'The Pleistocene development of the Severn from Bridgnorth to the sea', *Quarterly Journal of the Geological Society of London*, **94**, 161-242.
- Wohl, E. E. 1992. 'Gradient irregularity in the Herbert Gorge of northeastern Australia', *Earth Surface Processes and Landforms*, **17**, 69-84.
- Wolcott, J. and Church, M. 1991. 'Strategies for sampling spatially heterogeneous phenomena: the example of river gravels', *Journal of Sedimentary Petrology*, **61**, 534-543.
- Wolff, C. G. and Burges, S. J. 1994. 'An analysis of the influence of river channel properties on flood frequency', *Journal of Hydrology*, **153**, 317-337.
- Wolman, M. G. 1954. 'A method of sampling coarse river-bed material', *Transactions of the American Geophysical Union*, **14**, 951-956.
- Wolman, M. G. and Leopold, L. B. 1957. 'River flood plains: some observations on their formation', *U. S. Geological Survey Professional Paper*, **282C**, 87-101.

- Wolman, M. G. and Miller, J. P. 1960. Magnitude and frequency of forces in geomorphic processes, *Journal of Geology*, **68**, 54-74.
- Wolman, M. G. and Gerson, R. 1978. 'Relative scales of time and effectiveness of climate in watershed geomorphology', *Earth Surface Processes*, **3**, 189-208.
- Woltemade, C. J. 1993. *Fluvial Geomorphology and Flood Hydraulics: Affects of Flood Peak Attenuation*, Unpublished Ph.D. thesis, Univeristy of Wisconsin.
- Woltemade, C. J. and Potter, K. W. 1994. 'A watershed modelling analysis of fluvial geomorphologic influences on flood peak attenuation', *Water Resources Research*, **30**, 1933-1942.
- Wood, T. R. 1987. 'The present-day hydrology of the River Severn', in Gregory, K. J., Lewin, J. and Thornes, J. B. (Eds), *Palaeohydrology in Practice*, John Wiley & Sons, Chichester, 79-97.
- Wyzga, B. 1996. 'Changes in the magnitude and transformation of flood waves subsequent to the channelization of the Raba River, Polish Carpathians', *Earth Surface Processes and Landforms*, **21**, 749-764.
- Yalin, M. S. 1992. *River Mechanics*, Pergammon Press, Oxford, 219pp.
- Yang, C. T. 1971a. 'Potential energy and stream morphology', *Water Resources Research*, **7**, 311-322.
- Yang, C. T. 1971b. 'On river meanders', *Journal of Hydrology*, **13**, 231-253.
- Yang, C. T. 1971c. 'Formation of riffles and pools', *Water Resources Research*, **7**, 1567-1574.
- Yang, C. T. 1972. 'Unit stream power and sediment transport', *Journal of the Hydraulics Division*, **98**, 1805-1825.
- Yang, C. T. 1973. 'Incipient motion and sediment transport', *Journal of the Hydraulics Division*, **99**, 1679-1703.
- Yang, C. T. 1976. 'Unit stream power and fluvial hydraulics', *Journal of the Hydraulics Division*, **107**, 919-934.
- Yang, C. T. and Stall, J. B. 1973. 'Unit stream power in dynamic stream systems', in Morisawa, M. (Ed) *Fluvial Geomorphology*, 4th Binghamton Symposium, 259-297.
- Yang, C. T. and Stall, J. B. 1976. 'Applicability of the unit stream power equation', *Journal of the Hydraulics Division*, **102**, 559-568.

- Yang, C. T. and Song, C. C. 1979. 'Dynamic adjustments of alluvial channels', in Rhodes, D.D. and Williams, G.P. (Eds), *Adjustments of the Fluvial System*. Kendall/Hunt Pub Co., Dubuque, Iowa, 55-67.
- Yang, C. T. and Molinas, A. 1982. 'Sediment transport and the unit stream power function', *Journal of the Hydraulics Division*, **108**, 774-79.
- Yatsu, E. 1955. 'On the longitudinal profile of the graded river', *Transactions of the American Geophysical Union*, **36**, 211-219.
- Young, A. 1972. *Slopes*, Longman, 218pp.
- Yu, B. and Wolman, M. G. 1987. 'Some dynamic aspects of river geometry', *Water Resources Research*, **23**, 501-509.
- Zippe, H. J. and Graf, W. H. 1983. 'Turbulent boundary layer flow from permeable and non-permeable rough surfaces', *Journal of Hydraulic Research*, **21**, 51-65.

# Appendix I

A summary of the study site locations, and the timing and measurement techniques applied to the collection of flow data.

Site number	Site name	Study site location					LOW-FLOW					MEDIUM-FLOW					HIGH-FLOW			
		Distance downstream (km)	Elevation (m) (a.s.l.)	Stage datum (m) (a.s.l.)	Easting	Northing	Survey date	Time (GMT)	Stage (m) (a.s.l.)	Discharge measurement technique	Velocity measurements - no. verticals (no. point measurements)	Survey date	Time (GMT)	Stage (m) (a.s.l.)	Discharge measurement technique	Velocity measurements - no. verticals (no. point measurements)	Survey date	Time (GMT)	Stage (m) (a.s.l.)	Discharge measurement technique
1	Upper Hafren 1	0.08	606.21	606.21	2823	2898	09-Jun-95	08.45	605.20	Bucket est.	-	09-Feb-95	14:35	605.11	Velocity-area	14 (21)	16-Jan-96	10:00	605.82	Trash lines
2	Upper Hafren 2	0.31	580.22	580.22	2825	2896	09-Jun-95	09:30	579.45	Bucket est.	-	09-Feb-95	13:30	579.55	Velocity-area	15 (21)	16-Jan-96	10:30	579.62	Trash lines
3	Upper Hafren 3	0.76	547.76	547.76	2828	2893	09-Jun-95	11:00	547.02	Bucket est.	-	09-Feb-95	12:30	547.25	Velocity-area	13 (26)	16-Jan-96	11:15	547.42	Trash lines
4	Hafren Forest	1.23	524.38	524.38	2829	2890	28-Jul-94	14:45	523.50	Velocity-area	10 (31)	09-Feb-95	10:45	523.70	Velocity-area	16 (31)	16-Jan-96	12:30	523.81	Trash lines
5	Hafren Falls	2.73	390.72	390.72	2837	2883	28-Jul-94	12:25	389.33	Velocity-area	10 (26)	31-Jan-95	13:15	389.90	Velocity-area	17 (100)	02-Jan-96	11:00	390.08	Trash lines
							09-Jun-95	12:45	389.77	Slope-area	-									
6	Tanllwyth	3.71	347.79	347.79	2843	2877	28-Jul-94	10:40	346.91	Velocity-area	10 (31)	31-Jan-95	16:15	347.17	Velocity-area	15 (107)	02-Jan-96	10:00	347.43	Trash lines
							09-Jun-95	13:20	347.04	Slope-area	-									
7	Severn Flume	4.26	334.33	334.33	2847	2873	28-Jul-94	09:00	332.94	Velocity-area	10 (75)	16-Feb-95	13:20	333.15	Velocity-area	12 (88)	16-Jan-96	13:20	333.67	Trash lines
							09-Jun-95	12:00	332.76	Slope-area	-									
8	Picnic Bridge	5.81	313.71	313.71	2856	2869	28-Jul-94	11:40	311.65	Velocity-area	9 (73)	01-Feb-95	11:15	311.90	Velocity-area	14 (87)	02-Jan-96	12:00	312.47	Trash lines
9	Severn Gorge	7.62	271.57	271.57	2868	2867	28-Jul-94	09:15	269.96	Velocity-area	11 (36)	23-Feb-95	16:15	271.04	Velocity-area	13 (125)				
10	Rhydyronnen	9.23	266.39	266.39	2871	2865	21-Jul-94	16:15	264.30	Velocity-area	13 (31)	16-Feb-95	12:10	265.87	Velocity-area	14 (107)	16-Jan-96	13:55	266.54	Trash lines
11	Severn Ford	11.11	204.27	204.27	2904	2846	21-Jul-94	14:00	201.81	Velocity-area	13 (40)	01-Feb-95	15:15	203.77	Velocity-area	22 (195)	16-Jan-96	14:35	204.07	Trash lines
12	Mount Severn	16.88	165.71	165.71	2947	2841	21-Jul-94	12:40	263.49	Velocity-area	25 (44)	23-Feb-95	12:15	163.86	Velocity-area	16 (259)	16-Jan-96	15:15	164.52	Trash lines
13	Dolwen	22.20	147.61	147.61	2996	2852	18-Jul-94	14:40	145.03	Velocity-area	10 (80)	24-Feb-95	11:20	146.40	Velocity-area	19 (239)	31-Jan-95	16:00	146.55	Slope-area
							20-Apr-95	12:00	146.28	Slope area	-						17-Feb-95	09:45	146.57	Slope-area
14	Llandinam	28.00	135.20	135.20	3000	2880	20-Apr-95	13:20	133.96	Slope area	-						17-Feb-95	16:00	135.15	Slope-area
15	Caersws	34.10	118.70	118.70	3036	2920	18-Jul-94	11:30	116.22	Velocity-area	14 (101)	24-Feb-95	16:00	117.94	Velocity-area	23 (272)	31-Jan-95	16:45	118.12	Slope-area
							20-Apr-95	14:30	117.57	Slope area	-						17-Feb-95	11:00	118.04	Slope-area
16	Newtown	44.93	109.00	109.00	3093	2910	26-Apr-95	11:45	106.85	Velocity-area	18 (187)						17-Feb-95	11:50	107.85	Slope-area
17	Abermule	55.92	83.00	83.00	3165	2958	28-Jul-95	14:15	77.23	Velocity-area	14 (71)	10-Mar-95	13:40	79.30	Velocity-area	18 (195)	17-Feb-95	13:15	81.18	Slope-area
18	Dyffryn	70.30	75.02	75.02	3211	3012	19-May-95	08:10	71.98	Velocity-area	21 (256)	09-Mar-95	15:15	72.87	Velocity-area	27 (287)	17-Feb-95	14:30	73.73	Slope-area
19	Pool Quay	83.20	63.03	63.03	3260	3118	19-May-95	15:05	55.33	Velocity-area	14 (195)	09-Jan-96	11:00	59.93	Slope-area	-	17-Feb-95	15:35	62.13	Slope-area
20	Crew Green	100.90	52.94	52.94	3345	3155	16-Jun-95	13:15	46.50	Velocity-area	15 (121)	09-Jan-96	13:00	50.35	Slope-area	-	17-Feb-95	16:35	51.94	Slope-area
21	Montford	115.46	52.00	52.00	3396	3147	16-Jun-95	10:00	47.61	Velocity-area	16 (92)	21-Mar-95	13:15	48.85	Velocity-area	16 (251)	09-Jan-96	14:00	50.64	Slope-area
22	Buildwas	166.45	39.25	39.25	3612	3048	22-Mar-95	13:30	36.10	Velocity-area	23 (60)	07-Mar-96	07:30	36.40	Slope-area	-	03-Feb-95	10:15	39.51	Slope-area
23	Bridgnorth	192.36	30.52	30.52	3722	2736	03-May-95	15:00	26.77	Velocity-area	26 (442)	06-Mar-96	09:00	27.14	Slope-area	-	03-Feb-95	14:00	29.13	Slope-area
24	Bewdley	209.00	20.89	20.89	3782	2762	27-Apr-95	14:30	17.44	Velocity-area	18 (350)	07-Mar-96	14:00	18.02	Slope-area	-	03-Feb-95	16:00	20.84	Slope-area
25	Saxons Lode	254.13	13.27	13.27	3886	2391	18-Oct-95	12:10	7.87	Velocity-area	16 (149)	06-Mar-96	14:00	9.97	Slope-area	-	20-Jan-96	15:00	11.62	Slope-area

## APPENDIX II

A FORTRAN 77 programme designed to convert the MIKE11 results into a format suitable for spreadsheet analysis

Written by John Couperthwaite and Dan Cornford, March 1995

### PROGRAM CONVERSION

This program is designed to link the results of the MIKE11 simulation with the raw cross-section data in order to calculate the hydraulic variables important for my study; these are: shear stress, stream power, water surface slope, mean velocity and discharge.

The REAL variables used in this program are:

Y	= chainages in the raw data file (km)
YMOD	= chainages in the result data file (km)
X	= horizontal distance across the cross-section (m)
Z	= elevation of the river bed in the cross-section (m)
TEMPDATA	= all simulated water elevations (m)
MODWATER	= water elevations from result file which match those in the raw data file (m)
RESIS	= normalised Manning's n values
DIFF	= difference between raw data and result file chainages
WELBX	= waters edge left bank, x-values (m)
WERBX	= waters edge right bank, x-values (m)
TX	= x-values between the wetted part of the river (m)
WWIDTH	= wetted width (m)
WDEPTH	= water depth for each x-z value in the wetted part of the river (m)
AREASEG	= area of each wetted segment of the river (m <sup>2</sup> )
WPERSEG	= wetted perimeter of each segment of the river (m)
TOTAREA	= area of the wetted cross-section (m <sup>2</sup> )
TOTWPER	= wetted perimeter of the wetted cross-section (m)
BEDMIN	= elevation of the lowest part of the wetted bed (m)
TOTHRAD	= hydraulic radius of the wetted cross-section (m)
WSSLOPE	= water surface slope (m.m <sup>-1</sup> )
VELSEG	= velocity of each wetted segment (m s <sup>-1</sup> )
MEANVEL	= mean cross-sectional velocity (m s <sup>-1</sup> )
DISCHARGE	= discharge of the cross-section (m <sup>3</sup> s <sup>-1</sup> )
SSTRESS	= reach mean shear stress (N m <sup>-2</sup> )
GPOWER	= gross stream power (W m <sup>-1</sup> )
UPOWER	= unit steam power (W m <sup>-2</sup> )

The INTEGER variables used in this program are:

MAXXSN	= maximum number of cross-sections
MAXINT	= maximum number of lines for each cross-section
NOXVALUE	= number of x-values for each cross-section
NOXSECT	= number of cross-sections in the raw data file
NOCHAIN	= number of cross-sections in the result file

NUM = counter for the number of wetted x-z values in a cross-section  
 START = number of x-z values in the cross-section array  
 FLAG = define whether or not the left bank has been identified  
 AMAX = maximum area value for each cross-section (= TOTAREA)  
 PMAX = maximum wetted perimeter value for each cross-section (= TOTWPER)  
 ZMIN = minimum z-value (m)  
 NT = number of time intervals in the simulation

C IF NT CHANGES, CHANGE FORMAT

```

PROGRAM CONVERSION
INTEGER MAXXSN,NT,MAXINT,MAXHT,TIME
PARAMETER (MAXXSN = 300, NT = 36, MAXINT = 300, MAXHT = 1000,
+ TIME = 36)
REAL MODWATER (MAXXSN, NT), DIFF
REAL TEMPDATA (MAXHT, NT), YMOD (MAXHT),YMODT(MAXHT),
+ CHAIN (MAXXSN), CHAINAGE (MAXXSN)
REAL Y (MAXXSN), YFIT (MAXXSN)
REAL X (MAXXSN, MAXINT)
REAL Z (MAXXSN, MAXINT)
REAL RESIS (MAXXSN, MAXINT)
REAL TX (MAXXSN, MAXINT), TZ (MAXXSN, MAXINT)
REAL WELBX (MAXXSN, NT)
REAL WERBX (MAXXSN, NT)
REAL WWIDTH (MAXXSN,NT)
REAL WDEPTH (MAXXSN, MAXINT), TOTWDEPTH(MAXXSN, NT),
+ AVEWDEPTH(MAXXSN,NT)
REAL BEDMIN (MAXXSN), MAXDEPTH(MAXXSN,NT)
REAL AREASEG (MAXXSN, MAXINT), WPERSEG(MAXXSN, MAXINT)
REAL AMAX (MAXXSN, NT), PMAX (MAXXSN,NT)
REAL TOTAREA (MAXXSN,NT), TOTWPER (MAXXSN,NT)
REAL TOTHRAD (MAXXSN,NT)
REAL WSSLOPE (MAXXSN,NT), SLOPE (MAXXSN,NT)
REAL Q(MAXHT,TIME), TQ(MAXHT,NT)
REAL SSTRESS(MAXXSN, NT), GPOWER(MAXXSN, TIME),
+ UPOWER(MAXXSN, TIME)
REAL DISCHARGE (MAXXSN,NT)
INTEGER NUM, TIMEMAX
INTEGER NOXVALUE (MAXXSN), NOXSECT, NOCHAIN, START, FLAG
INTEGER YR(NT), DAY(NT), HR(NT), MIN(NT), QYR(TIME),
+ QMON(TIME), QDAY(TIME), QHR(TIME), QMIN(TIME), TMON(NT)
INTEGER MONI(NT), XVALUES(MAXXSN), MAP(MAXHT)
CHARACTER DUMMY*7, MON(NT)*3
  
```

C OPEN DATA FILE CONTAINING RAW X-Z VALUES FOR EACH  
 C CROSS-SECTION

C OPEN (6, FILE = 'A:\')

```

OPEN (6, FILE = 'C:\DBOS.DIR\SEVERN\ABERBEWD.TXT')
NOXSECT = 0

C READ IN ALL SECTIONS IN THE PRESCRIBED FORMAT

DO J = 1, MAXXSN
  READ(6,*,END=100)
  READ(6,*)
  READ(6,*) Y(J)
  DO L = 1,8
    READ(6,*)
  ENDDO
  READ(6,10) DUMMY, NOXVALUE(J)
100 FORMAT(A7,5X,I7)

C READ IN X-VALUES, Z-VALUES, RESISTANCE VALUES

DO K = 1, NOXVALUE(J)
  READ(6,*) X(J,K), Z (J,K), RESIS(J,K)
  IF (X(J,K).EQ.X(J,K-1).AND.(K.NE.1)) THEN
    X(J,K) = (X(J,K) + 0.01)
  ENDIF
ENDDO
NOXSECT = NOXSECT+1

  READ(6,*, END = 100)
  READ(6,*, END = 100)
ENDDO
100 CLOSE(6)

C CALCULATE THE MIN BED LEVEL

PRINT*, 'READ IN THE MIKE11 RESULT FILE'

  NLIST = 9999
C NT SHOULD BE ALTERED TO THE CORRECT NUMBER OF TIME INTERVALS

  OPEN (7, FILE = 'C:\DBOS.DIR\SEVERN\PLYNABEH.TXT', RECL = 700)
  PRINT*, 'STAGE-FILE OPENED'
C READ IN THE CHAINAGE AND SIMULATED WATER ELEVATIONS FOR
C ALL INTERPOLATED POINTS
  NORES= 1
  READ(7,19) (YR(I), MONI(I), DAY(I), HR(I), MIN(I), I=1, NT)
19 FORMAT (36(I2, I1, I2, I2, I2, 7X))
  PRINT*, 'MONTHS READ IN'
  DO I = 1, NT
    YR(I) = YR(I)+1900
    PRINT*, YR(I), MONI(I), DAY(I), HR(I)
  ENDDO

```

```

NOCHAIN = 0

DO J = 1, MAXHT
  READ(7,*, END = 200) YMODT(J), (TEMPDATA(J,K), K = 1, NT)
  DO K = 1, NOXSECT
    DIFF = ABS(YMODT(J) - Y(K))

    IF (DIFF.LT.0.02) THEN

      NOCHAIN = NOCHAIN + 1
      DO L = 1, NT
        MODWATER(NOCHAIN,L) = TEMPDATA(J,L)
        YMOD(NOCHAIN) = YMODT(J)
        XVALUES(NOCHAIN) = NOXVALUE(K)
        MAP(NOCHAIN) = K
      ENDDO
    ENDIF
  ENDDO
  NORES = NORES + 1
ENDDO
200 CLOSE(7)

  NORES = NORES - 1

C  IDENTIFY WHETHER ASSIMILATED CHAINAGES AND CROSS-SECTION
C  CHAINAGES CORRESPOND

C  CREATE NEW ARRAYS: TX(MAXXSN,MAXINT), TZ(MAXXSN,MAXINT)
C  FOR THE X-Z VALUES BETWEEN (AND INCLUDING) THE
C  WATERS EDGE VALUES

TOTAREA(J,L) = 0.0
TOTWPER(J,L) = 0.0

DO J = 1, NOCHAIN
  DO L = 1, NT
    NUM = 1
    FLAG = 0
    WWIDTH(J,L) = 0.0

C  IDENTIFY THE LEFT AND RIGHT BANK, USING SIMULATED WATER
C  ELEVATION AND THE MORPHOLOGY OF THE CHANNEL

C  IF WATER ELEVATION IS EQUAL TO AN ACTUAL Z-VALUE ON THE
C  LEFT BANK, MARK IT TZ

    DO K = 1, XVALUES(J)
      IF ((K.EQ.1).AND.MODWATER(J,L).GT.Z(MAP(J,1))) THEN
        TX(J,1) = X(MAP(J,1)) - 0.1
        WDEPTH(J,NUM) = MODWATER(J,L) - Z(MAP(J),K)

```

NUM = NUM + 1  
START = 1  
FLAG = 1

+ ELSEIF ((MODWATER(J,L).EQ.Z(MAP(J),K)).AND.  
(Z(MAP(J),K).GT.Z(MAP(J),K+1)).AND.(FLAG.EQ.0)) THEN  
TX(J,1) = X(MAP(J),K)  
WDEPTH(J,NUM) = 0.0  
START = K  
FLAG = 1  
NUM = NUM+1

C IF WATER ELEVATION FALL BETWEEN TWO Z-VALUES ON THE LEFT  
C BANK, PERFORM FOLLOWING CALCULATION TO IDENTIFY  
C TX, TZ = MODWATER  
C  $X = ((WE - Y1)/m) + X1$

+ ELSEIF ((MODWATER(J,L).LT.Z(MAP(J),K)).AND.  
(MODWATER(J,L).GT.Z(MAP(J),K+1)).AND.  
(FLAG.EQ.0)) THEN  
TX(J,1) = ((MODWATER(J,L)-Z(MAP(J),K))/  
((Z(MAP(J),K+1)-Z(MAP(J),K))/  
(X(MAP(J),K+1)-X(MAP(J),K)))) + (X(MAP(J),K))  
WDEPTH(J,NUM) = 0.0  
START = K  
FLAG = 1  
NUM = NUM+1

ELSEIF (MODWATER(J,L).GE.Z(MAP(J),K)) THEN  
WDEPTH(J,NUM) = MODWATER(J,L) - Z(MAP(J),K)  
TX(J,NUM) = X(MAP(J),K)  
NUM = NUM + 1  
START = START + 1  
TOTWDEPTH(J,L) = WDEPTH(J,NUM) + TOTWDEPTH(J,L)

ENDIF

ENDDO

C ONCE LEFT BANK IS IDENTIFIED, LABEL ALL X-Z VALUES UP TO  
C Z = MODWATER, TX AND TZ

C WATER DEPTH IS CALCULATED BY SUBTRACTING INDIVIDUAL  
C TZ-VALUES FROM MODWATER

C IF WATER ELEVATION IS EQUAL TO AN ACTUAL Z-VALUE ON  
C THE RIGHT BANK, MARK IT TZ

```

DO K = (START-1), XVALUES(J)
  IF ((MODWATER(J,L).EQ.Z(MAP(J),K)).AND.
+ (Z(MAP(J),K).LT.Z(MAP(J),K+1))) THEN
    TZ(J,NUM) = X(MAP(J),K)
    WDEPTH(J,NUM) = 0.0

C   IF WATER ELEVATION FALL BETWEEN Z-VALUES ON RIGHT BANK,
C   PERFORM FOLLOWING CALCULATION TO IDENTIFY TX, TZ = MODWATER

    ELSEIF ((MODWATER(J,L).GT.Z(MAP(J),K)).AND.
+ (MODWATER(J,L).LT.Z(MAP(J),K+1))) THEN
      TZ(J,NUM) = ((MODWATER(J,L)-Z(MAP(J),K+1))/
+ ((Z(MAP(J),K+1)-Z(MAP(J),K))/
+ (X(MAP(J),K+1)-X(MAP(J),K)))) + (X(MAP(J),K+1))
      WDEPTH(J,NUM) = 0.0

    ELSEIF ((K.EQ.XVALUES(J)).AND.(MODWATER(J,L).GT.
+ Z(MAP(J),K))) THEN
      TZ(J,NUM) = X(MAP(J),K) + 0.1
      WDEPTH(J,NUM) = (MODWATER(J,L)) - Z(MAP(J),K)
    ENDIF

ENDDO

C   CALCULATE THE AREA AND WETTED PERIMETER FOR EACH CROSS- SECTION
C   THIS INVOLVES SUMMING THE INDIVIDUAL SEGMENT VALUES

C   AREA OF SEGMENT = 0.5.(WD(K)+WD(K+1)).(TX(K+1)-TX(K))
C   WETTED PERIMETER OF EACH SEGMENT =
C   (((WD(K+1)-WD(K))^2)+(TX(K+1)-TX(K))^2)^0.5

DO K = 1, NUM

  IF (K.EQ.2) THEN
    AREASEG(J,K) = ABS(0.5*(WDEPTH(J,NUM)+WDEPTH(J,K))*
+ (TX(J,K)-TX(J,1)))
    WPERSEG(J,K) = (((WDEPTH(J,K)-WDEPTH(J,NUM))**2)
+ ((TX(J,K)-TX(J,1))**2))**0.5

  ELSEIF ((K.GE.3).AND.(K.LT.NUM)) THEN
    AREASEG(J,K) = ABS(0.5*(WDEPTH(J,K)+WDEPTH(J,K-1))*
+ (TX(J,K-1)-TX(J,K)))
    WPERSEG(J,K) = (((WDEPTH(J,K-1)-WDEPTH(J,K))**2)
+ ((TX(J,K-1)-TX(J,K))**2))**0.5

  ELSEIF (K.EQ.NUM) THEN
    AREASEG(J,K) = ABS(0.5*(WDEPTH(J,K-1)+WDEPTH(J,NUM))*
+ (TZ(J,NUM)-TX(J,K-1)))
    WPERSEG(J,K) = (((WDEPTH(J,NUM)-WDEPTH(J,K-1))**2)

```

```

+          +((TZ(J,NUM)-TX(J,K-1))**2)**0.5
  ENDIF

C  TOTAL AREA AND WETTED PERIMETER EQUAL THE SUM OF THE      SEGMENTS

      TOTAREA(J,L) = AREASEG(J,K) + TOTAREA(J,L)
      TOTWPER(J,L) = WPERSEG(J,K) + TOTWPER(J,L)

  ENDDO

      TOTHRAD(J,L) = TOTAREA(J,L) / TOTWPER(J,L)

C  WATERS EDGE LEFT AND RIGHT BANK (X-VALUES) = TX(J,1), TX(J,NUM)
C  WATERS EDGE LEFT AND RIGHT BANK (Z-VALUES) = TZ(J,1), TZ(J,NUM)

      WELBX(J,L) = TX(J,1)
      WERBX(J,L) = TZ(J,NUM)
      WWIDTH(J,L) = ABS(WELBX(J,L) - WERBX(J,L))

C  WETTED WIDTH IS EQUAL TO THE RIGHT BANK X-VALUE MINUS THE LEFT

      ENDDO

      ENDDO

PRINT*, 'NUMBER OF MODEL CHAINAGES =', NORES
PRINT*, 'NUMBER OF X-SECTIONS =', NOXSECT
PRINT*, 'NUMBER OF LINKED CHAINAGES =', NOCHAIN

IF (NOCHAIN.GT.NOXSECT) THEN
  PRINT*, 'GREATER NUMBER OF MODEL CHAINAGES'
ELSE IF (NOCHAIN.LT.NOXSECT) THEN
  PRINT*, 'GREATER NUMBER OF CROSS SECTIONS'
ENDIF

C  WSSLOPE = WATER SURFACE SLOPE IS AVERAGED FROM:
C      (MODWATER(J+1)-MODWATER(J-1))/(Y(J+1)-Y(J-1))
C  AT THE BOUNDARIES, DO NOT USE (J-1) & (J+1), BUT JUST
C  (J) AND (J) FOR THE UPPER AND LOWER ENDS, RESPECTIVELY

DO L = 1, NT
DO M = 1, NORES
  IF (M.EQ.1) THEN
    SLOPE(M,L) = ABS((TEMPDATA(M,L)-TEMPDATA(M+1,L))/
+      ((YMODT(M+1)-YMODT(M))*1000))
  ELSEIF ((M.GE.2).AND.(M.LT.NORES)) THEN
    SLOPE(M,L) = ABS((TEMPDATA(M-1,L)-TEMPDATA(M+1,L))/
+      ((YMODT(M+1) - YMODT(M-1))*1000))
  ELSEIF (M.EQ.NORES) THEN

```

```

      SLOPE(M,L) = ABS((TEMPDATA(M-1,L)-TEMPDATA(M,L))/
+      ((YMODT(M) - YMODT(M-1))*1000))
      ENDIF
      PRINT*, L, M, SLOPE(M,L)

```

```

      DO J = 1, NOCHAIN
        DIFF = ABS(YMODT(M) - Y(MAP(J)))
        IF (DIFF.LT.0.02) THEN
          WSSLOPE(J,L) = SLOPE(M,L)
        ENDIF
      ENDDO
    ENDDO
  ENDDO

```

```

PRINT*, 'CALCULATING THE MINIMUM BED LEVEL'
DO J = 1, NOCHAIN
  BEDMIN(J) = 700.00
  DO K = 1, XVALUES(J)
    IF (Z(MAP(J),K).LT.BEDMIN(J)) THEN
      BEDMIN(J) = Z(MAP(J),K)
    ENDIF
  ENDDO
  DO L = 1, NT
    MAXDEPTH(J,L) = MODWATER(J,L) - BEDMIN(J)
  ENDDO
ENDDO

```

```

AMAX(1,L) = 0.0
PMAX(1,L) = 0.0
MAX = 1
AMAX(1,L) = TOTAREA(1,L)
PMAX(1,L) = TOTWPER(1,L)

```

C IDENTIFY THE LAST VALUE IN THE CUMULATIVE SUMMATION OF AREA

```

DO L = 1, NT
  DO J = 1, NOCHAIN
    IF (TOTAREA(J,L).GT.AMAX(J,L)) THEN
      AMAX(J,L) = TOTAREA(J,L)
      MAX = J
    ENDIF
  ENDDO
ENDDO

```

C IDENTIFY THE LAST VALUE IN THE CUMULATIVE SUMMATION OF W.PER

```

DO L = 1, NT
  DO J = 1, NOCHAIN
    IF (TOTWPER(J,L).GT.PMAX(J,L)) THEN
      PMAX(J,L) = TOTWPER(J,L)
    ENDIF
  ENDDO
ENDDO

```

```

    MAX = J
    ENDIF
ENDDO
ENDDO

TIMEMAX = 0
OPEN (7, FILE = 'A:\PLYNABER\PLYNABEQ.TXT')
PRINT*, 'OPENING DISCHARGE FILE'
NCHAIN = 1
DO J = 1, 50
  READ(7,*, end = 700)
  READ(7,*)
  READ(7,*)
  READ(7,*)
  READ(7,*)
  READ(7,*)
  READ(7,*) (CHAIN(N), N = NCHAIN, NCHAIN + 4)
  READ(7,*)
  DO L = 1, time
    READ(7,37) QYR(L), QMON(L), QDAY(L), QHR(L), QMIN(L),
+ (Q(N,L), N = NCHAIN, NCHAIN + 4)
37  FORMAT (I4, 4X, I2, 6X, I2, 6X, I2, 6X, I2, 6X, F8.2,
+      F8.2, F8.2, F8.2, F8.2)
    ENDDO
    NCHAIN = NCHAIN + 5
  ENDDO
  NCHAIN = NCHAIN - 1
700 CLOSE(7)

CHAINAGE(1) = YMOD(1)

DO M = 1, TIME
  DISCHARGE(1,M) = Q(1,M)
ENDDO

DO J = 1, NCHAIN
  DO K = 1, NOCHAIN
    DIFF = ABS (((CHAIN(J) + CHAIN(J+1)) / 2) - Y(MAP(K)))
    IF (DIFF.LT.1.0) THEN
      IF ((K.GE.2).AND.(J.LT.NCHAIN)) THEN
        CHAINAGE(K) = Y(MAP(K))
        DO M = 1, TIME
          DISCHARGE(K,M) = Q(J,M)
        IF (K.EQ.NOCHAIN) THEN
          DISCHARGE(NOCHAIN,M) = Q(NCHAIN,M)
          CHAINAGE(K+1) = Y(NOCHAIN)
        ENDIF
      ENDDO
    DO M = 1, TIME
  ENDDO
ENDIF
ENDIF

```

```
ENDDO
ENDDO
```

```
C CALCULATE THE REACH MEAN SHEAR STRESS, GROSS STREAM POWER
C AND UNIT STREAM POWER USING CALCULATED VARIABLES
```

```
SSTRESS(J,L) = 0.0
GPOWER(J,K) = 0.0
UPOWER(J,K) = 0.0
DENS = 1000
GRAV = 9.81
DO L = 1, NT
DO J = 1, NOCHAIN
    SSTRESS(J,L) = GRAV*DENS*TOTHRAD(J,L)*WSSLOPE(J,L)
    DO K = 1, TIME
        GPOWER(J,K) = GRAV*DENS*DISCHARGE(J,K)*WSSLOPE(J,L)
        UPOWER(J,K) = ((GRAV*DENS*DISCHARGE(J,K)*WSSLOPE(J,L))
+ /WWIDTH(J,L))
    ENDDO
ENDDO
ENDDO
```

```
PRINT*, 'OPENING RESULT-FILE'
```

```
OPEN (8, FILE = 'C:\DBOS.DIR\PLYNABER.TXT', RECL = 130)
```

```
WRITE(8,38) 'ABERMULE - BEWDLEY: 15 - 23 FEB 1989'
```

```
38 FORMAT (A37)
```

```
DO L = 1, NT
```

```
WRITE(8,40) DAY(L),' ',MONI(L),' ',YR(L),' ',HR(L),' ',
```

```
+ MIN(L),' '
```

```
40 FORMAT(I2,A1,I1,A1,I4,A2,I2,A1,I2,A1)
```

```
WRITE(8,39) 'NO,', 'CHAIN,', 'WWIDTH,', 'BEDMIN,', 'WELEV,',
```

```
+ 'MAXDEPTH,', 'AREA,', 'WPER,', 'HYDRRAD,', 'WSSLOPE,',
```

```
+ 'SSTRESS,', 'DISCHARGE,', 'GPOWER,', 'UPOWER,'
```

```
39 FORMAT(A3, A6, A7, A7, A6, A9, A5, A5, A8, A8, A8, A11,
```

```
+ A7, A7)
```

```
WRITE(8,250) '(KM)', '(M)', '(M)', '(M)', '(M)',
```

```
+ '(M2)', '(M)', '(M)', '(M/M)', '(N M-2)', '(M3 S-1),
```

```
+ '(W M-1)', '(W M-2),'
```

```
250 FORMAT (3X, A1, A5, A4, A4, A4, A4, A5, A4, A4, A6, A8, A9,
```

```
+ A8, A8)
```

```
WRITE(8,*)
```

```
DO J = 1, NOCHAIN
```

```
WRITE(8,41) J, ', ', YMOD(J), ', ', WWIDTH(J,L), ', ',
```

```
+ BEDMIN(J), ', ', MODWATER(J,L), ', ', MAXDEPTH(J,L),
```

```
+ ', ', TOTAREA(J,L), ', ', TOTWPER(J,L), ', ', TOTHRAD(J,L),
```

```
+ ', ', WSSLOPE(J,L), ', ', SSTRESS(J,L), ', ', DISCHARGE(J,L),
```

```
+ ', ', GPOWER(J,L), ', ', UPOWER(J,L)
```

```
41  FORMAT(I3, A1, F8.3, A1, F9.3, A1, F8.3, A1, F8.3, A1, F8.3,  
+   A1, F9.3, A1, F9.3, A1, F8.3, A1, F9.7, A1, F9.3, A1, F9.3,  
+   A1, F9.3, A1, F9.3)
```

```
ENDDO  
ENDDO
```

```
CLOSE(8)
```

```
STOP  
END
```

## APPENDIX II

A FORTRAN 77 program designed to convert EA data files from ASCII format into a MIKE11 input-file format

Written by John Couperthwaite and Dan Cornford, December 1994

### PROGRAM XSECTION

```
REAL CHAIN
INTEGER I
CHARACTER*12 FILES(700), FILEN
OPEN (6,FILE = 'A:\WORC\DESIGN.CAT')
PRINT*, 'CAT OPEN'
READ(6,*)
READ(6,*)
READ(6,*) NFILES
CHAIN = 0
DO I = 1, NFILES
  READ(6,10) FILEN
10  FORMAT (A12)
  FILES (NFILES+1-I) = FILEN
ENDDO
CLOSE(6)

OPEN (6, FILE = 'C:\DBOS.DIR\SEVERN\XSECTION.TXT',
+ RECL = 50)
DO I = 1, NFILES
  FILEN = FILES (I)
  CALL READFILE (FILEN, CHAIN)
ENDDO

CLOSE(6)
CLOSE(8)

STOP
END

SUBROUTINE READFILE (FILEN, CHAIN)
CHARACTER FILEN*12, FILENM*20
REAL XSN(1000,2)
REAL LB, RB, X, Y, CHAIN, DUMMY, NMOD(5)
REAL NM(5), MAXDEPTH, LBY, RBY
INTEGER I, MIN, COUNT
FILENM (1:8) = 'A:\WORC\'
FILENM (9:20) = FILEN (1:12)
CHAIN = 14244
OPEN (7, FILE = FILENM)
READ(7,*) XCHAIN
```

```
READ(7,*)
CHAIN = (ABS(XCHAIN - CHAIN)) * 10
CHAIN = (CHAIN + 207740) / 1000
READ(7,*) NM(1), NM(2), NM(3), NM(4), NM(5)
PRINT*, CHAIN, NM(1), NM(2), NM(3), NM(4), NM(5)
READ(7,*) LB, RB, DUMMY
READ(7,*)
```

```
COUNT = 0
DO I = 1, 1000
  READ(7,19, END = 99) X, Y
  COUNT = COUNT + 1
  XSN(I,1) = X
  XSN(I,2) = Y
ENDDO
```

```
99 CLOSE(7)
```

```
  WRITE(6,40) 'ABER-BEWD'
40  FORMAT (A9)
  WRITE(6,41) 'SEVERN'
41  FORMAT (A6)
  WRITE(6,12) CHAIN
12  FORMAT (F11.3)
  WRITE(6,42) 'COORDINATES'
42  FORMAT (A11)
  WRITE(6,13) '1 0', CHAIN
13  FORMAT (A4, F13.3)
  WRITE(6,43) 'FLOW'
43  FORMAT (A4)
  WRITE(6,*) '0'
  WRITE(6,44) 'DATUM'
44  FORMAT (A5)
  WRITE(6,*) '0'
  WRITE(6,45) 'RADIUS TYPE'
45  FORMAT (A11)
  WRITE(6,*) '0'
  WRITE(6,14) 'PROFILE', COUNT
14  FORMAT (A7, I7)
```

```
MIN = 1
YMIN = XSN(1,2)
DO I = 2, COUNT
  IF (XSN(I,2).LT.YMIN) THEN
    YMIN = XSN(I,2)
    MIN = I
  ENDIF
ENDDO
```

```
DO I = 1, COUNT
```

```

IF (XSN(I,1).EQ.LB) THEN

  LBY = XSN(I,2)
ENDIF
ENDDO

DO I = 1, COUNT
  IF (XSN(I,1).EQ.RB) THEN
    RBY = XSN(I,2)
  ENDIF
ENDDO

MAXDEPTH = ABS(((LBY+RBY)/2) - YMIN)

DO I = 1, 5
  NMOD(I) = NM(I)*30
ENDDO

DO I = 1, COUNT
  IF (XSN(I,1).EQ.LB) THEN
    WRITE(6,15) XSN(I,1), XSN(I,2), NMOD(1)
15  FORMAT (2F12.2, F7.3)
  ELSEIF (XSN(I,1).EQ.RB) THEN
    WRITE(6,15) XSN(I,1), XSN(I,2), NMOD(2)
  ELSEIF (XSN(I,2).EQ.YMIN) THEN
    WRITE(6,155) XSN(I,1), XSN(I,2), NMOD(3), '<2>'
155  FORMAT (2F12.2, F7.3, A5)
  ELSEIF (XSN(I,1).LT.LB) THEN
    WRITE(6,16) XSN(I,1), XSN(I,2), NMOD(1)
16  FORMAT (2F12.2, F7.3)
  ELSEIF (XSN(I,1).GT.RB) THEN
    WRITE(6,16) XSN(I,1), XSN(I,2), NMOD(2)
  ELSEIF (XSN(I,2).LE.(YMIN + (0.2*MAXDEPTH))) THEN
    WRITE(6,16) XSN(I,1), XSN(I,2), NMOD(3)
  ELSEIF (XSN(I,2).LE.(YMIN + (0.8*MAXDEPTH))) THEN
    WRITE(6,16) XSN(I,1), XSN(I,2), NMOD(4)
  ELSEIF (XSN(I,2).GT.(YMIN + (0.8*MAXDEPTH))) THEN
    WRITE(6,16) XSN(I,1), XSN(I,2), NMOD(5)
  ENDIF
ENDDO

  WRITE(6,46) 'H-LEVELS 10'
46  FORMAT (A13)
  WRITE(6,47) '****'
47  FORMAT (A3)
  RETURN

END

```

John S. Couperthwaite

*Downstream change in channel hydraulics along the River Severn, UK*

Thesis (PhD.) - University of Birmingham, School of Geography, Faculty of Science, 2007

Appendix 3 is not available in this digital version